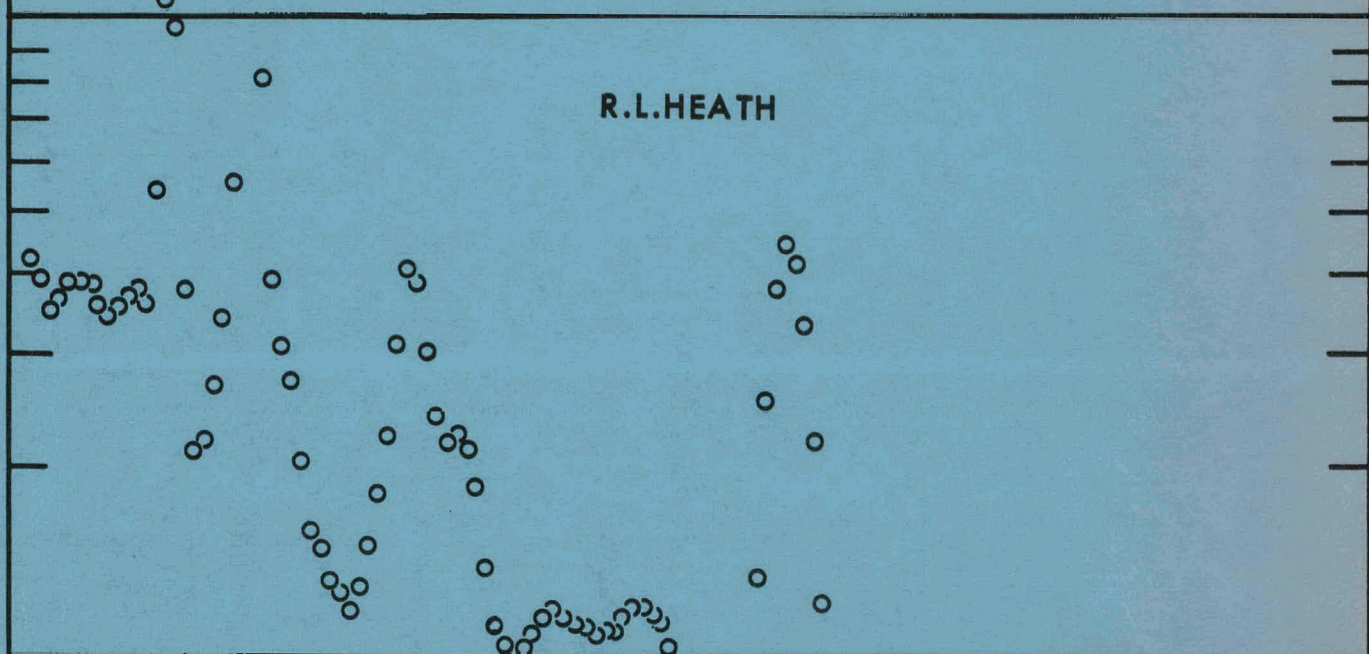


PHYSICS AND MATHEMATICS  
(TID-4500, Ed. 13)

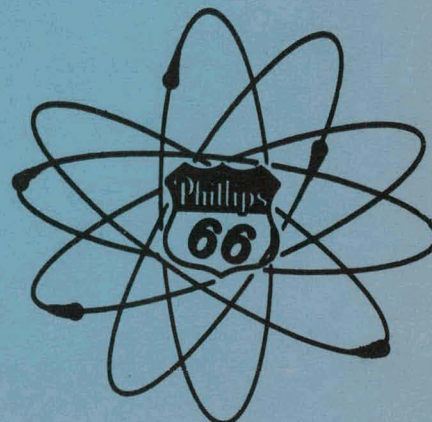
# SCINTILLATION SPECTROMETRY GAMMA-RAY SPECTRUM CATALOGUE

BY

R.L. HEATH



**PHILLIPS PETROLEUM CO.**  
**ATOMIC ENERGY DIVISION**  
SUBDER CONTRACT NO. AT (20-8-209)  
**IDAHO OPERATIONS OFFICE**  
**U. S. ATOMIC ENERGY COMMISSION**



971-001

## **DISCLAIMER**

**This report was prepared as an account of work sponsored by an agency of the United States Government. Neither the United States Government nor any agency Thereof, nor any of their employees, makes any warranty, express or implied, or assumes any legal liability or responsibility for the accuracy, completeness, or usefulness of any information, apparatus, product, or process disclosed, or represents that its use would not infringe privately owned rights. Reference herein to any specific commercial product, process, or service by trade name, trademark, manufacturer, or otherwise does not necessarily constitute or imply its endorsement, recommendation, or favoring by the United States Government or any agency thereof. The views and opinions of authors expressed herein do not necessarily state or reflect those of the United States Government or any agency thereof.**

## **DISCLAIMER**

**Portions of this document may be illegible in electronic image products. Images are produced from the best available original document.**

The following pages are an exact representation of what is in the original document folder.

PRICE \$4.75

Available from the  
Office of Technical Services  
U. S. Department of Commerce  
Washington 25, D. C.

DO NOT PHOTOSTAT

### LEGAL NOTICE

This report was prepared as an account of Government sponsored work. Neither the United States, nor the Commission, nor any person acting on behalf of the Commission:

A. Makes any warranty or representation, express or implied, with respect to the accuracy, completeness, or usefulness of the information contained in this report, or that the use of any information, apparatus, method, or process disclosed in this report may not infringe privately owned rights; or

B. Assumes any liabilities with respect to the use of, or for damages resulting from the use of any information, apparatus, method, or process disclosed in this report.

As used in the above, "person acting on behalf of the Commission" includes any employee or contractor of the Commission to the extent that such employee or contractor prepares, handles or distributes, or provides access to, any information pursuant to his employment or contract with the Commission.

**SCINTILLATION SPECTROMETRY**  
**GAMMA-RAY SPECTRUM CATALOGUE**

**BY**

**R. L. HEATH**

**July 1, 1957**

**PHILLIPS PETROLEUM CO.**  
**ATOMIC ENERGY DIVISION**  
**Idaho Falls, Idaho**

**LEGAL NOTICE**

This report was prepared as an account of Government sponsored work. Neither the United States, nor the Commission, nor any person acting on behalf of the Commission:

A. Makes any warranty or representation, expressed or implied, with respect to the accuracy, completeness, or usefulness of the information contained in this report, or that the use of any information, apparatus, method, or process disclosed in this report may not infringe privately owned rights; or

B. Assumes any liabilities with respect to the use of, or for damages resulting from the use of any information, apparatus, method, or process disclosed in this report.

As used in the above, "person acting on behalf of the Commission" includes any employee or contractor of the Commission, or employee of such contractor, to the extent that such employee or contractor of the Commission, or employee of such contractor prepares, disseminates, or provides access to, any information pursuant to his employment or contract with the Commission, or his employment with such contractor.

# TABLE OF CONTENTS

	Page
ACKNOWLEDGEMENTS	
I. PREFACE . . . . .	9
II. METHODS OF MEASUREMENT . . . . .	11
A. The Standard Detector . . . . .	11
B. The Detector Shield . . . . .	12
C. Source-Detector Configuration . . . . .	13
D. The Scintillation Spectrometer . . . . .	15
E. Data Processing . . . . .	15
F. The Quantitative Method . . . . .	16
III. INDEX OF GAMMA-RAY SPECTRA . . . . .	24
APPENDIX I - Detection Efficiency Curves	
APPENDIX II - Peak-To-Total Ratios	

## ACKNOWLEDGEMENTS

The collection of data contained in this catalogue represents the combined efforts of many people on the MTR technical staff. It is a pleasure for the author to acknowledge the support of those individuals who have contributed to this work.

In particular, the author wishes to express his appreciation to Miss Wanda Hammer, whose efforts have made this publication possible. Miss Hammer has been largely responsible for the reduction of data and the preparation of all material for publication.

Source preparation and chemical purification of source material were carried out by members of the Radiochemistry group. This work included the efforts of N. P. Alley, R. B. Regier, T. O. Passell, D. R. Reeder, E. H. Turk, R. P. Schumann and W. H. Burgus. The preparation of the plates for reproduction was under the direction of F. E. Payne and A. D. Lintelmann of the drafting section.

The author wishes to express his gratitude to Dr. S. H. Vegors, who assisted in the collection of some of the data and the preparation of the text; and to Mr. G. O. English for assistance in the calibration and maintenance of the electronic equipment. Special thanks are due Mr. D. R. DeBoisblanc, director of the Reactor Physics Branch, for constant encouragement and support.

The development of many of the techniques which were used in obtaining the data contained in this catalogue has been largely due to the work of Dr. P. R. Bell and co-workers at the Oak Ridge National Laboratory.

## I - PREFACE

Gamma scintillation spectrometry as a method of radioactivity measurement has gained wide acceptance in the past few years. It would seem, however, that its general use has been limited severely both in scope and precision by the lack of adequate published information on the characteristics of the detectors. The techniques have been in general use in the research laboratories for several years now, but the information needed to promote their general use has remained largely in unpublished form.

In view of possibilities which this method offers in applied radiation measurement studies, for both qualitative and quantitative application, it was felt that an effort should be made to make available the necessary information in a form which can be readily applied in the routine laboratory.

In the experience of personnel at this laboratory, a comprehensive catalogue of the response of a scintillation detector to individual nuclides has been a useful tool in the routine analysis of radioactive samples. The compilation of this catalogue is an effort to present such information in a usable form.

In order to make a collection of data such as this useful for quantitative as well as qualitative

application, it has been necessary to adopt certain criteria for the method employed in obtaining the so-called "standard" response curves. Among these are the following:

1. Choice of detector size and geometrical shape.
2. Source-detector configuration.
3. Detector shield design.
4. Methods of data collection and analysis.

This collection of gamma spectra contains samples of the response of NaI(Tl) scintillation detectors to a large number of the more frequently encountered radioactive nuclides. These data have been assembled under very carefully controlled experimental conditions to permit reproduction in any laboratory with a reasonable amount of care. These "spectral shapes" may be used together with techniques of graphical analysis to provide quick, accurate analysis of unknown samples, both in a qualitative and quantitative sense.

Any future extension of the catalogue to include samples of activities omitted or modification of the data presentation will depend upon its acceptance by measurement laboratories. Any suggestions which might make this information more useful would be welcomed by the author.

## II - METHODS OF MEASUREMENT

### A. The Standard Detector

In this laboratory the 3" diameter x 3" cylinder of NaI(Tl) has become the standard reference detector for precision gamma-ray scintillation spectrometry. The choice of this size detector is based upon a consideration of several factors. Fig. 1 shows the pulse-height distribution obtained for the single 662 Kev gamma-ray emitted in the decay of Cs<sup>137</sup>.

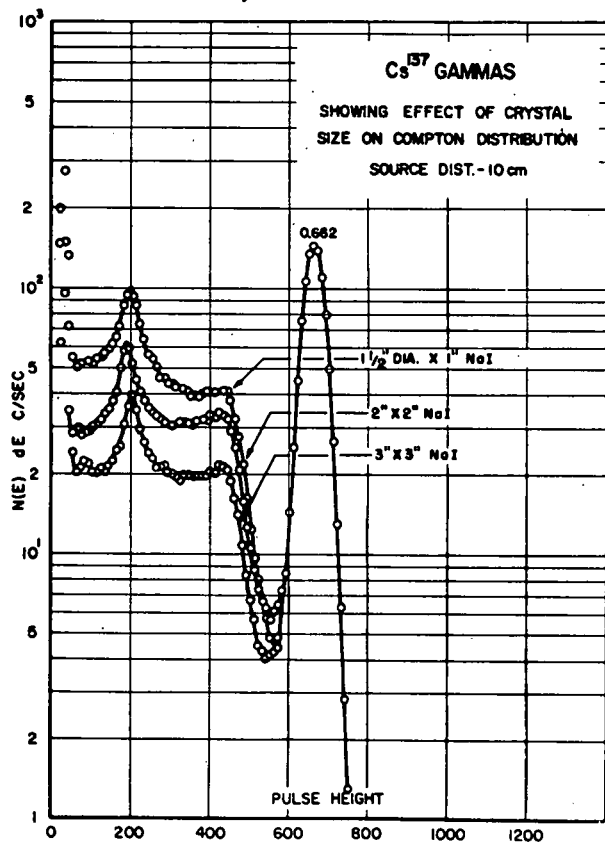


Fig. 1. Effect of Detector Size on Compton Distribution.

To permit a comparison the response of 1 1/2" diameter x 1", 2" diameter x 2" and 3" diameter x 3" cylinders of NaI are shown normalized at the photo-electric peak. As the detector size, and hence the path length traversed by a photon increases, the probability for the occurrence of multiple Compton processes increases markedly. Since the resolution time of the phosphor is long compared with the time for many collisions, the events will add. This results in relatively more events which ultimately leave the total photon energy in the detector. At 0.662 Mev. 55% of the events result in total energy loss in the 3" x 3"

detector as opposed to 33% for the 1 1/2" diameter x 1" detector.

In the analysis of complex spectra it would be ideal to completely suppress the Compton electron distribution. For a number of reasons, however, a compromise is necessary. A 3" diameter x 3" detector, together with phototube, costs around \$1000. To go to a larger phosphor would require the use of a larger phototube with an appreciable increase in cost and loss of resolution. With 3" x 3" crystals and DuMont 6363 phototubes it is possible to obtain better than 8% resolution for the Cs<sup>137</sup> line with little selection necessary.

The crystal mounting technique which has been adopted is that developed by P. R. Bell, et al,<sup>1</sup> at ORNL and is shown in Fig. 2. In this

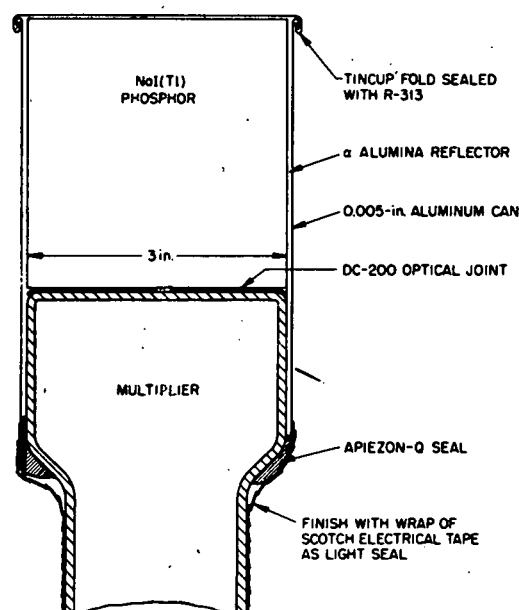


Fig. 2. Standard Method of Phosphor Preparation

method the phosphor and phototube are mounted as one integral unit with the crystal surrounded by a 0.005" aluminum can.

The reflecting surface is a thin coating of  $\alpha$ -alumina sprayed on the inside surface, using sodium silicate as a binder. The primary reason for using a can of this type is to minimize the amount of scattering material in the near vicinity of the phosphor, thus reducing any distortion due to spurious scattered radiation.

<sup>1</sup>P. R. Bell,  *$\beta$  and  $\gamma$ -Ray Spectroscopy*, K. Siegbahn ed., p 161, North-Holland, Amsterdam, 1955.

## B. The Detector Shield

One of the most important considerations in obtaining good data in scintillation spectrometry is the design of the detector radiation shield. For convenience it is desirable to reduce the background radiation level to a point where corrections to the data will be small for the moderate strength sources usually prepared in the laboratory.

In any type of analysis of data obtained on the scintillation spectrometer a differentiation must be made between the response of the detector to direct radiation from the source and spurious scattered radiation arising from interaction with the surrounding material; i.e., source holder, beta absorber and radiation shield.

This scattered radiation results from two types of interaction: (1) the photoelectric process and (2) Compton scattering.

### 1. Photoelectric Effect

The photo-effect is of particular importance in shield design since the cross section for this process is high for low energy photons, particularly in materials such as Pb. This process results in the production of x-rays characteristic of the absorbing material. Spurious radiation from this source is generally reduced by the use of graded shields. In an arrangement of this type the Pb radiation shield is lined with one or more materials in descending order of Z. These materials are chosen to have a high cross section for the absorption of fluorescent radiation from the preceding one. The usual arrangement is to line the Pb shield with 0.030" to 0.060" of Cd and 0.005" of Cu, in that order. Fig. 3 shows the effect of fluorescent radiation produced in a Pb shield and its reduction by this procedure. This figure is a plot of the response of a 3" x 3" detector to the 0.32 Mev gamma-ray of Cr<sup>51</sup>. For this series of measurements the detector was mounted in a 6" x 6" shield with the source at 10 cm. In this configuration a strong "line" is observed at 0.072 Mev resulting from the production of Pb x-rays in the shield. The second curve (shown by the solid line in the x-ray region) indicates the response following the addition of a 0.030" Cd lining to the shield, indicating a considerable reduction of the x-ray peak. Finally, the lowest line shows the response of the detector in a larger shield which is lined with 0.060" Cd and 0.005" Cu sheet in that order. The combination of reduced solid-angle for scattering and the "graded" lining have re-

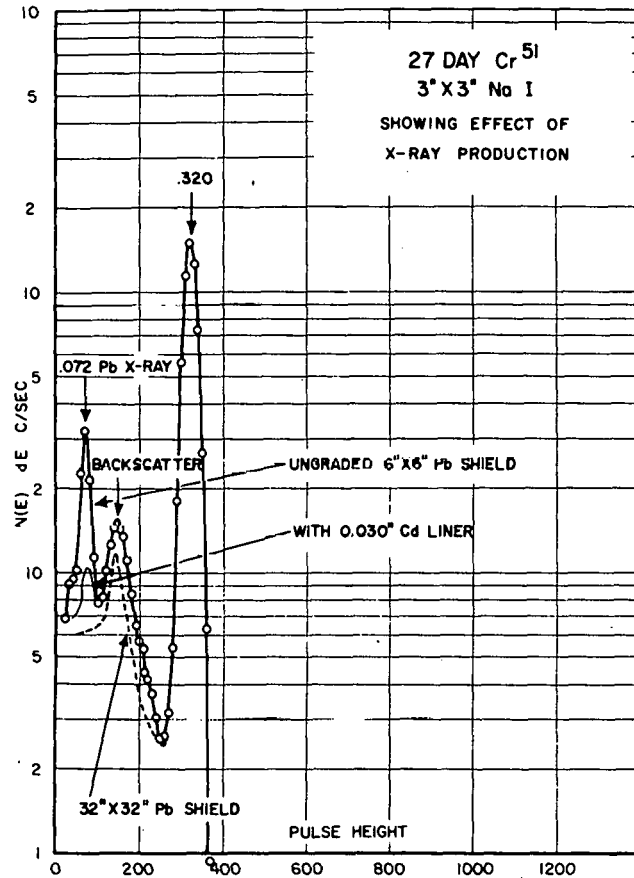


Fig. 3. Effect of X-ray Production in Pb Shield reduced the fluorescent radiation below the limits of detection.

### 2. Compton Scattering

The major source of spurious radiation from the shield is due to Compton scattering, where the energy of the scattered electron,  $E_e$ , (and hence the scattered photon) is related to the energy of the primary photon,  $E_\gamma$ , by the relationship:

$$E_e = \frac{E_\gamma}{1 + \frac{mc^2}{(1 - \cos \theta) E_\gamma}}$$

where  $\theta$  is the angle between the primary photon direction and the secondary scattered gamma-ray. This indicates that the spectrum of scattered radiation will vary from the energy of the primary photon down to a minimum value corresponding to 180° scattering. The energy distribution observed by a detector from Compton scattering off the walls of the radiation shield will then depend upon the particular geometrical arrangement of source, shield and detector. To illustrate the effect of shield

configuration upon the scattered component, data was obtained using three different shielding geometries. These are shown in Fig. 4. The three

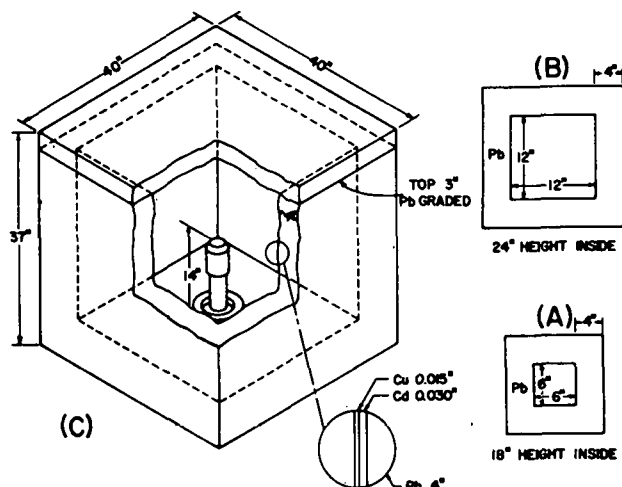


Fig. 4 Shield Configurations.

shields were constructed with 4'' Pb walls with inside dimensions of 6'' x 6'' x 18''(A), 12'' x 12'' x 24''(B), and 32'' x 32'' x 32''(C). Shield A was duplicated using Fe to demonstrate the relative effect of Z upon the scattering properties. Fig. 5 indicates the response of a 3'' x 3'' detector to the 0.835 Mev gamma-ray of Mn<sup>54</sup>, mounted at 10 cm. from the detector, for three cases. The top curve, indicated by the open circles, was obtained in shield A (Fe). The middle and lower curves, indicated by the solid lines in the low energy region represent the response in shield A (Pb) and shield C respectively. Comparison of the two curves taken in the 6'' x 6'' shield show a large difference in the magnitude of the scattered component. This is due to the difference in the relative magnitude of the absorption cross sections for the various processes which can occur in the shield material.

It is interesting to make a comparison of the general features of the spectrum of scattered radiation for all three cases. Scattering from the small shield gives rise to a broad spectrum with evidence for two major components at approximately 150 and 200 Kev. This structure is attributed to multiple and single scattering. The peak at 72 Kev in the 6'' x 6'' (Pb) case is due to Pb x-ray production. Comparing shield A with the large shield (C), there are two distinct differences in the scattered spectrum. The magnitude is considerably reduced and the spectrum assumes the shape of a fairly sharp line at approximately

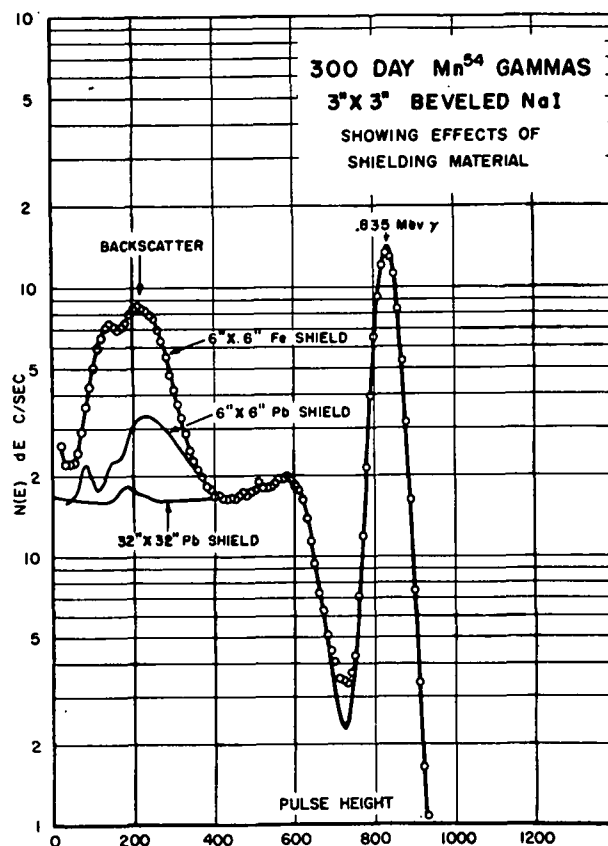


Fig. 5. Effect of Shield Configuration.

190 Kev. Both of these effects are due to a decrease in the solid-angle subtended by the detector for scattering from a point on the surface of the shield wall. In most shield geometries this characteristic "line" is referred to as the "backscatter peak". A consideration of these factors would lead one to conclude that the detector shield should be as large as cost and space will permit. The detector shield geometry used for each spectrum contained in this catalogue is indicated in the index.

One further point to recall is that the relative magnitude of the scattering effect will depend upon the source-detector configuration. For most shield arrangements the magnitude of the scattered component will be relatively independent of source distance,  $h$ , while the efficiency for the detection of direct radiation will be proportional to  $1/h^2$ .

### C. Source-Detector Configuration

#### 1. Geometry

The necessity for selecting a standard source-detector geometry is dictated largely by the fact that the response of the detector is intimately

related to the solid-angle. The probability for the occurrence of multiple events depends primarily upon the average path length traversed by a photon in passing through the detector. For this reason the "shape" of the pulse-height distribution obtained for a single gamma-ray photon will depend upon geometry. Since source strength is a prime consideration in many cases, a wide range of detector efficiency has been provided by studying the response of the standard detector to monoenergetic radiation for point sources mounted at 0.2, 3, 5 and 10 cm. (See Section II-F.) In general, sources are mounted on thin films held in cardboard or thin aluminum frames to minimize scattering. The arrangement used in this laboratory is shown in Fig. 6. The convention adopted for positioning beta absorbing material is to place it directly on top of the detector can. This mini-

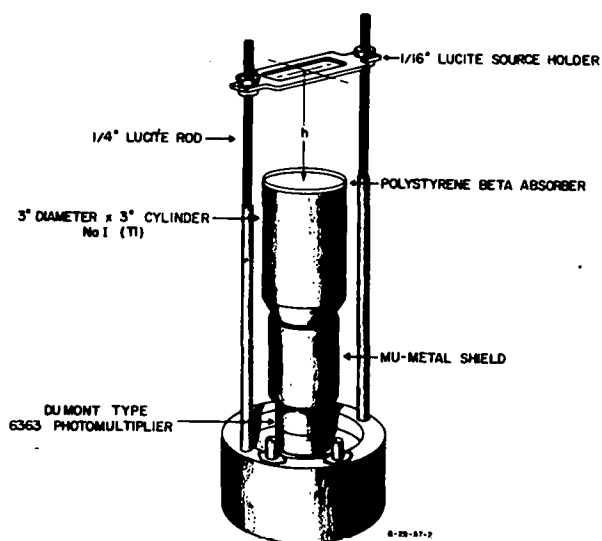


Fig. 6. Source-Detector Arrangement.

mizes the geometry for the production of external bremsstrahlung in the absorbing material. In cases where the beta energies are known, only sufficient absorber to stop the most energetic beta is used since any absorber will result in degradation of the spectrum. (See Section II-F.) In measuring the spectrum from positron emitters, sources were evaporated from solution onto a thin film and sandwiched between copper discs approximately 0.2 cm. in diameter. In each case the discs were of

sufficient thickness to insure annihilation of the positrons. In this manner a "point-source" geometry is maintained for the annihilation radiation.

## 2. Coincidence Effects

Although the response of the detector is known for several source positions, the standard source-detector geometry used for most data in the catalogue is that of a point source mounted 10 cm. from the top of the detector, on the central axis. In the more complicated decay schemes beta emission may be followed by two or more cascade gamma-rays emitted simultaneously. There is, then, a finite probability that more than one gamma-ray from the same disintegration will be detected. The light pulse produced following such an event will then be representative of the sum of the energies left by the two photons. The result will be a distribution of pulses extending in energy up to the sum of the energies of the two coincident gamma-rays. This is termed the "coincidence sum spectrum". The probability for detecting coincident radiation in this manner is just the product of the probability for detecting each of the gamma-rays individually. In effect, then, the probability for "summing" is proportional to the square of the solid-angle, whereas the probability for detecting a single event is directly proportional to the solid-angle. Increasing the source distance will then reduce the "sum spectrum" appreciably. Fig. 7 shows the spectrum of 20,000 yr  $Nb^{94}$  which decays with the emission of two cascade gamma-rays of 705 and 878 Kev. The "coincidence sum spectrum" is characterized by a smear of pulses and a sharp peak at 1.59 Mev. This "sum peak" represents the simultaneous detection of two coincident photons with total loss of energy in both cases. To demonstrate the effect of geometry on the magnitude of this effect, the source was measured at 0.4 cm. and at 10 cm. Both spectra are shown normalized to the 878 Kev gamma-ray peak. It is evident that the analysis of complex spectra would be hampered considerably by this effect if the spectrum is obtained under conditions of large solid-angle. On the other hand, in certain cases, use is made of this effect to permit identification of particular nuclides. In this manner it may be established that two photons are coincident, without the use of electronic coincidence circuitry. It should be evident that the geometry afforded by the

<sup>2</sup>Bell, Kelley and Goss, ORNL Report 1278, 1951 (unpublished), p. 27.

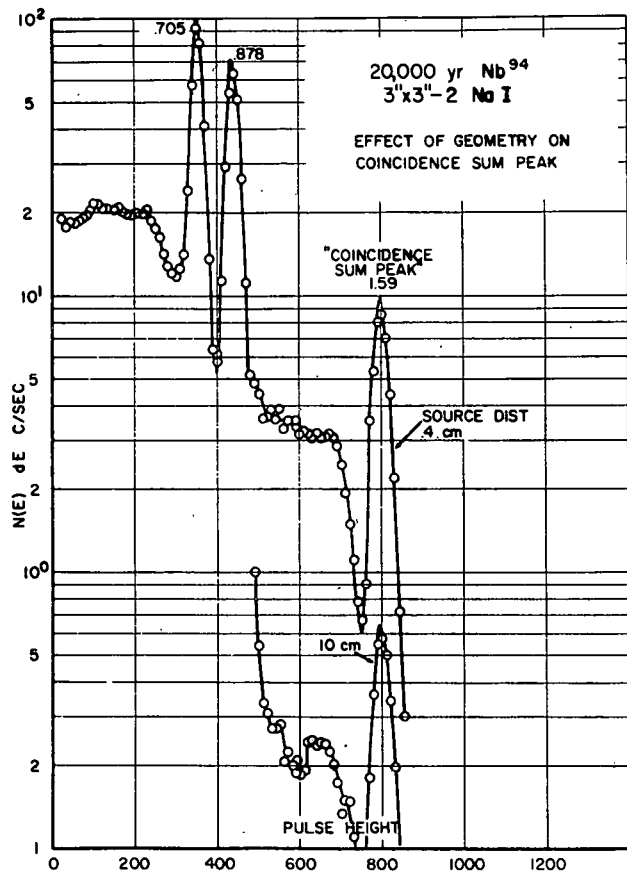


Fig. 7. Effect of Geometry on Coincidence Sum Spectrum.

well-type detectors will result in an appreciable coincidence effect. The adoption of a source distance,  $h$ , of 10 cm. is considered to be a reasonable compromise for the reduction of this effect.

#### D. The Scintillation Spectrometer

The scintillation spectrometer used to obtain the data contained in this catalogue consisted of an A-1D linear pulse amplifier operated in conjunction with a 20-channel discriminator-type pulse sorter designed by Bell, Kelley and Goss.<sup>2</sup> The pulse sorter is provided with a data storage unit with 100 channels of storage capacity. Each channel consists of a GC-10B decade glow-transfer tube and a Sodeco electro-mechanical register. These are arranged in five banks of twenty channels with twenty binary scale-of-four "pre-scalers" common to all five banks. Automatic control is provided to permit sequence programming to obtain 100 channels of pulse-height information. A block diagram of this system is shown in Fig. 8. The equipment is operated in a temperature-controlled environment and exhibits excellent long-time stability. Long-time drifts in gain and window-amplifier zero do not

exceed 1% per day. The window-width stability of the sorter is better than 2% per day under normal operating conditions. Total input counting rates of up to 20,000 per second may be handled with negligible spectrum distortion.

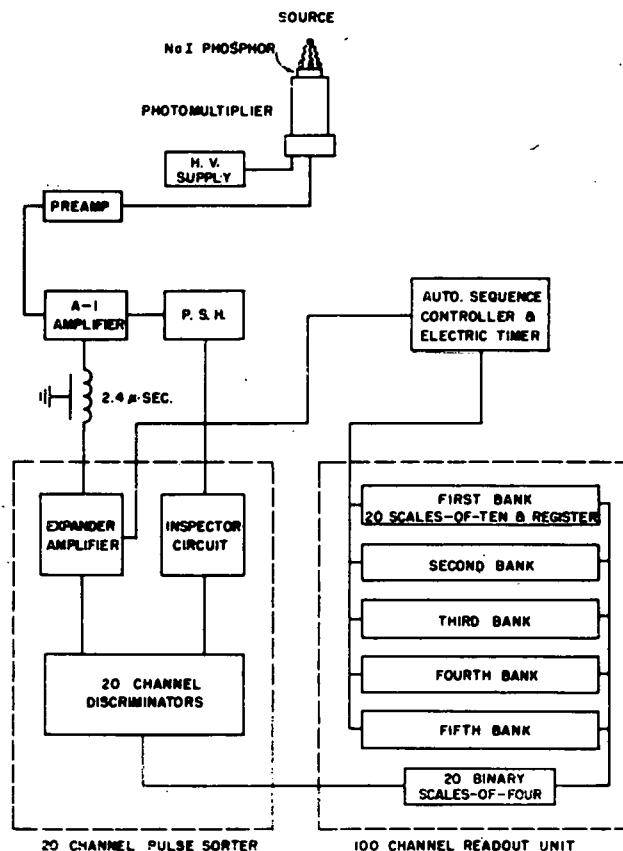


Fig. 8. Block Diagram of Scintillation Spectrometer.

#### E. Data Processing

All pulse-height distributions or gamma-ray "spectra" contained in the catalogue have been represented as plots on a standard Keuffel and Esser semi-logarithmic grid (No. 359-73). The use of the log scale on the ordinate greatly facilitates graphical analyses since the shape of the spectrum is independent of amplitude. Considerable care has been taken in the printing process to insure that the plates are exactly the same size as the original grids. This permits the use of the plates as templates for comparison with new data.

The convention adopted has been to plot the channel counting rate (ordinate) against an arbitrary scale in pulse-height units (abscissa). In the 20-channel pulse sorter this scale is obtained from the ten-turn helipot which establishes the win-

low-amplifier threshold for the bottom edge of the first channel. The window in this case is always 10 PHU wide. The relationship between this pulse-height scale and gamma-ray energy is determined by the energy range to be covered, the resolution of the detector relative to window-width and other requirements for a particular experiment. To provide a wide range of selection of energy range the following standard "gain scales" have been adopted: 0.25, 0.50, 1, 2 and 4 Kev/PHU. These scales provide energy ranges of zero to 0.25, 0.50, 1.0, 2.0 and 4.0 Mev, respectively. Some spectra have been repeated in the catalogue on more than one gain scale. This was for the purpose of showing details in the low energy region or to provide examples of the response of the detector to monoenergetic radiation on each gain scale for quantitative analysis. The use of a standard plotting technique for published spectra should greatly increase the value of such information.

#### F. The Quantitative Method

##### 1. Detector Response to Monoenergetic Radiation

In order to fully utilize phosphor detectors in gamma-ray spectrometry it is necessary to have a good understanding of the nature of the relationship between the energy of an electron produced in the detector and the energy of the incident photon. Gamma-rays may interact with matter by one of several processes: the photoelectric process, the Compton process, pair production and coherent scattering by bound electrons in the detector. Since a complete discussion of these processes as related to phosphor detectors could not be included in this brief introduction, the reader is referred to an excellent description by P. R. Bell in Chapter V of reference 1. In the interest of orientation, however, three typical gamma-ray spectra of monoenergetic radiation are presented here to illustrate the response of the standard detector as a function of energy. Fig. 9 shows the response of the detector to the single 0.155 Mev gamma emitted in the decay of 3.4 day  $Sc^{47}$ . In this energy region the pulse distribution indicates mostly response by the photoelectric process. On the low energy side of the "photo-peak" at 127 Kev is the "escape-peak" which results from escape of the iodine K x-ray following photoelectric interaction. These pulses are included by definition in the photoelectric response for quantitative analysis. It will be noted that the Compton electron distribution in this region is characterized by a rather sharp peak corresponding to  $180^\circ$  scattering. Fig. 10 is the response to

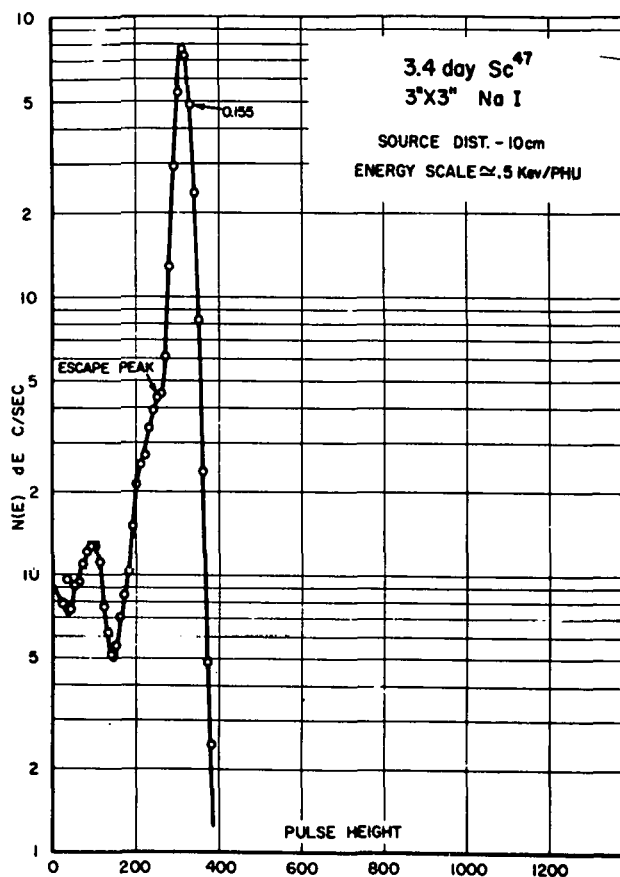


Fig. 9. Gamma-ray Spectrum of 3.4 day  $Sc^{47}$ .

the 0.835 Mev gamma-ray of  $Mn^{54}$ . In this region we see that the Compton electron distribution is much more prominent, but with a rather constant intensity from zero up to the maximum electron energy. Fig. 11 shows the response to the 3.13 Mev gamma-ray emitted by 5 min.  $S^{37}$ . At this energy the pair process is becoming quite evident. Superimposed upon the Compton electron distribution are the three (3) peaks which are characteristic of interaction by the pair process.

In this process all energy in excess of the 1.02 Mev threshold is carried away as kinetic energy of the electron-positron pair. Subsequent annihilation of the positron will yield two (2) 0.511 Mev photons. If both of these annihilation quanta escape detection in the crystal, the resultant energy loss in the detector will be 1.02 Mev less than the energy of the incident photon. In this case a single peak will appear at that energy representing the collection of only the kinetic energy of the pair. This peak is called the "double escape peak". In the event that one of the annihilation quanta is detected by the photo process following

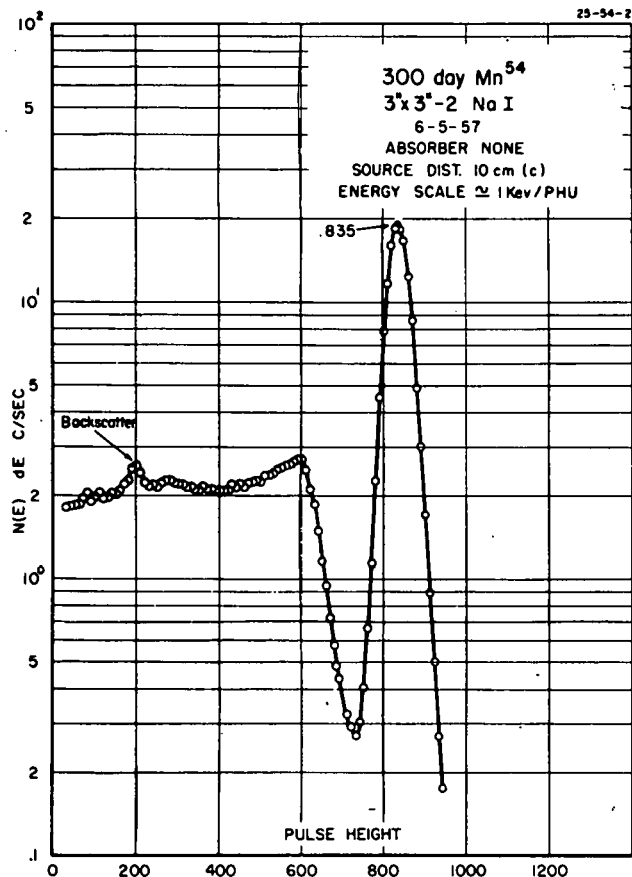


Fig. 10. Gamma-ray Spectrum of 300 day  $Mn^{54}$ .

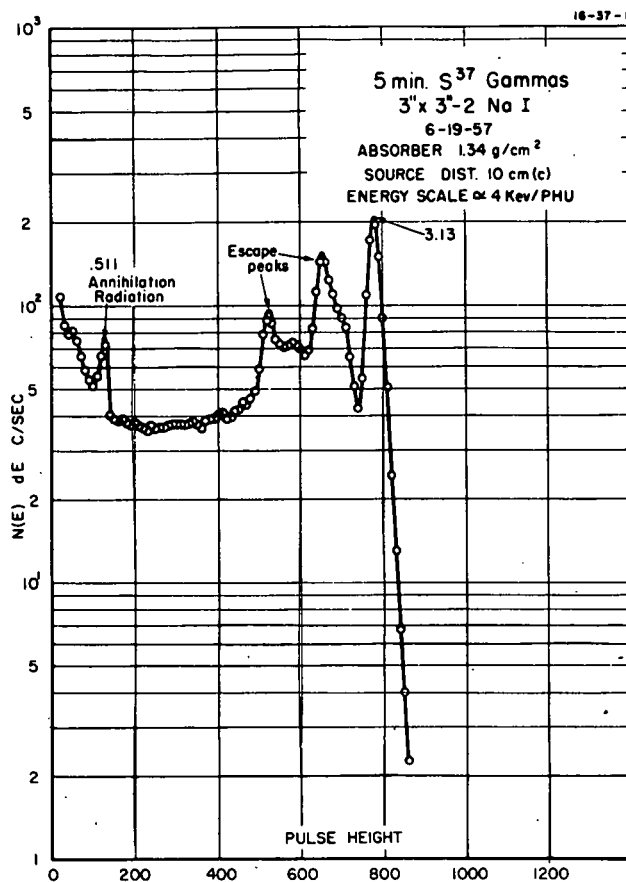


Fig. 11. Gamma-ray Spectrum of 5 min.  $S^{37}$ .

pair production in the detector, or by any combination of multiple processes which result in total energy loss, then a peak will appear at 0.511 Mev less than that of the incident photon. This peak is termed the "single escape peak". If both annihilation quanta are detected with total energy loss, the addition of the energy left in the detector by all processes for one pair event will produce pulses in the "full-energy peak". The total result of interaction by the pair process will then be a distribution of pulses from  $(E\gamma - 1.02 \text{ Mev})$  to the energy of the incident photon, including the three prominent peaks just described. The true shape of this pulse distribution due to the pair process is always obscured by the Compton electron distribution, which is characterized in this energy region by a rather sharp peak corresponding to  $180^\circ$  scattering.

In the  $S^{37}$  spectrum a low intensity peak is seen at 0.511 Mev. This is due to interaction of the high energy photons by the pair process in the detector shield and other material in the vicinity of the detector. The escape and subsequent detection of annihilation radiation from these e-

vents represents an additional background effect in the high energy region. This peak does not represent the detection of primary photons incident upon the detector from the source (neglecting internal pair formation).

## 2. Calculation of Absolute Photon Emission Rates

### (a) Absolute Efficiency of the Detector

The scintillation phosphor detector may be considered as a primary detector. By this it is meant that the detection efficiency of a solid phosphor detector may be calculated with a high degree of precision. If one knows the absorption cross section of NaI,  $\tau$ , for gamma-rays of a given energy and the source-detector geometry, then it is possible to derive an exact expression for the absolute detection efficiency of the detector. Calculations have been made at this laboratory by Vegors, Marsden and Heath<sup>3</sup> for the case of a point source and a disk source located on the central axis of a cylindrical detector. The detection efficiency for the point source configuration is given by the following relationship:

<sup>3</sup>S. H. Vegors, Jr., L. L. Marsden and R. L. Heath, AEC Report IDO-16370 (unpublished).

$$T(E) = \frac{1}{2} \left\{ \int_0^{\tan^{-1} \frac{r_0}{h_0 + t_0}} \left( 1 - e^{-\tau(E) \frac{t_0}{\cos \theta}} \right) \sin \theta d\theta + \int_{\tan^{-1} \frac{r_0}{h_0 + t_0}}^{\tan^{-1} \frac{r_0}{h_0}} \left[ 1 - e^{-\tau(E) \left( \frac{r_0}{\sin \theta} - \frac{h_0}{\cos \theta} \right)} \right] \sin \theta d\theta \right\}$$

### DETECTION EFFICIENCY - POINT SOURCE

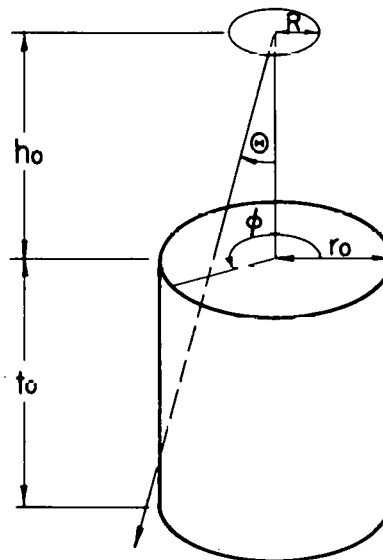
for a source a distance  $h_0$  on the extended axis of a right circular cylinder of NaI of radius  $r_0$  and height  $t_0$ . These calculations included 32 different detector sizes for values of  $h$  from 0 to 100 cm. and photon energies from 10 Kev to 10 Mev. Values of  $\tau$  used were those of Gladys White Grodstein<sup>4</sup> of the National Bureau of Standards with the coherent scattering cross section removed. Curves of detection efficiency for a point source (3" x 3" detectors) are given in Appendix I.

<sup>4</sup>Gladys White Grodstein, National Bureau of Standards circular NBS-583.

The detection efficiency for an extended disk source whose center is on the central axis of the detector and whose plane is parallel to the top of the detector is given by the following relationship for a source of radius  $R$ . In this case machine computing time was prohibitive so only values for the 3" diameter x 3", 1-3/4" x 2", and 1-1/2" x 1" detectors were computed. These sizes were selected as those most frequently used in most laboratories. The quantity  $T(E)$ , the absolute detection efficiency, obtained from these relationships is the total probability that a photon emitted from

$$T(E) = \frac{1}{\pi R^2} \int_0^R x dx \int_{-\pi/2}^{\pi/2} d\phi \left\{ \int_0^{\tan^{-1} \left( \frac{-x \sin \phi + \sqrt{x^2 \sin^2 \phi - (x^2 - r_0^2)}}{h_0 + t_0} \right)} \left[ 1 - e^{-\tau(E) \frac{t_0}{\cos \theta}} \right] \sin \theta d\theta \right.$$

$$\left. + \int_{\tan^{-1} \left( \frac{-x \sin \phi + \sqrt{x^2 \sin^2 \phi - (x^2 - r_0^2)}}{h_0} \right)}^{\tan^{-1} \left( \frac{-x \sin \phi + \sqrt{x^2 \sin^2 \phi - (x^2 - r_0^2)}}{h_0 + t_0} \right)} \left[ 1 - e^{-\tau(E) \left( \frac{-x \sin \phi + \sqrt{x^2 \sin^2 \phi - (x^2 - r_0^2)}}{\sin \theta} - \frac{h_0}{\cos \theta} \right)} \right] \sin \theta d\theta \right\}$$



### DETECTION EFFICIENCY - DISK SOURCE

the source will interact in the detector with the loss of a finite amount of energy. In a solid material such as NaI, which has a density of 2.67, the sensitive volume is very clearly defined. Since the amount of material which a secondary electron produced in the solid phosphor must traverse to leave a measurable amount of energy is negligible, edge effects are insignificant. Any error to be expected will be due to uncertainty in the value of  $\tau$  used in the calculation. Fig. 12 is a plot of the percent error in detection efficiency versus percent error in absorption cross section for the detection

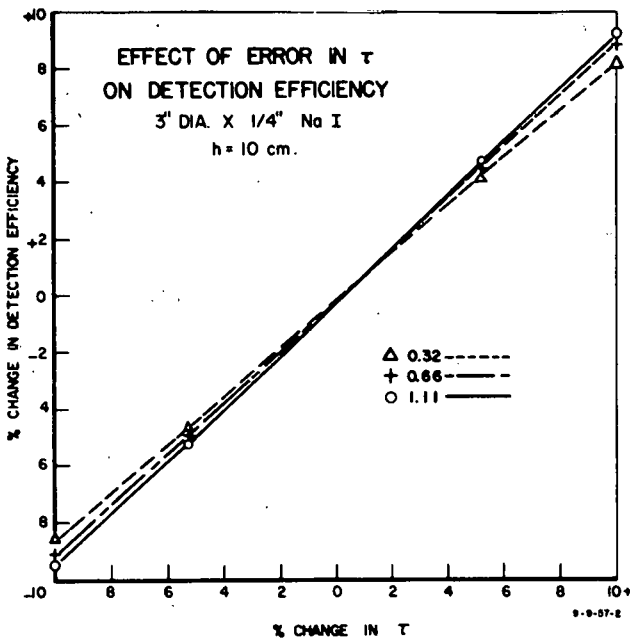


Fig. 12. Error in Detection Efficiency vs. Error in  $\tau$  (1/4" x 3" detector).

of 0.32, 0.66 and 1.11 Mev gamma rays in a 1/4" thick x 3" diameter NaI phosphor. As one might expect, for small values of  $t$ , the absorber thickness, the error will vary linearly with  $\tau$ . As the absorber thickness increases a photon traverses several relaxation lengths in passing through the detector. Fig. 13 shows a similar plot for the 3" x 3" detector. For the large phosphor the error in detection efficiency due to uncertainty in  $\tau$  has been reduced appreciably. Even at 1.11 Mev a 10% error in  $\tau$ , which is considerably more than currently expected for calculated values, will result in an error of only 5% in detection efficiency. For lower energies the error will be considerably reduced since the detector is almost black to gamma

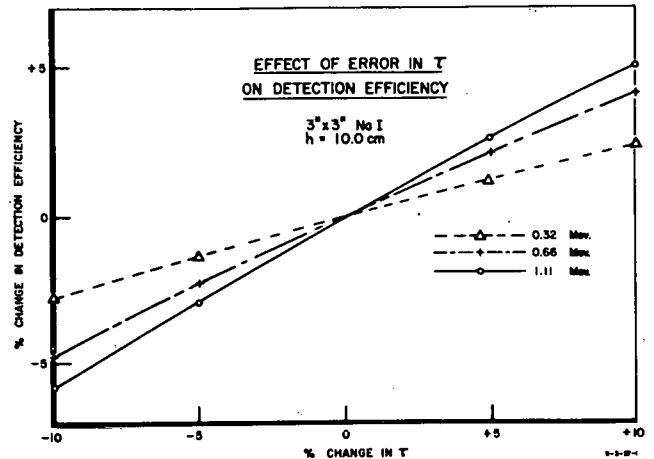


Fig. 13. Error in Detection Efficiency vs. Error in  $\tau$  (3" x 3" detector).

radiation of less than 0.5 Mev.

(b) Calculation of Emission Rates (single  $\gamma$ -ray)

Knowing the probability for the detection of a photon by a particular detector and source-detector geometry, it is then possible to reduce the data obtained on the scintillation spectrometer to obtain the absolute emission rate from the source. The pulse-height distribution obtained from the detector for a monoenergetic gamma-ray will be unique. If all pulses due to the detection of radiation scattered off the radiation shield, beta absorber or other material in the vicinity of the detector are accounted for and subtracted from the total spectrum, then integration under the resultant pulse-height distribution will yield the total number of photons detected by the phosphor in a given time. If a multi-channel differential pulse-height analyzer is used, this integration can be accomplished by the simple addition of the channel counting rates, since all pulses are accounted for in one channel or another. The use of a sliding-window single channel pulse analyzer requires more complicated treatment of the data. This case has been discussed in an earlier report issued from this laboratory.<sup>5</sup>

The "true" response of the 3" x 3" detector to monoenergetic photons has been obtained by the measurement of a series of "line" sources. To reduce spurious effects due to scattering, electron-capture sources or low energy beta emitters were used in most cases and measurements were made

<sup>5</sup> R. L. Heath and F. Schroeder, AEC Report IDO-16149.

either with the source and detector mounted in an open room or in the large shield previously described. Fig. 14 illustrates the effect of even a moderate amount of beta-absorbing material upon the "shape" of the detector response. The pulse-height spectrum obtained from Be<sup>7</sup> is shown with and without a 1.34 g/cm<sup>2</sup> polystyrene beta absorber, an amount sufficient to stop a 1.5 Mev beta particle. Note that the attenuation of the photopeak is small, but that there is considerable distortion in the Compton region due to small-angle Compton scattering in the beta absorber. This distortion must be considered in absorption corrections and in the analysis of complex spectra.

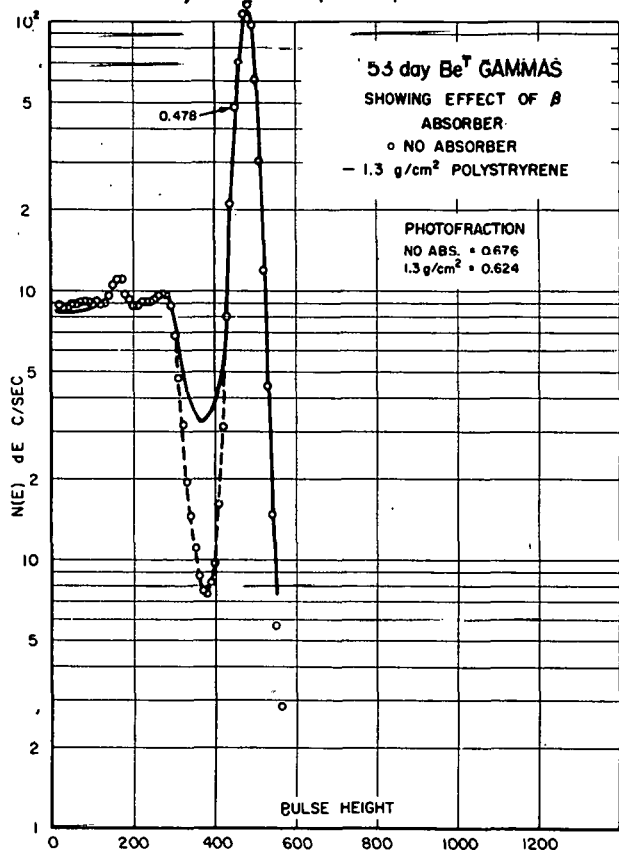


Fig. 14. Effect of beta absorber on detector response.

Since it is normally difficult to obtain measurements under ideal conditions, use is made of a very convenient quantity: the photo-efficiency or peak-to-total ratio. This quantity,  $P$ , is the fraction of the total number of events which fall in the photo-electric peak as shown in Fig. 15. For this purpose the peak area is defined as that of a symmetrical "gaussian" shape, fit to the high energy side of the experimental photo-peak. Use of experimentally determined values for the peak-to-total

ratio, obtained under conditions of negligible scattering, permits analysis of data obtained under less than ideal conditions. Determination of the peak-to-total ratio as a function of gamma-ray energy and source distance has been made for the 3" x 3" detector at this laboratory and by P. R. Bell, et al., at the Oak Ridge National Laboratory.<sup>6</sup> A tabulation of values obtained at the MTR will be found in Appendix II.

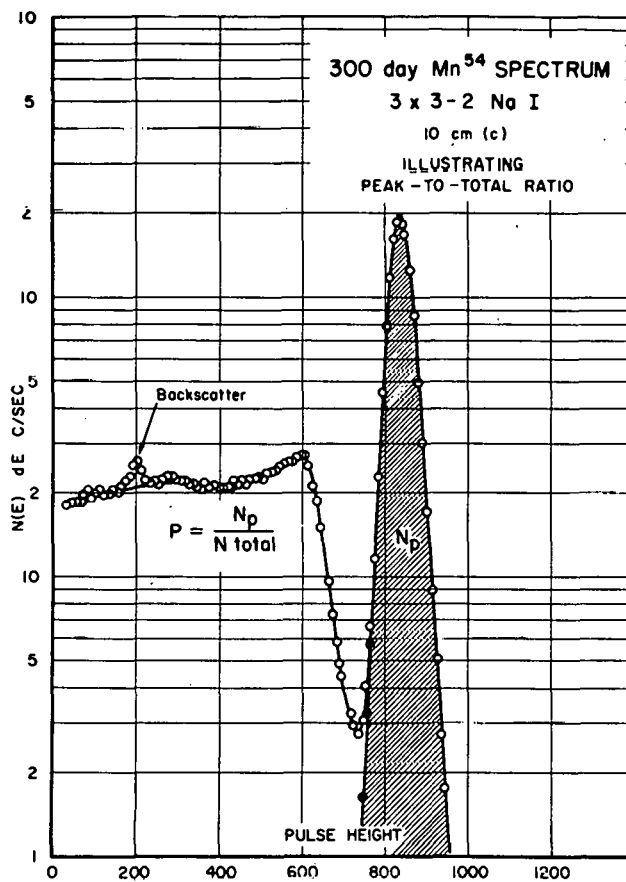


Fig. 15. Illustration of Peak-To-Total Ratio.

Using this convention, the emission rate of a single gamma-ray will then be given by the following relationship:

$$N_0 = \frac{N_p}{\epsilon_t P A} \quad (1)$$

where  $N_0$  is the number of gamma-rays emitted/sec by the source,  $N_p$  is the area under the photo-peak in c/sec,  $\epsilon_t$  is the total absolute detection efficiency for the source-detector geometry used,  $P$  is the

<sup>6</sup>P. R. Bell, R. C. Davis, N. H. Lazar, ORNL Report 1975 (unpublished) p.72.

appropriate value for the peak-to-total ratio, and  $A$  is the correction factor for absorption in source and any beta absorber used in the measurement.

### C. Calculation of Emission Rate (complex spectrum)

In the decay of most radioactive nuclides the gamma-ray spectrum observed is considerably more complex than that for one single gamma-ray. In every case to a first approximation the observed detector response represents the summation of the response to the individual gamma rays. To illustrate the methods of data reduction with no further complication due to the complex nature of the decay scheme, the response to a source emitting several

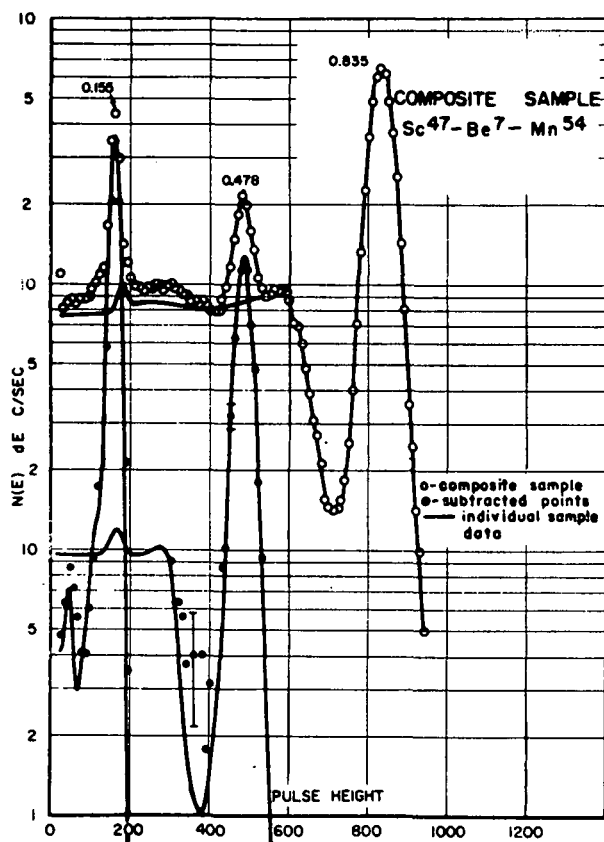


Fig. 16. Spectrum of Composite Sample.

gamma rays is shown in Fig. 16. A composite sample was made up of three activities each emitting one single gamma-ray— $\text{Sc}^{47}$ ,  $\text{Be}^7$  and  $\text{Mn}^{54}$ . The two low energy sources were intentionally less than 10% of the  $\text{Mn}^{54}$  activity to provide a moderately troublesome case. The sources were prepared so that each could be measured separately and as

one source. The composite response is shown by the open circles, the individual source measurements by the solid lines and the closed circles represent the actual subtracted points obtained by successive subtraction of standard "spectral" shapes taken from the catalogue, for measurements of the three nuclides under these conditions.

The general procedure which is used is straightforward. Inspection of the observed gross spectrum indicates that the highest energy gamma-ray observed was at 0.835 Mev. The spectrum "shape" representing the response of the detector to a gamma-ray of this energy is fitted (channel-by-channel) to the photo-peak and subtracted from the gross spectrum. The residuals are observed, and if found to be statistical, the process is repeated for the next gamma-ray. In this manner, by successive subtraction of the response of the detector to each gamma-ray, the gross spectrum is divided into its components. Should the gross spectrum be made up of several nuclides, each characterized by a more complex spectrum, then the same procedure would be followed using the detector response to each nuclide. In the simple case given, the absolute emission rate for each gamma-ray would be determined by application of formula (1) to the respective components. As an indication of the precision which one might expect in such a quantitative analysis, Table 1 summarizes the results obtained from the composite sample and the three components measured individually. Even in this moderately difficult case the maximum deviation is 3.2%. In general, the error to be expected will be determined by the energies and relative intensities of the gamma rays being measured.

In the example above the analysis was somewhat simplified by a knowledge of the exact detect-

TABLE I

### QUANTITATIVE ANALYSIS OF COMPOSITE SOURCE

	Gammas Emitted/ Sec		Percent of Total Gammas Emitted		Percent Error
	SINGLE SPECTRA	COMPOSITE SPECTRUM	SINGLE SPECTRA	COMPOSITE SPECTRUM	
$\text{Mn}^{54}$	54.731		87.4%	87.3%	0.1
$\text{Be}^7$	4.256	4.393	6.8%	7.0%	3.2
$\text{Sc}^{47}$	3.633	3.567	5.8%	5.7%	1.8

or response to each of the components of the gross spectrum. Since the detector response to monoenergetic radiation cannot be described by an analytic function, empirical methods must be employed. The general shape of the pulse-height distribution is known from the measurement of monoenergetic sources over a wide energy range. Other known parameters include the resolution of the detector (photo-peak width) as a function of gamma-ray energy and the Compton electron distribution end-point energy. It is then possible to fit a given photo-peak with a "gaussian" of the proper width corresponding to the measured energy. A Compton electron distribution characteristic of the geometry used is then obtained from the pulse spectrum of a monoenergetic source with energy as near as possible to the measured energy of the gamma-ray in question. The intensity and Compton end-point energy are adjusted in relation to the assumed "photo-peak" in such a manner that their relative areas correspond to the experimentally determined peak-to-total ratio for a gamma-ray of that energy measured in similar geometry. This "synthesized" response curve is then subtracted from the gross spectrum and the process repeated for the next gamma-ray as indicated above. For examples of this type of analysis see  $^{135}$  (Plate 53-135-1) and  $^{93}$  (Plate 39-93-1). A compilation of convenient sources which are used for energy calibration of the spectrometer and to obtain "response functions" for single gamma rays is given in Table II.

TABLE II

CALIBRATION SOURCES FOR  
DETECTOR RESPONSE AND ENERGY CALIBRATION

NUCLIDE	T 1/2	$E_\gamma$ (Mev)
$^{60m}\text{Co}$	10 min.	0.059
$^{141}\text{Ce}$	32 day	0.142
$^{47}\text{Sc}$	3.4 day	0.155
$^{51}\text{Cr}$	27 day	0.322
$^7\text{De}$	53 day	0.478
$^{85}\text{Sr}$	65 day	0.510
$^{207}\text{Bi}$	0 year	0.569
		1.063
$^{137}\text{Cs}$	30 year	0.662
$^{54}\text{Mn}$	300 day	0.835
$^{88}\text{Y}$	105 day	0.900
		1.830
$^{65}\text{Zn}$	250 day	1.114
$^{24}\text{Na}$	14.9 hr.	1.368
		2.753
$^{37}\text{S}$	5 min.	3.13

Up to this point in the discussion no consideration has been given to several factors which somewhat complicate the quantitative analysis of complex gamma-ray spectra emitted in the decay of radioactive nuclides. Perhaps the most important is "coincidence summing" of gamma rays emitted in cascade. (See Section II-C.) Although the effect of summing is somewhat difficult to analyze in every detail the total area associated with the sum spectrum and the "sum peak" may be calculated from the known efficiencies and solid angle. Considering a simple scheme characterized by the emission of two cascade gamma-rays (e.g.  $\text{Co}^{60}$ ), and adopting a nomenclature similar to Lazar and Klema,<sup>7</sup> the emission rate of  $\gamma_1$  will be given by equation (2).

$$N_1 = \frac{N_p(\gamma_1)}{\epsilon_1 P_1 [1 - \epsilon_2 \bar{W}(0^0) q_{2,1}]} \quad (2)$$

where  $N_p$  is the area under the photopeak of  $\gamma_1$  (with any contribution due to  $\gamma_2$  or the sum spectrum subtracted),  $\epsilon_1$  and  $\epsilon_2$  are the total absolute efficiencies for  $\gamma_1$  and  $\gamma_2$ ,  $P_1$  is the peak-to-total ratio for  $\gamma_1$  (experimental),  $q_{2,1}$  is the fraction of  $\gamma_2$  in coincidence with  $\gamma_1$ , and  $\bar{W}(0^0)$  is a factor to take into account the angular distribution function of the two gamma rays integrated over the face of the crystal, evaluated by the methods described by Rose.<sup>8</sup> The third term in the denominator accounts for those pulses which would normally appear in the photo-peak but, due to simultaneous detection of the other cascade gamma-ray, appear in the coincidence sum spectrum. Another convenient expression is that for the area under the coincidence sum peak, or the probability that two coincident gamma rays will be detected simultaneously, with total energy loss in the detector. This quantity is given by equation (3).

$$N_{c.s.} = \frac{N_p(\gamma_1) \epsilon_2 P_2 q_{2,1} \bar{W}(0^0)}{[1 - \epsilon_2 \bar{W}(0^0) q_{2,1}]} \quad (3)$$

An additional complicating factor in the measurement of gamma-ray spectra is the production of bremsstrahlung in the absorption of beta radiation accompanying the decay. This results in a continuous energy distribution of photons extending from zero energy to the beta end-point. The mag-

<sup>7</sup>N. H. Lazar and E. D. Klema, *Phys. Rev.* 91, 610 (1953).

<sup>8</sup>M. E. Rose, *Phys. Rev.* 91, 610 (1953).

nitude of this effect depends upon beta energy, the Z of the material used to absorb the beta particles, and the geometrical configuration. In general the intensity of the bremsstrahlung spectrum is negligible, excepting those cases where a major fraction of the decay is accompanied by the emission of a high energy beta group to the ground state of the daughter nucleus, with only very weak gamma transitions. As an example of this effect, Fig. 17 shows the gamma-ray spectrum obtained from 58 day  $Y^{91}$ .

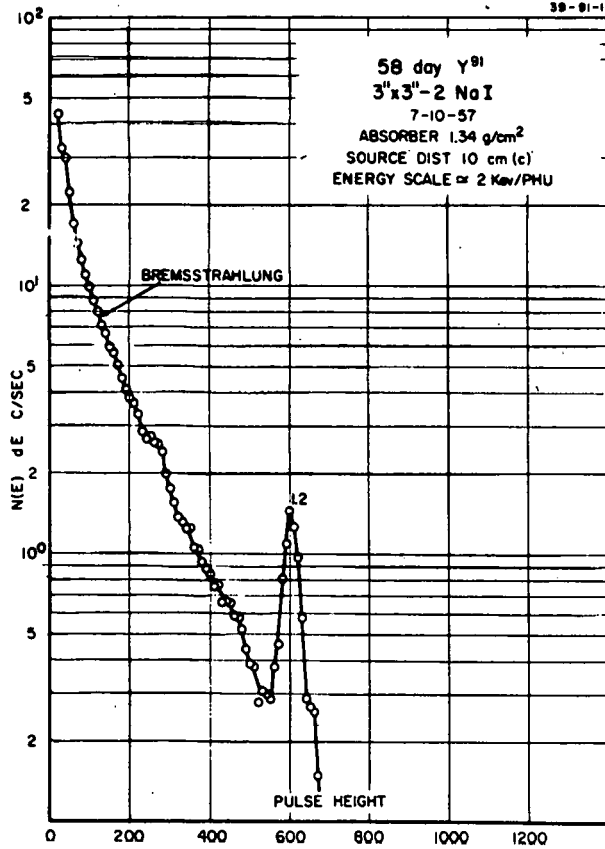


Fig. 17. Spectrum of 58 day  $Y^{91}$ .

This nuclide decays with the emission of a 1.5 Mev beta group to the ground state of the daughter (99.8%) with a very weak 1.2 Mev gamma-ray (0.2%). An additional example of the presence of considerable bremsstrahlung may be seen in the spectrum of gamma radiation emitted in the decay of 11 hr.  $Y^{93}$ . (See Plate 39-93-1.)

One additional point which should be included in a discussion of quantitative methods is the conversion from absolute gamma-ray emission rates to disintegration rate. This demands a detailed knowledge of the complete "decay scheme" which describes the pattern of decay for a particular nuclide. For this purpose one must know the branching ratio for at least one of the major gamma rays emitted. This usually requires consideration of the process of internal conversion as a result of the interaction of gamma-ray photons with external bound electrons. In the event that the details of the decay scheme are not known for a particular nuclide, one may determine the branching ratio for a major gamma-ray by comparison of the gamma emission rate for a given source with a carefully determined total beta disintegration rate.

In conclusion, the discussion above is to be considered as a general outline of the problems of measurement using the techniques of gamma-ray scintillation spectrometry. In practice each problem must be carefully analyzed to determine the applicability of these techniques. It is hoped that the material contained in this catalogue will serve to illustrate both the utility and limitations of the method.

### III - INDEX OF GAMMA-RAY SPECTRA

---

#### A. Notes on Index

##### 1. General Arrangement

For convenience, the spectra have been indexed by chemical element, listed in alphabetical order. Under each element the individual nuclides are listed in ascending order of A. Values given for half-life are those listed in current literature. Each pulse spectrum has been assigned a "plate number" which is given in column (7). The plate numbers signify the proton number, Z, the mass number A and a serial number in that order (e.g. Cs<sup>138</sup> would be represented by the series 55-138-x). The plates are arranged in ascending order of Z and A.

##### 2. Detectors

Most of the spectra contained in the catalogue were obtained with four NaI(Tl) detectors mounted in the manner described in section II-A. Two of these detectors were 3" diameter x 3" cylinders of NaI and are identified in column (4) as 3" x 3" and 3" x 3"-2. The third detector was a 3" x 3" cylinder bevelled at 45° for 1/2" from the top surface. This detector is indicated as 3" x 3"-bev. The fourth detector was a 1 3/4" diameter x 2" cylinder, used in a few cases to illustrate the response of this size detector to

monoenergetic radiation. The resolution of these detectors for the 0.662 Mev gamma-ray of Cs<sup>137</sup> is shown below:

Detector	Resolution
3" x 3"	8.8%
3" x 3"-2	7.9%
3" x 3"-bev	7.9%
1 3/4" x 2"	8.5%

##### 3. Experimental Details

To facilitate the reproduction of the experimental conditions for each spectrum, the source distance, *h*, is given in column (5), together with the detector shield configuration.

Measurement with no shield is denoted by the suffix (A), the shield with inside dimensions of 12" x 12" x 24" by (B), and the large 32" x 32" x 32" shield by (C). (See section II.) Column (6) lists the gain scale relating gamma-ray energy in Kev to the arbitrary pulse-height unit scale. The accuracy of this conversion factor is better than 5% over the entire energy range. The quantity of polystyrene or other absorbing material used to absorb beta-rays or low energy photons is given on each plate.

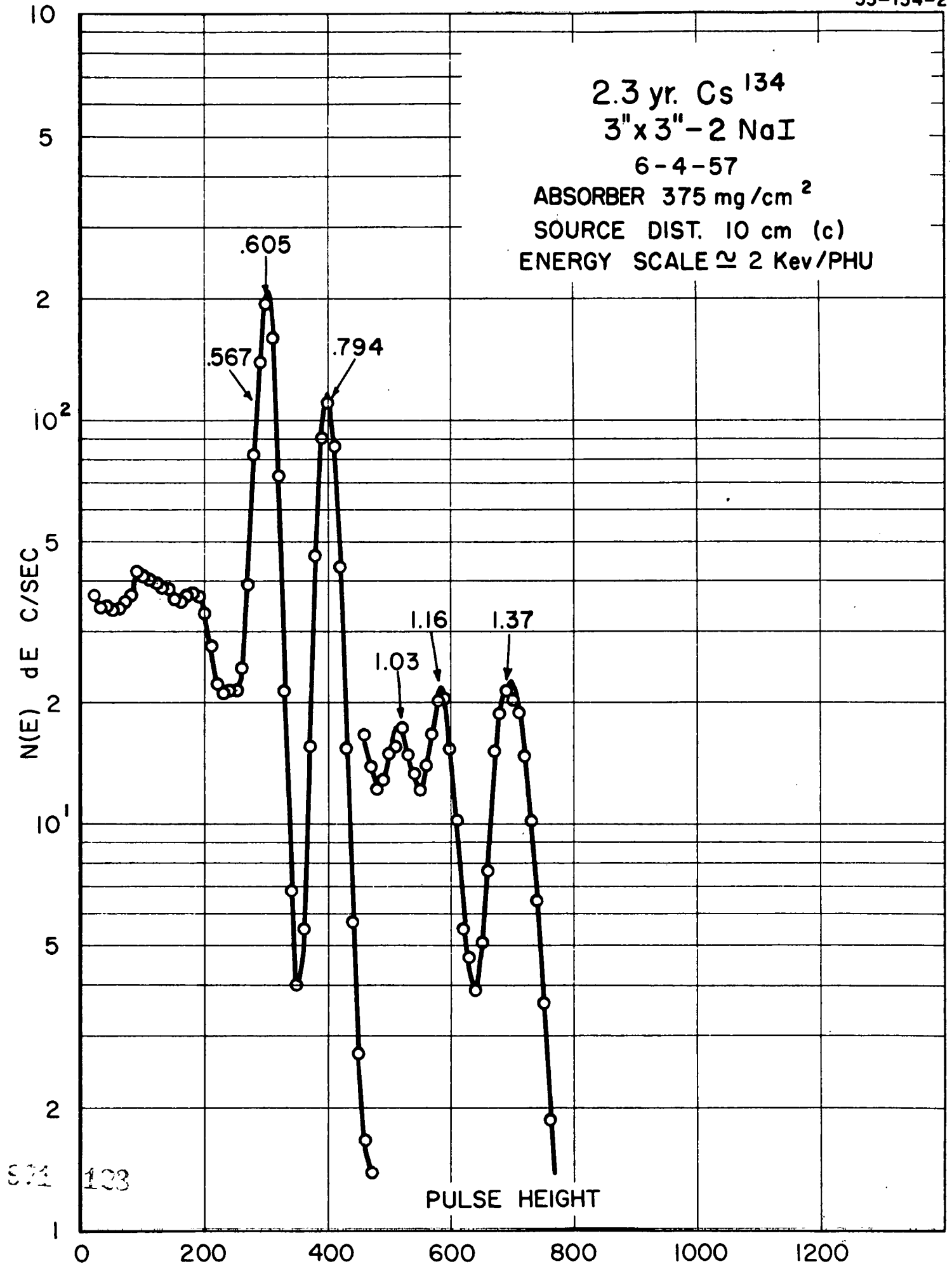
ELEMENT	ISOTOPE	HALF-LIFE	DETECTOR	GEOMETRY	ENERGY SCALE	PLATE NUMBER	
Aluminum	28	2.3 Min.	3" x 3" - 2	10 Cm (C)	~ 2 Kev/PHU	13-28-1	
	(With 21.3 Hr Mg <sup>28</sup> )	28	2.3 Min.	3" x 3" - 2	7 Cm (C)	~ 2 Kev/PHU	12-28(13-28)1
Antimony	122	2.8 Day	3" x 3"	10 Cm (B)	~ 2 Kev/PHU	51-122-1	
	124	60 Day	3" x 3"	10 Cm (B)	~ 2 Kev/PHU	51-124-1	
	125	2.7 Yr.	3" x 3"	10 Cm (B)	~ 1 Kev/PHU	51-125-1	
Argon	41	1.82 Hr.	3" x 3" - 2	10 Cm (C)	~ 2 Kev/PHU	18-41-1	
Arsenic	76	26.7 Hr.	3" x 3"	10 Cm (B)	~ 2 Kev/PHU	33-76-1	
Barium	139	85 Min.	3" x 3" - 2	10 Cm (C)	~ 1 Kev/PHU	56-139-1	
	139	85 Min.	3" x 3" - 2	10 Cm (C)	~ 2 Kev/PHU	56-139-2	
	(With 40.2 Hr La <sup>140</sup> )	140	12.8 Day	3" x 3"	10 Cm (B)	~ 2 Kev/PHU	56-140(57-140)1
	140	12.8 Day	3" x 3"	10 Cm (B)	~ 2 Kev/PHU	56-140-2	
	140	12.8 Day	3" x 3"	10 Cm (B)	~ 1 Kev/PHU	56-140-3	
Beryllium	7	54 Day	3" x 3" - 2	10 Cm (C)	~ 1 Kev/PHU	4-7-1	
	7	54 Day	3" x 3" - 2	10 Cm (C)	~ 2 Kev/PHU	4-7-2	
	7	54 Day	3" x 3" bev.	10 Cm (B)	~ 1 Kev/PHU	4-7-3	
Bismuth	205	15 Day	3" x 3" - 2	10 Cm (C)	~ 2 Kev/PHU	83-205-1	
	207	8.0 Yr.	3" x 3" - 2	10 Cm (C)	~ 2 Kev/PHU	83-207-1	
Bromine	82	36 Hr.	3" x 3" - 2	10 Cm (C)	~ 2 Kev/PHU	35-82-1	
Cadmium	115m	43 Day	3" x 3" - 2	10 Cm (C)	~ 2 Kev/PHU	48-115-1	
	115	54 Hr.	3" x 3" - 2	10 Cm (C)	~ 1 Kev/PHU	48-115-2	
	(With 4.5 Hr. In <sup>115</sup> )	115	54 Hr.	3" x 3" - 2	10 Cm (C)	~ 2 Kev/PHU	48-115(49-115)1
	(With 4.5 Hr. In <sup>115</sup> )	115	54 Hr.	3" x 3" - 2	10 Cm (C)	~ 1 Kev/PHU	48-115(49-115)2
Calcium	47	4.7 Day	3" x 3" - 2	10 Cm (C)	~ 2 Kev/PHU	20-47-1	
Cerium	141	32 Day	3" x 3" - 2	10 Cm (C)	~ 0.5 Kev/PHU	58-141-1	
	141	32 Day	3" x 3" - 2	10 Cm (C)	~ 1 Kev/PHU	58-141-2	
	141	32 Day	3" x 3" bev.	10 Cm (B)	~ 1 Kev/PHU	58-141-3	
	141	32 Day	3" x 3" bev.	10 Cm (B)	~ 0.5 Kev/PHU	58-141-4	
	141	32 Day	1 1/2" x 2"	10 Cm (A)	~ 0.5 Kev/PHU	58-141-5	
	143	33 Hr.	3" x 3"	10 Cm (B)	~ 1 Kev/PHU	58-143-1	
	143	33 Hr.	3" x 3"	12 Cm (B)	~ 0.5 Kev/PHU	58-143-2	
	(With 17 Min Pr <sup>144</sup> )	144	290 Day	3" x 3"	10 Cm (B)	~ 2 Kev/PHU	58-144-1
Cesium	134	2.3 Yr.	3" x 3" bev.	10 Cm (B)	~ 2 Kev/PHU	55-134-1	
	134	2.3 Yr.	3" x 3" - 2	10 Cm (C)	~ 2 Kev/PHU	55-134-2	
	137	30 Yr.	3" x 3"	10 Cm (B)	~ 1 Kev/PHU	55-137-1	
	137	30 Yr.	3" x 3" bev.	10 Cm (B)	~ 1 Kev/PHU	55-137-2	
	137	30 Yr.	3" x 3" - 2	10 Cm (C)	~ 1 Kev/PHU	55-137-3	
	137	30 Yr.	1 1/2" x 2"	3 Cm (A)	~ 1 Kev/PHU	55-137-4	
	137	30 Yr.	1 1/2" x 2"	10 Cm (A)	~ 1 Kev/PHU	55-137-5	
	138	33 Min.	3" x 3"	10 Cm (B)	~ 4 Kev/PHU	55-138-1	
138	33 Min.	3" x 3"	10 Cm (B)	~ 2 Kev/PHU	55-138-2		
Chlorine	38	37 Min.	3" x 3" - 2	10 Cm (C)	~ 4 Kev/PHU	17-38-1	
	38	37 Min.	3" x 3" - 2	10 Cm (C)	~ 2 Kev/PHU	17-38-2	
Chromium	51	27 Day	3" x 3" - 2	10 Cm (C)	~ 0.5 Kev/PHU	24-51-1	
	51	27 Day	3" x 3" - 2	10 Cm (C)	~ 1 Kev/PHU	24-51-2	
	51	27 Day	3" x 3" bev.	10 Cm (B)	~ 1 Kev/PHU	24-51-3	
	51	27 Day	3" x 3" bev.	10 Cm (B)	~ 0.5 Kev/PHU	24-51-4	
	51	27 Day	1 1/2" x 2"	10 Cm (A)	~ 0.5 Kev/PHU	24-51-5	

ELEMENT	ISOTOPE	HALF-LIFE	DETECTOR	GEOMETRY	ENERGY SCALE	PLATE NUMBER	
Cobalt	58	71 Day	3" x 3"	10 Cm (B)	~ 2 Kev/PHU	27-58-1	
	58	71 Day	3" x 3" bev	10 Cm (B)	~ 2 Kev/PHU	27-58-2	
	60	5.3 Yr.	3" x 3" -2	0.3 Cm (C)	~ 4 Kev/PHU	27-60-1	
	60	5.3 Yr.	3" x 3" -2	10 Cm (C)	~ 2 Kev/PHU	27-60-2	
	60	5.3 Yr.	3" x 3" -2	10 Cm (C)	~ 4 Kev/PHU	27-60-3	
	60	5.3 Yr.	3" x 3" bev	10 Cm (B)	~ 2 Kev/PHU	27-60-4	
Copper	60m	10 Min.	3" x 3" - 2	10 Cm (C)	~0.25 Kev/PHU	27-60m-1	
	64	12.8 Hr.	3" x 3"	10 Cm (B)	~ 2 Kev/PHU	29-64-1	
Gallium	66	5 Min.	3" x 3"	12 Cm (B)	~ 2 Kev/PHU	29-66-1	
	72	14.1 Hr.	3" x 3"	10 Cm (B)	~ 2 Kev/PHU	31-72-1	
Gold	72	14.1 Hr.	3" x 3"	10 Cm (B)	~ 4 Kev/PHU	31-72-2	
	198	2.7 Day	3" x 3" - 2	10 Cm (C)	~ 1 Kev/PHU	79-198-1	
Hafnium	181	46 Day	3" x 3" - 2	10 Cm (C)	~ 1 Kev/PHU	72-181-1	
Indium (With 43 day Cd <sup>115</sup> )	115	4.5 Hr.	3" x 3" - 2	10 Cm (C)	~ 2 Kev/PHU	48-115(49-115)1	
	115	4.5 Hr.	3" x 3" - 2	10 Cm (C)	~ 1 Kev/PHU	48-115(49-115)2	
	116	54 Min.	3" x 3" - 2	10 Cm (C)	~ 2 Kev/PHU	49-116-1	
	116	54 Min.	3" x 3" - 2	10 Cm (C)	~ 4 Kev/PHU	49-116-2	
Iodine	128	25 Min.	3" x 3" - 2	10 Cm (C)	~ 2 Kev/PHU	53-128-1	
	131	8.0 Day	3" x 3" - 2	10 Cm (C)	~ 1 Kev/PHU	53-131-1	
	132	2.3 Hr.	3" x 3" - 2	10 Cm (C)	~ 2 Kev/PHU	53-132-1	
	(With 77 hr Tc <sup>132</sup> )	132	2.3 Hr.	3" x 3" bev	10 Cm (B)	~ 2 Kev/PHU	52-132(53-132)3
	135	6.7 Hr.	3" x 3"	9 Cm (B)	~ 2 Kev/PHU	53-135-1	
Iridium	192	74 Day	3" x 3"	10 Cm (B)	~ 1 Kev/PHU	77-192-1	
Iron	59	45 Day	3" x 3" - 2	10 Cm (C)	~ 2 Kev/PHU	26-59-1	
Krypton	85m	4.4 Hr.	3" x 3" - 2	10 Cm (C)	~ 1 Kev/PHU	36-85m-1	
	85	10.4 Yr.	3" x 3" - 2	10 Cm (C)	~ 1 Kev/PHU	36-85-1	
Lanthanum	140	40.2 Hr.	3" x 3" - 2	10 Cm (C)	~ 2 Kev/PHU	57-140-1	
	140	40.2 Hr.	3" x 3" - 2	10 Cm (C)	~ 4 Kev/PHU	57-140-2	
	(With 12.8 day Ra <sup>140</sup> )	140	40.2 Hr.	3" x 3"	10 Cm (B)	~ 2 Kev/PHU	56-140(57-140)1
	142	77 Min.	3" x 3" - 2	10 Cm (C)	~ 4 Kev/PHU	57-142-1	
Lutetium	176	3.6 Hr.	3" x 3"	10 Cm (B)	~ 0.5 Kev/PHU	71-176-1	
	177	6.8 Day	3" x 3"	10 Cm (B)	~ 0.5 Kev/PHU	71-177-1	
Magnesium	27	9.6 Min.	3" x 3" - 2	10 Cm (C)	~ 2 Kev/PHU	12-27-1	
	27	9.6 Min.	3" x 3" bev	10 Cm (B)	~ 2 Kev/PHU	12-27-2	
	(With 2.3 min Al <sup>28</sup> )	28	21.3 Hr.	3" x 3" - 2	7 Cm (C)	~ 2 Kev/PHU	12-28(13-28)1
Manganese	54	300 Day	3" x 3" -2	10 Cm (C)	~ 2 Kev/PHU	25-54-1	
	54	300 Day	3" x 3" - 2	10 Cm (C)	~ 1 Kev/PHU	25-54-2	
	54	300 Day	3" x 3" bev	10 Cm (B)	~ 2 Kev/PHU	25-54-3	
	54	300 Day	3" x 3" bev	10 Cm (B)	~ 1 Kev/PHU	25-54-4	
	54	300 Day	1 1/2" x 2"	3 Cm (A)	~ 1 Kev/PHU	25-54-5	
	56	2.6 Hr.	3" x 3" - 2	10 Cm (C)	~ 2 Kev/PHU	25-56-1	
	56	2.6 Hr.	3" x 3" - 2	10 Cm (C)	~ 4 Kev/PHU	25-56-2	
	Mercury	197	65 Hr.	3" x 3"	10 Cm (B)	~ 0.5 Kev/PHU	80-197-1
		197	65 Hr. M1				
		23 Hr. M2	3" x 3"	10 Cm (B)	~ 0.5 Kev/PHU	80-197-2	
Molybdenum	203	48 Day	3" x 3"	10 Cm (B)	~ 0.5 Kev/PHU	80-203-1	
	99	68 Hr.	3" x 3" - 2	10 Cm (C)	~ 2 Kev/PHU	42-99(43-99)1	
(With 6 hr Tc <sup>99m</sup> )	99	68 Hr.	3" x 3" - 2	10 Cm (C)	~ 1 Kev/PHU	42-99(43-99)2	

ELEMENT	ISOTOPE	HALF-LIFE	DETECTOR	GEOMETRY	ENERGY SCALE	PLATE NUMBER
Neptunium	239	2.33 Day	3" x 3" - 2	10 Cm (C)	~ 1 Kev/PHU	93-239-1
Nickel	65	2.56 Hr.	3" x 3" - 2	10 Cm (C)	~ 2 Kev/PHU	28-65-1
Niobium	94	20,000 Yr.	3" x 3" - 2	10 Cm (C)	~ 2 Kev/PHU	41-94-1
	95	35 Day	3" x 3" - 2	10 Cm (C)	~ 2 Kev/PHU	41-95-1
	95	35 Day	3" x 3" - 2	10 Cm (C)	~ 1 Kev/PHU	41-95-2
(With 65 day Zr <sup>95</sup> )	95	35 Day	3" x 3" - 2	10 Cm (C)	~ 1 Kev/PHU	40-95(41-95)1
Palladium	109	13.6 Hr.	3" x 3" - 2	10 Cm (C)	~ 0.5 Kev/PHU	46-109-1
Potassium	42	12.8 Hr.	3" x 3" - 2	10 Cm (C)	~ 2 Kev/PHU	19-42-1
Praseodymium	142	19.1 Hr.	3" x 3"	10 Cm (B)	~ 2 Kev/PHU	59-142-1
(With 290 day Ce <sup>144</sup> )	144	17 Min.	3" x 3"	10 Cm (B)	~ 2 Kev/PHU	58-144-1
Protactinium	233	27.4 Day	3" x 3"	2 Cm (B)	~ 1 Kev/PHU	91-233-1
Radium	226	1,620 Yr.	3" x 3"	10 Cm (B)	~ 4 Kev/PHU	88-226-1
	226	1,620 Yr.	3" x 3"	10 Cm (B)	~ 2 Kev/PHU	88-226-2
Rhodium (With 1 yr Ru <sup>106</sup> )	106	40 Sec.	3" x 3" - 2	10 Cm (C)	~ 2 Kev/PHU	44-106(45-106)1
	106	40 Sec.	3" x 3"	16 Cm (B)	~ 4 Kev/PHU	44-106-2
Rubidium	88	18 Min.	3" x 3"	3 Cm (B)	~ 4 Kev/PHU	37-88-1
	89	15 Min.	3" x 3"	10 Cm (B)	~ 4 Kev/PHU	37-89-1
Ruthenium	97	2.3 Day	3" x 3" - 2	10 Cm (C)	~ 1 Kev/PHU	44-97-1
	103	40 Day	3" x 3" - 2	10 Cm (C)	~ 1 Kev/PHU	44-103-1
	105	4.5 Hr.	3" x 3" - 2	10 Cm (C)	~ 1 Kev/PHU	44-105-1
(With 40 sec Rh <sup>106</sup> )	106	1.0 Yr.	3" x 3" - 2	10 Cm (C)	~ 2 Kev/PHU	44-106(45-106)1
	106	1.0 Yr.	3" x 3"	16 Cm (B)	~ 4 Kev/PHU	44-106-2
Scandium	46	85 Day	3" x 3" - 2	10 Cm (C)	~ 2 Kev/PHU	21-46-1
	47	3.4 Day	3" x 3" - 2	10 Cm (C)	0.5 Kev/PHU	21-47-1
Silver	110	270 Day	3" x 3"	10 Cm (B)	~ 2 Kev/PHU	47-110-1
Sodium	22	2.6 Yr.	3" x 3" bev	10 Cm (B)	~ 2 Kev/PHU	11-22-1
	22	2.6 Yr.	3" x 3" - 2	10 Cm (C)	~ 2 Kev/PHU	11-22-2
	24	15 Hr.	3" x 3" - 2	10 Cm (C)	~ 4 Kev/PHU	11-24-1
	24	15 Hr.	3" x 3" bev	10 Cm (B)	~ 4 Kev/PHU	11-24-2
	24	15 Hr.	1X" x 2"	10 Cm (A)	~ 4 Kev/PHU	11-24-3
Strontium	91	9.7 Hr.	3" x 3"	3 Cm (B)	~ 2 Kev/PHU	38-91-1
	92	2.7 Hr.	3" x 3"	3 Cm (B)	~ 2 Kev/PHU	38-92-1
	93	7.0 Min.	3" x 3"	10 Cm (B)	~ 2 Kev/PHU	38-93-1
Sulphur	37	5 Min.	3" x 3" - 2	10 Cm (C)	~ 4 Kev/PHU	16-37-1
	37	5 Min.	3" x 3" bev	10 Cm (B)	~ 4 Kev/PHU	16-37-2
	37	5 Min.	1X" x 2"	10 Cm (A)	~ 4 Kev/PHU	16-37-3
Tantalum	182	111 Day	3" x 3" - 2	10 Cm (C)	~ 2 Kev/PHU	73-182-1
Technetium (With 68 hr Mo <sup>99</sup> )	99m	6.0 Hr.	3" x 3" - 2	10 Cm (C)	~ 2 Kev/PHU	42-99(43-99)1
	99m	6.0 Hr.	3" x 3" - 2	10 Cm (C)	~ 1 Kev/PHU	42-99(43-99)2
Tellurium	132	77 Hr.	3" x 3"	9 Cm (B)	~ 1 Kev/PHU	52-132-1
	132	77 Hr.	3" x 3"	9 Cm (B)	~ 0.5 Kev/PHU	52-132-2
(With 2.3 hr I <sup>132</sup> )	132	77 Hr.	3" x 3" bev	10 Cm (B)	~ 2 Kev/PHU	52-132(53-132)3
Terbium	160	72 Day	3" x 3" - 2	10 Cm (C)	~ 2 Kev/PHU	65-160-1
	160	72 Day	3" x 3" - 2	10 Cm (C)	~ 1 Kev/PHU	65-160-2
Tungsten	187	24 Hr.	3" x 3"	10 Cm (B)	~ 1 Kev/PHU	74-187-1
Uranium	(Ore)		3" x 3"	10 Cm (B)	~ 2 Kev/PHU	92-Ore-1
	237	6.7 Day	3" x 3" - 2	10 Cm (C)	~ 0.5 Kev/PHU	92-237-1

ELEMENT	ISOTOPE	HALF-LIFE	DETECTOR	GEOMETRY	ENERGY SCALE	PLATE NUMBER	
Vanadium	52	3.77 Min.	3" x 3" - 2	10 Cm (C)	~ 2 Kev/PHU	23-52-1	
Xenon	133	5.3 Day	3" x 3"	10 Cm (B)	~ 0.5 Kev/PHU	54-133-1	
	135	9.2 Hr.	3" x 3"	15 Cm (B)	~ 1 Kev/PHU	54-135-1	
Yttrium	88	105 Day	3" x 3" - 2	10 Cm (C)	~ 2 Kev/PHU	39-88-1	
	88	105 Day	3" x 3" bev	10 Cm (B)	~ 2 Kev/PHU	39-88-2	
	91	58 Day	3" x 3" - 2	10 Cm (C)	~ 2 Kev/PHU	39-91-1	
	93	10 Hr.	3" x 3"	10 Cm (B)	~ 2 Kev/PHU	39-93-1	
	93	10 Hr.	3" x 3"	10 Cm (B)	~ 2 Kev/PHU	39-93-2	
Zinc	65	250 Day	3" x 3" - 2	10 Cm (C)	~ 2 Kev/PHU	30-65-1	
	65	250 Day	3" x 3" bev	10 Cm (B)	~ 2 Kev/PHU	30-65-2	
	65	250 Day	1X" x 2"	3 Cm (A)	~ 2 Kev/PHU	30-65-3	
	69	14 Hr.	3" x 3"	10 Cm (B)	~ 1 Kev/PHU	30-69-1	
Zirconium	95	65 Day	3" x 3" - 2	10 Cm (C)	~ 2 Kev/PHU	40-95-1	
	95	65 Day	3" x 3" - 2	10 Cm (C)	~ 1 Kev/PHU	40-95-2	
	(With 95 day Nb <sup>95</sup> )	95	65 Day	3" x 3" - 2	10 Cm (C)	~ 1 Kev/PHU	40-95(41-95)1
	97	17 Hr.	3" x 3" - 2	10 Cm (C)	~ 2 Kev/PHU	40-97-1	

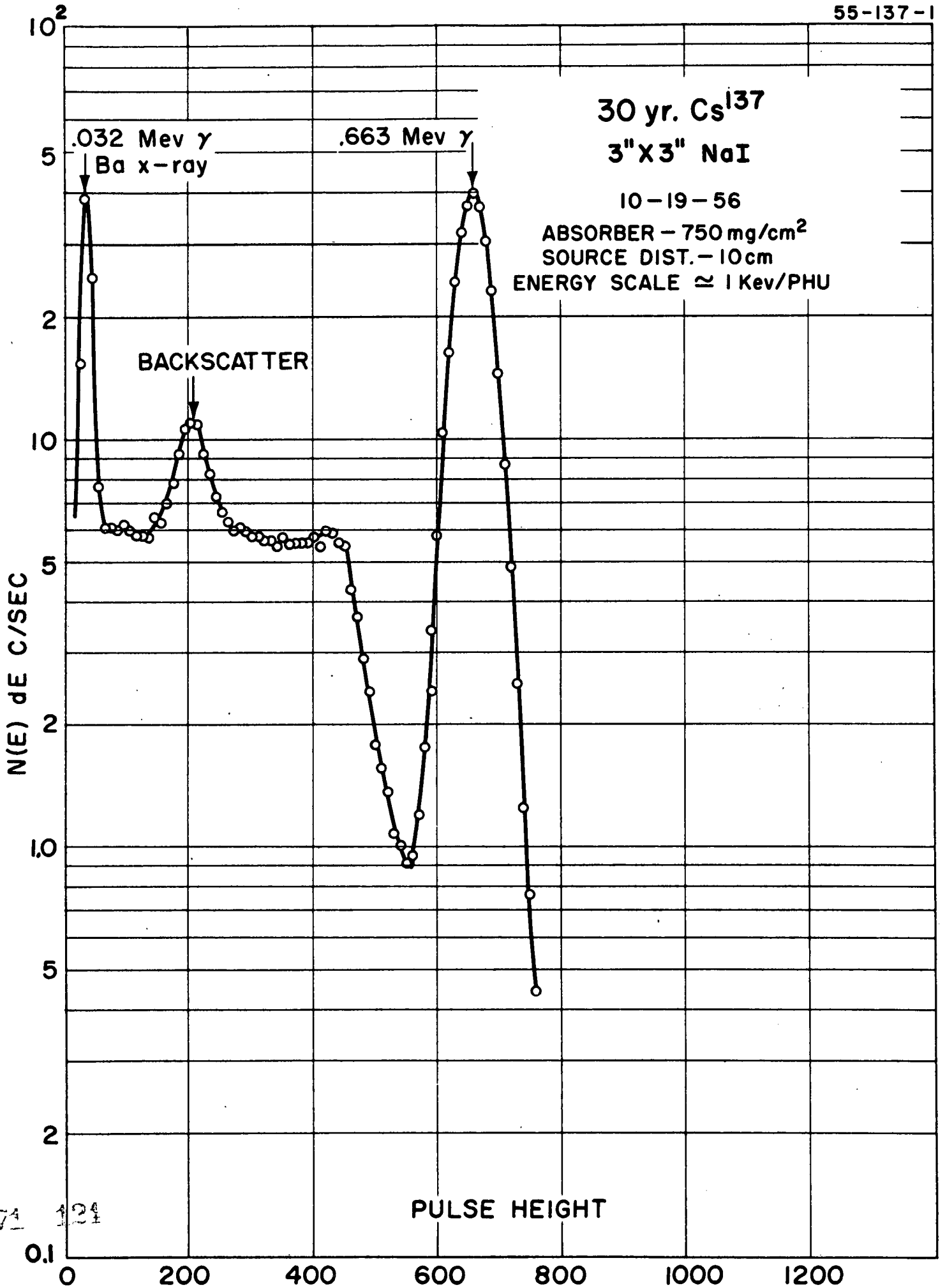
971-023



30 yr. Cs<sup>137</sup>  
3"X3" NaI

10-19-56

ABSORBER - 750 mg/cm<sup>2</sup>  
SOURCE DIST. - 10cm  
ENERGY SCALE  $\approx$  1 Kev/PHU

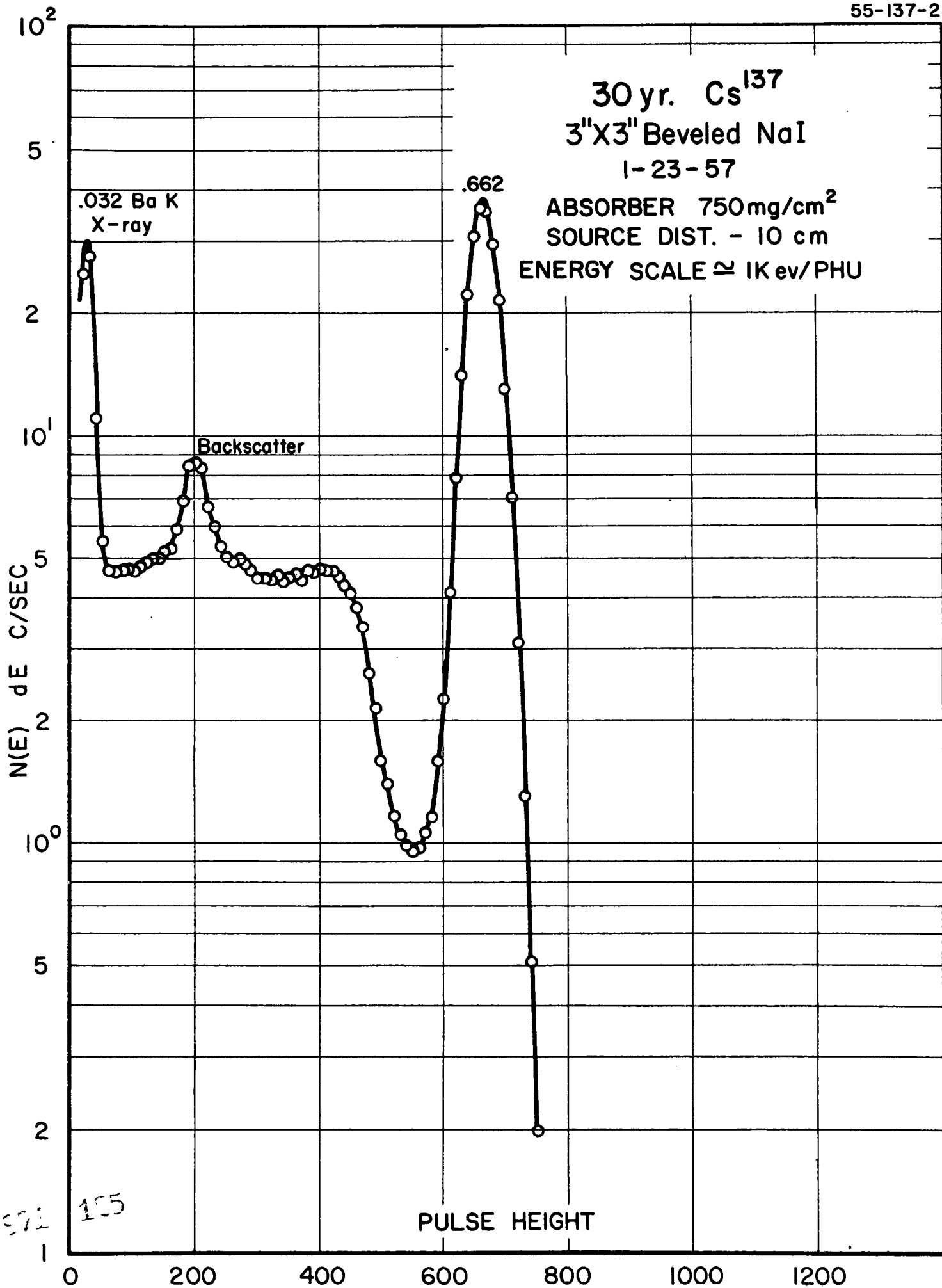


974 124

PULSE HEIGHT

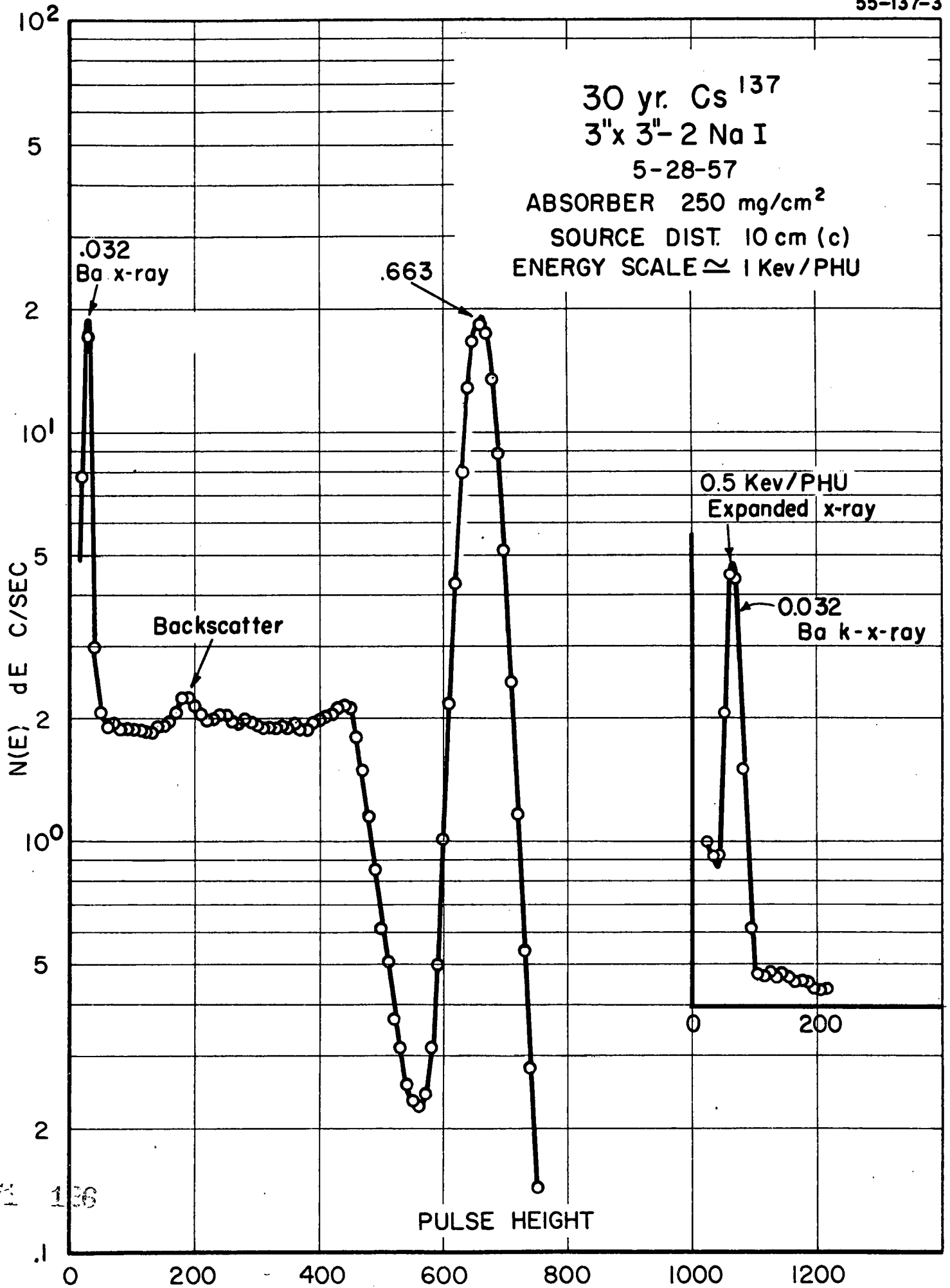
30 yr. Cs<sup>137</sup>  
3"X3" Beveled NaI  
1-23-57

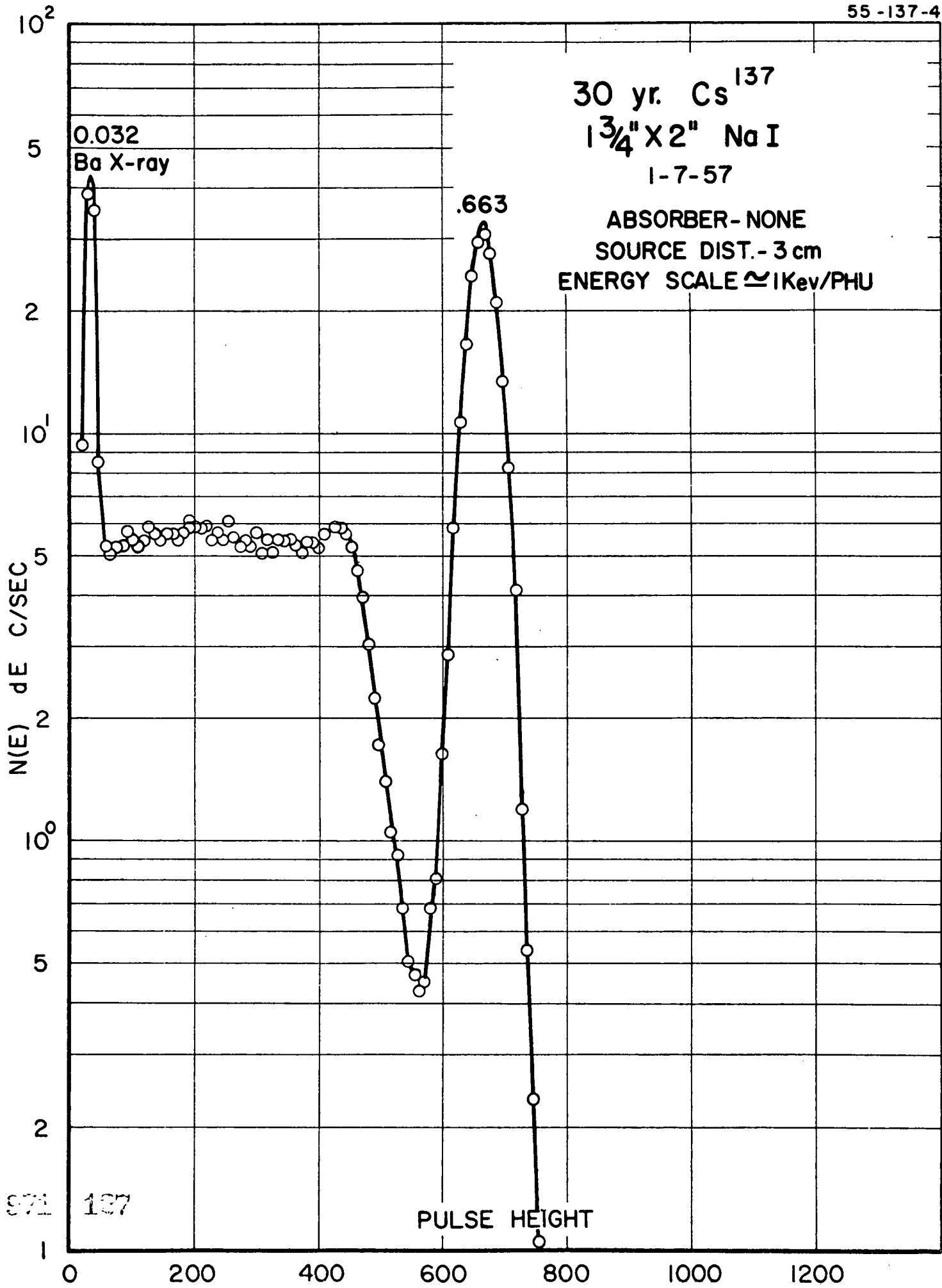
ABSORBER 750mg/cm<sup>2</sup>  
SOURCE DIST. - 10 cm  
ENERGY SCALE  $\approx$  1Kev/PHU



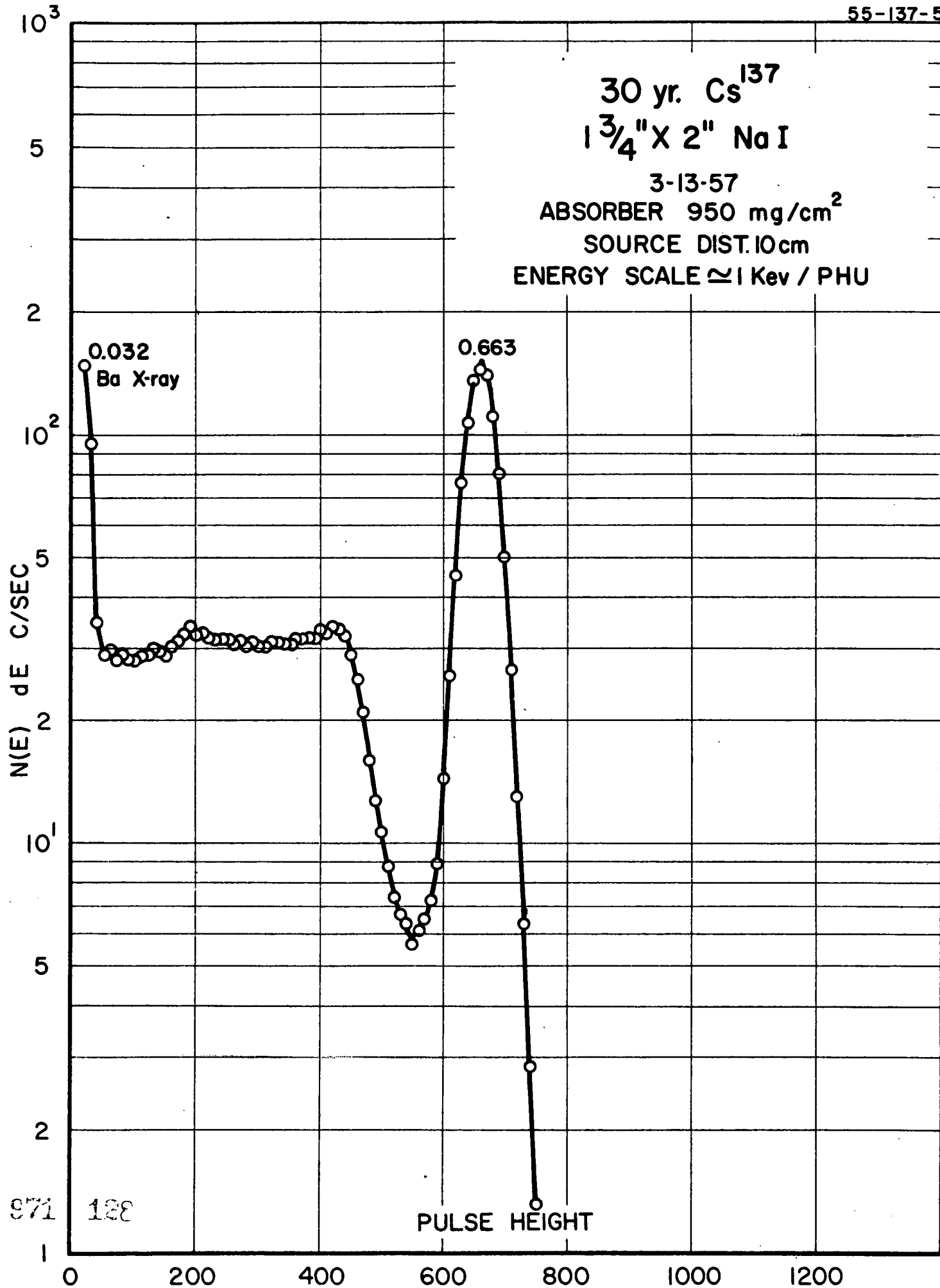
105  
1

PULSE HEIGHT





971 137



971

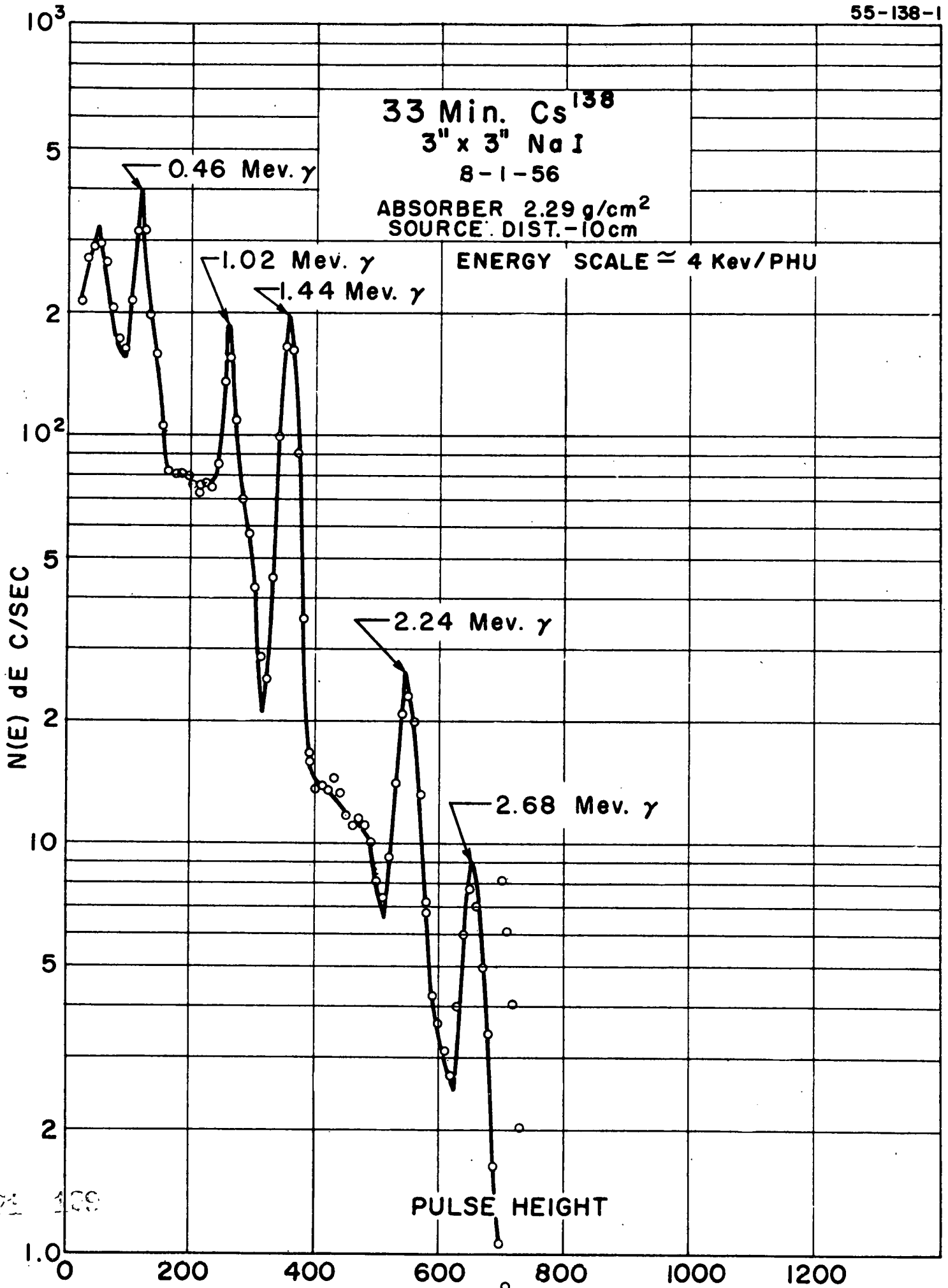
128

PULSE HEIGHT

33 Min. Cs<sup>138</sup>  
3" x 3" NaI  
8-1-56

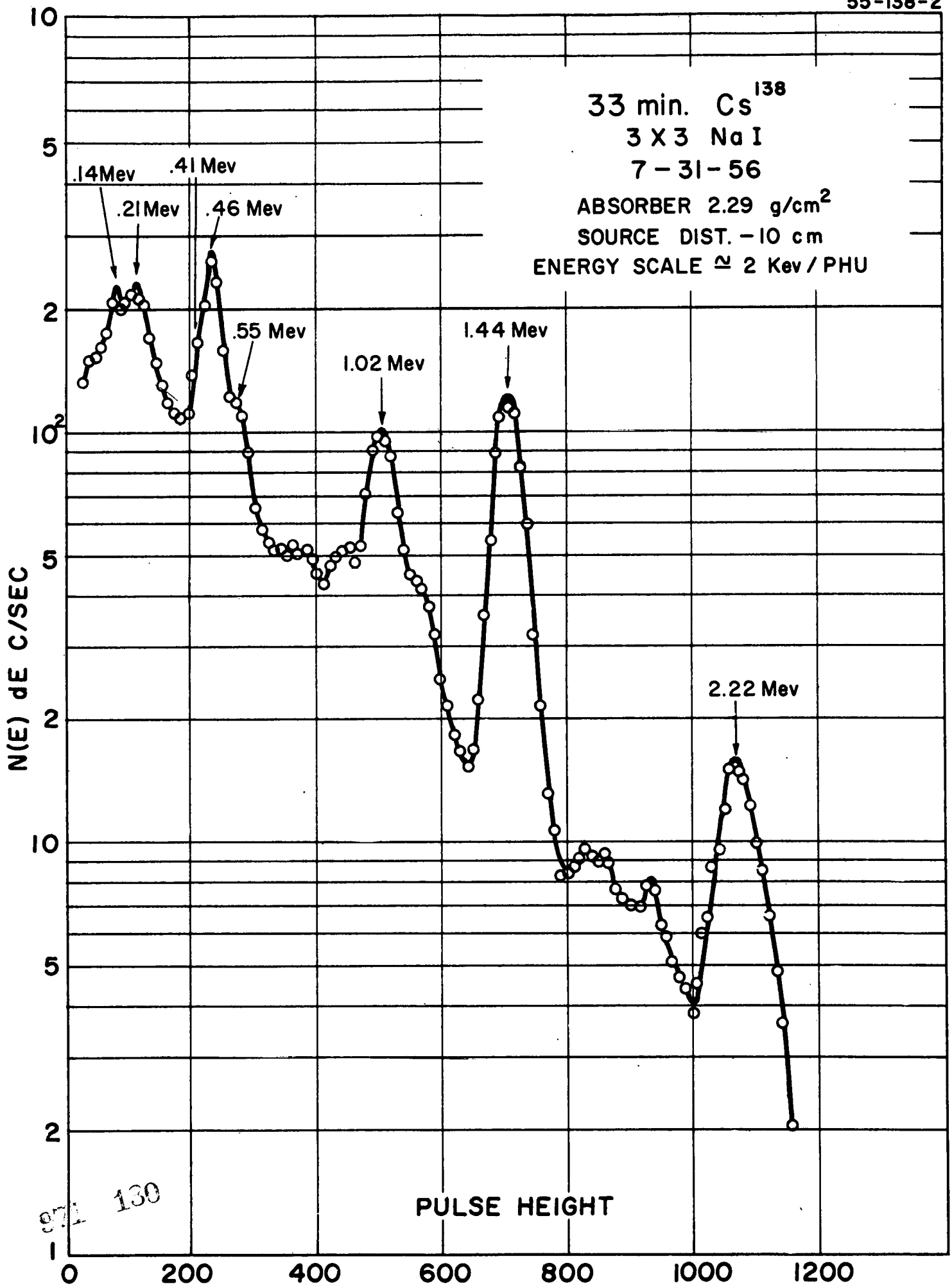
ABSORBER 2.29 g/cm<sup>2</sup>  
SOURCE DIST. -10cm

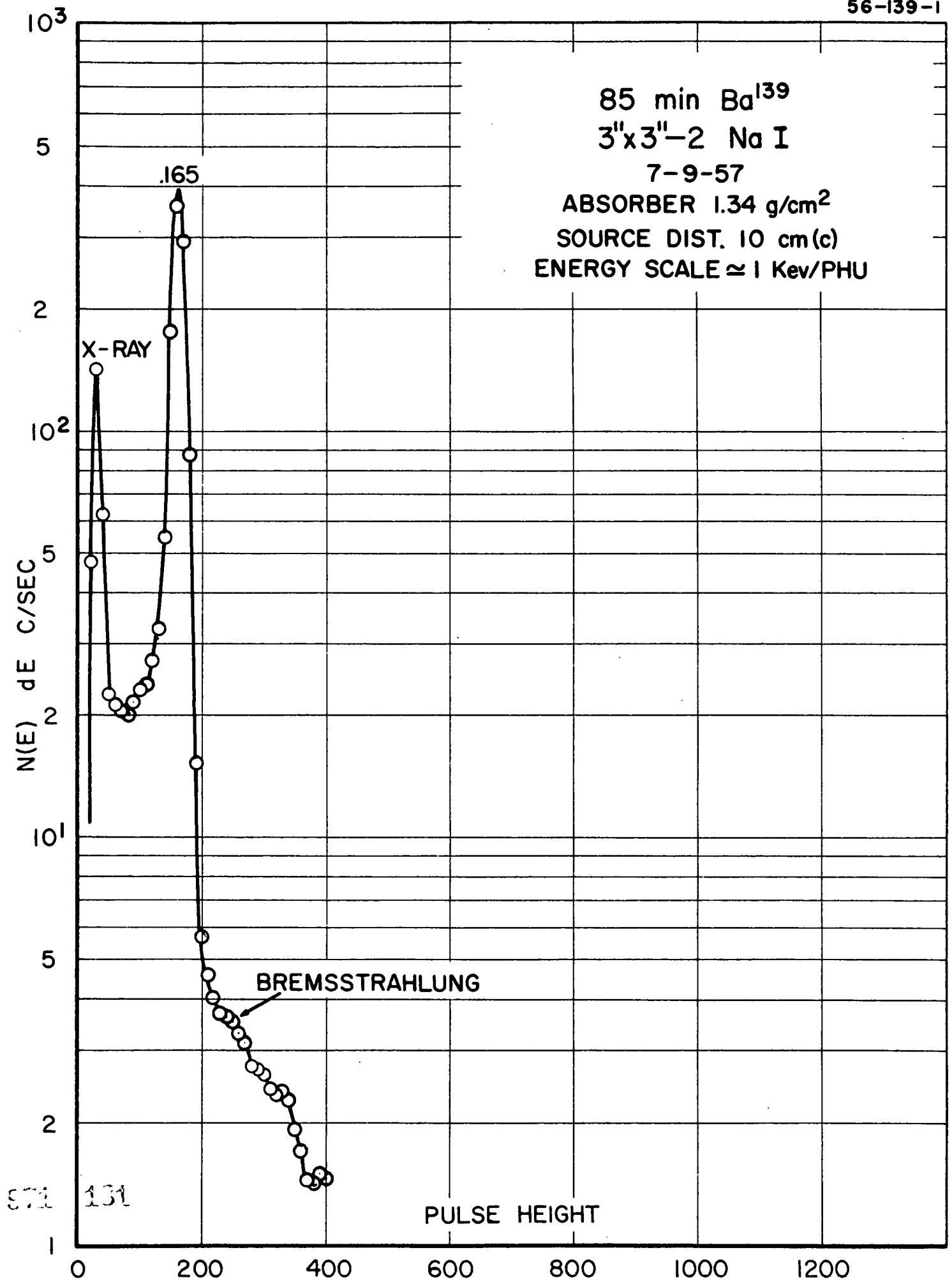
ENERGY SCALE  $\approx$  4 Kev/PHU



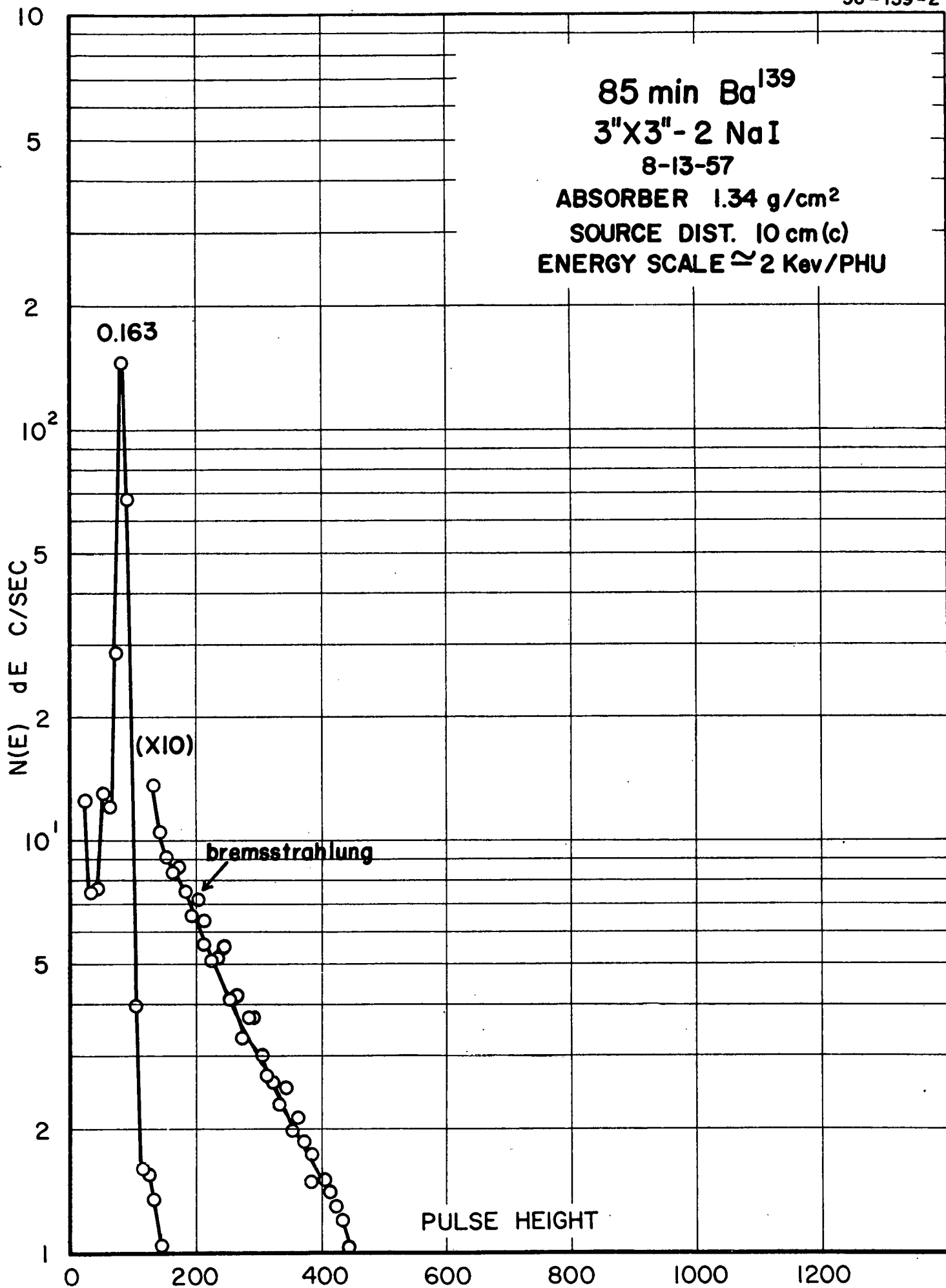
971 100

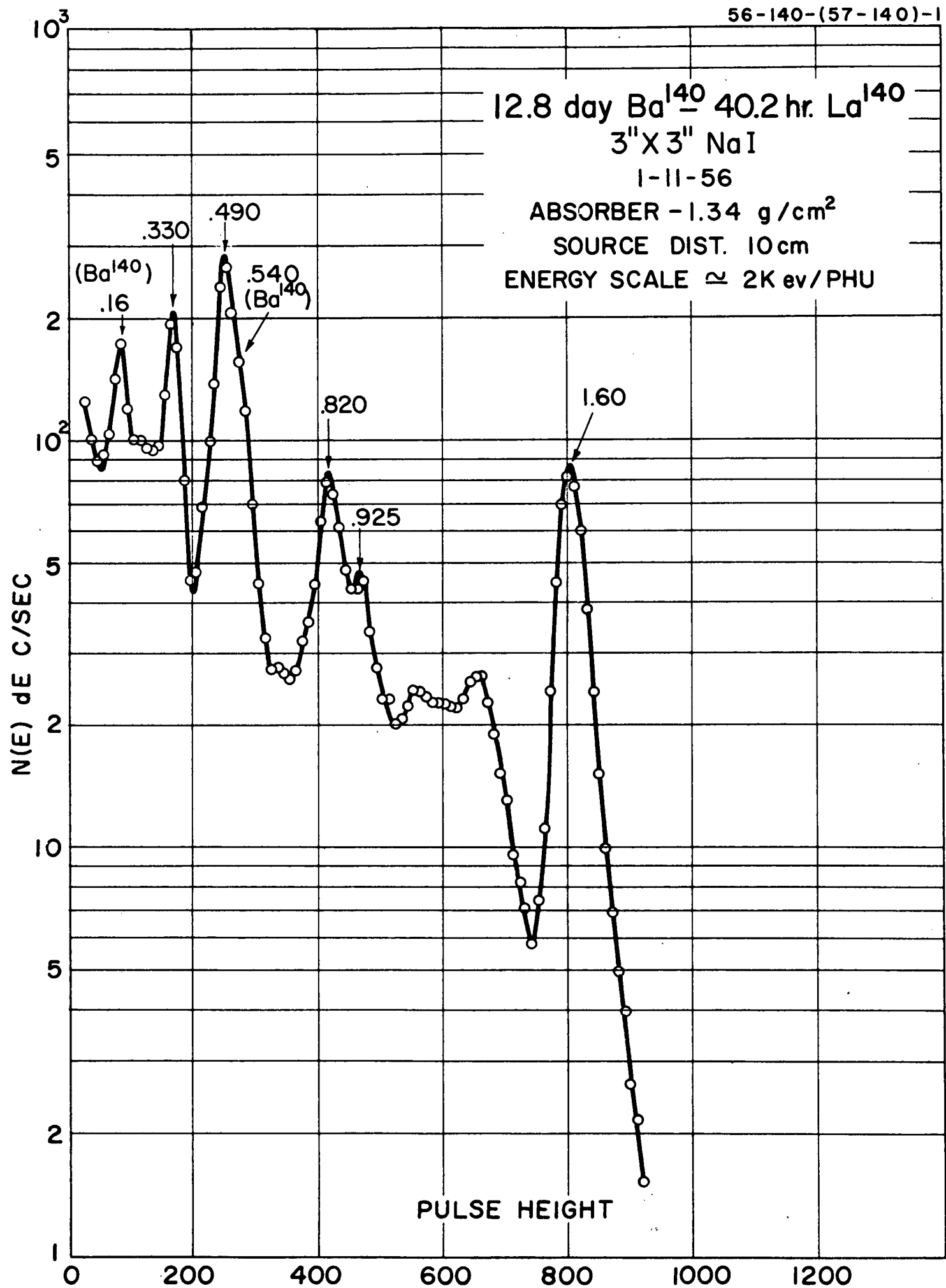
PULSE HEIGHT

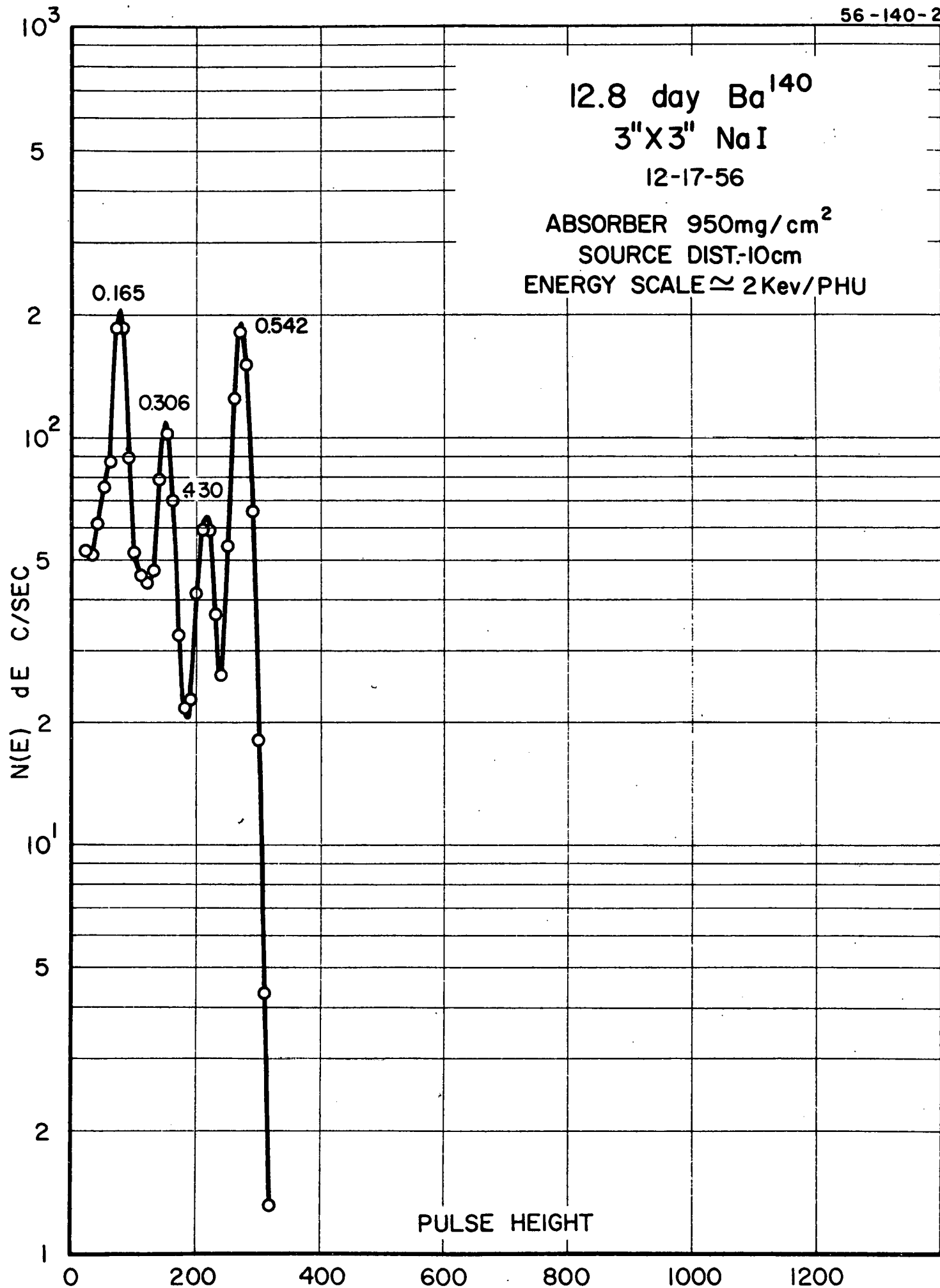




85 min Ba<sup>139</sup>  
3"X3"-2 NaI  
8-13-57  
ABSORBER 1.34 g/cm<sup>2</sup>  
SOURCE DIST. 10 cm(c)  
ENERGY SCALE ≈ 2 Kev/PHU







12.8 day Ba<sup>140</sup>

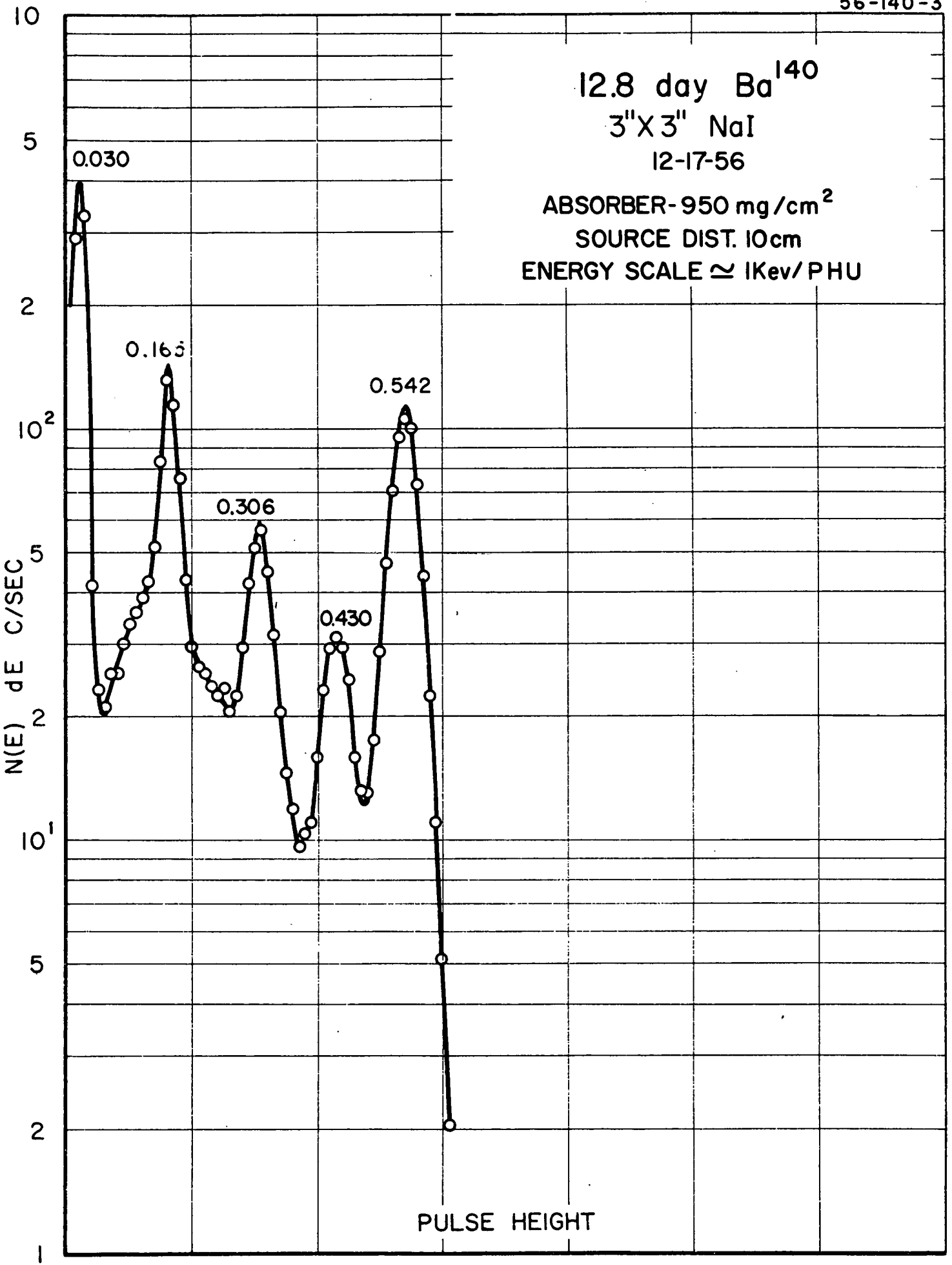
3"X3" NaI

12-17-56

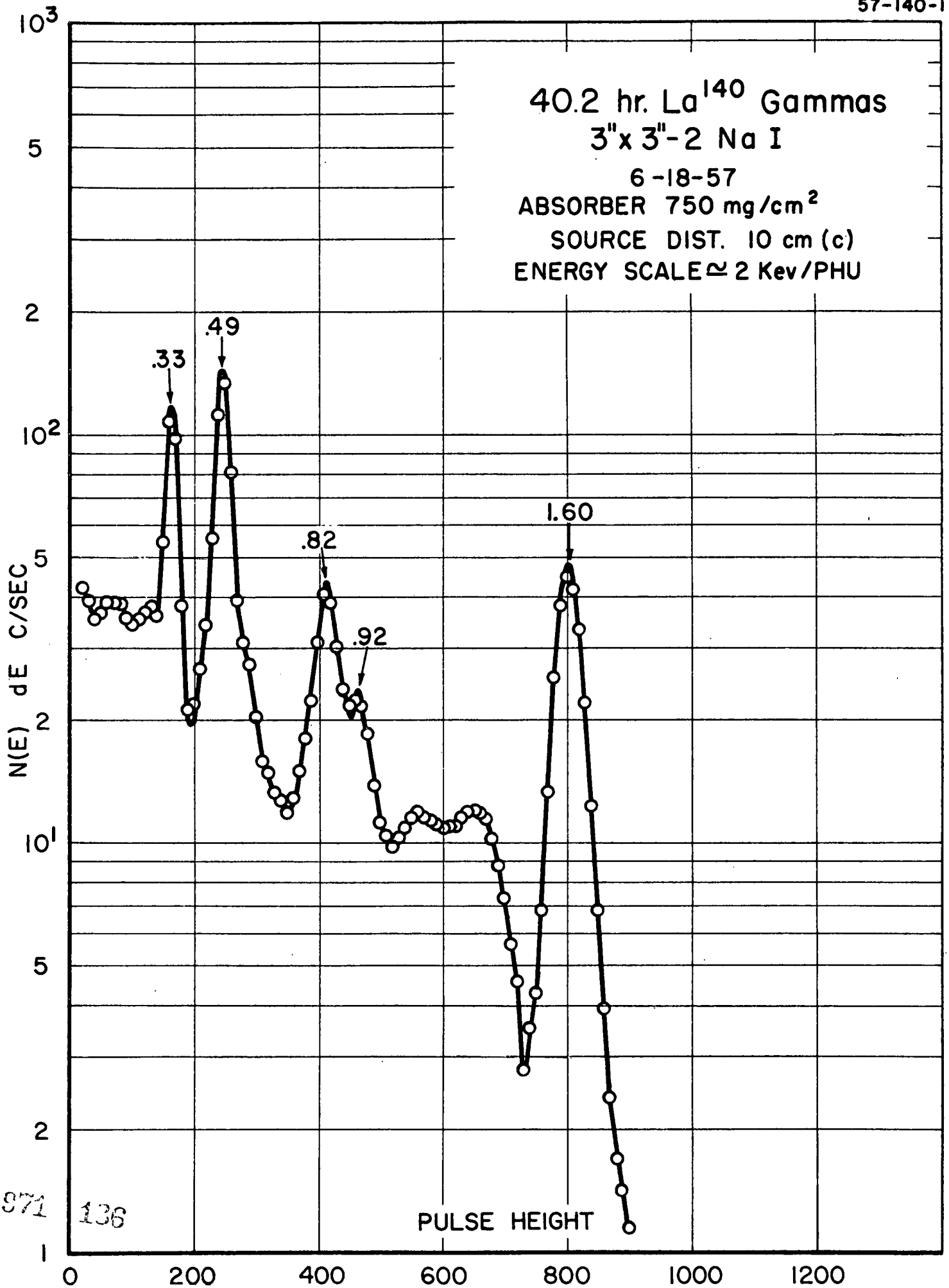
ABSORBER-950 mg/cm<sup>2</sup>

SOURCE DIST. 10cm

ENERGY SCALE  $\approx$  1Kev/PHU

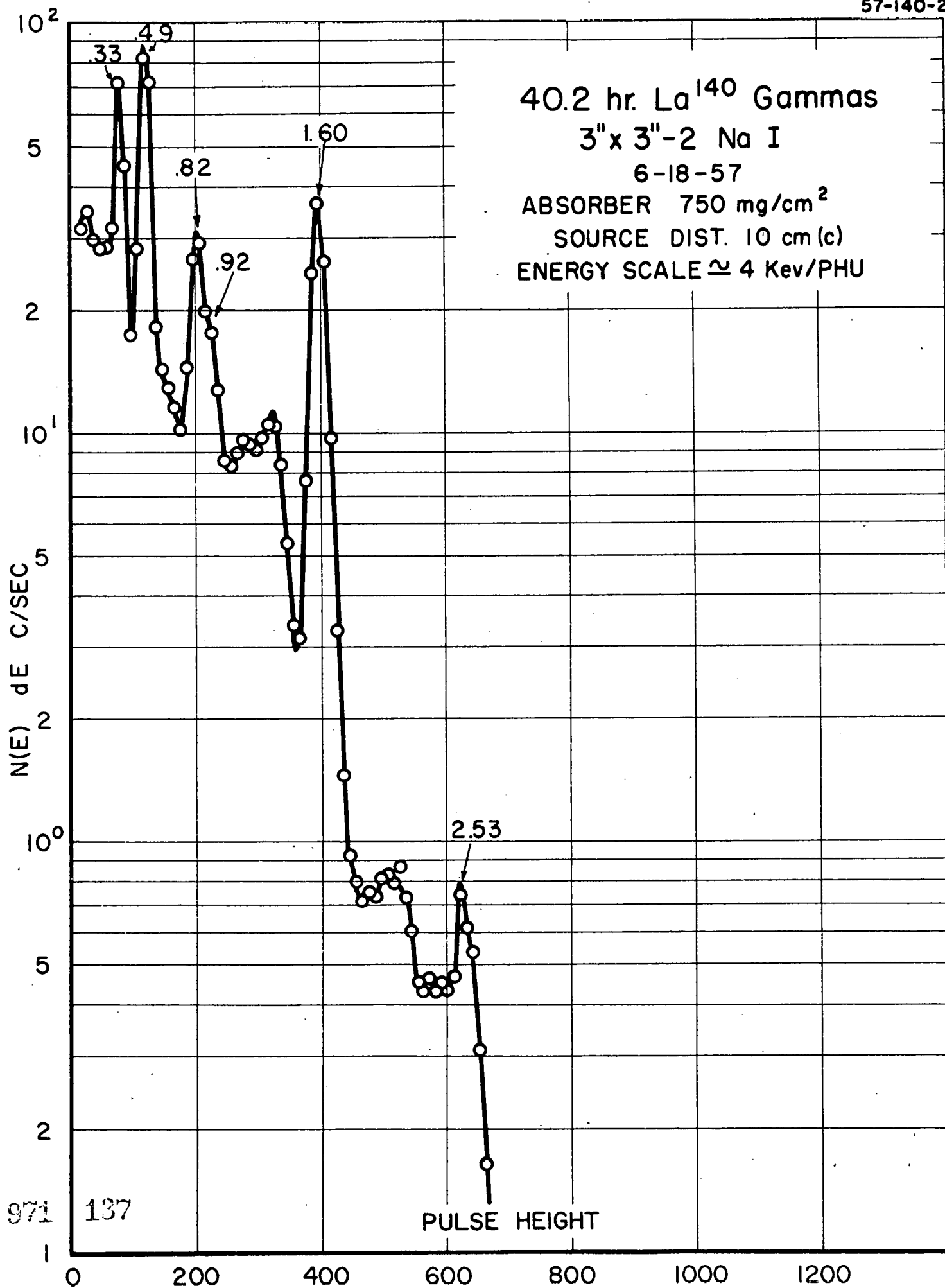


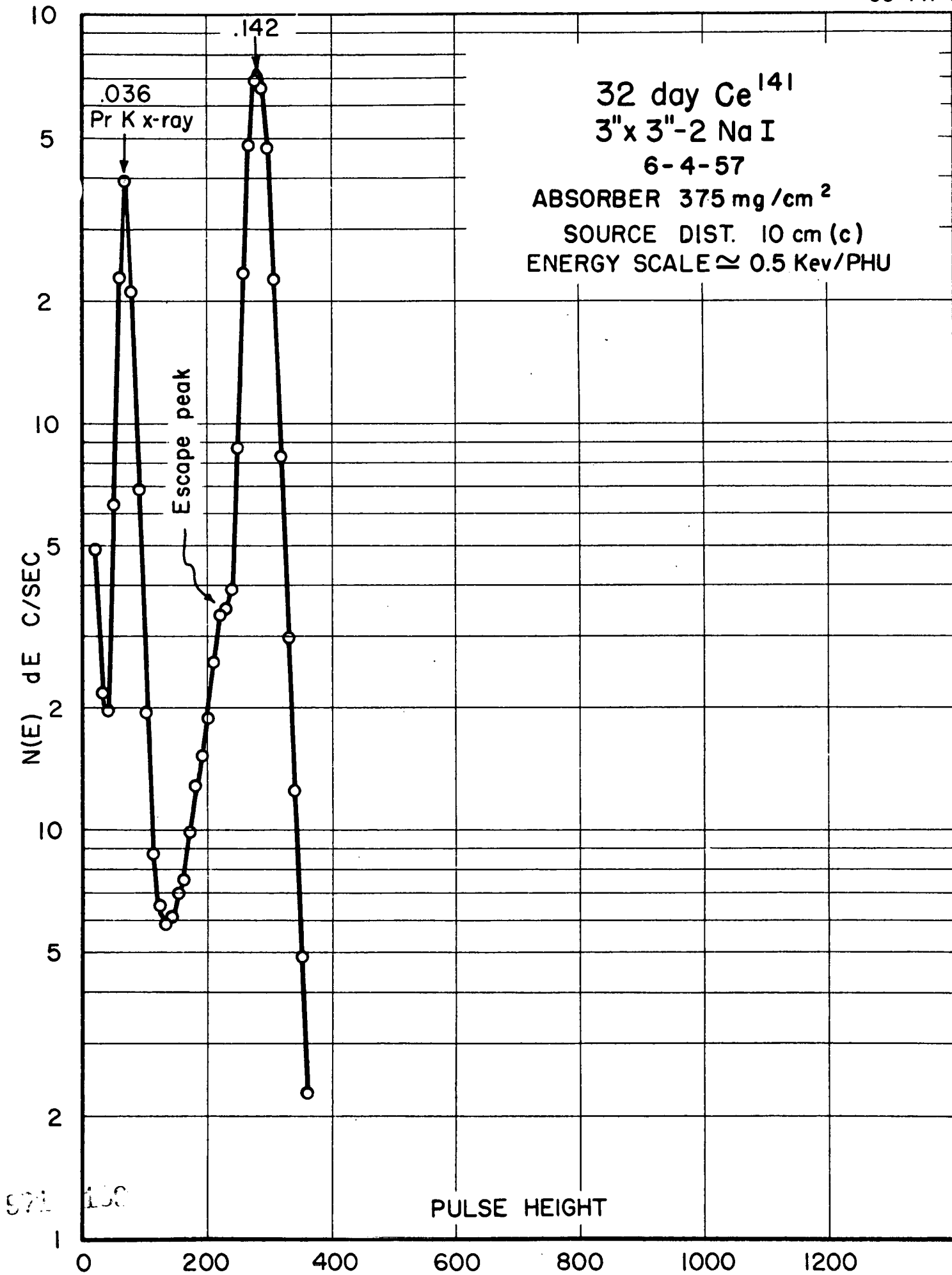
40.2 hr.  $\text{La}^{140}$  Gammas  
 3" x 3"-2 Na I  
 6-18-57  
 ABSORBER 750 mg/cm<sup>2</sup>  
 SOURCE DIST. 10 cm (c)  
 ENERGY SCALE  $\approx$  2 Kev/PHU



971 136

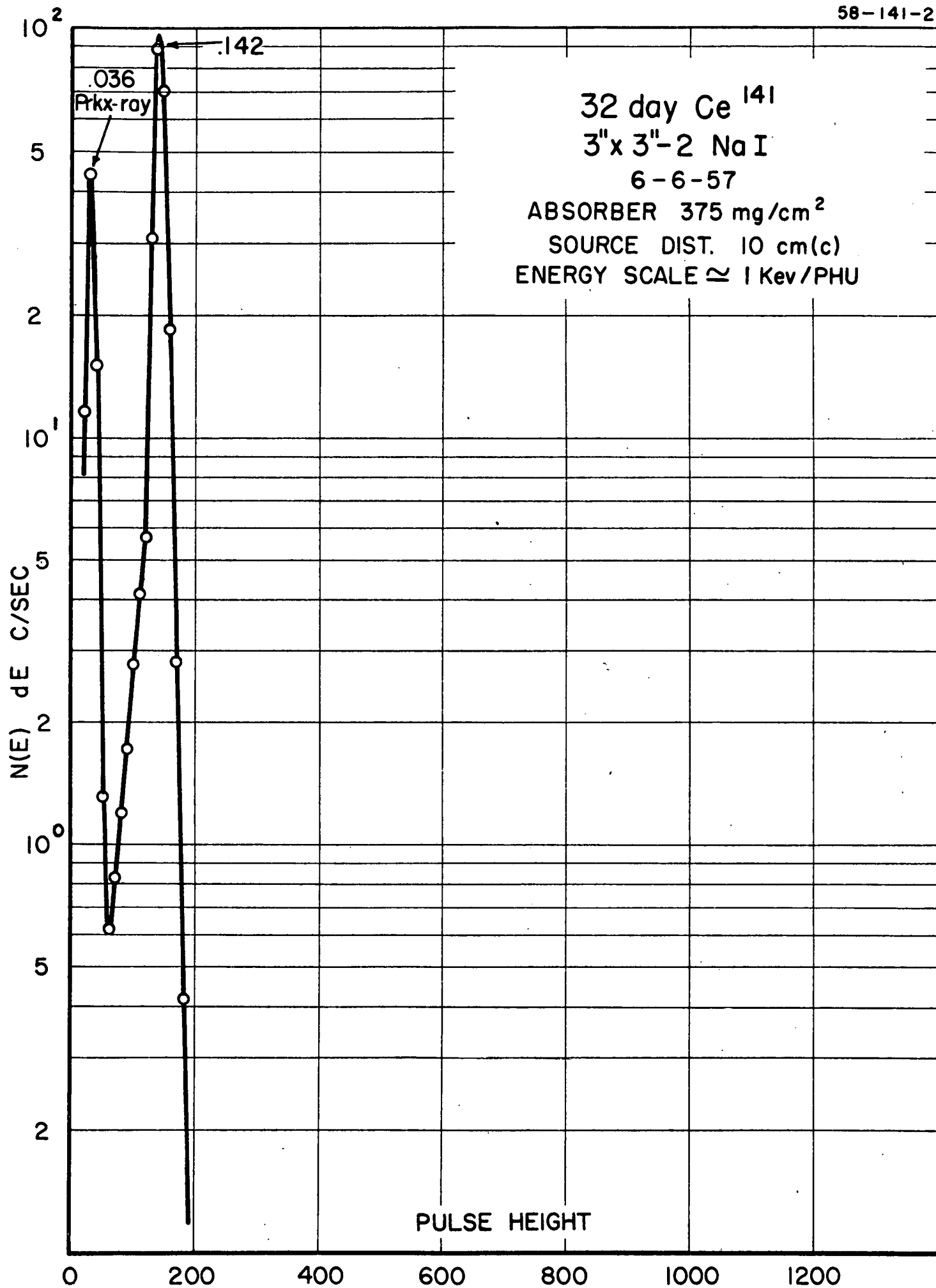
PULSE HEIGHT





971 150

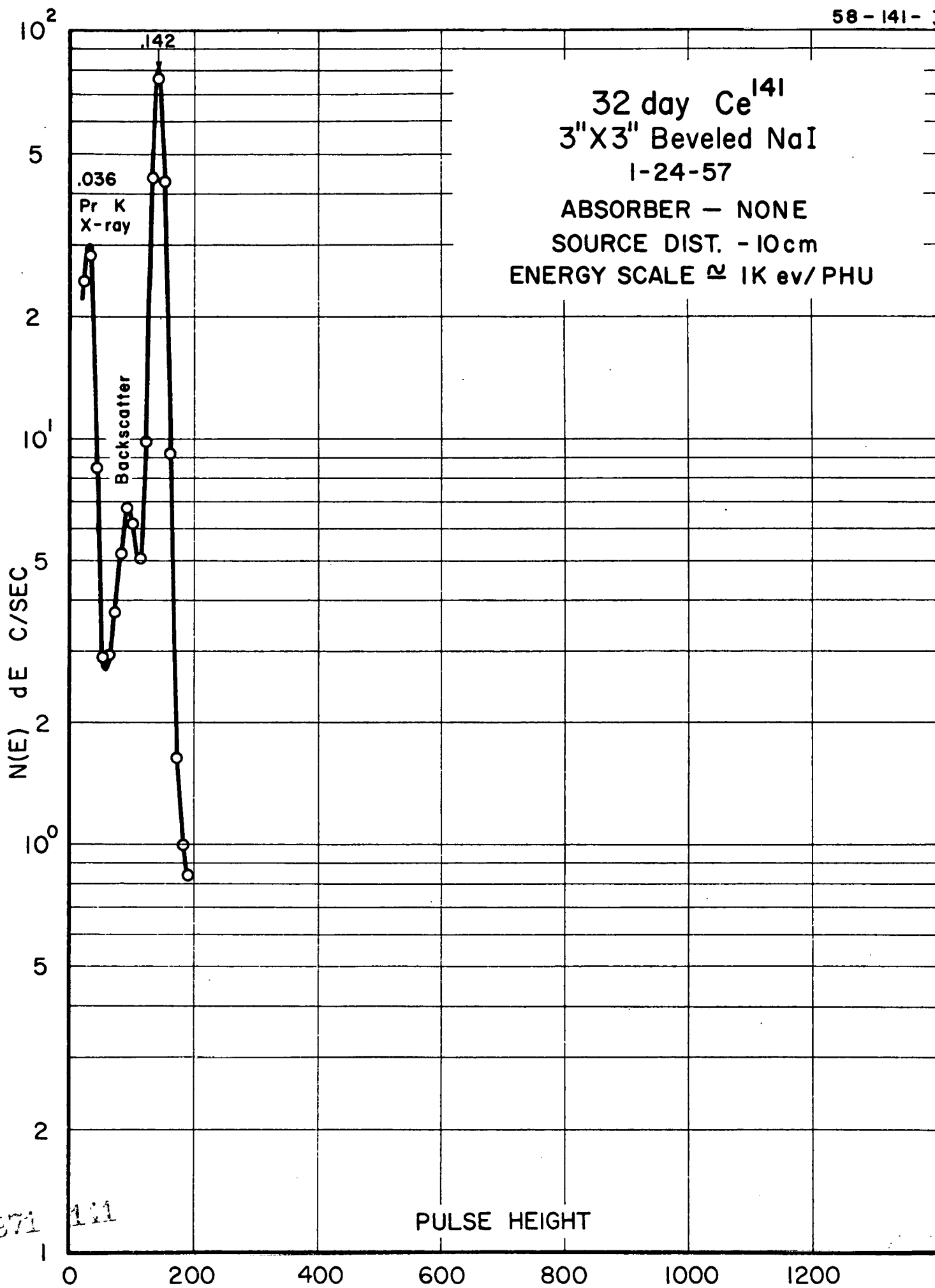
32 day  $Ce^{141}$   
3" x 3"-2 NaI  
6-6-57  
ABSORBER 375 mg/cm<sup>2</sup>  
SOURCE DIST. 10 cm(c)  
ENERGY SCALE  $\approx$  1 Kev/PHU



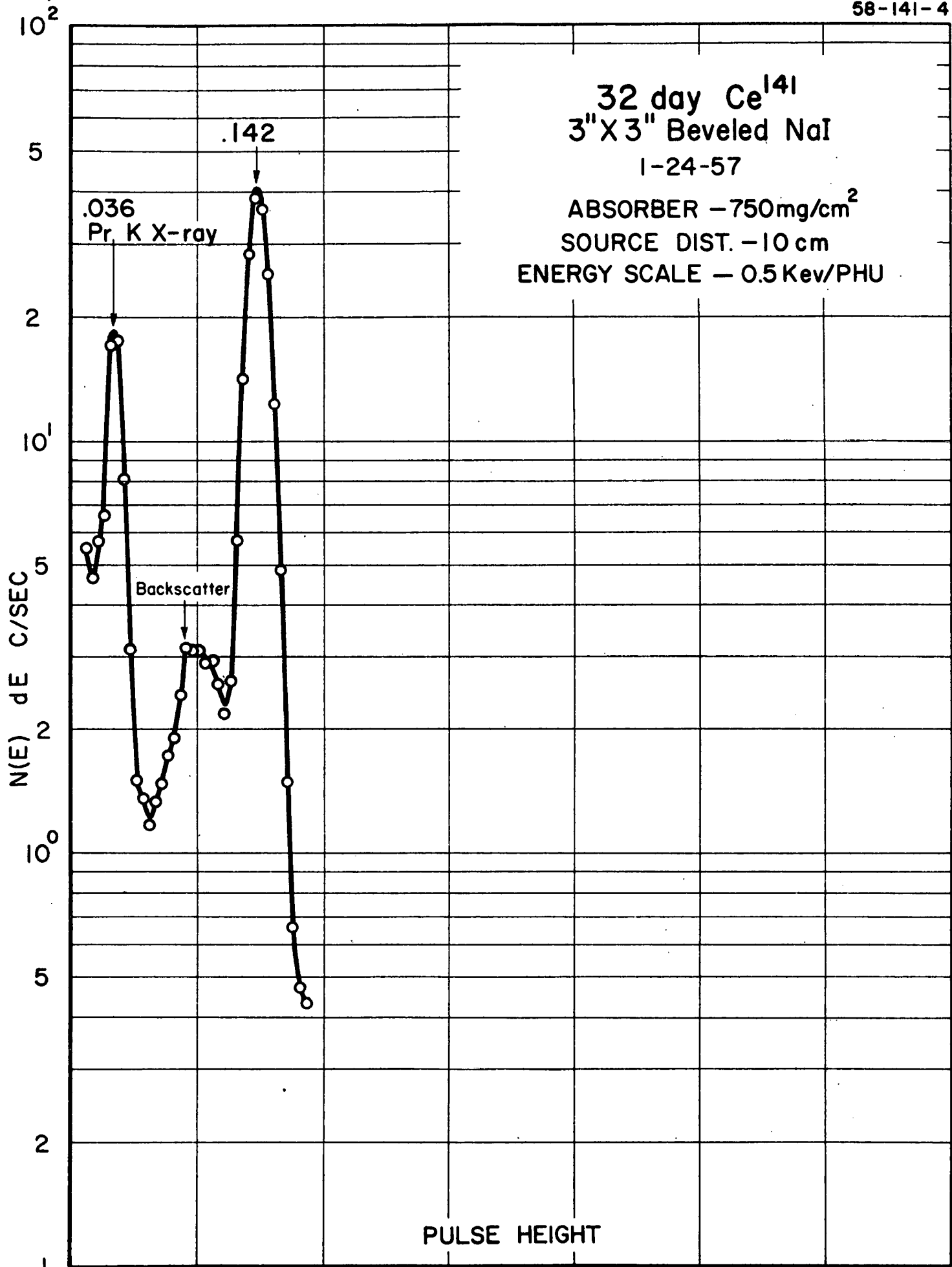
971 140

32 day  $\text{Ce}^{141}$   
 3"X3" Beveled NaI  
 1-24-57

ABSORBER - NONE  
 SOURCE DIST. - 10cm  
 ENERGY SCALE  $\approx$  1K ev/PHU

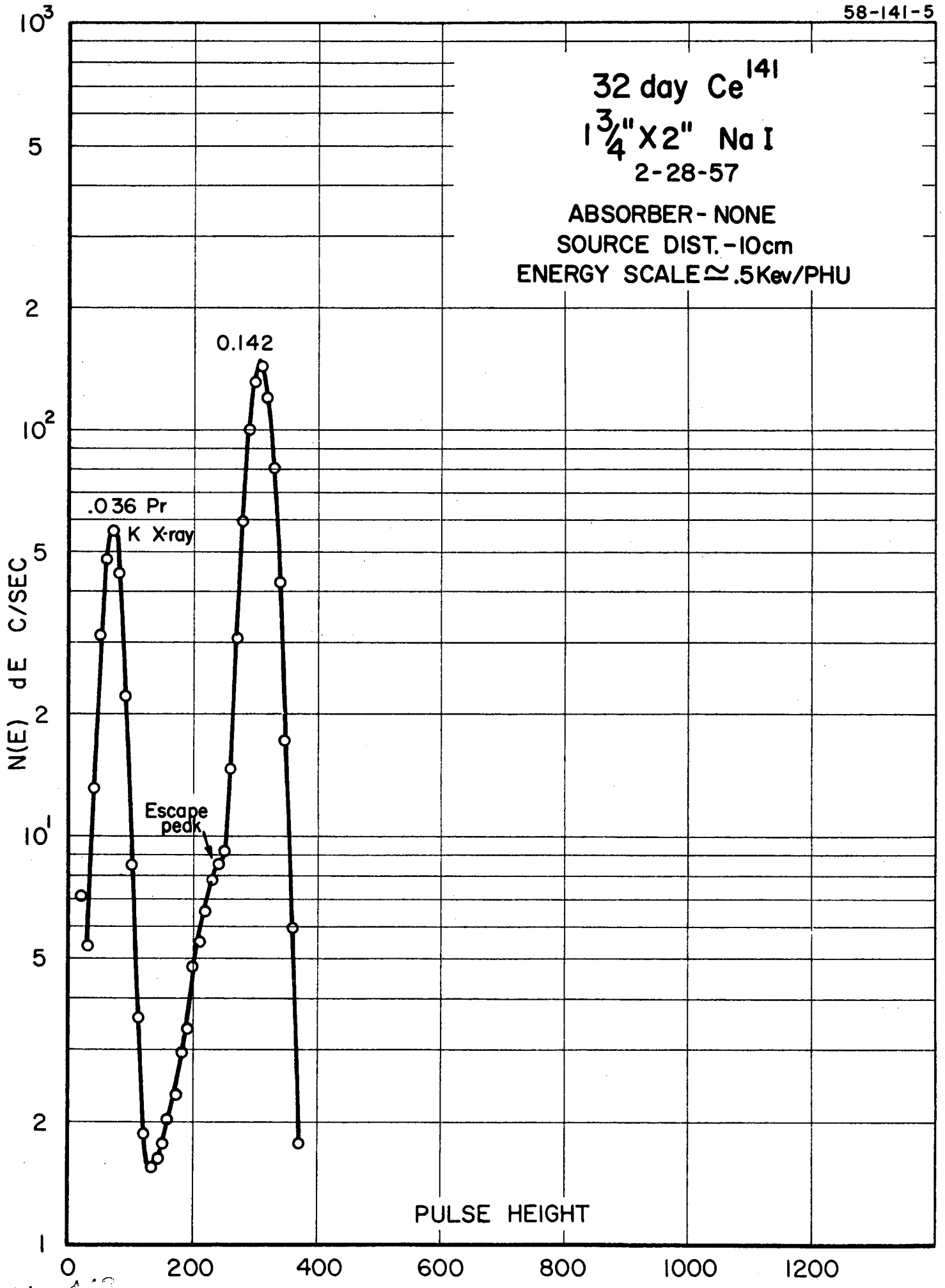


32 day  $Ce^{141}$   
3" X 3" Beveled NaI  
1-24-57  
ABSORBER - 750mg/cm<sup>2</sup>  
SOURCE DIST. - 10 cm  
ENERGY SCALE - 0.5 Kev/PHU



32 day  $Ce^{141}$   
 $1\frac{3}{4}'' \times 2''$  Na I  
2-28-57

ABSORBER - NONE  
SOURCE DIST. - 10cm  
ENERGY SCALE  $\approx .5$ Kev/PHU



77 min. -  $\text{La}^{142}$

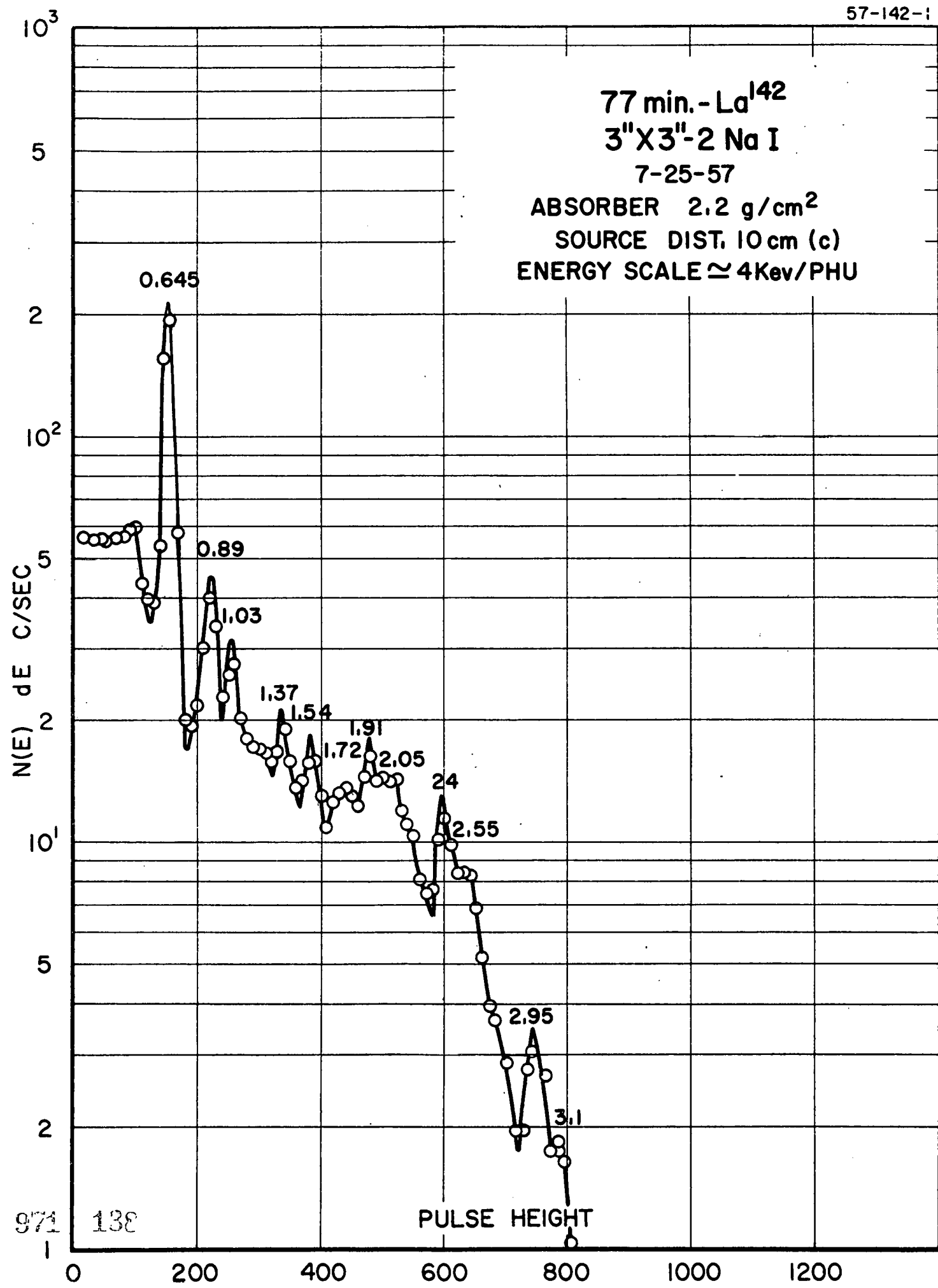
3" X 3" - 2 Na I

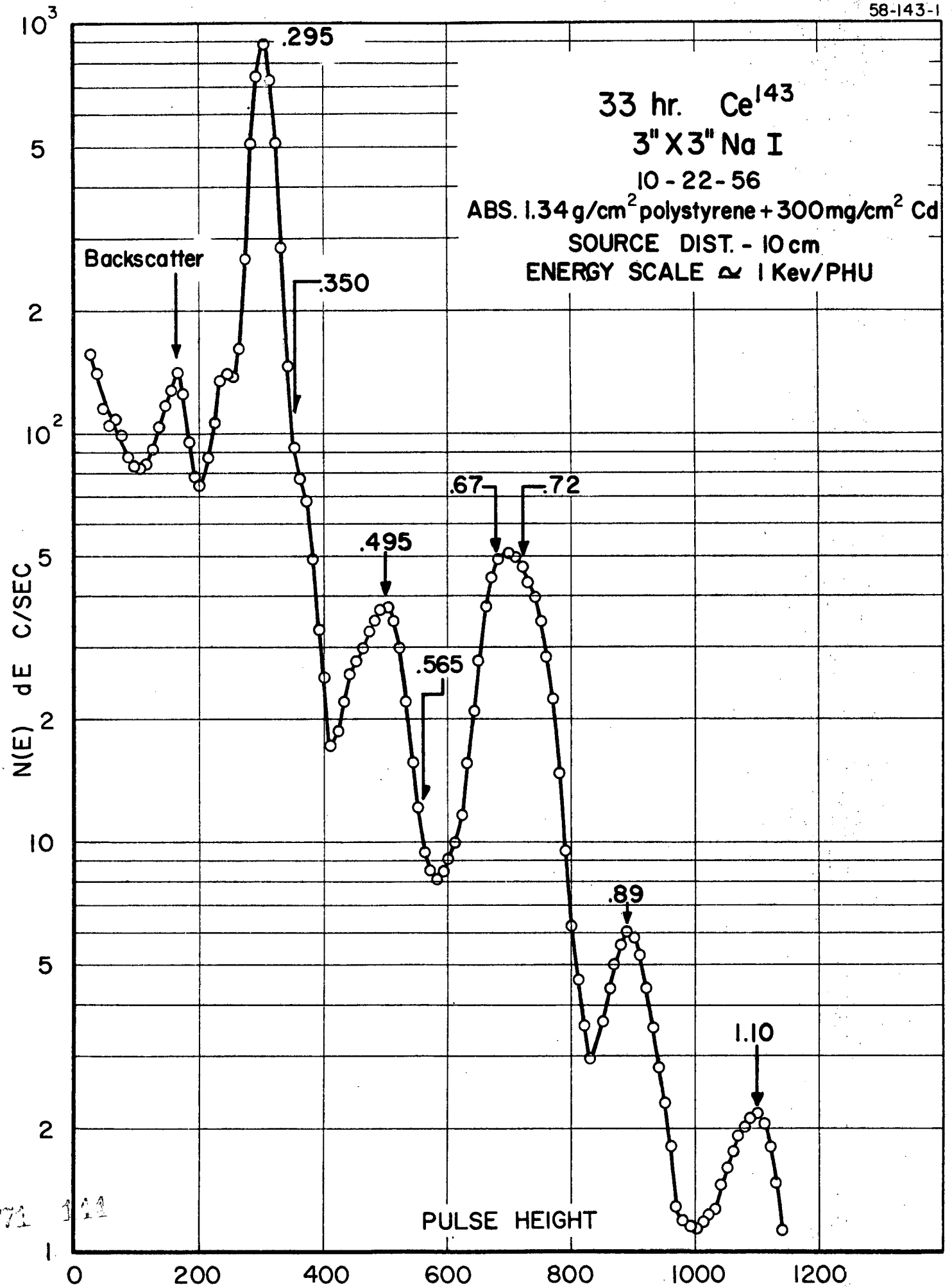
7-25-57

ABSORBER 2.2 g/cm<sup>2</sup>

SOURCE DIST. 10 cm (c)

ENERGY SCALE  $\approx$  4Kev/PHU



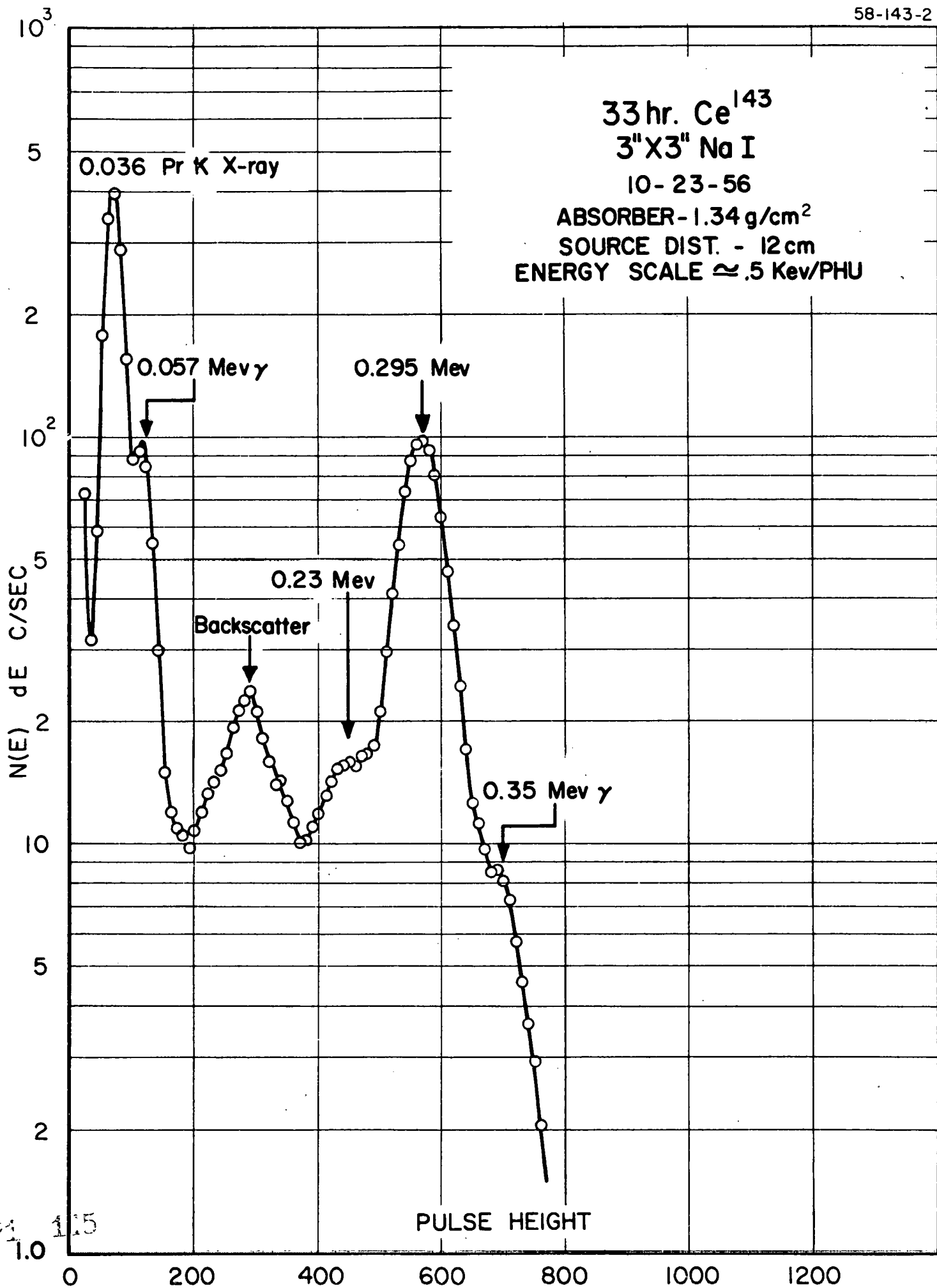


371 111

33 hr.  $Ce^{143}$   
3" X 3" Na I

10-23-56

ABSORBER - 1.34 g/cm<sup>2</sup>  
SOURCE DIST. - 12 cm  
ENERGY SCALE  $\approx$  .5 Kev/PHU



974 115

# 19.1 hr Pr<sup>142</sup> GAMMAS

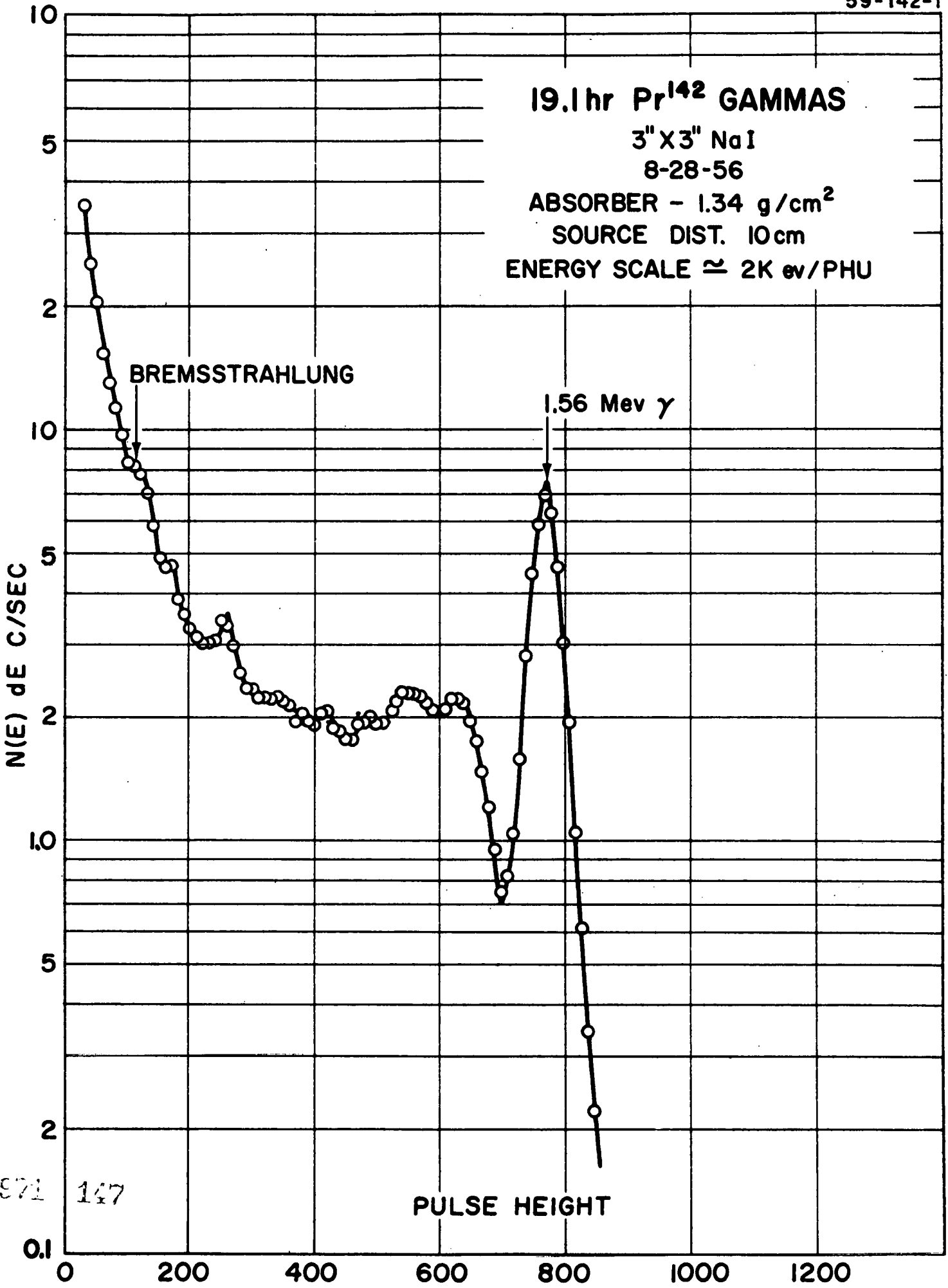
3" X 3" NaI

8-28-56

ABSORBER - 1.34 g/cm<sup>2</sup>

SOURCE DIST. 10cm

ENERGY SCALE  $\approx$  2K ev/PHU



BREMSSTRAHLUNG

1.56 Mev  $\gamma$

$N(E) dE$  C/SEC

PULSE HEIGHT

871 147

0.1

0

200

400

600

800

1000

1200

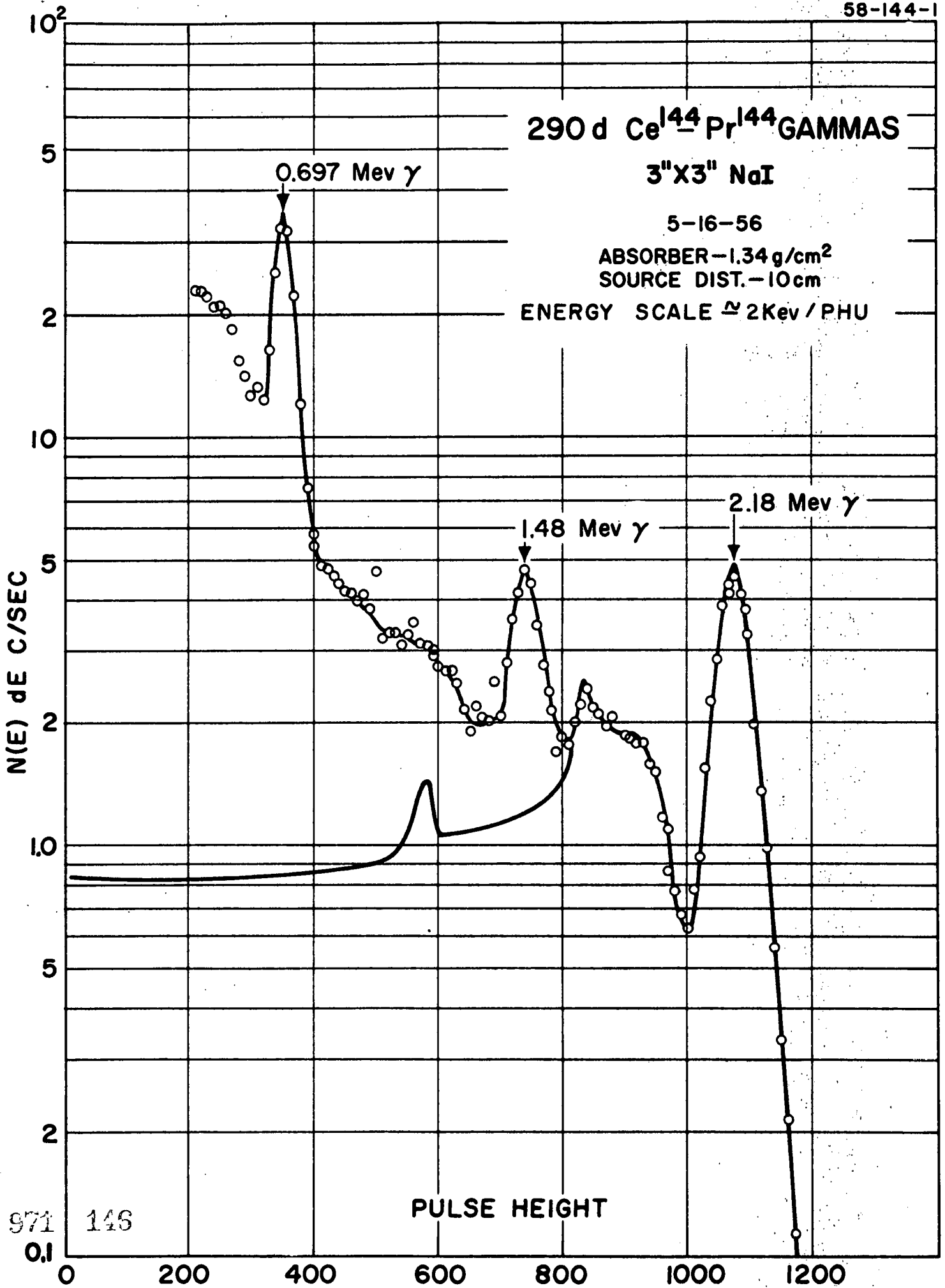
# 290 d $Ce^{144}$ $Pr^{144}$ GAMMAS

3"X3" NaI

5-16-56

ABSORBER-1.34 g/cm<sup>2</sup>  
SOURCE DIST.-10cm

ENERGY SCALE  $\approx$  2Kev/PHU

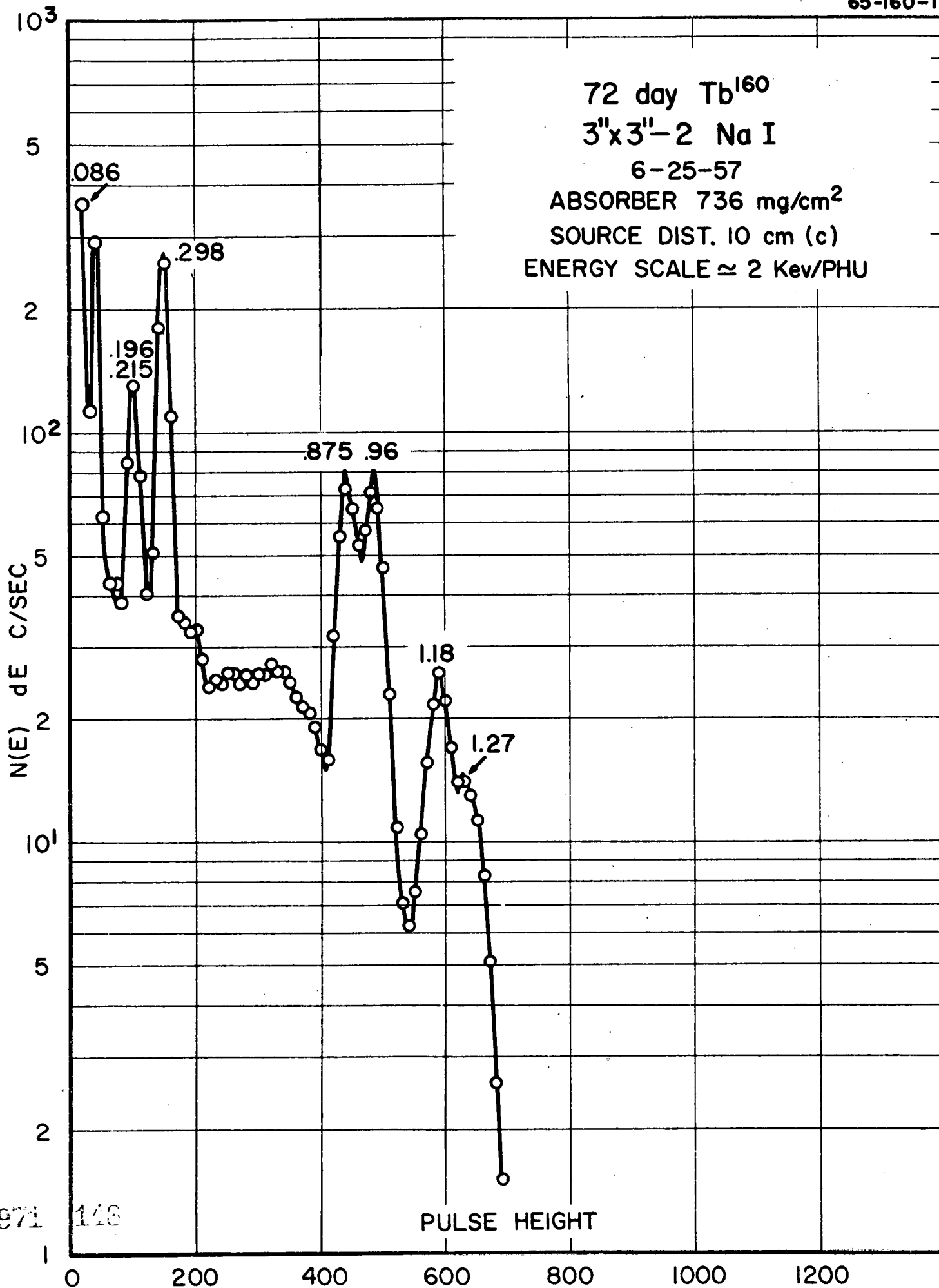


971 146  
0.1

PULSE HEIGHT

0 200 400 600 800 1000 1200

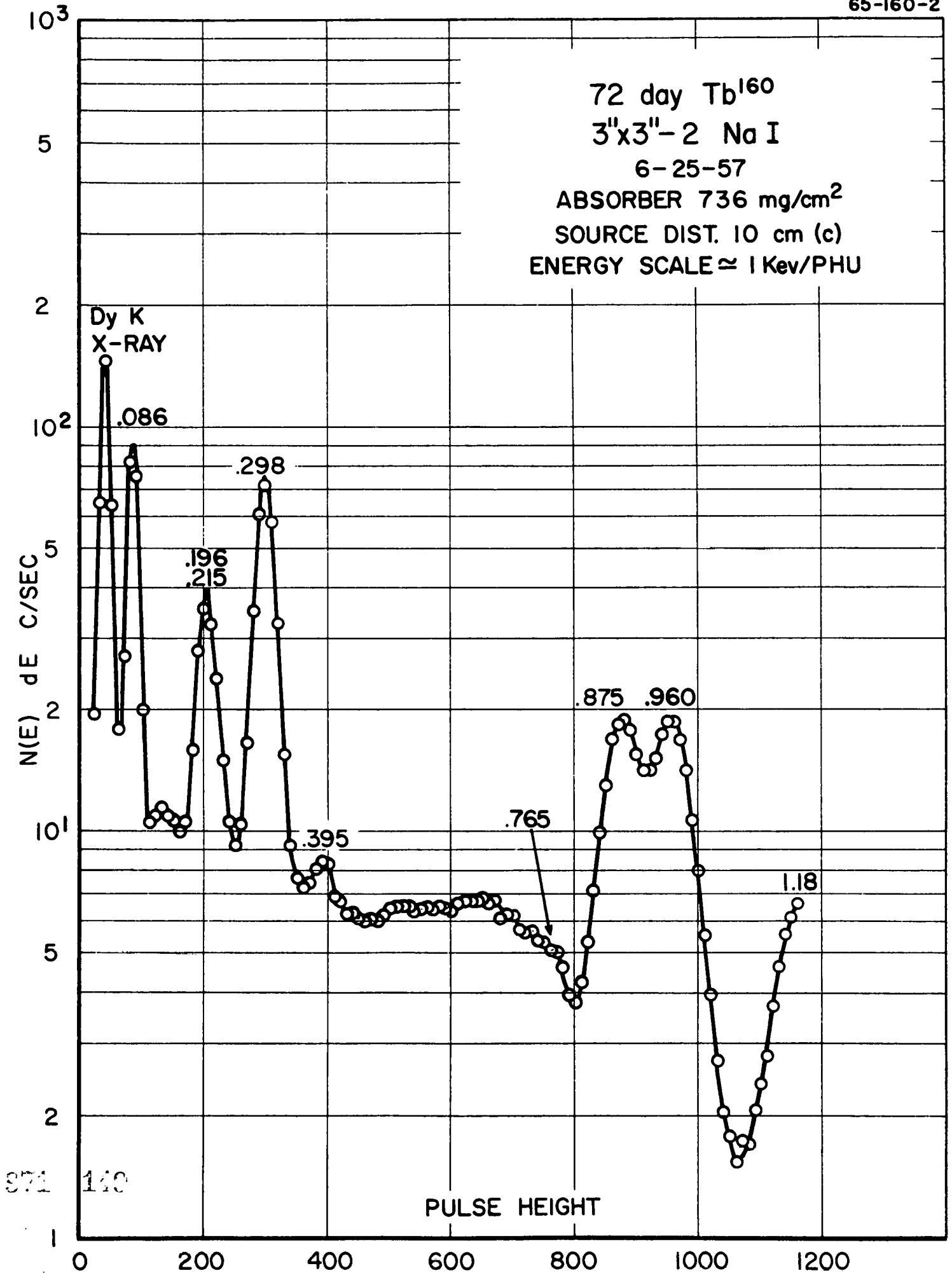
72 day Tb<sup>160</sup>  
3"x3"-2 Na I  
6-25-57  
ABSORBER 736 mg/cm<sup>2</sup>  
SOURCE DIST. 10 cm (c)  
ENERGY SCALE ≈ 2 Kev/PHU



971 148

PULSE HEIGHT

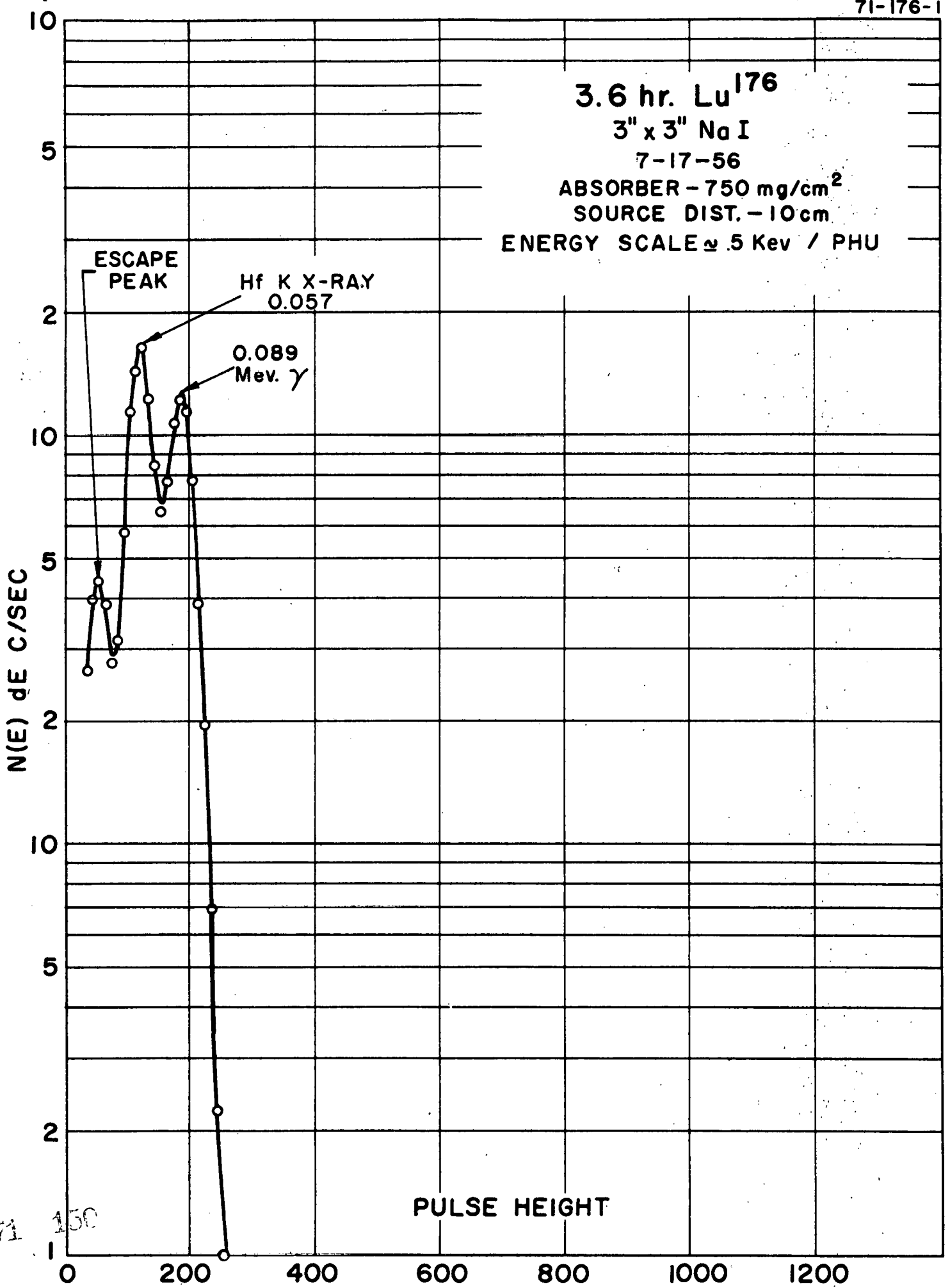
72 day  $Tb^{160}$   
3"x3"-2 Na I  
6-25-57  
ABSORBER 736 mg/cm<sup>2</sup>  
SOURCE DIST. 10 cm (c)  
ENERGY SCALE  $\approx$  1 Kev/PHU



371 140

PULSE HEIGHT

3.6 hr. Lu<sup>176</sup>  
3" x 3" NaI  
7-17-56  
ABSORBER - 750 mg/cm<sup>2</sup>  
SOURCE DIST. - 10 cm  
ENERGY SCALE  $\approx$  .5 Kev / PHU



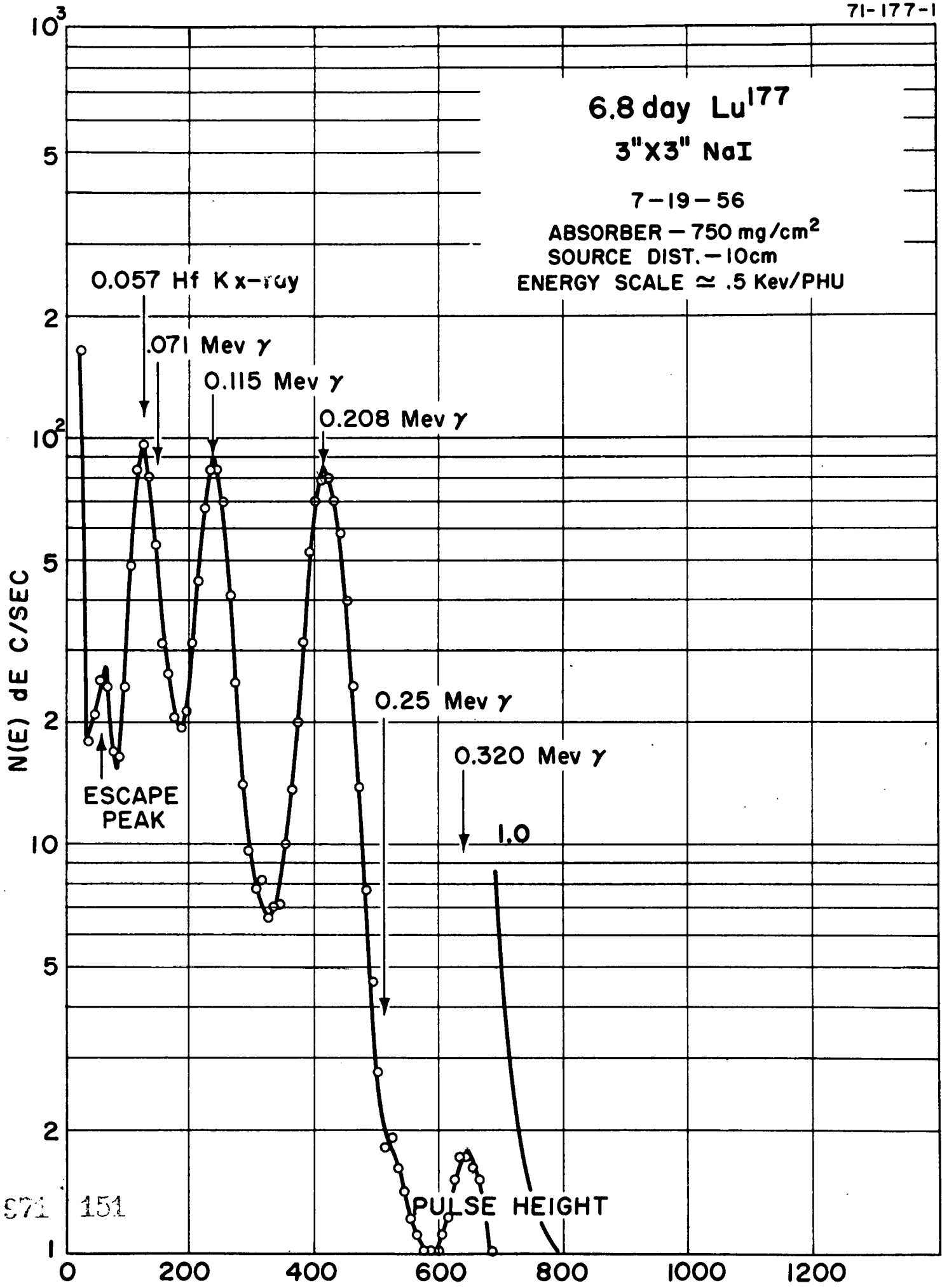
971 150

PULSE HEIGHT

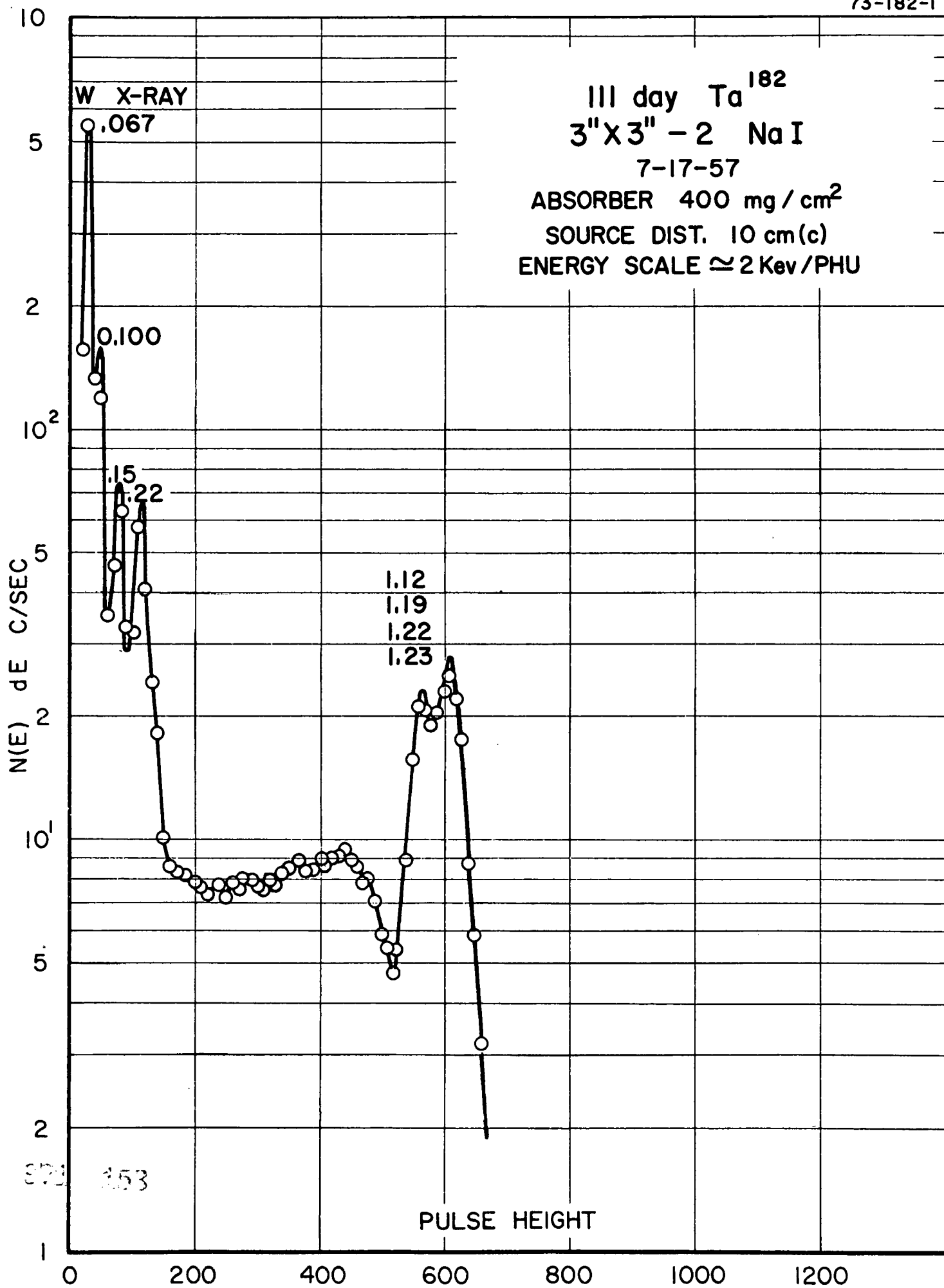
6.8 day  $\text{Lu}^{177}$   
3"X3" NaI

7-19-56

ABSORBER - 750 mg/cm<sup>2</sup>  
SOURCE DIST. - 10cm  
ENERGY SCALE  $\approx$  .5 Kev/PHU









74 day Ir<sup>192</sup>

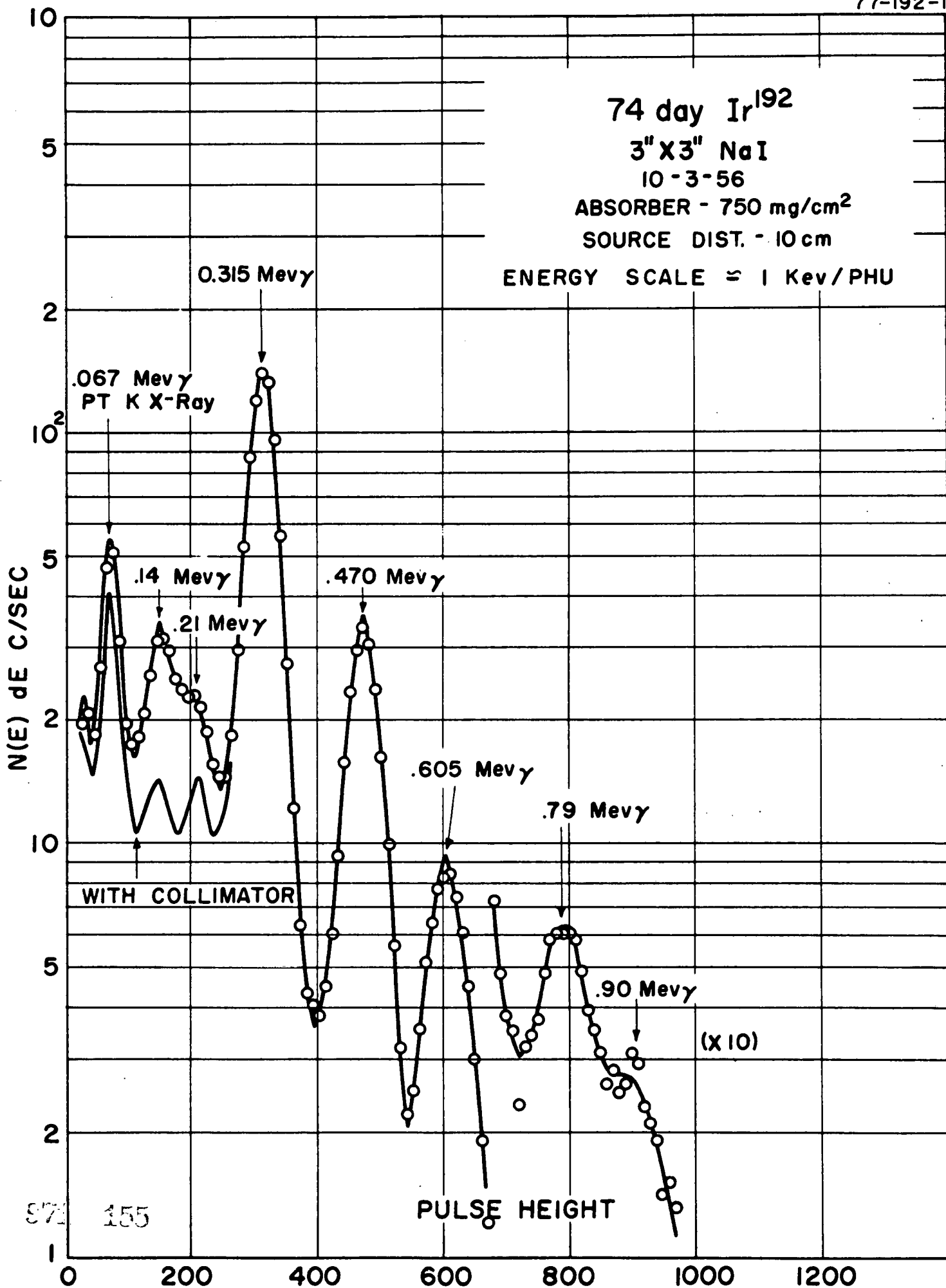
3" X 3" NaI

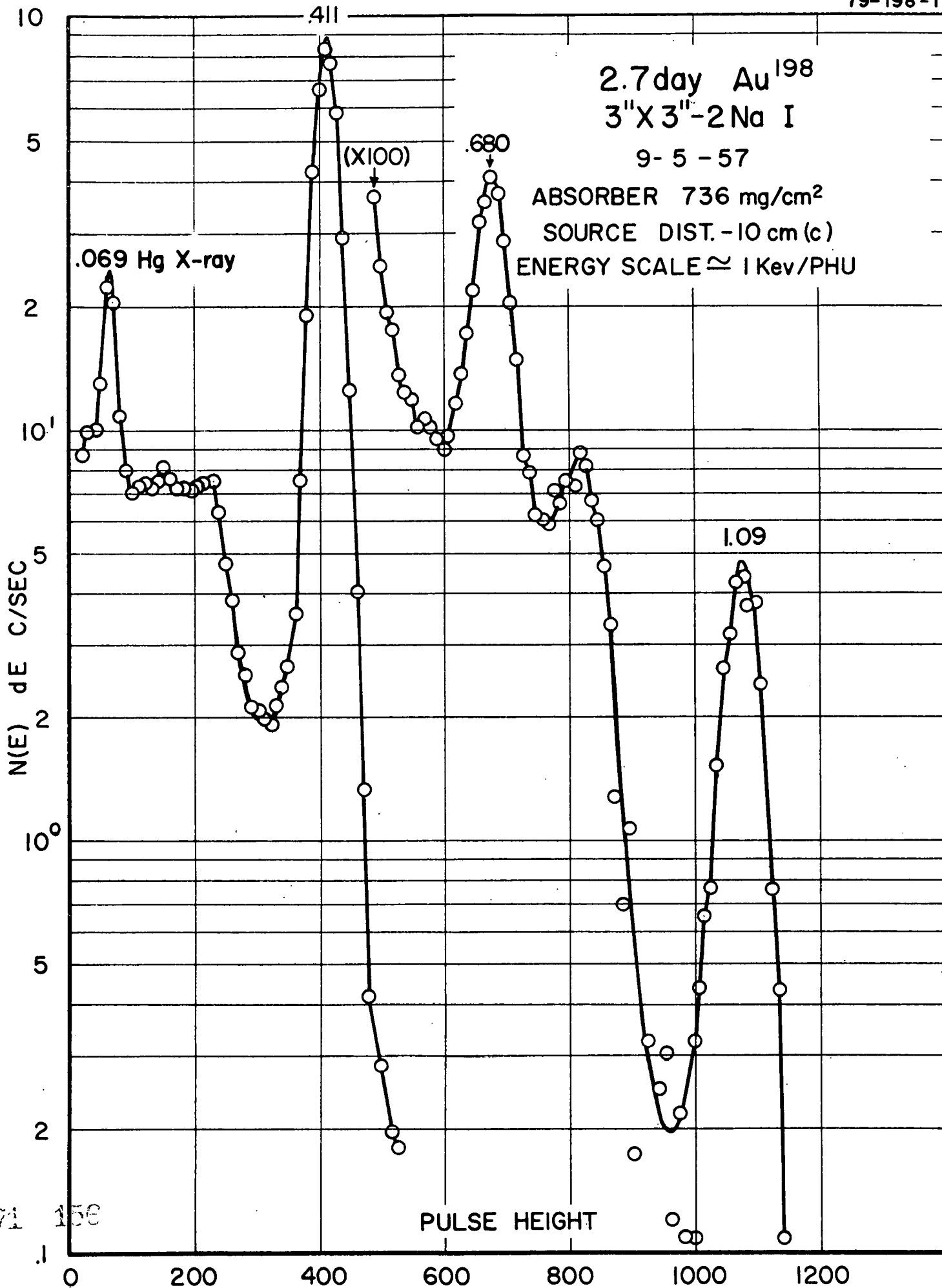
10-3-56

ABSORBER - 750 mg/cm<sup>2</sup>

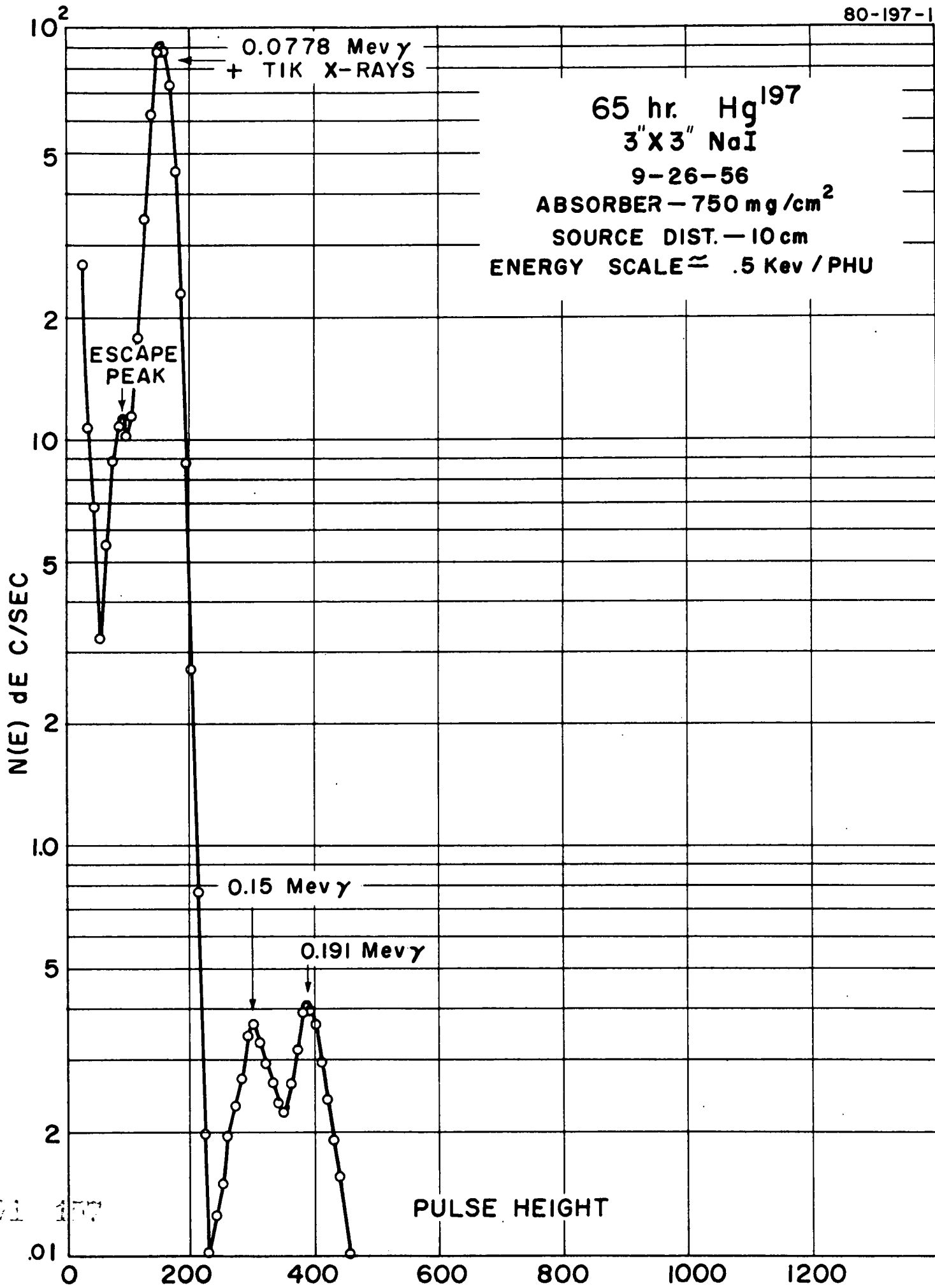
SOURCE DIST. - 10 cm

ENERGY SCALE  $\approx$  1 Kev/PHU





971 156



071 177

23 hr. Hg<sup>197m1</sup> + 65 hr. Hg<sup>197m2</sup>

3" X 3" NaI

9-21-56

ABSORBER - 750 mg/cm<sup>2</sup>

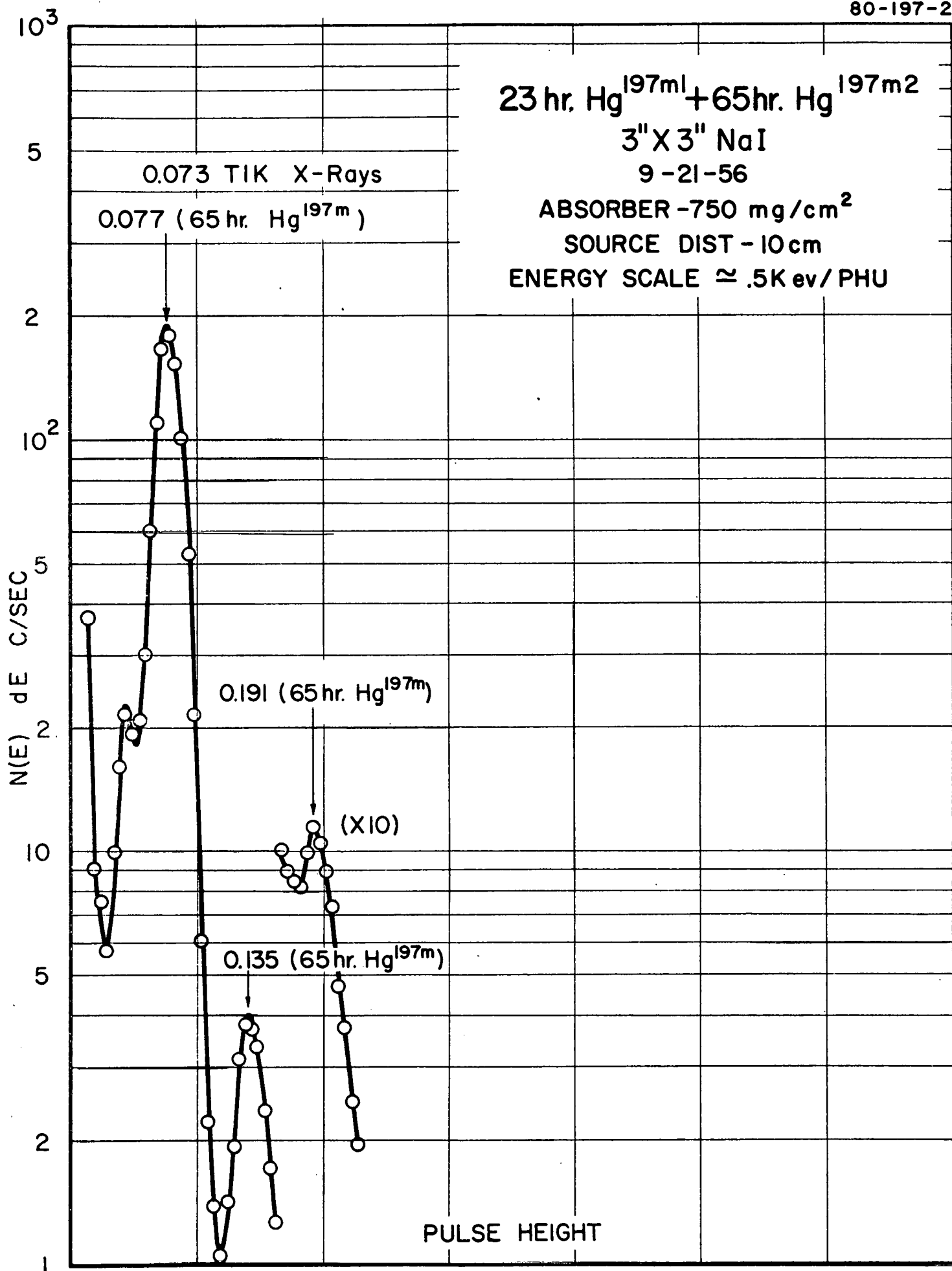
SOURCE DIST - 10 cm

ENERGY SCALE  $\approx$  .5K ev/PHU

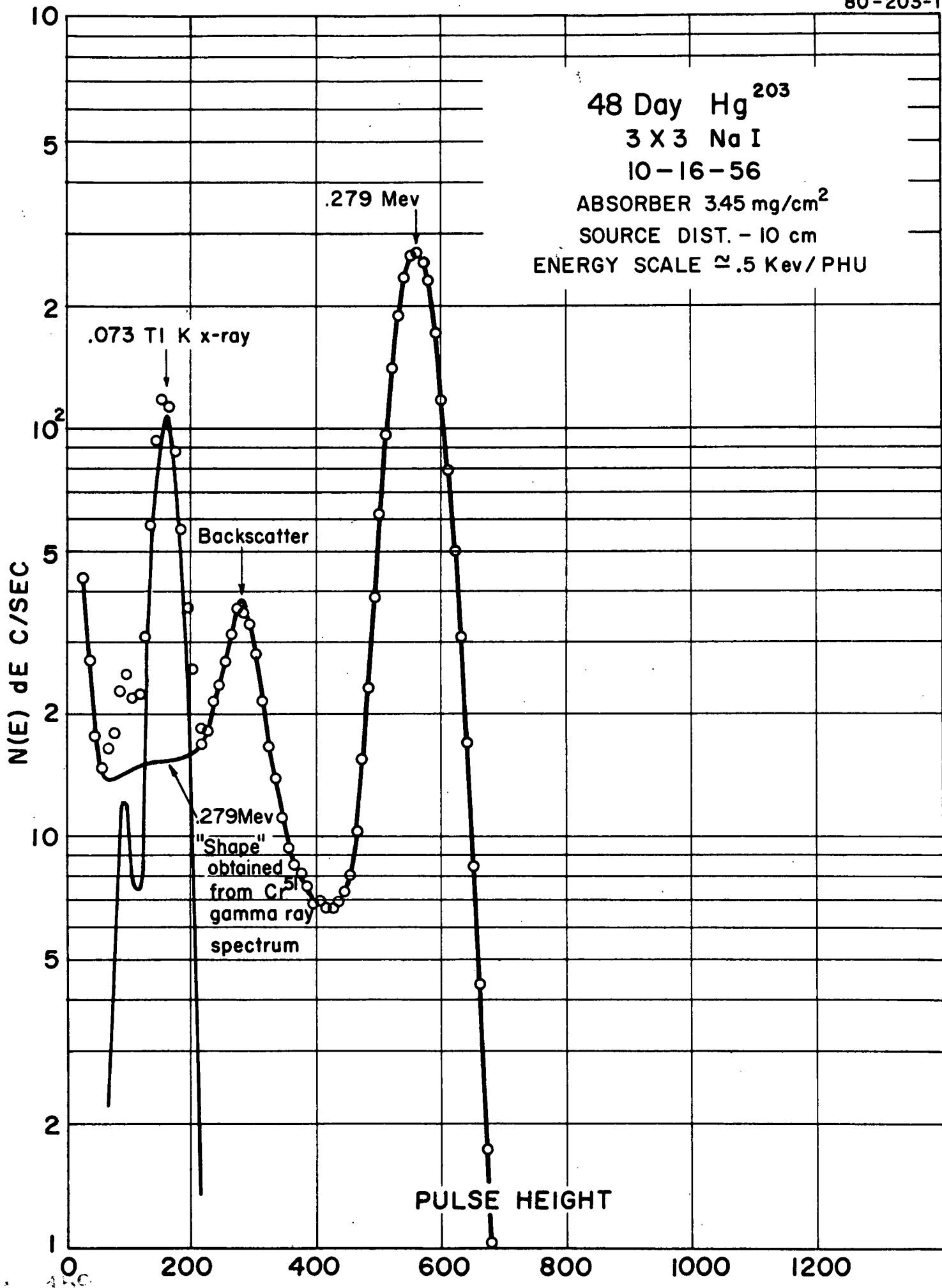
0.073 TIK X-Rays

0.077 (65 hr. Hg<sup>197m</sup>)0.191 (65 hr. Hg<sup>197m</sup>)

(X10)

0.135 (65 hr. Hg<sup>197m</sup>)

PULSE HEIGHT



15 day Bi<sup>205</sup>

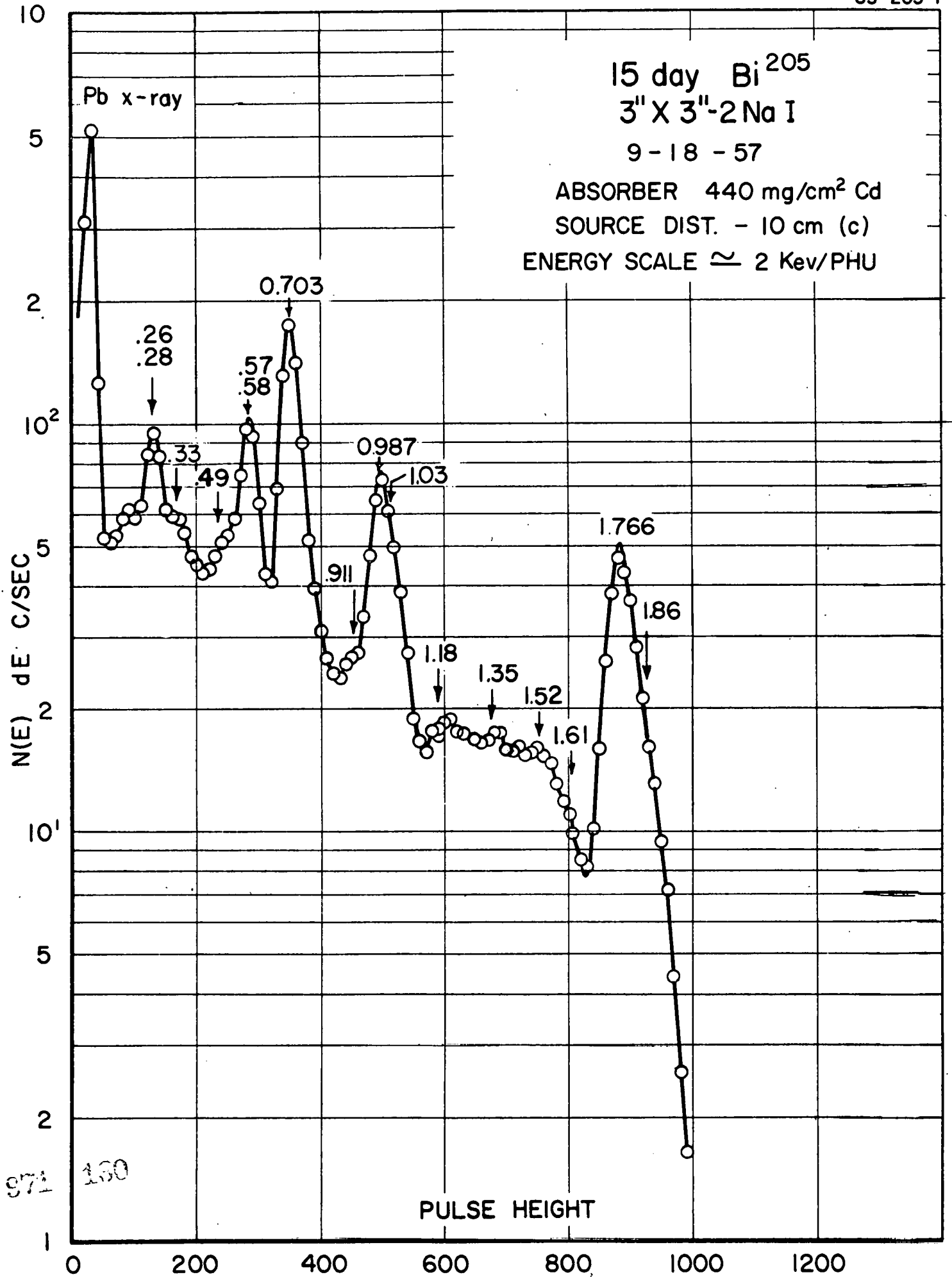
3" X 3"-2Na I

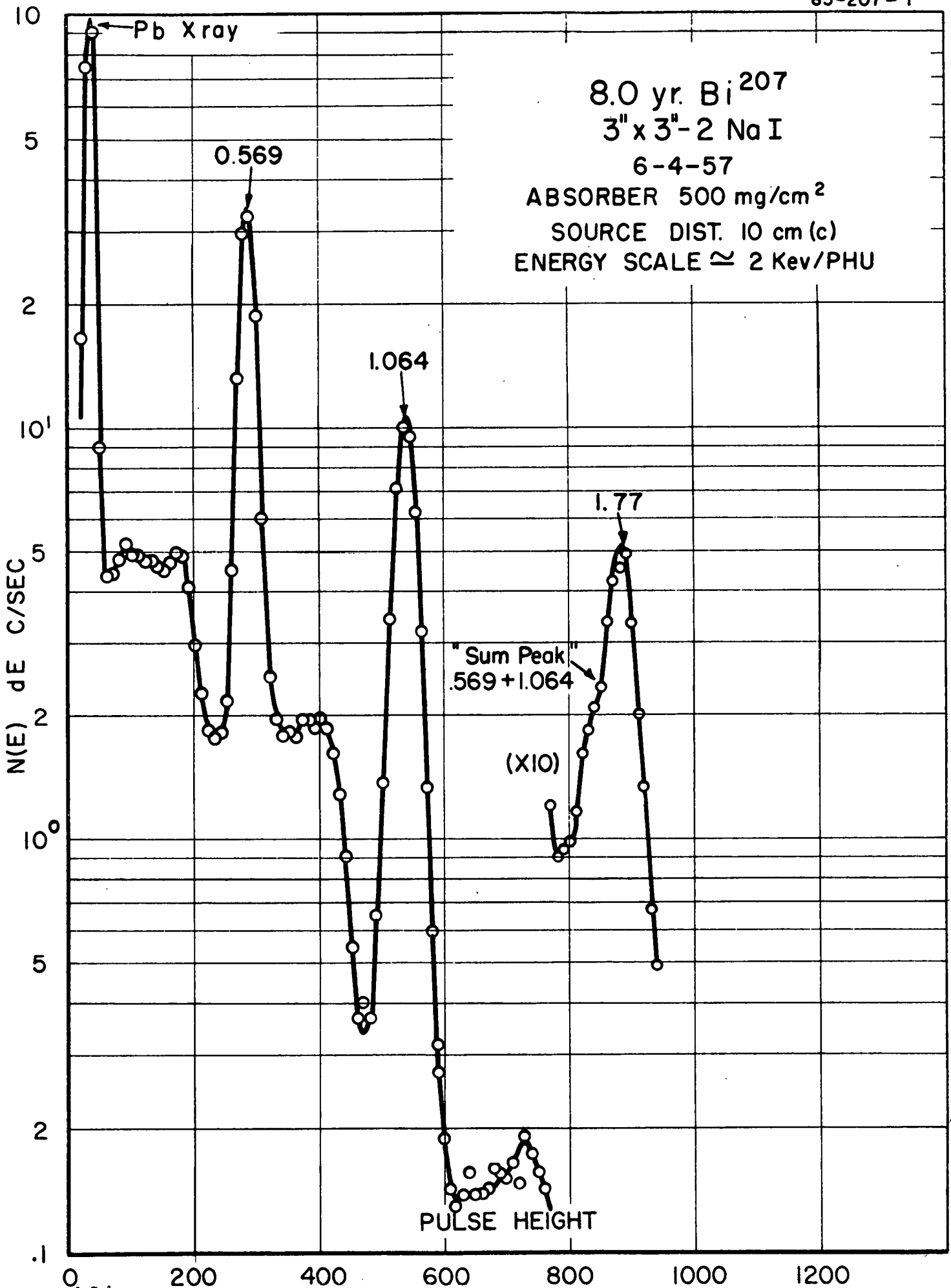
9-18-57

ABSORBER 440 mg/cm<sup>2</sup> Cd

SOURCE DIST. - 10 cm (c)

ENERGY SCALE  $\approx$  2 Kev/PHU





# 1620 yr. Ra<sup>226</sup> AND DECAY PRODUCTS—4 d FOLLOWING SEPARATION

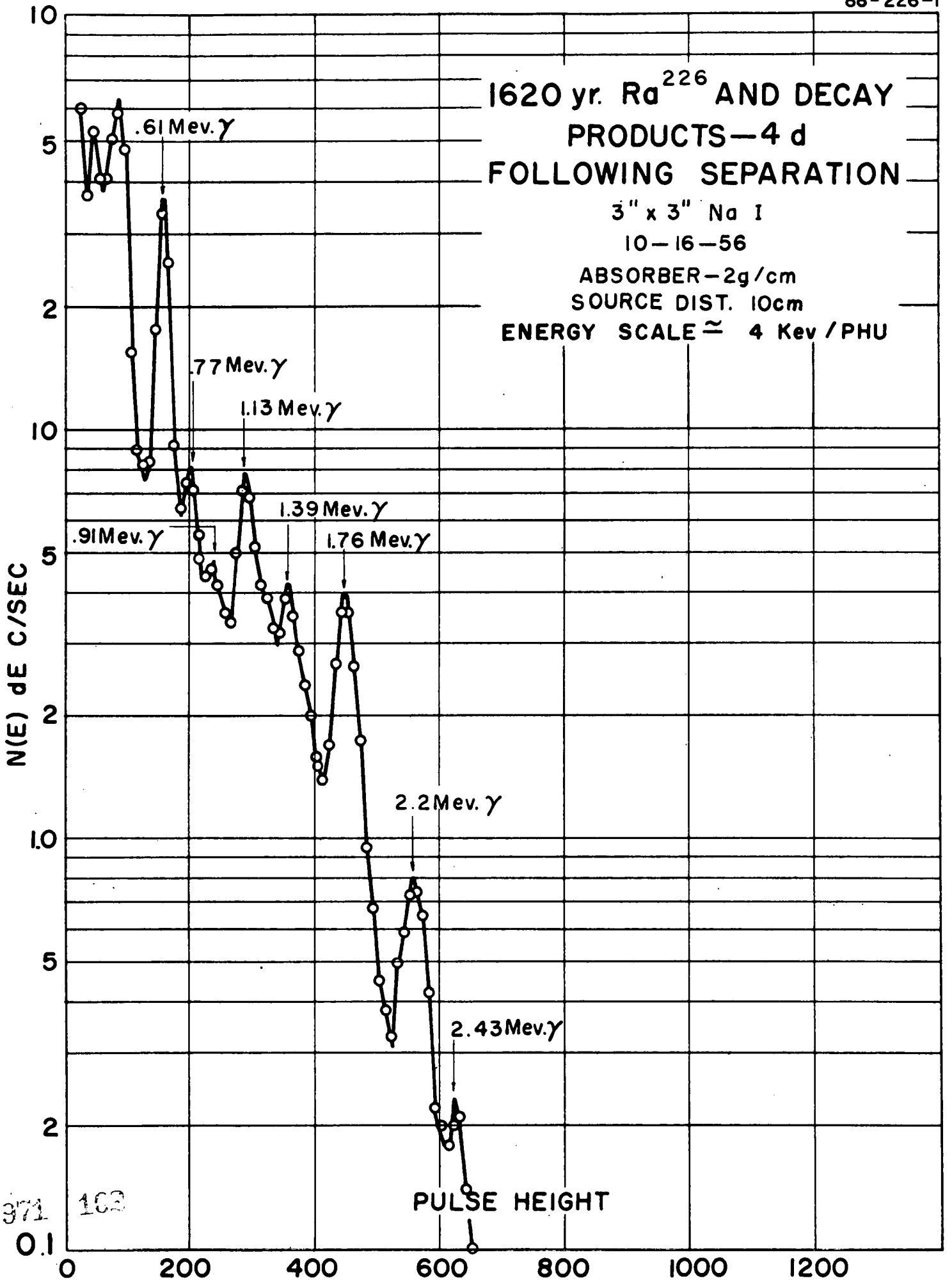
3" x 3" Na I

10-16-56

ABSORBER—2g/cm

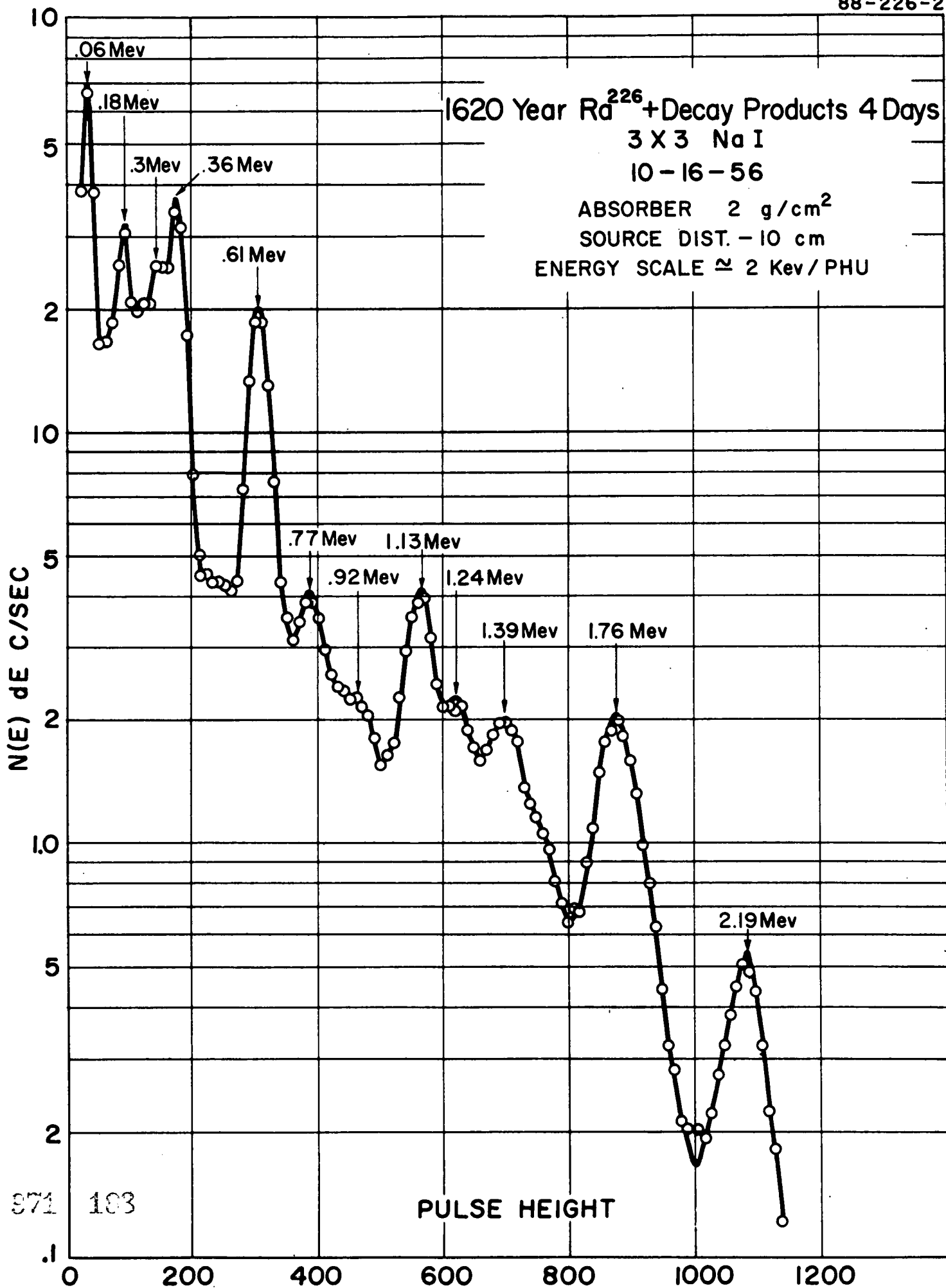
SOURCE DIST. 10cm

ENERGY SCALE  $\approx$  4 Kev / PHU



371 162  
0.1

PULSE HEIGHT



371 183

# 27.4 day Pa<sup>233</sup> GAMMAS

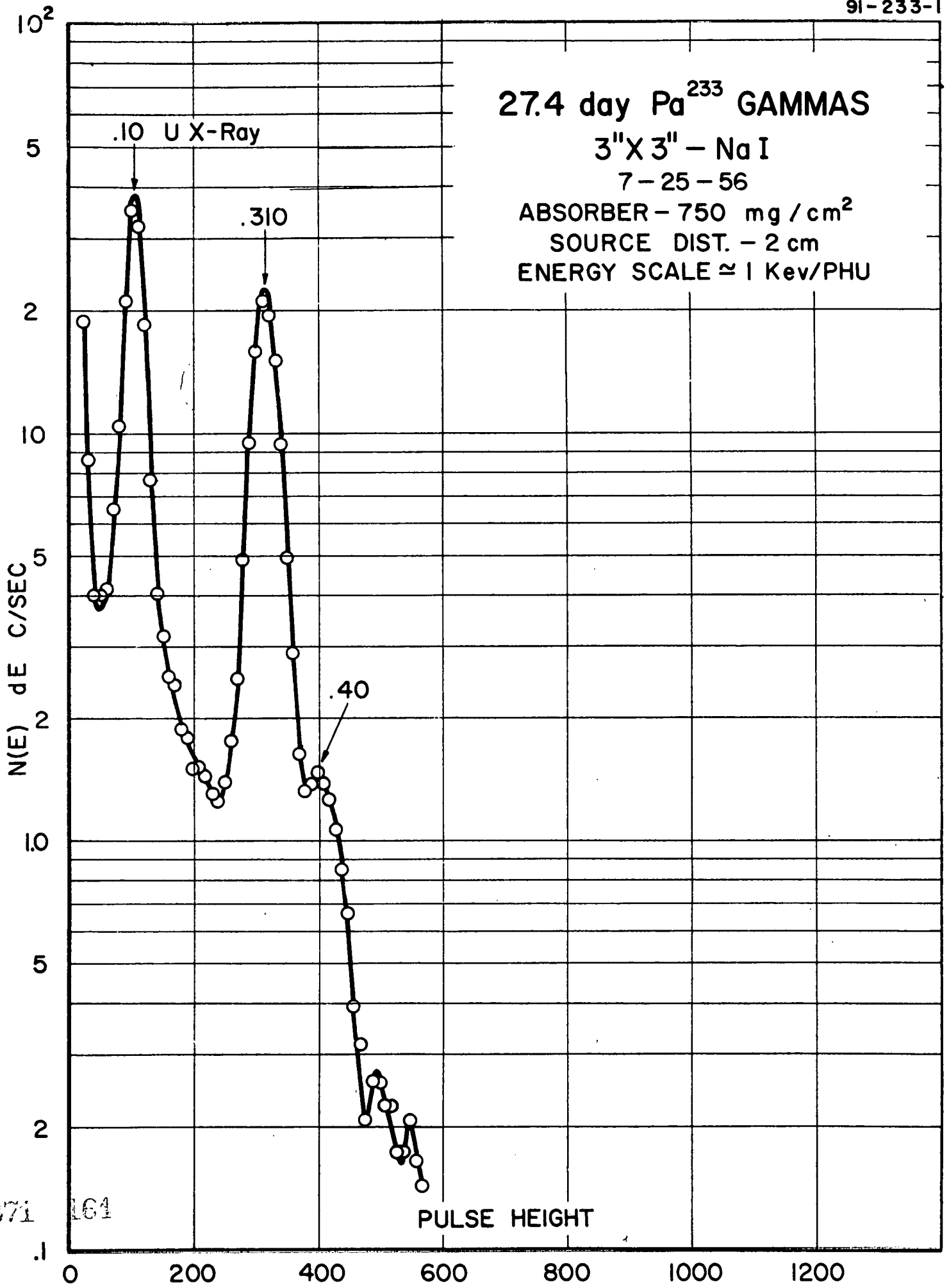
3" X 3" - Na I

7-25-56

ABSORBER - 750 mg/cm<sup>2</sup>

SOURCE DIST. - 2 cm

ENERGY SCALE  $\approx$  1 Kev/PHU



971 164

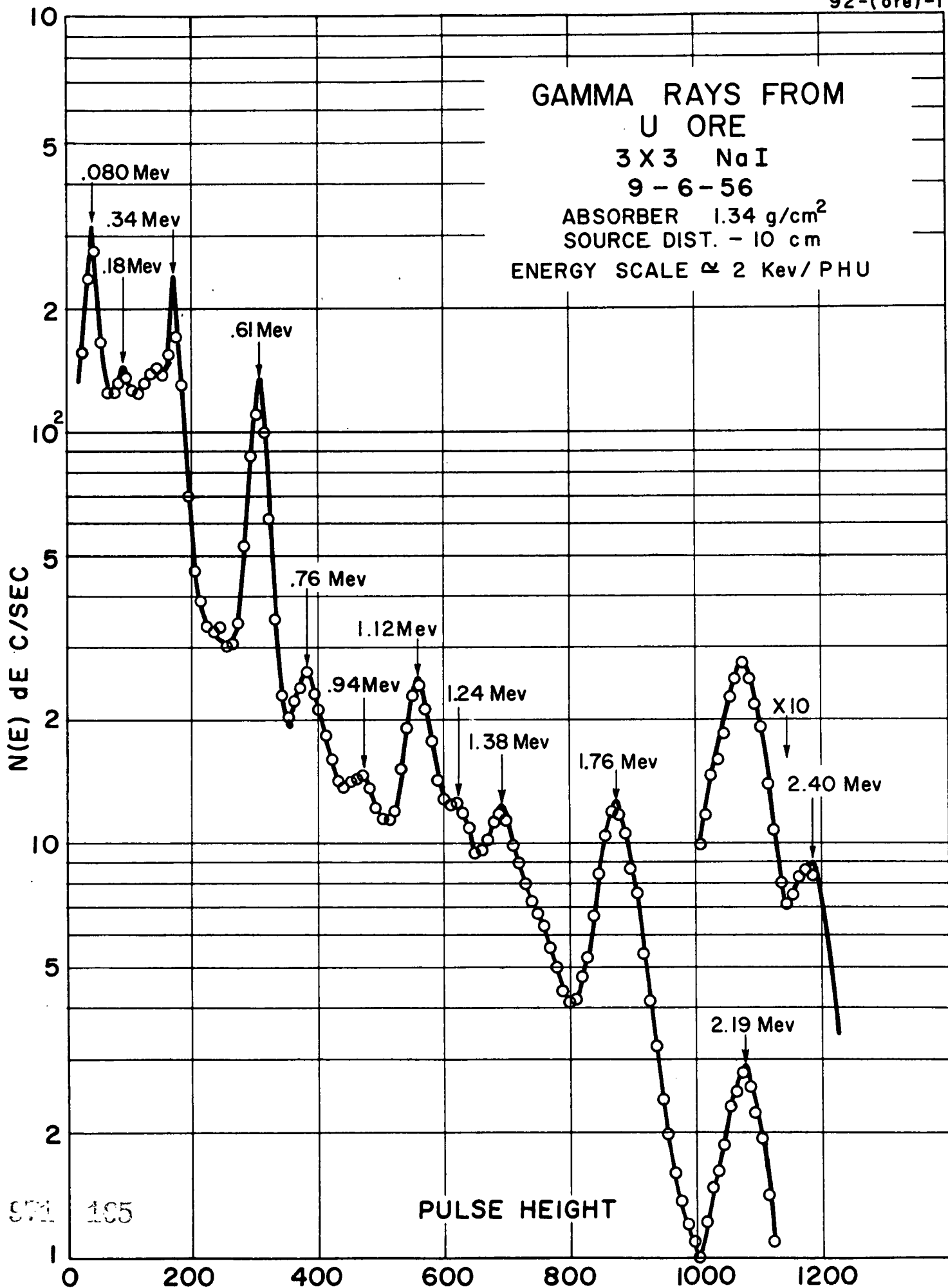
PULSE HEIGHT

# GAMMA RAYS FROM U ORE

3 X 3 NaI  
9 - 6 - 56

ABSORBER 1.34 g/cm<sup>2</sup>  
SOURCE DIST. - 10 cm

ENERGY SCALE  $\approx$  2 Kev/PHU



971 105

21.3 hr. Mg<sup>28</sup> - 2.3 min. Al<sup>28</sup>

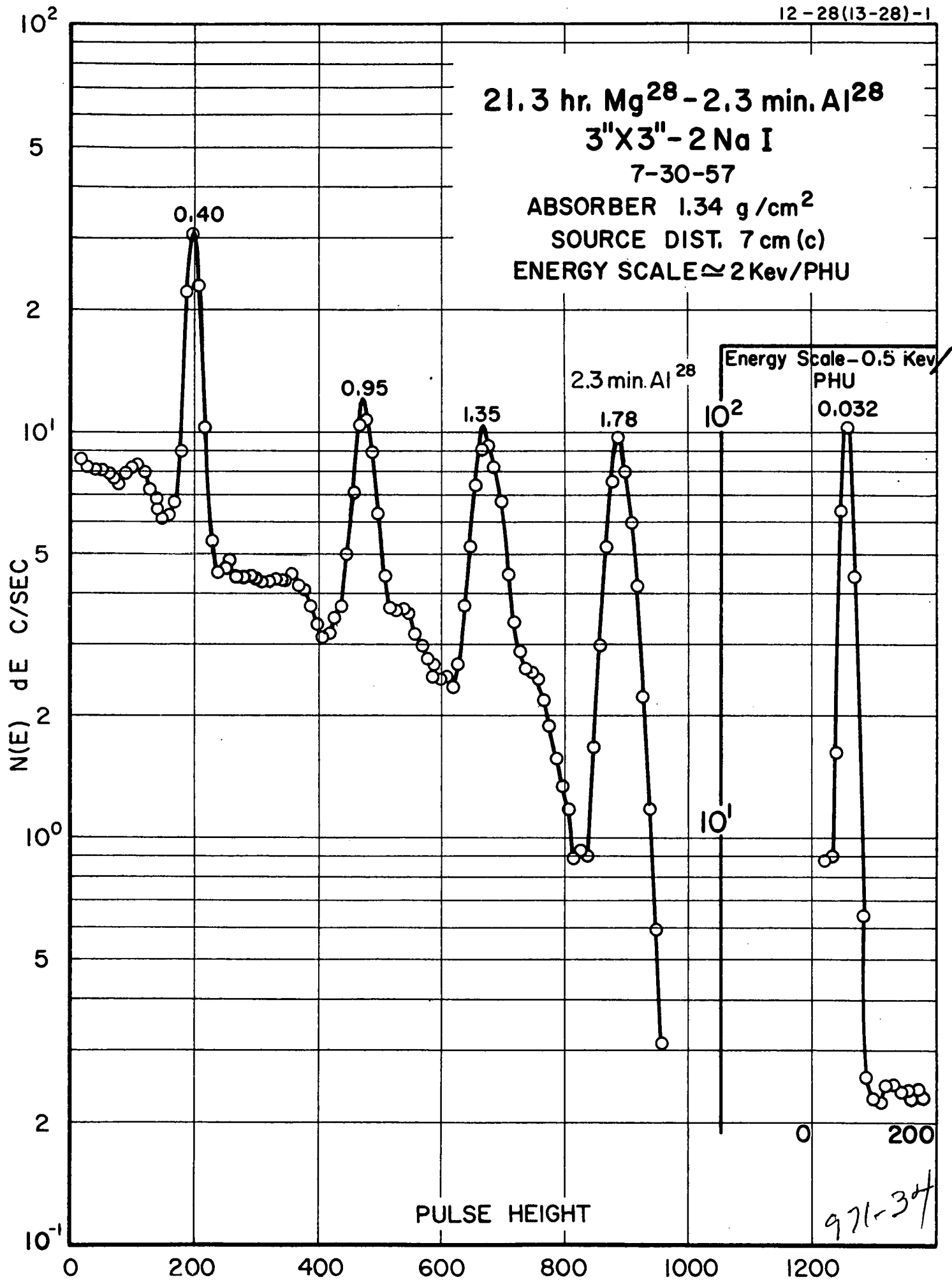
3"X3" - 2 Na I

7-30-57

ABSORBER 1.34 g/cm<sup>2</sup>

SOURCE DIST. 7 cm (c)

ENERGY SCALE  $\approx$  2 Kev/PHU



6.7 day U<sup>237</sup>

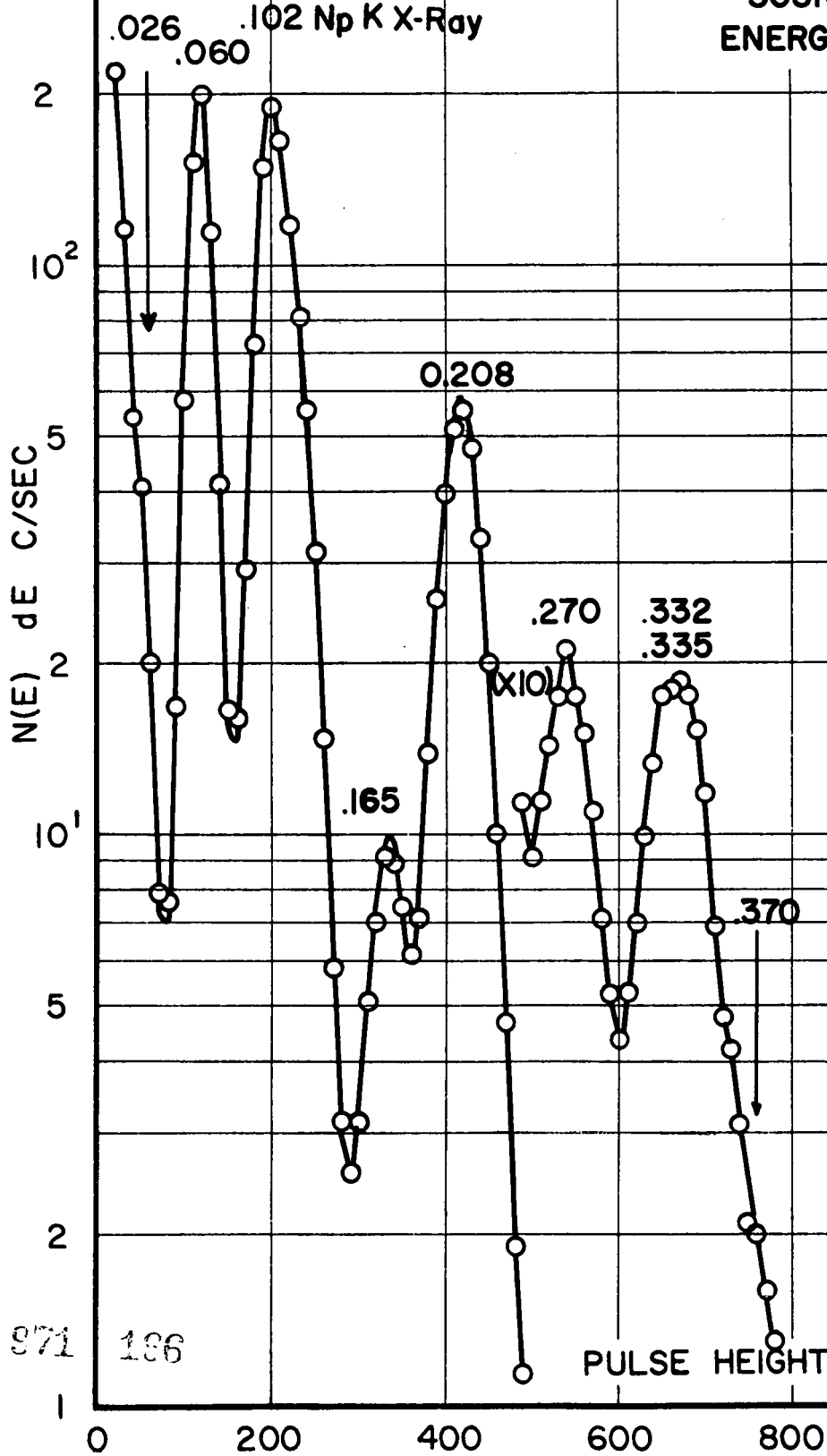
3"X3"-2 NaI

8-27-57

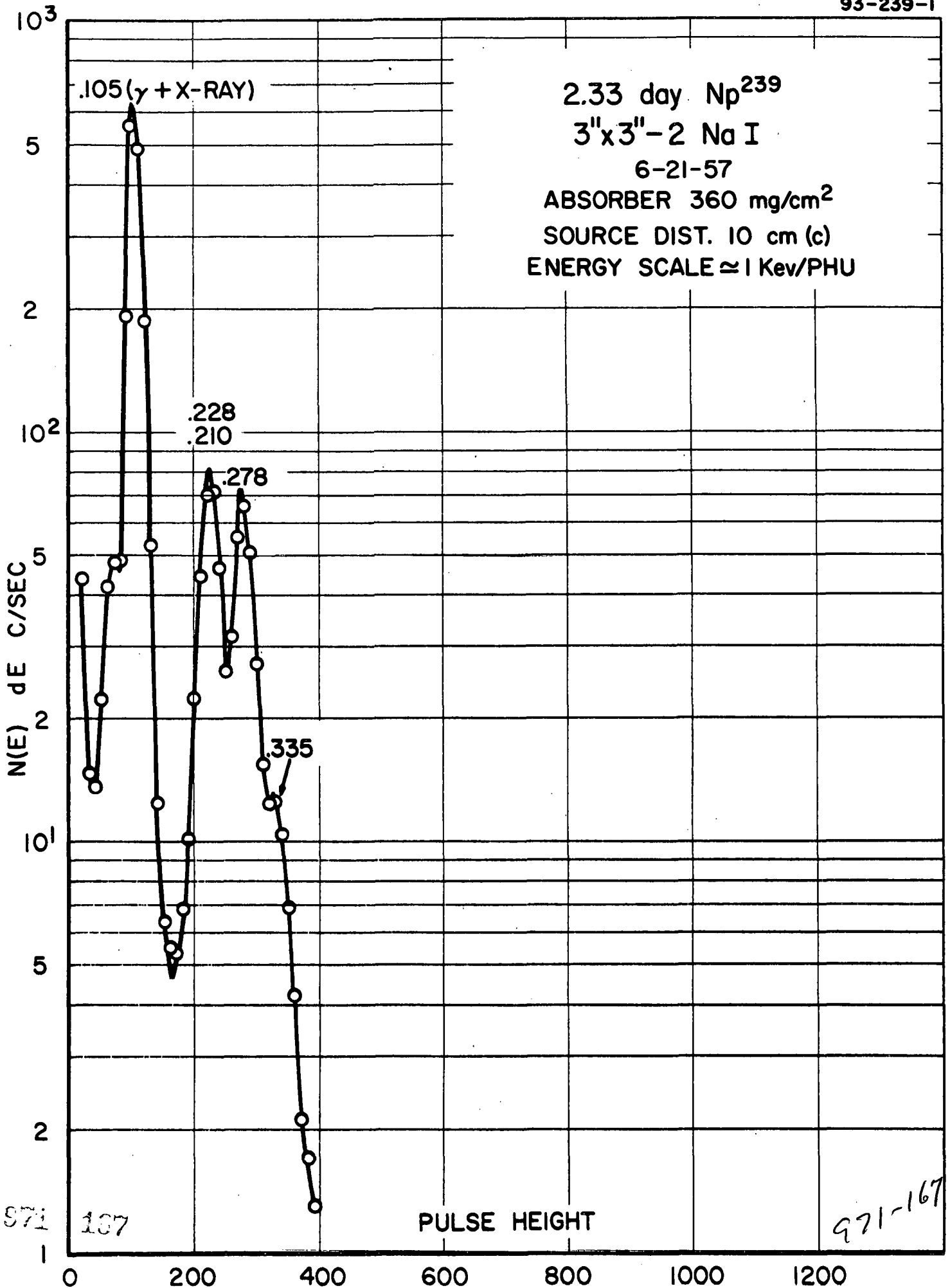
ABSORBER 200 mg/cm<sup>2</sup>

SOURCE DIST. 10 cm(c)

ENERGY SCALE ≈ 0.5 Kev/PHU



971

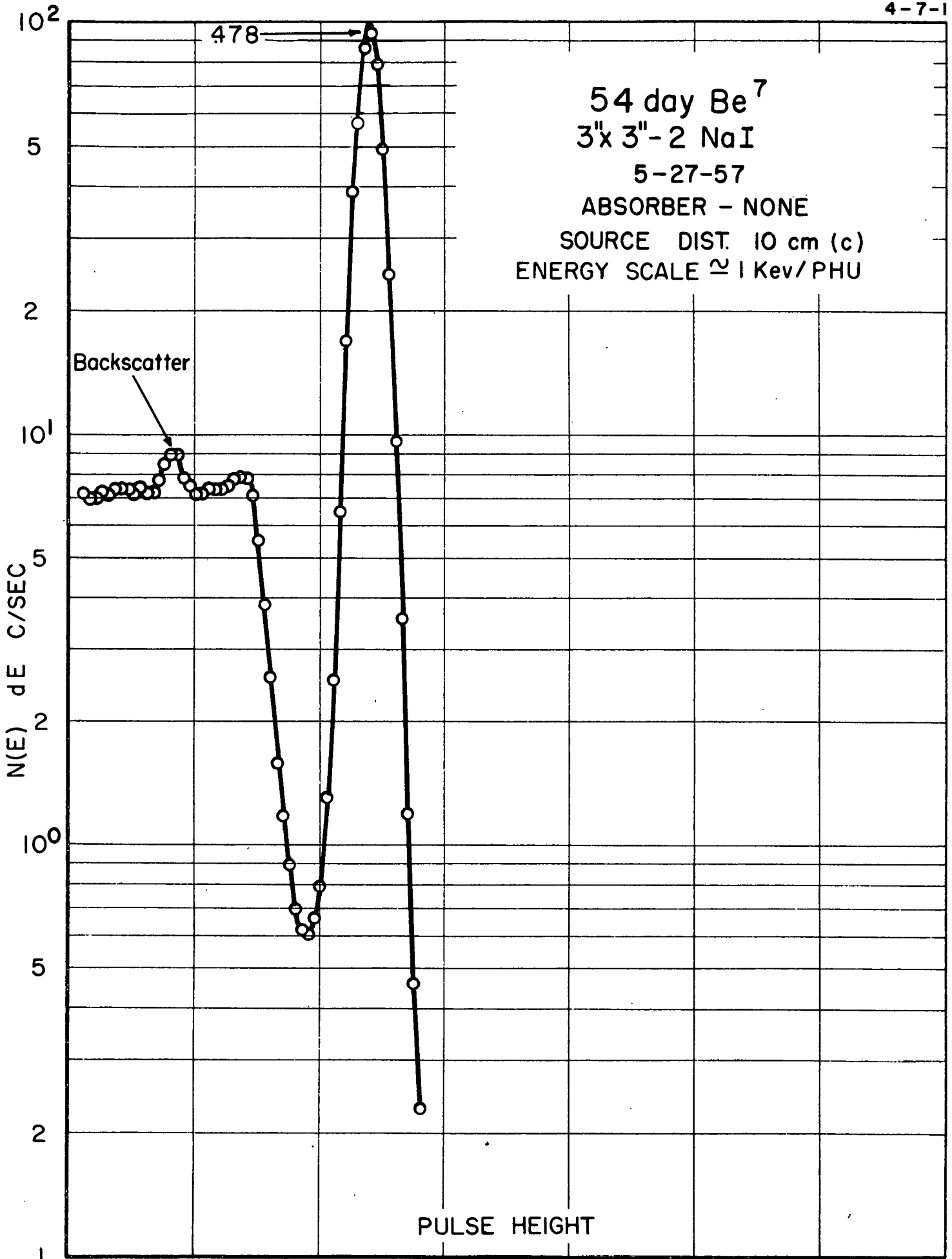


APPENDIX I

DETECTOR EFFICIENCY CURVES

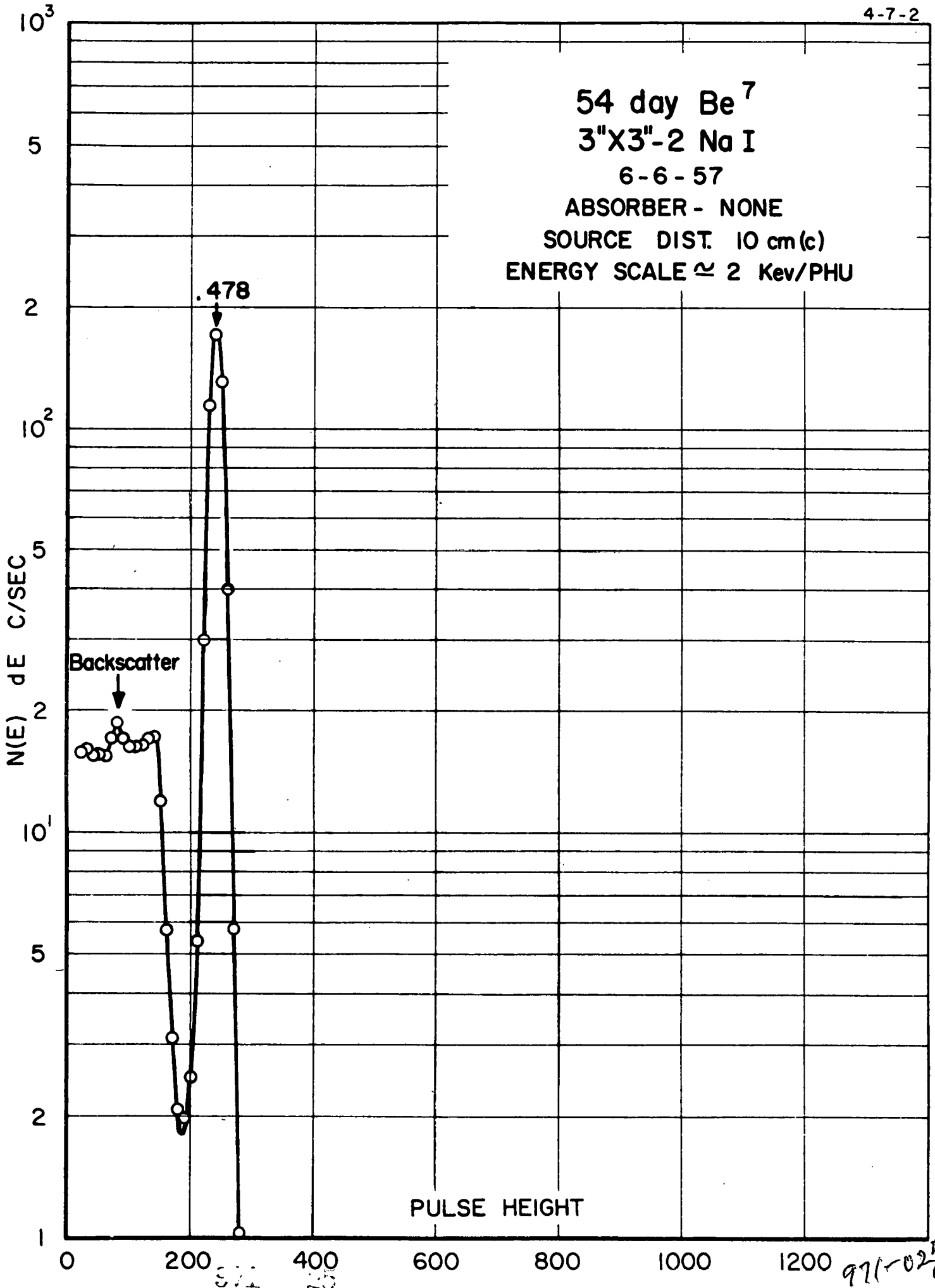
---

~~971~~ 971-168



971-024

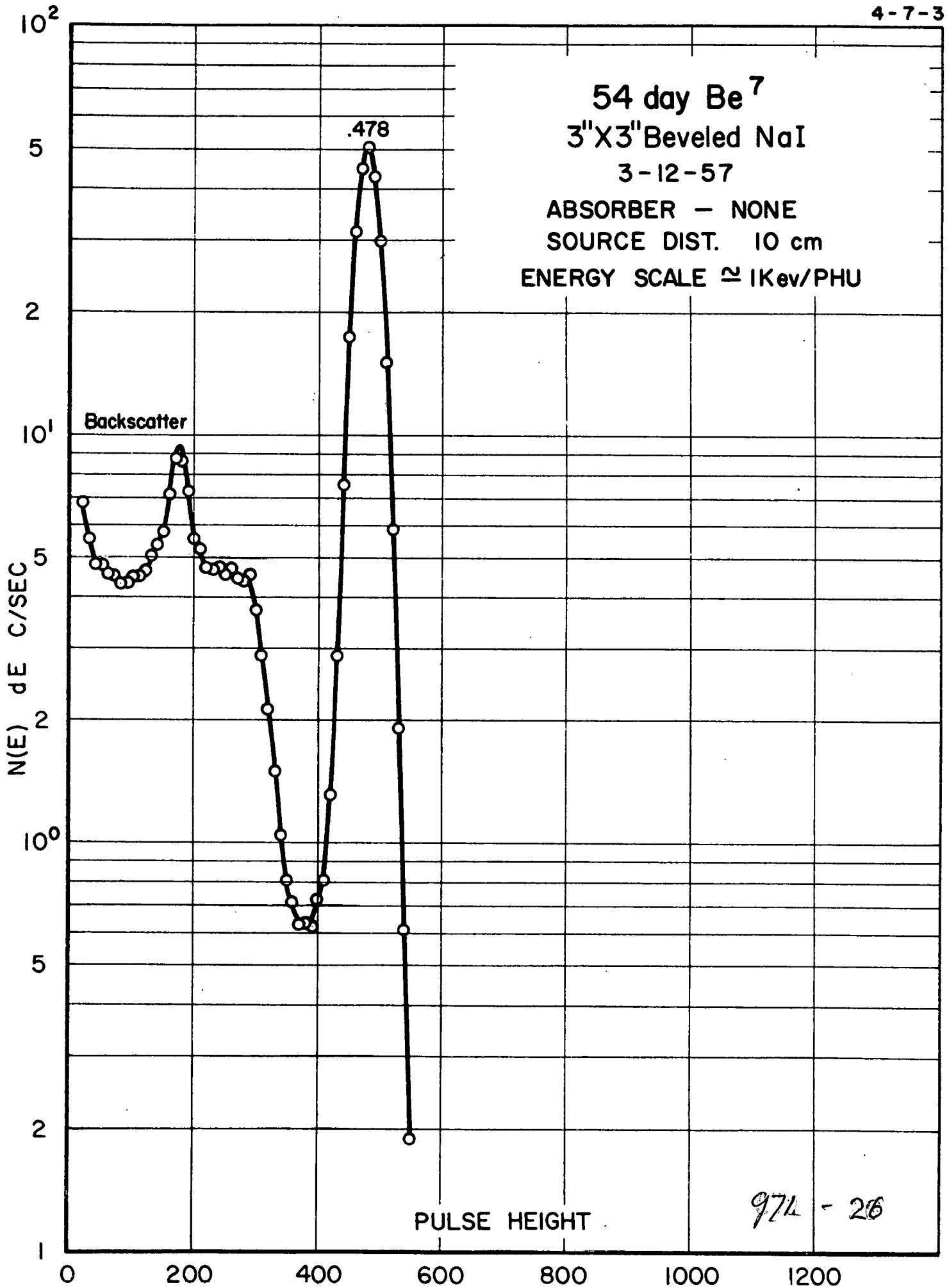
54 day Be<sup>7</sup>  
3"X3"-2 Na I  
6-6-57  
ABSORBER - NONE  
SOURCE DIST. 10 cm(c)  
ENERGY SCALE ≈ 2 Kev/PHU

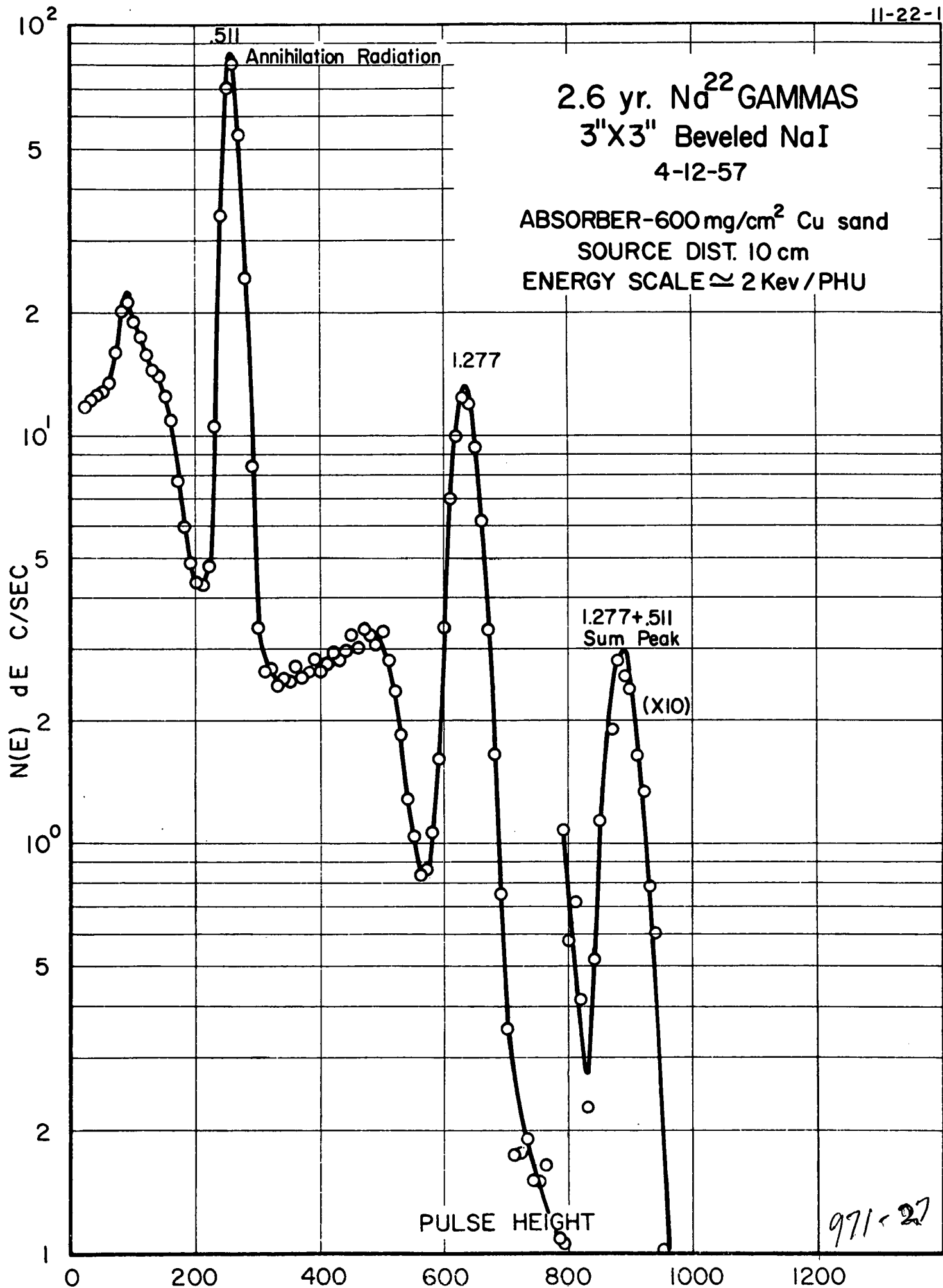


371

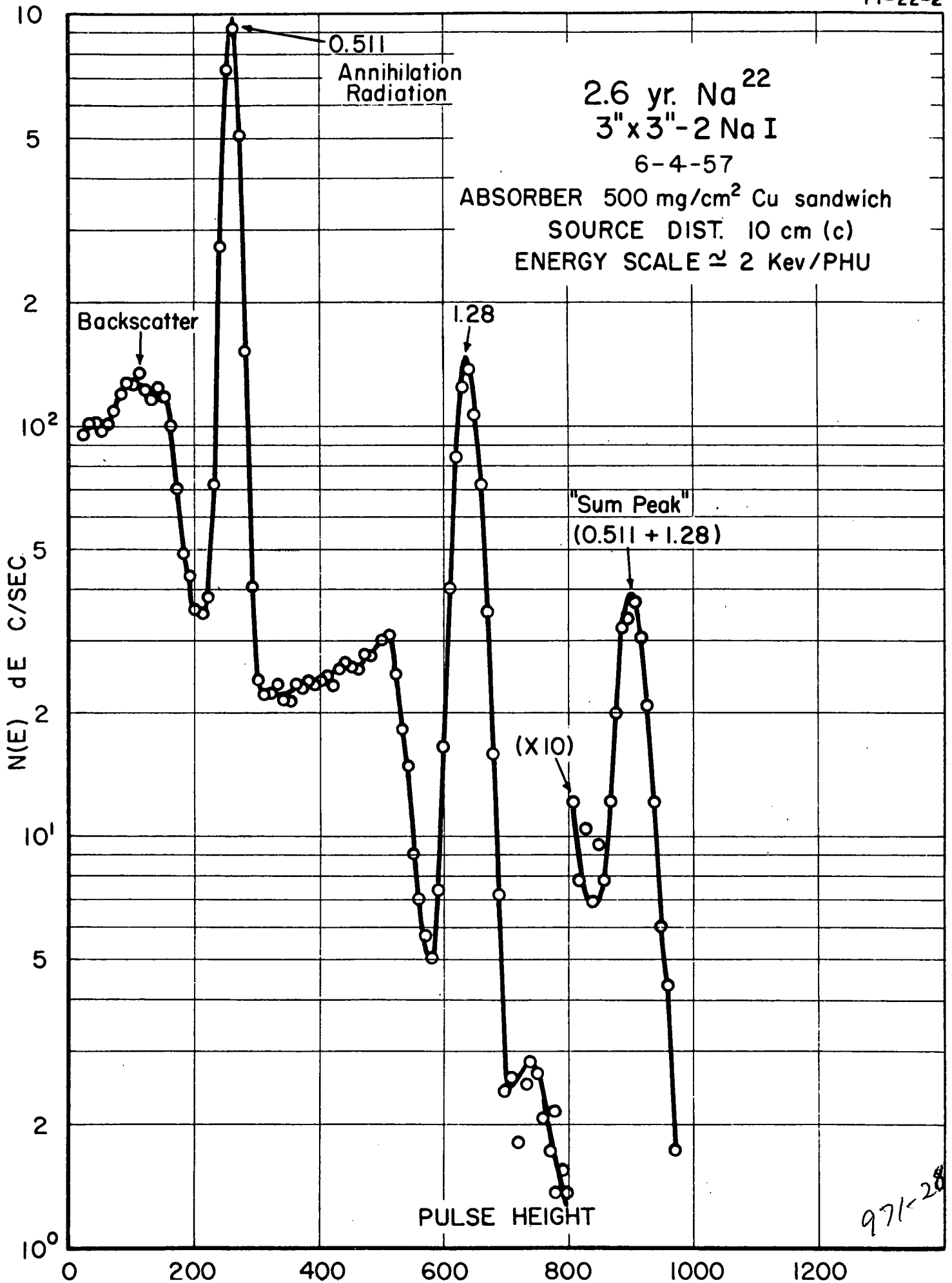
25

971-025

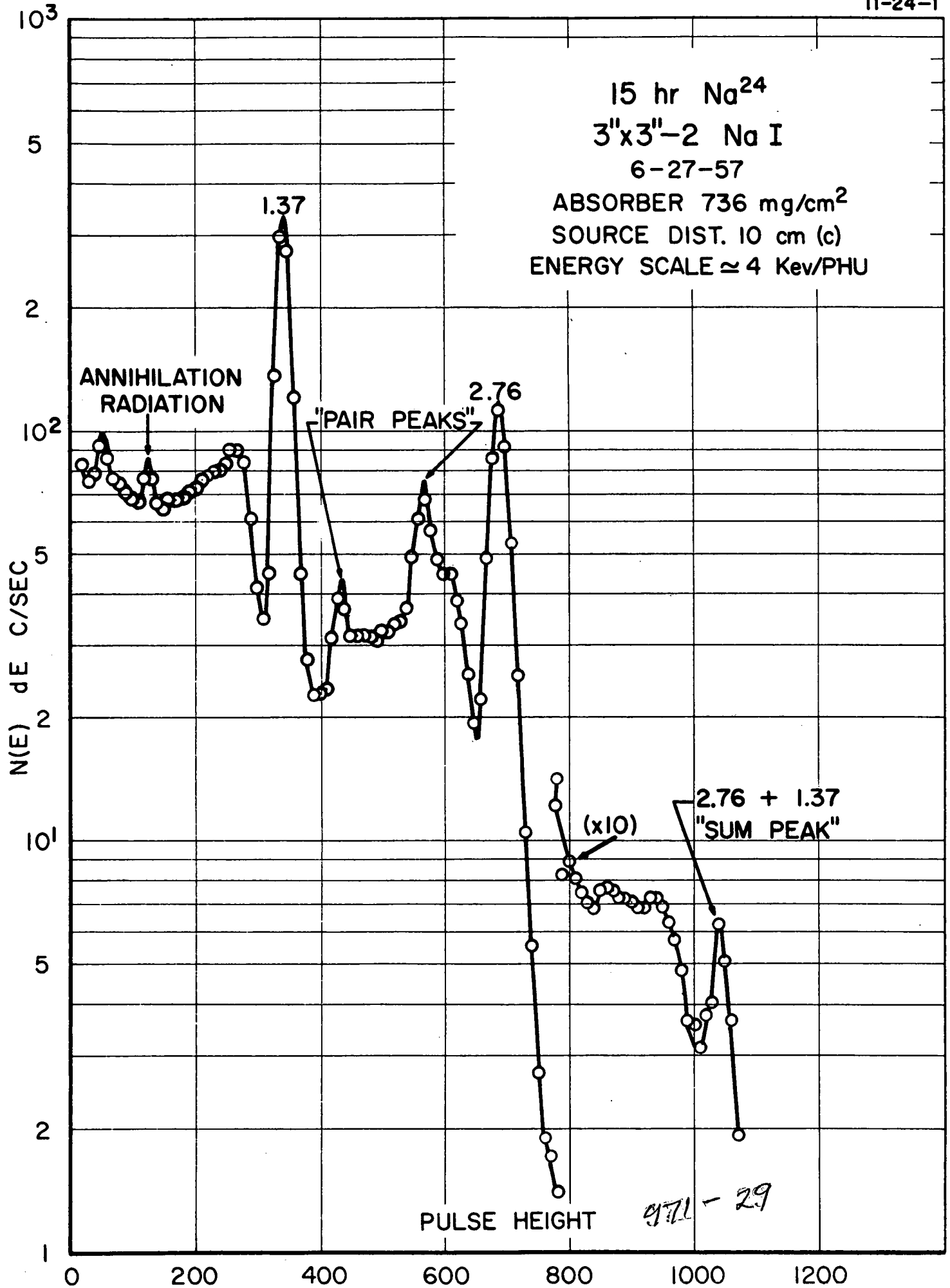


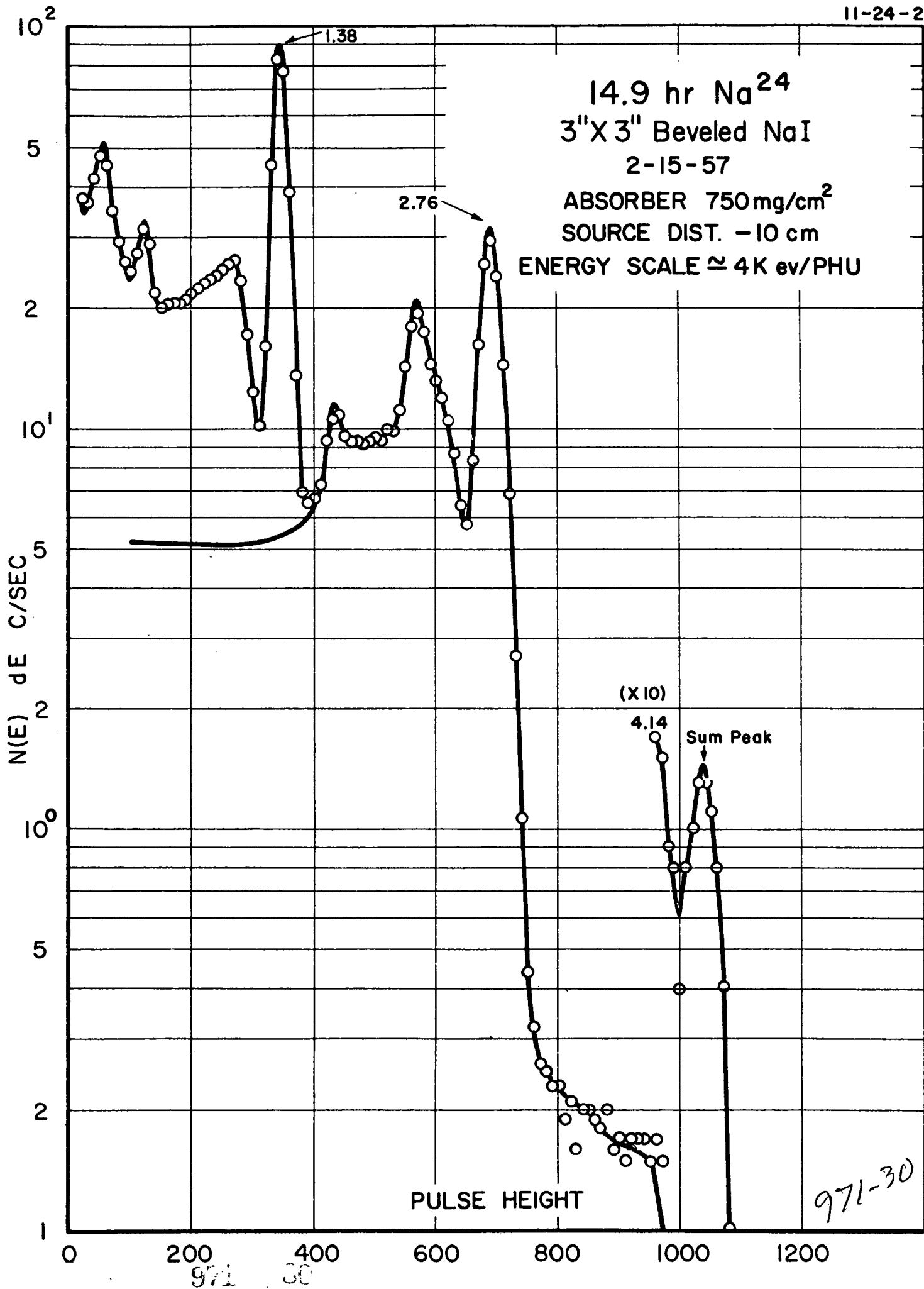


971-27



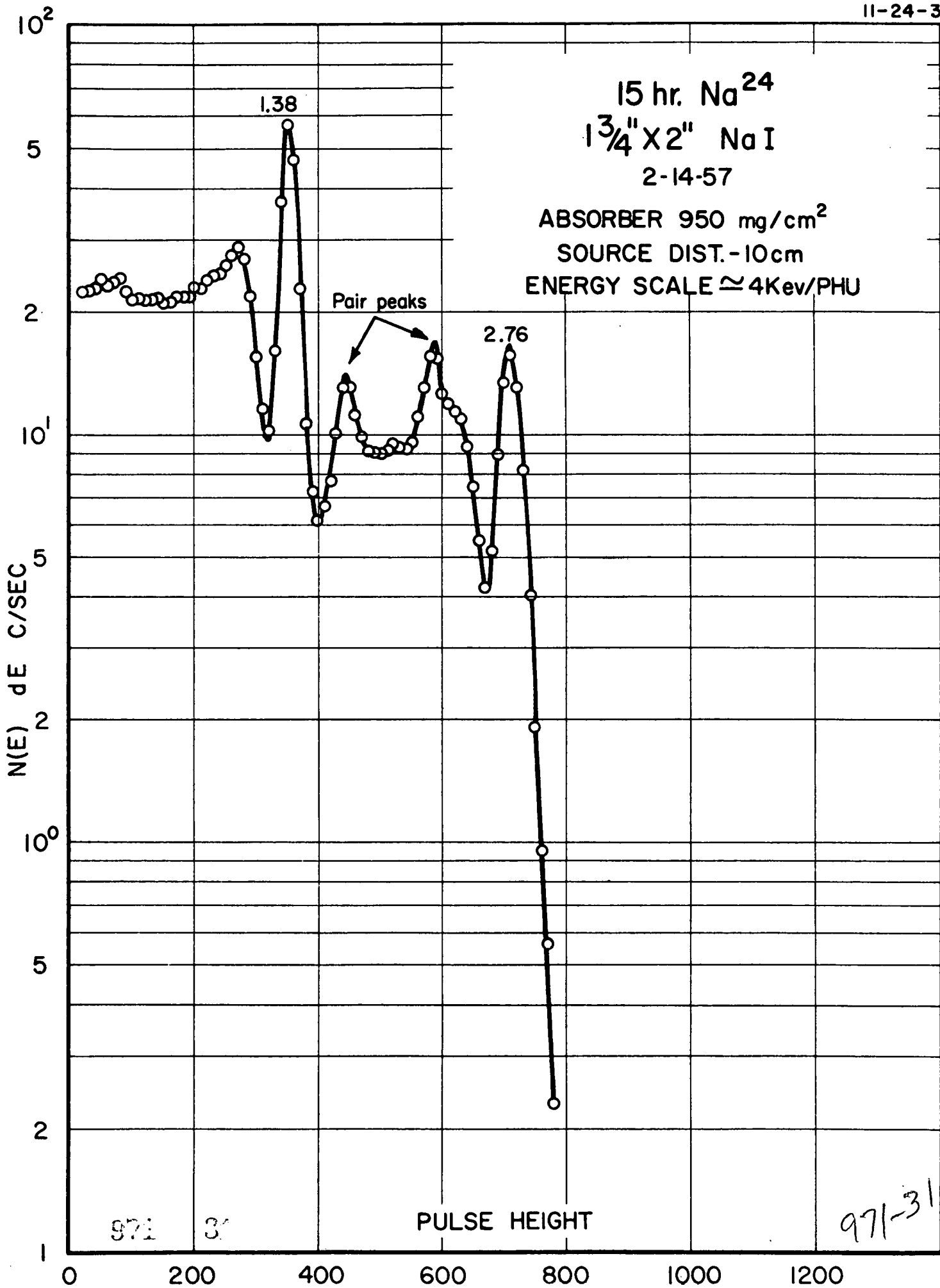
971-28

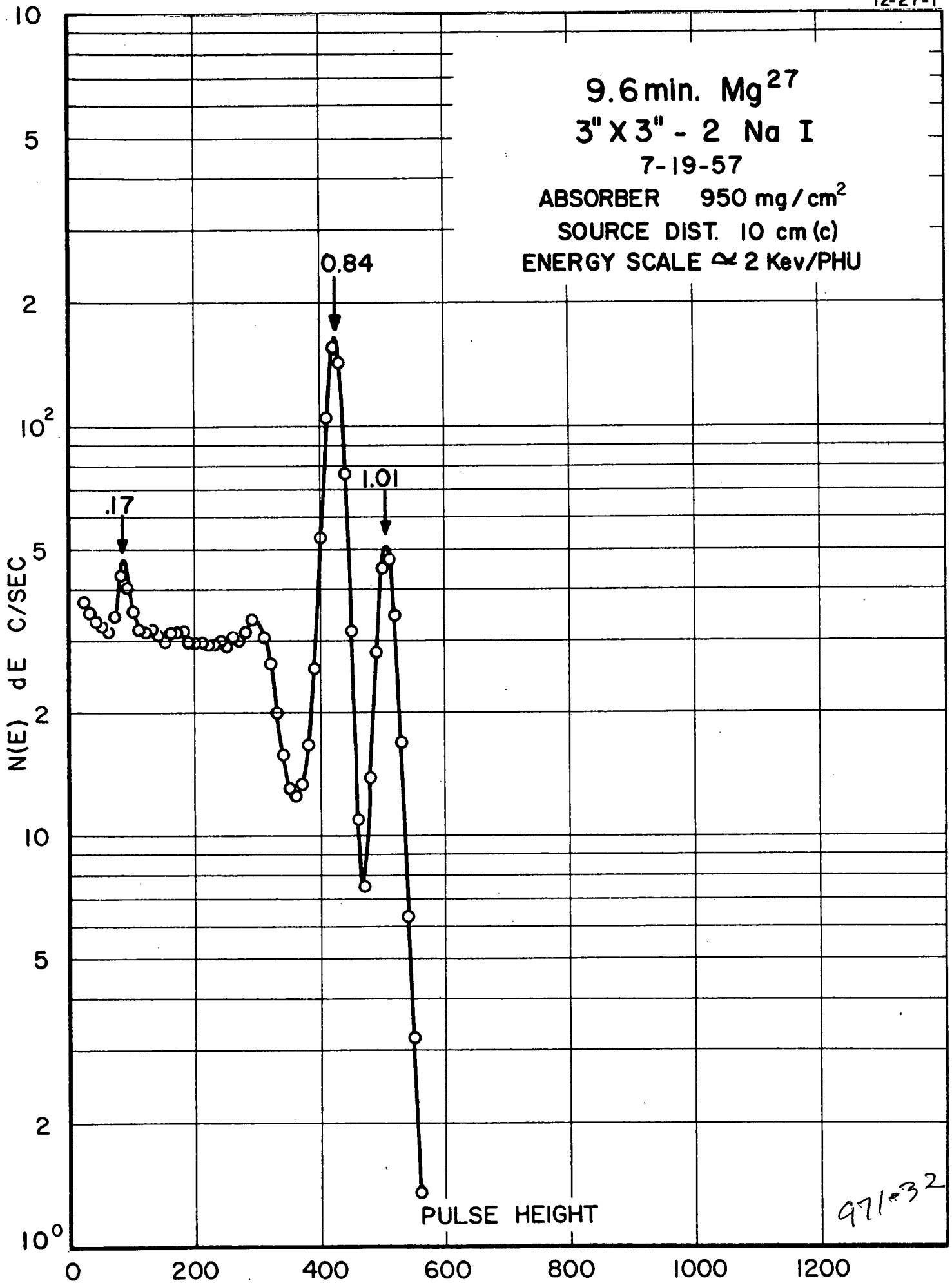




15 hr. Na<sup>24</sup>  
1 3/4" X 2" Na I  
2-14-57

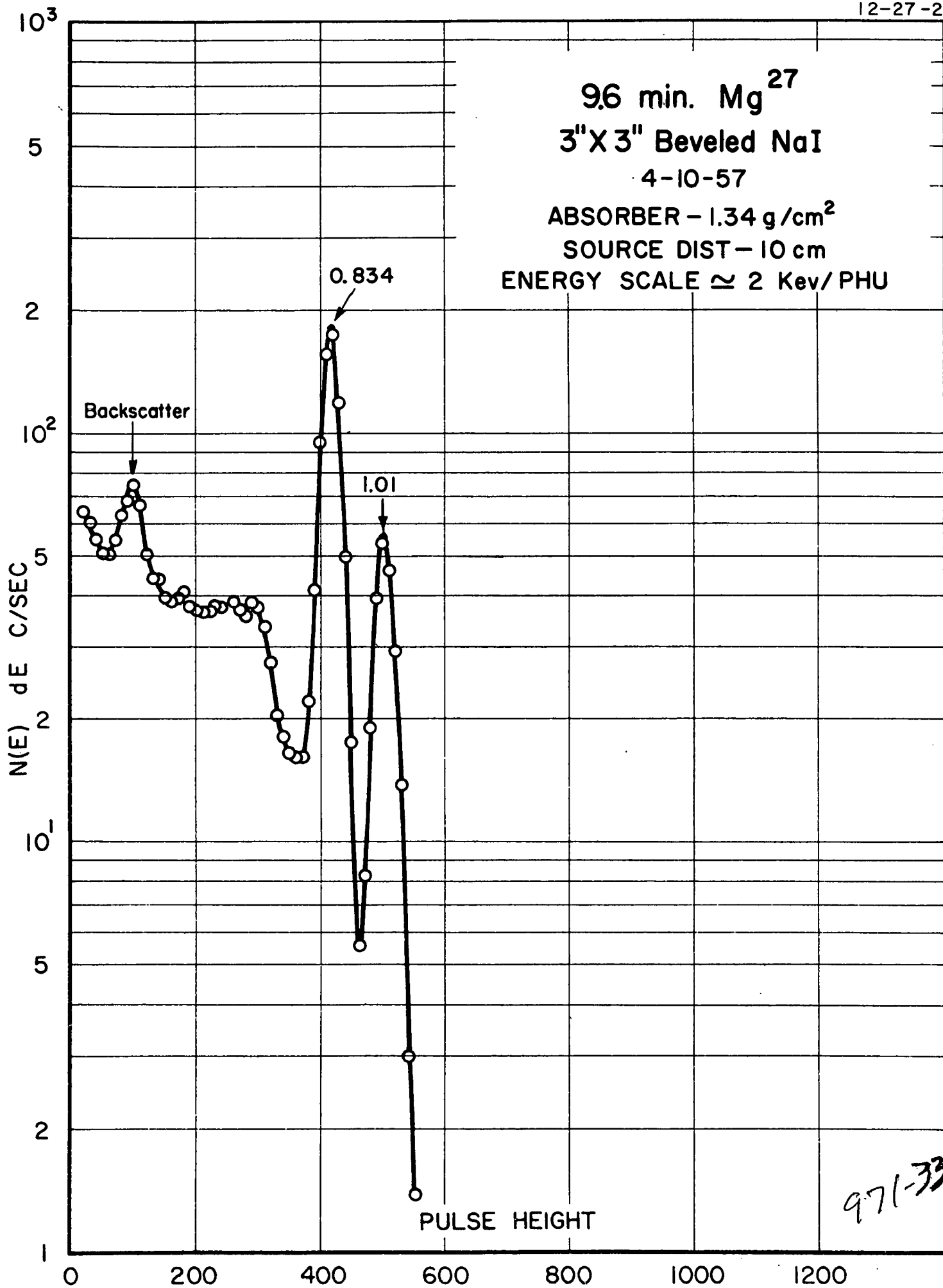
ABSORBER 950 mg/cm<sup>2</sup>  
SOURCE DIST. - 10cm  
ENERGY SCALE  $\approx$  4Kev/PHU





971e32

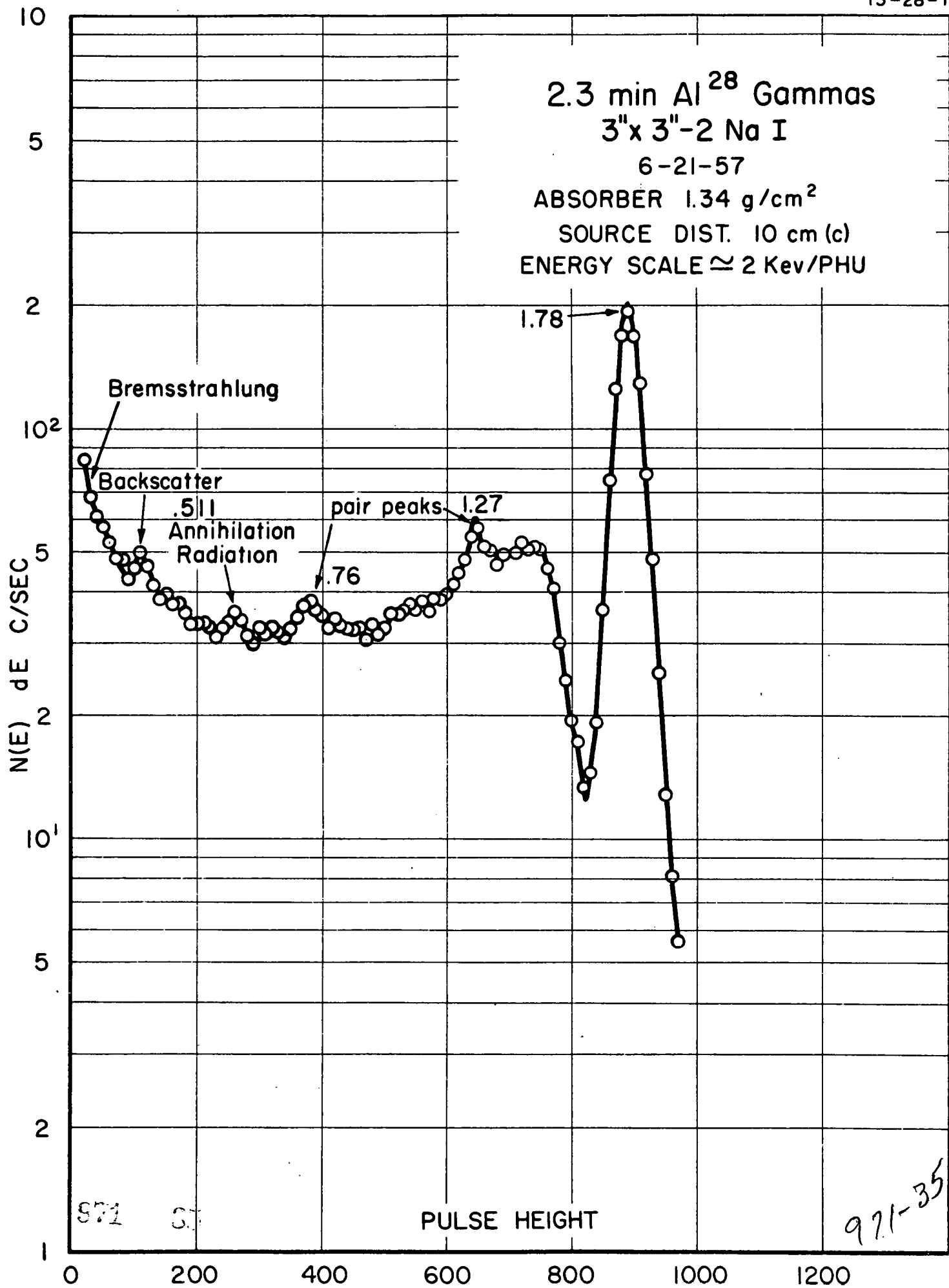
9.6 min.  $Mg^{27}$   
3" X 3" Beveled NaI  
4-10-57  
ABSORBER - 1.34 g/cm<sup>2</sup>  
SOURCE DIST - 10 cm  
ENERGY SCALE  $\approx$  2 Kev/PHU

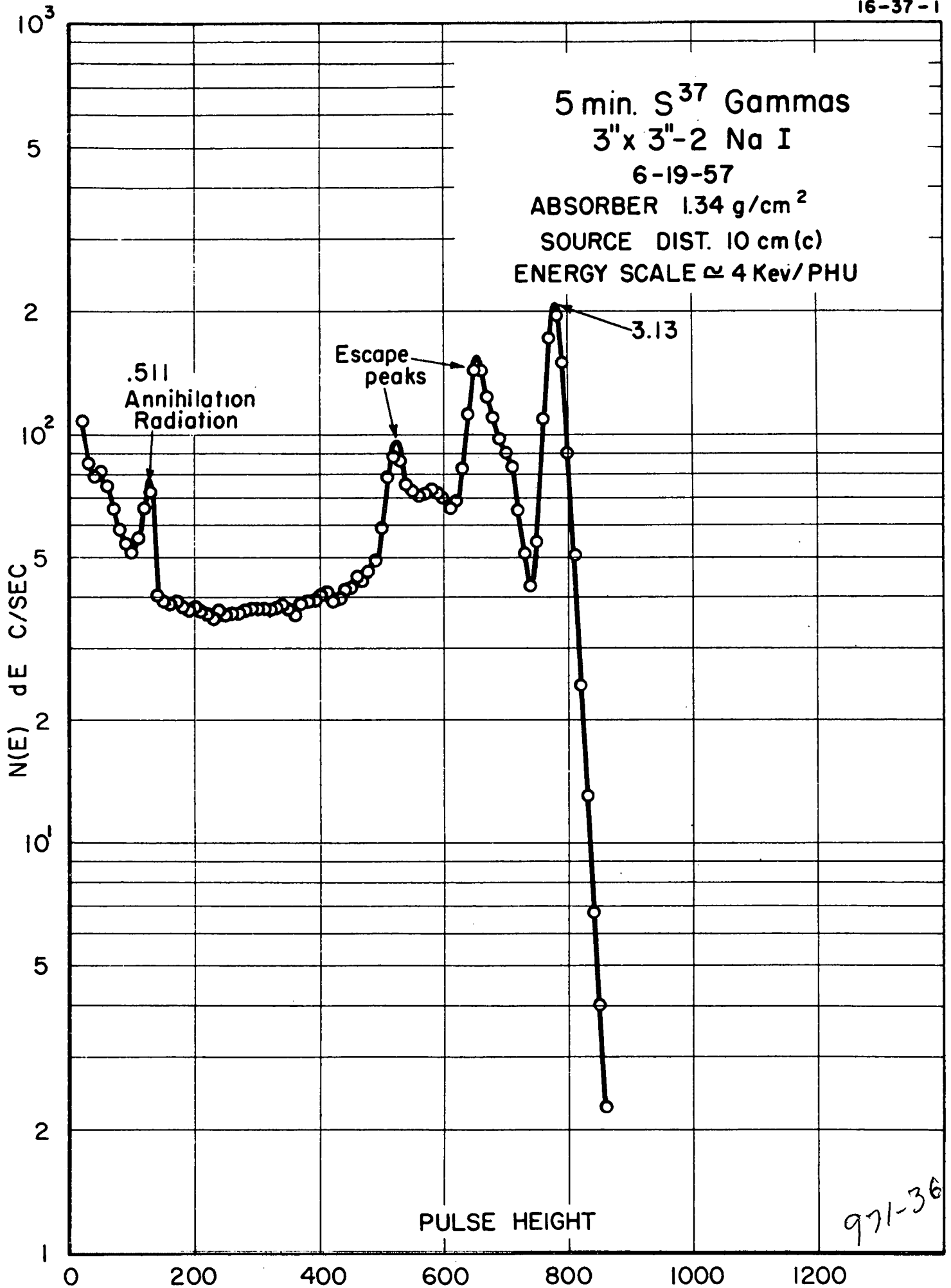


971-33

971 33

2.3 min  $Al^{28}$  Gammas  
3" x 3"-2 Na I  
6-21-57  
ABSORBER 1.34 g/cm<sup>2</sup>  
SOURCE DIST. 10 cm (c)  
ENERGY SCALE  $\approx$  2 Kev/PHU

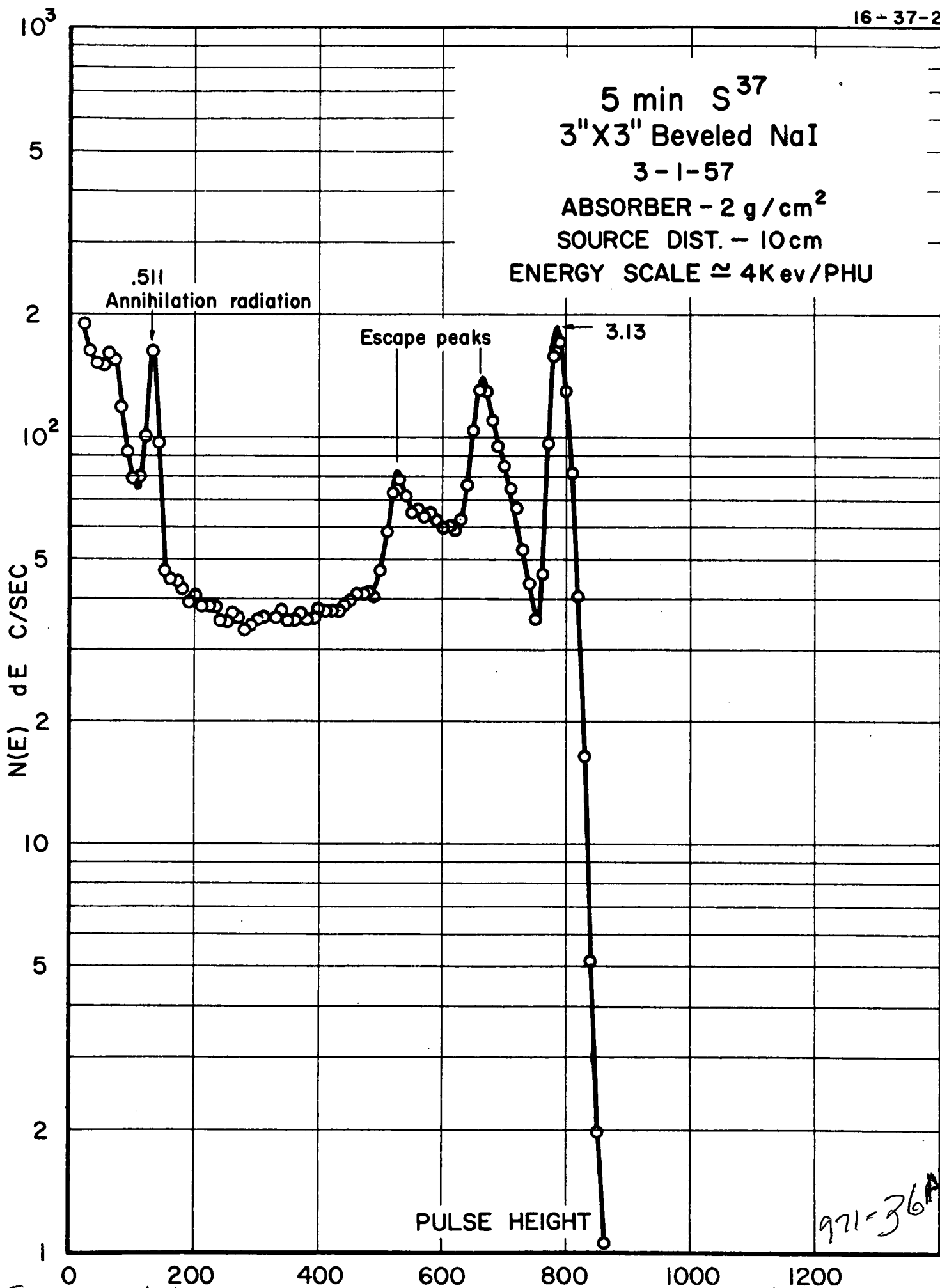


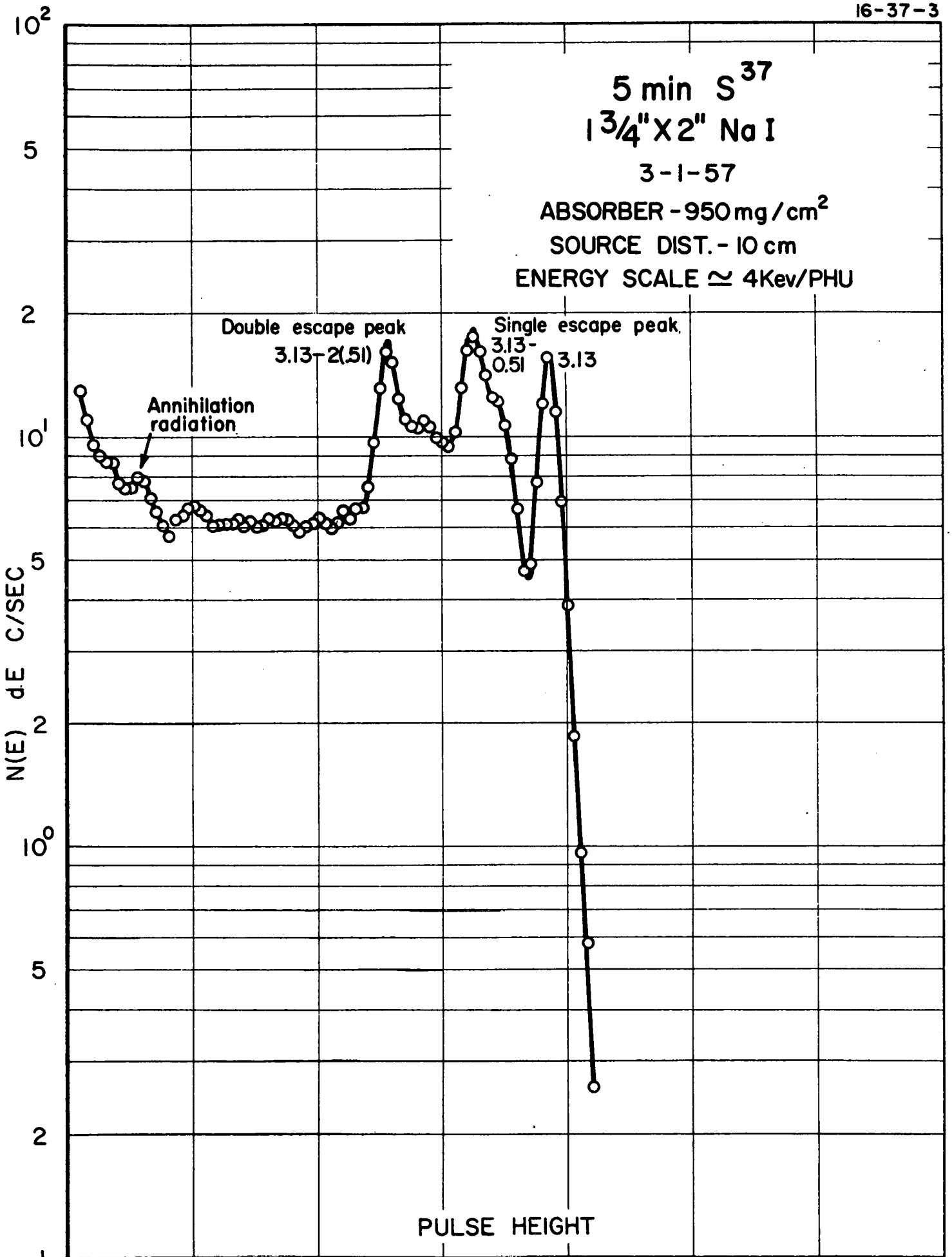


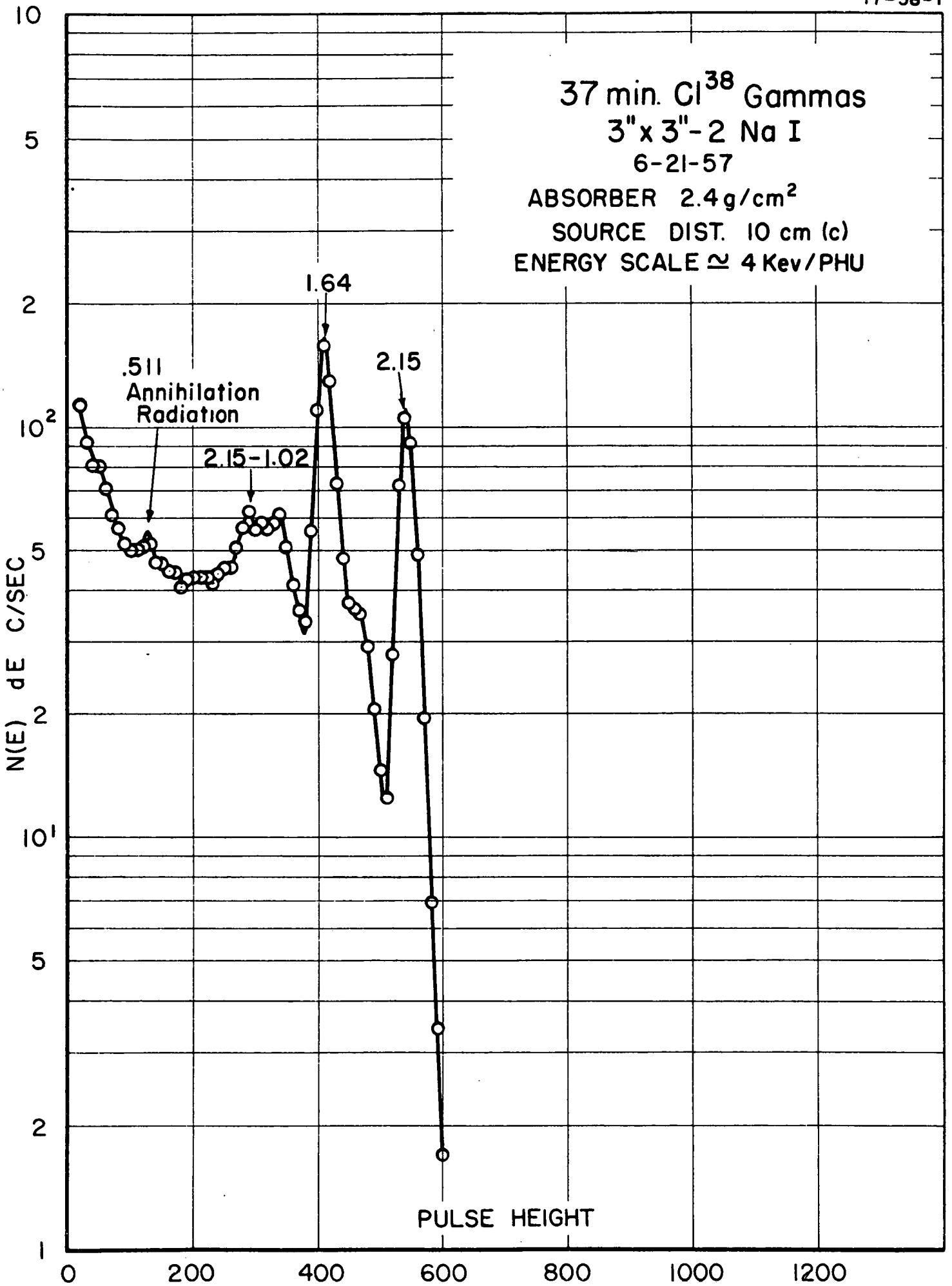
971-36

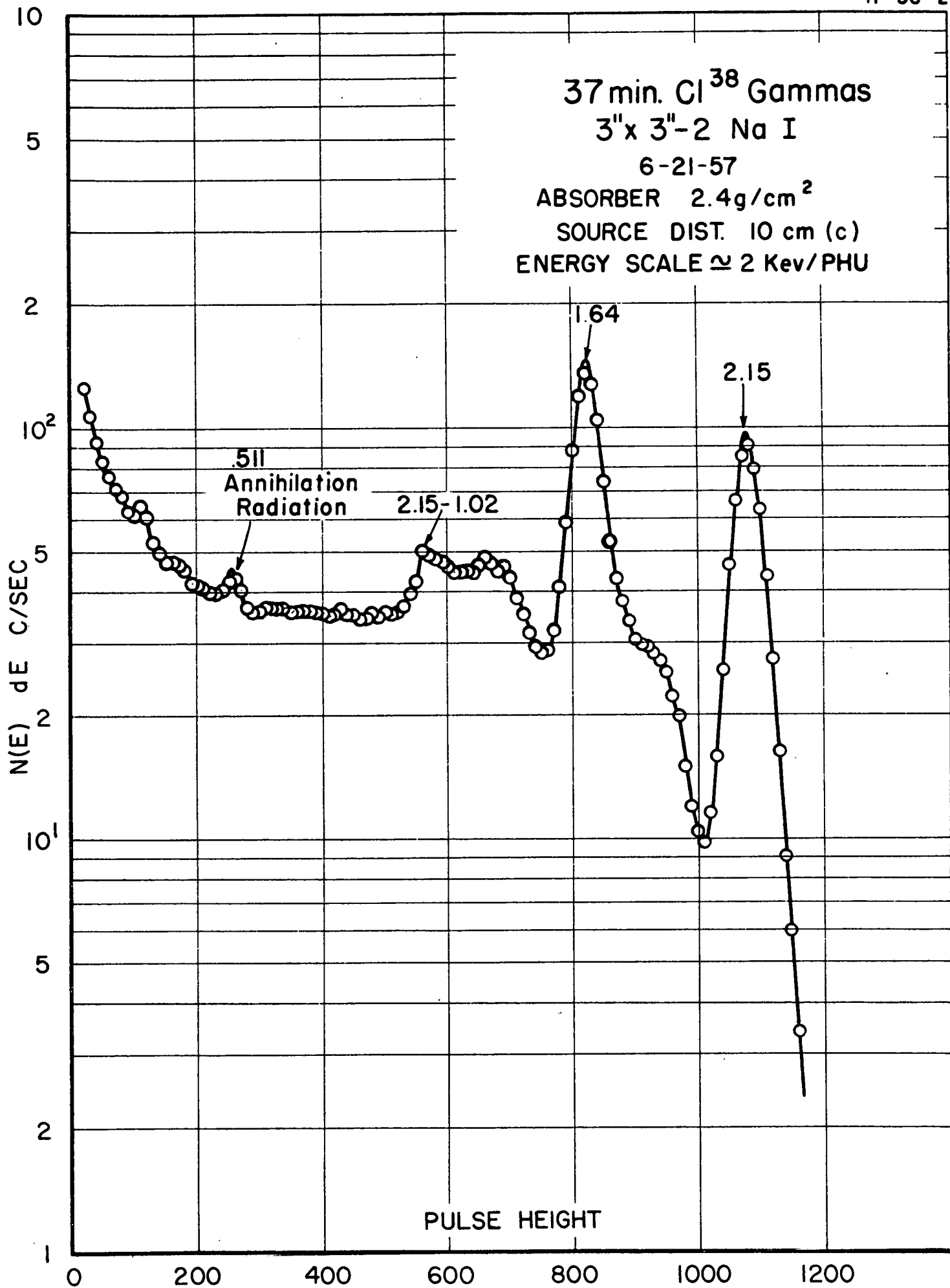
5 min  $S^{37}$   
3"X3" Beveled NaI  
3-1-57

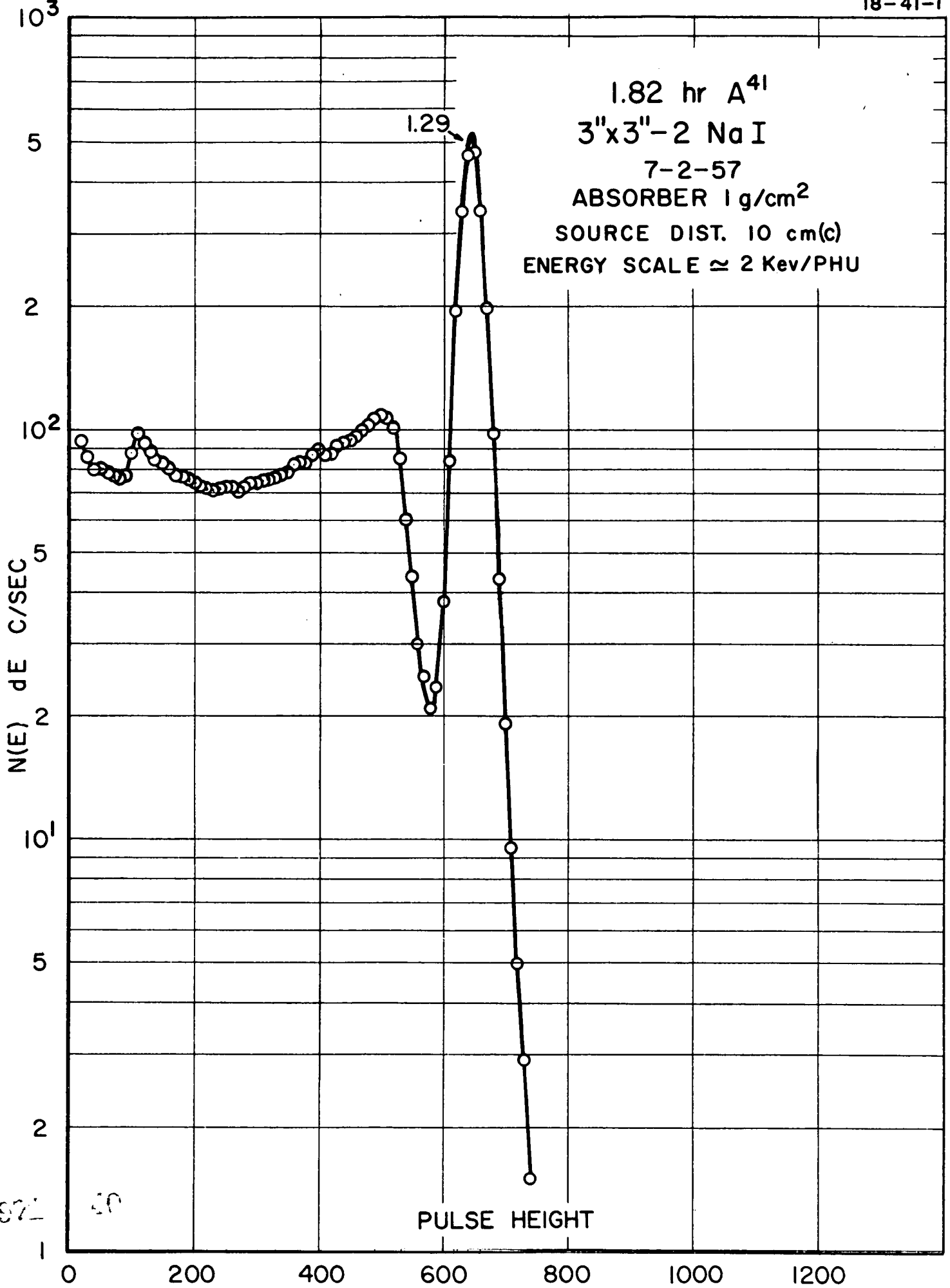
ABSORBER -  $2 \text{ g/cm}^2$   
SOURCE DIST. - 10cm  
ENERGY SCALE  $\approx 4 \text{ KeV/PHU}$



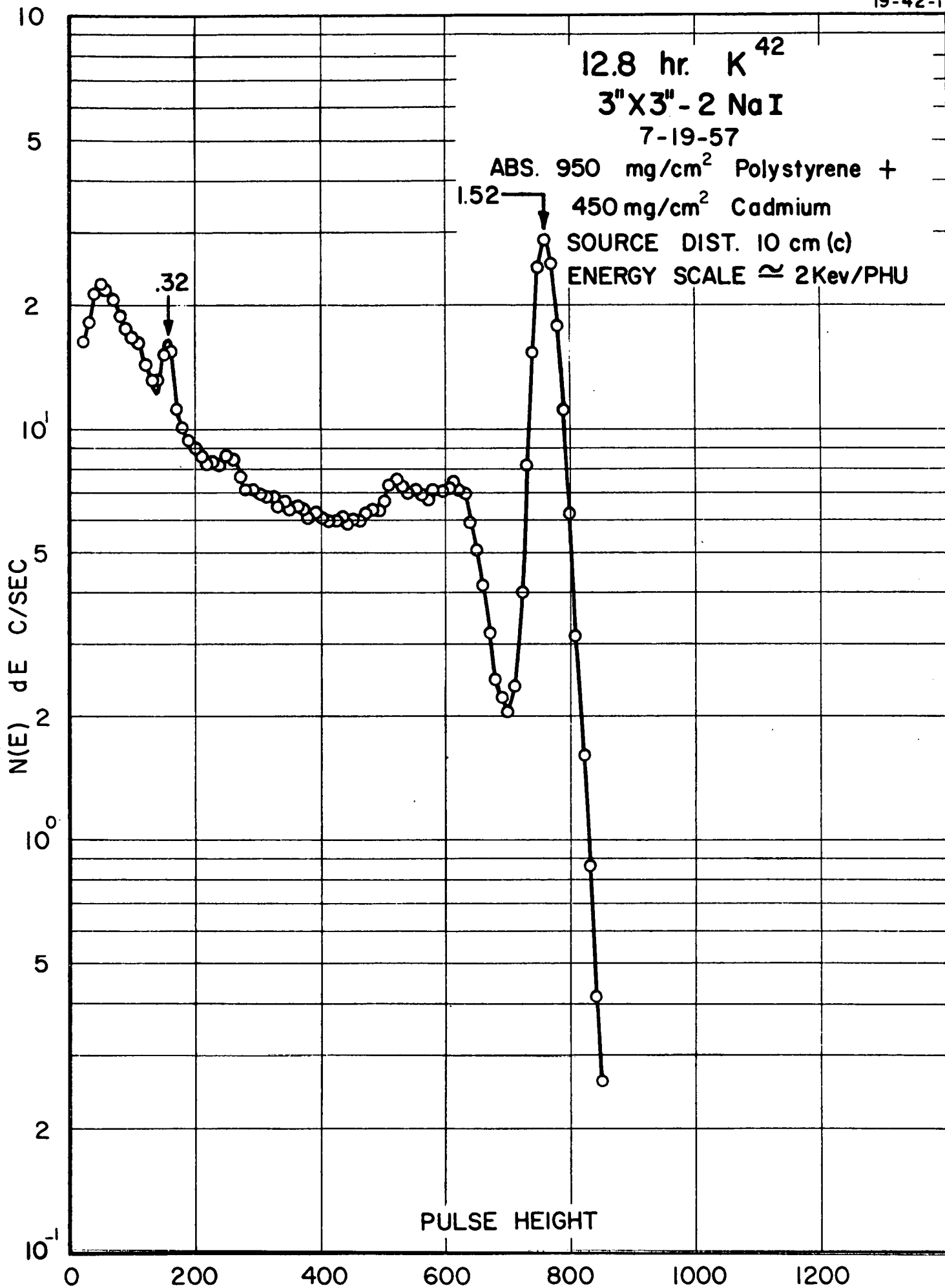


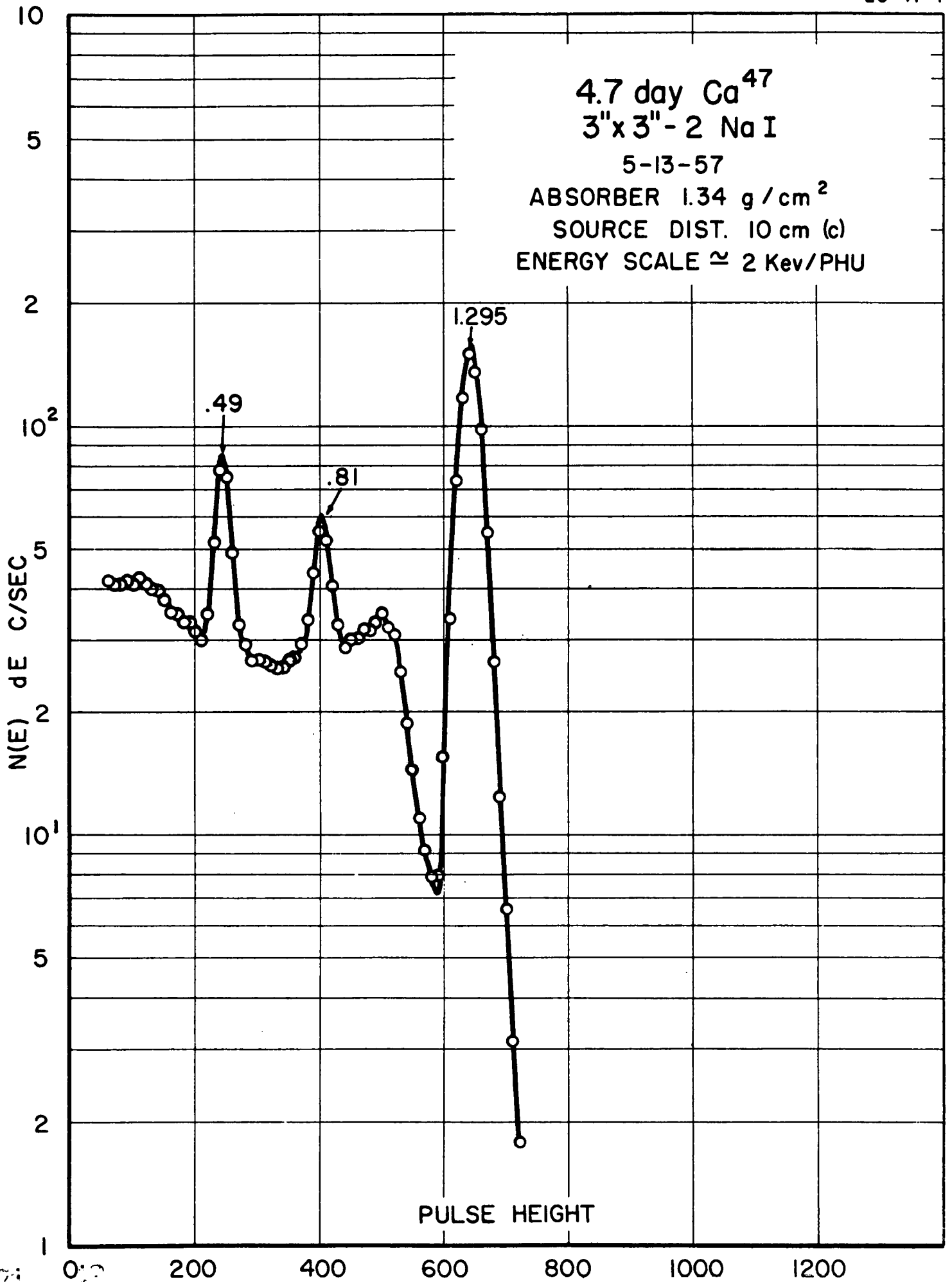


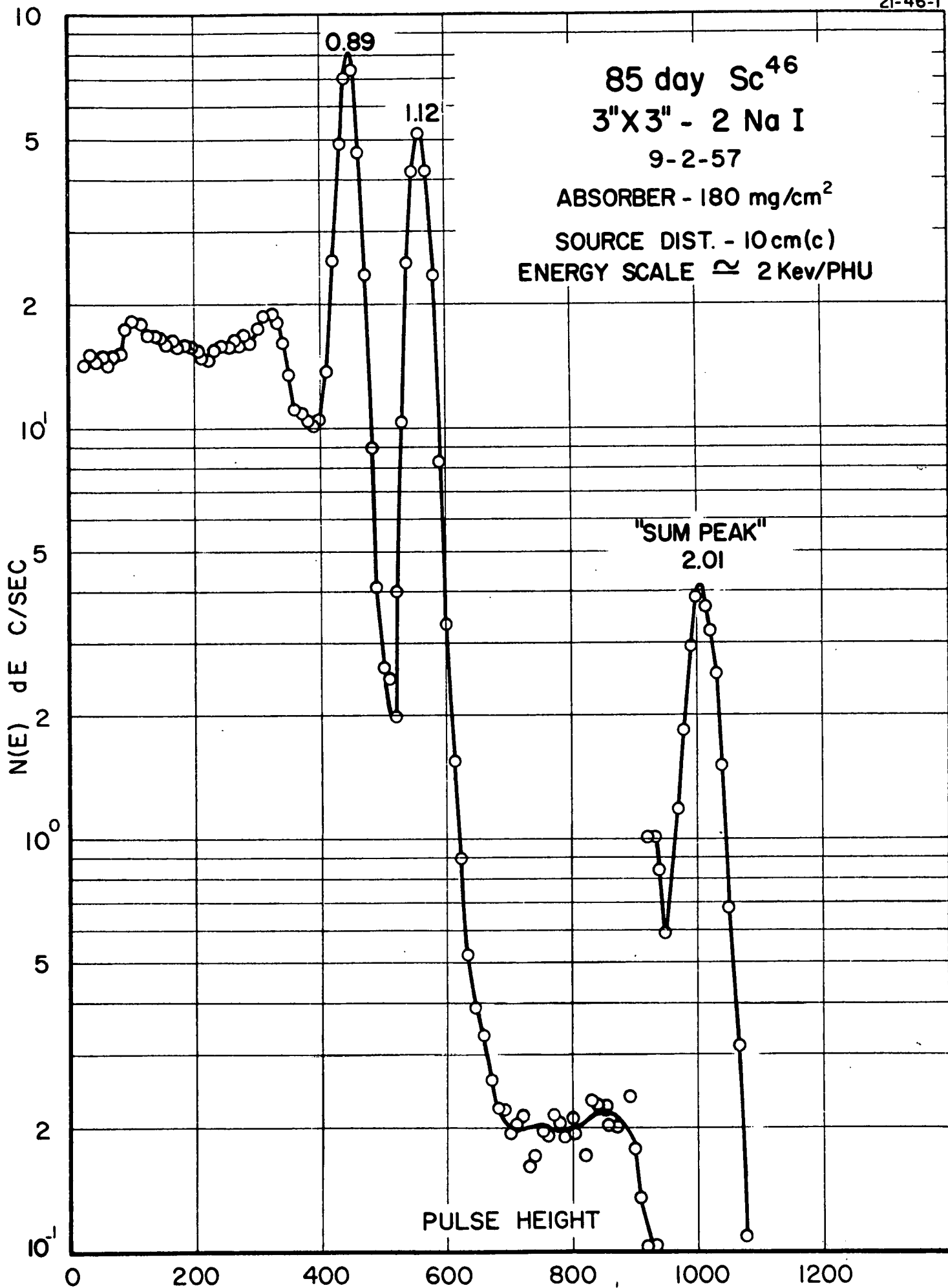


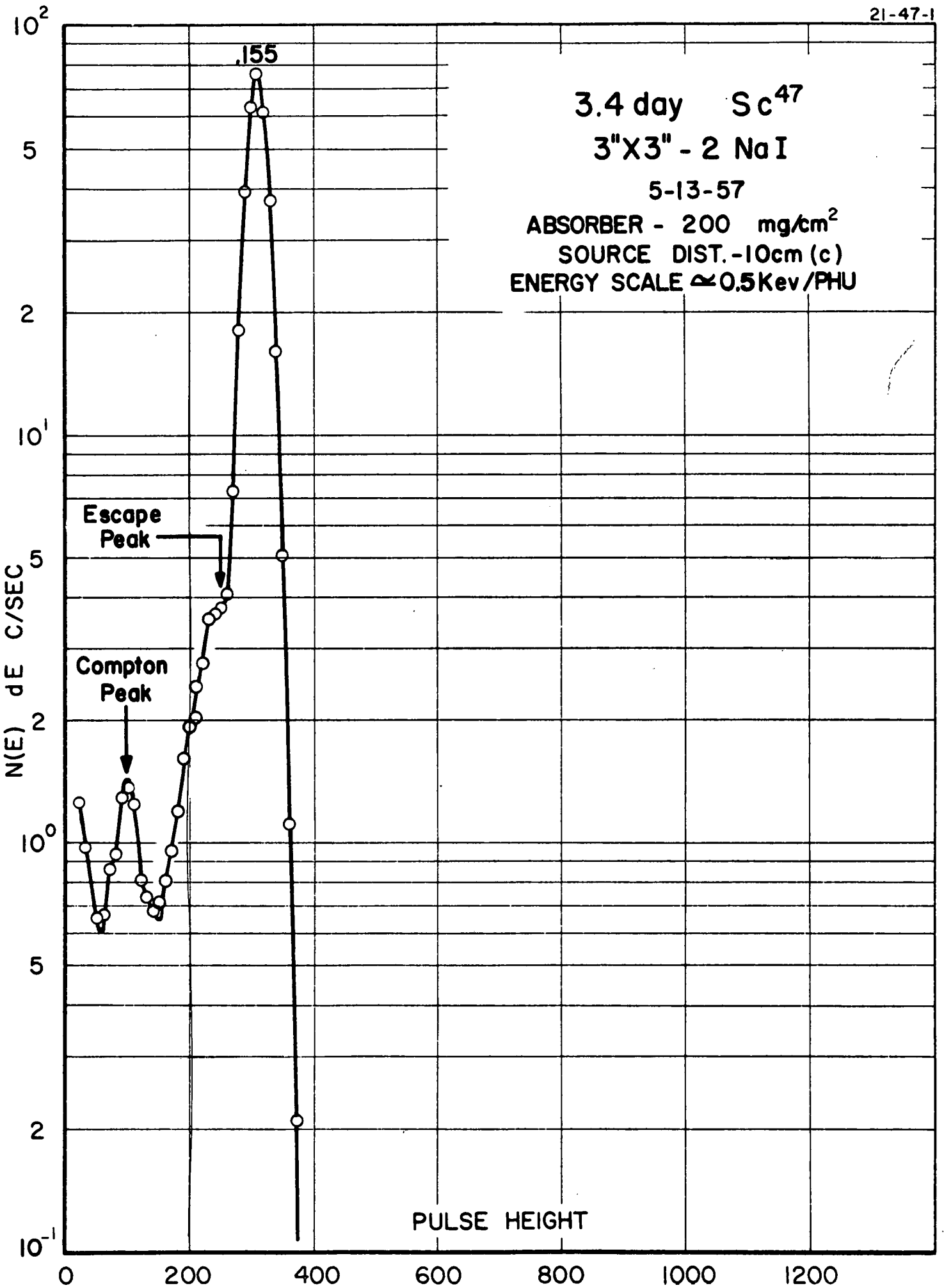


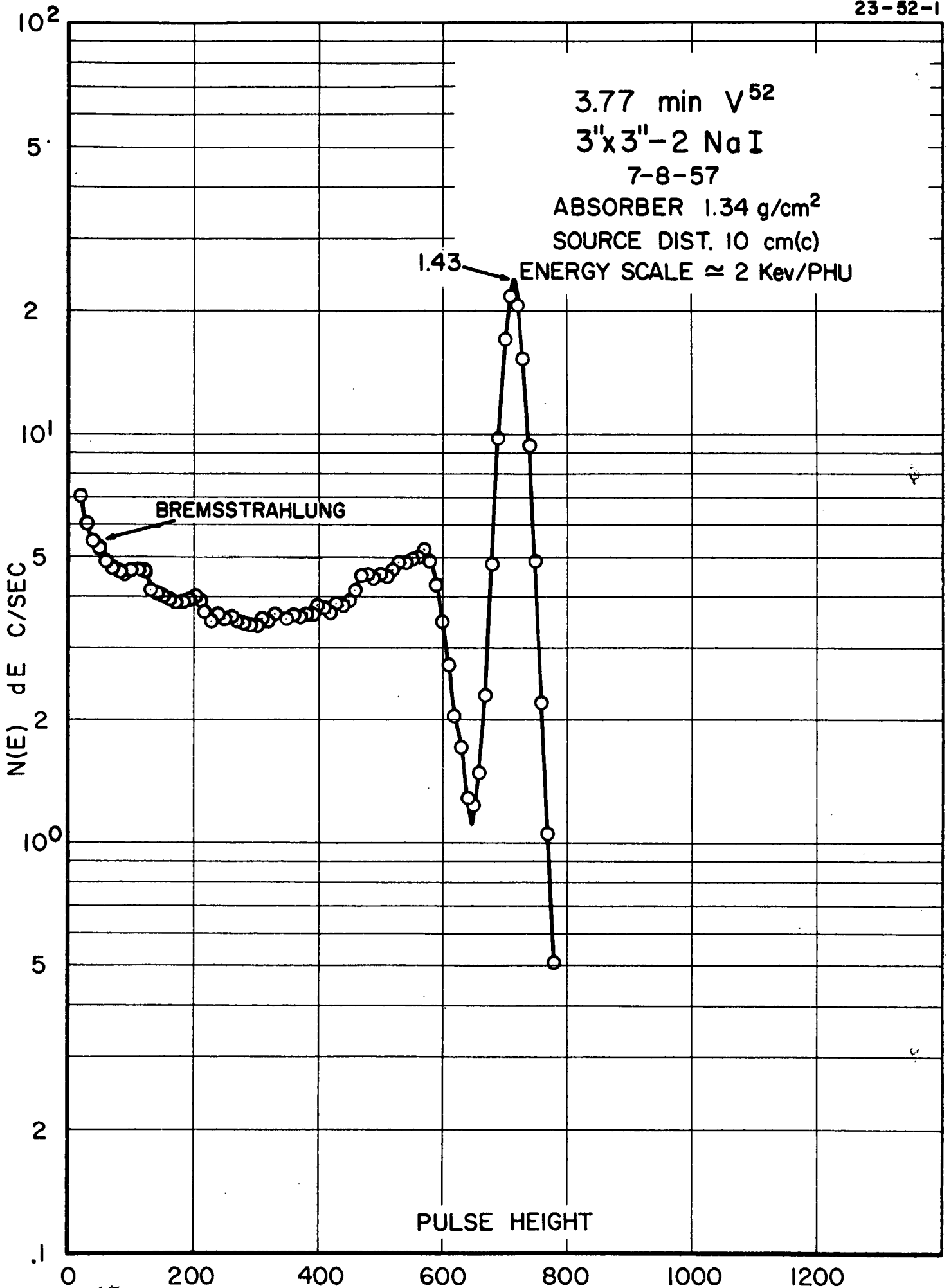
972 50

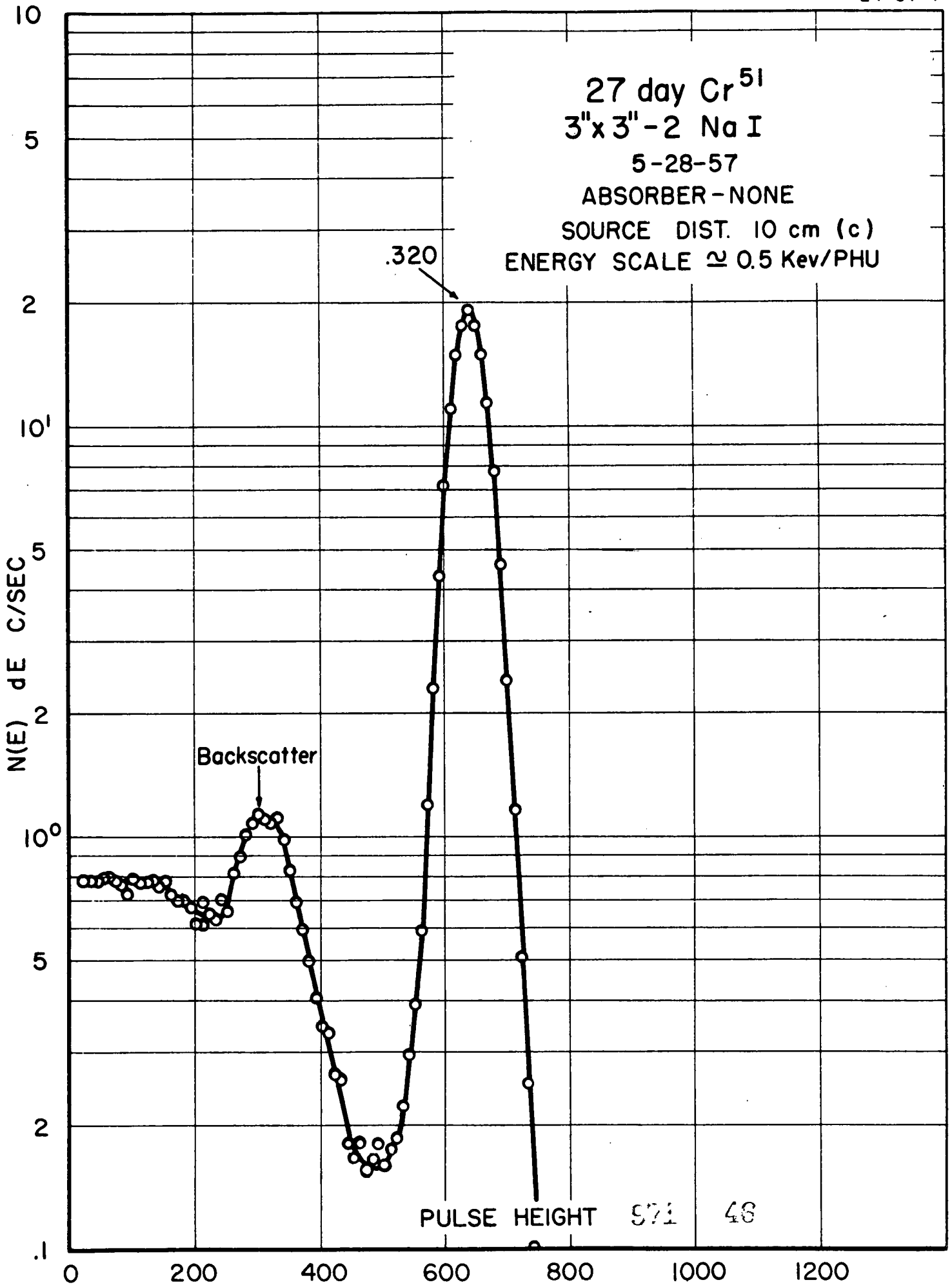


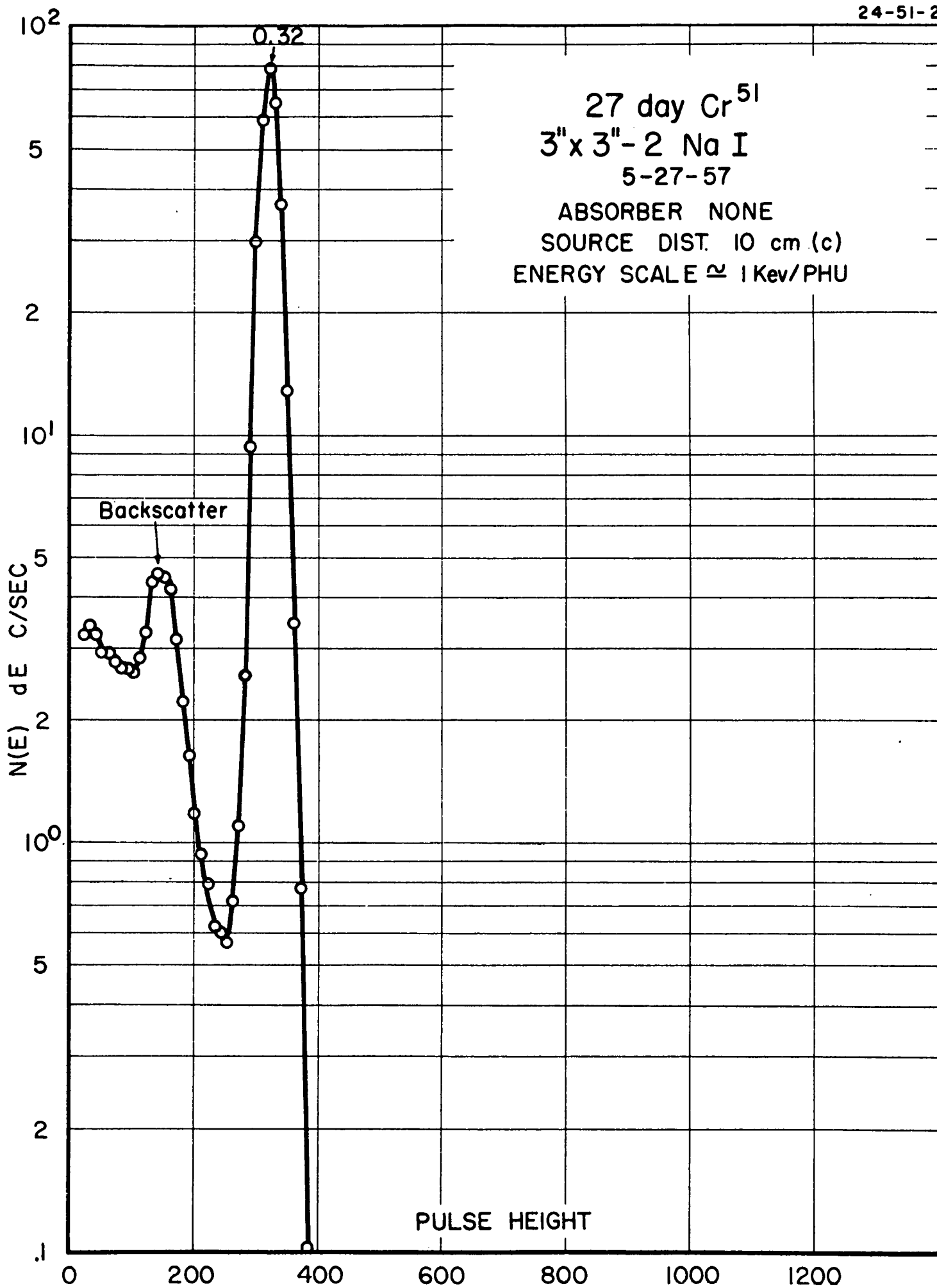




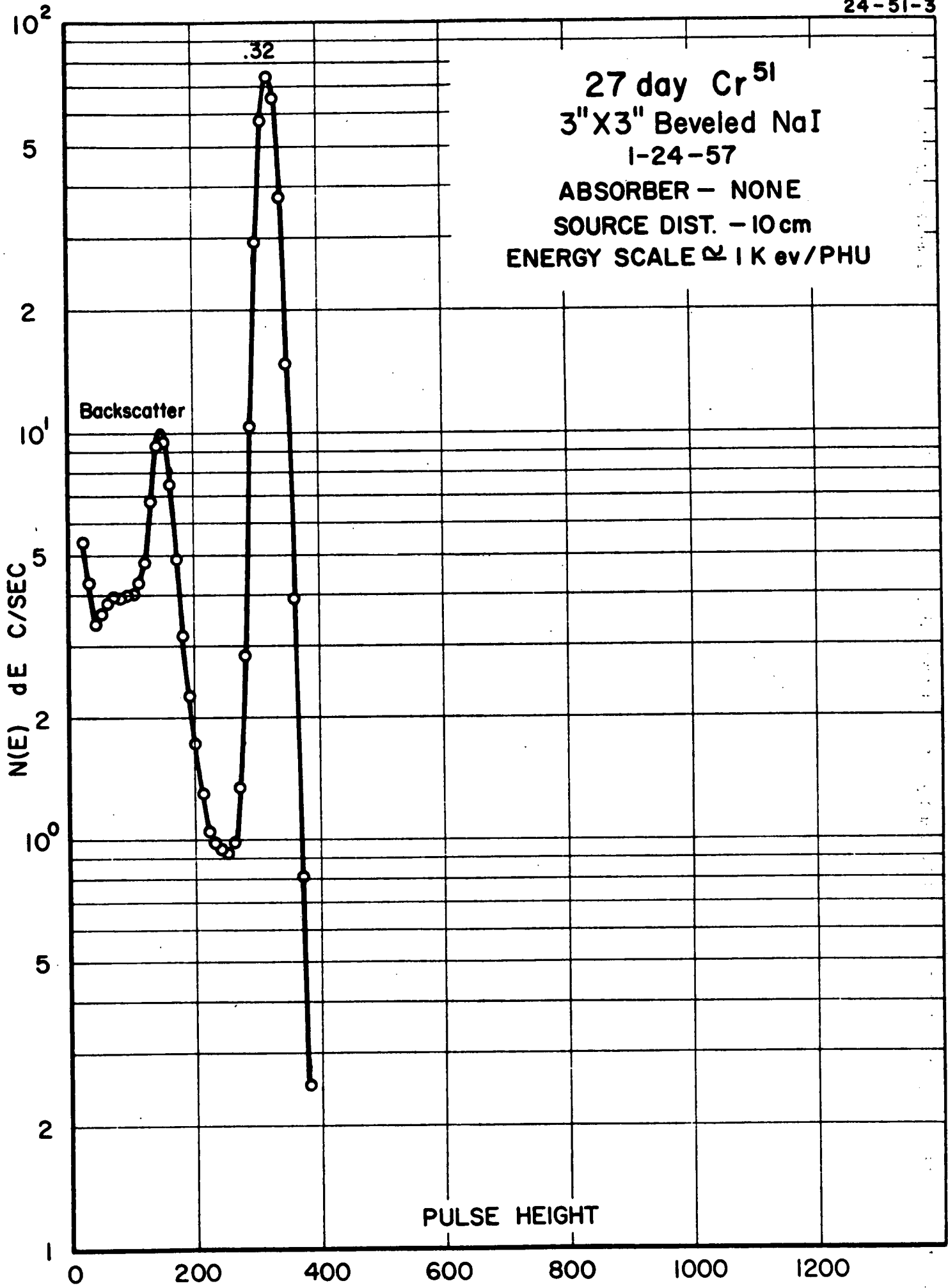




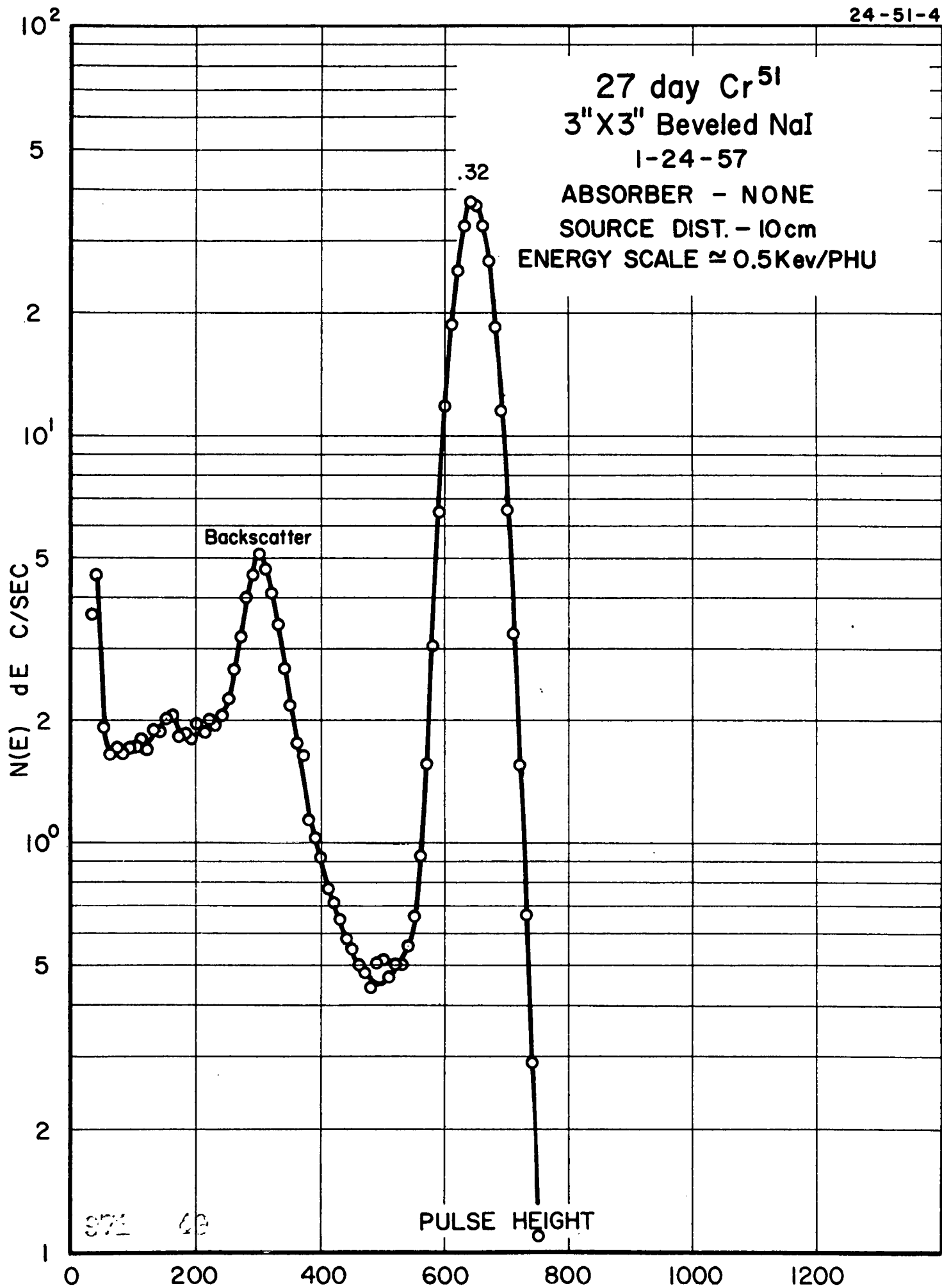




27 day Cr<sup>51</sup>  
3"X3" Beveled NaI  
1-24-57  
ABSORBER - NONE  
SOURCE DIST. - 10 cm  
ENERGY SCALE  $\approx$  1 K ev/PHU



077 18



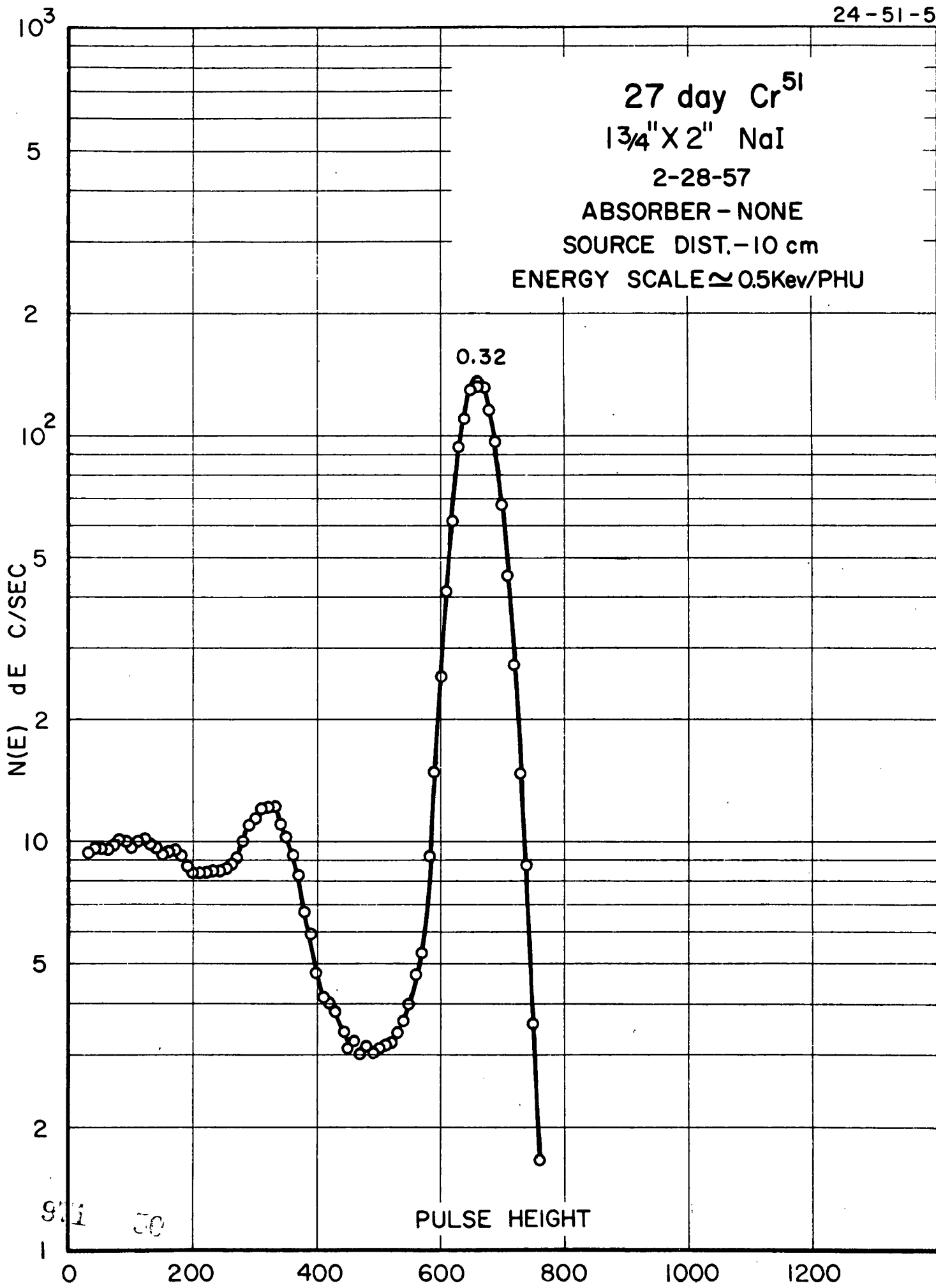
27 day Cr<sup>51</sup>  
1 3/4" X 2" NaI

2-28-57

ABSORBER - NONE

SOURCE DIST. - 10 cm

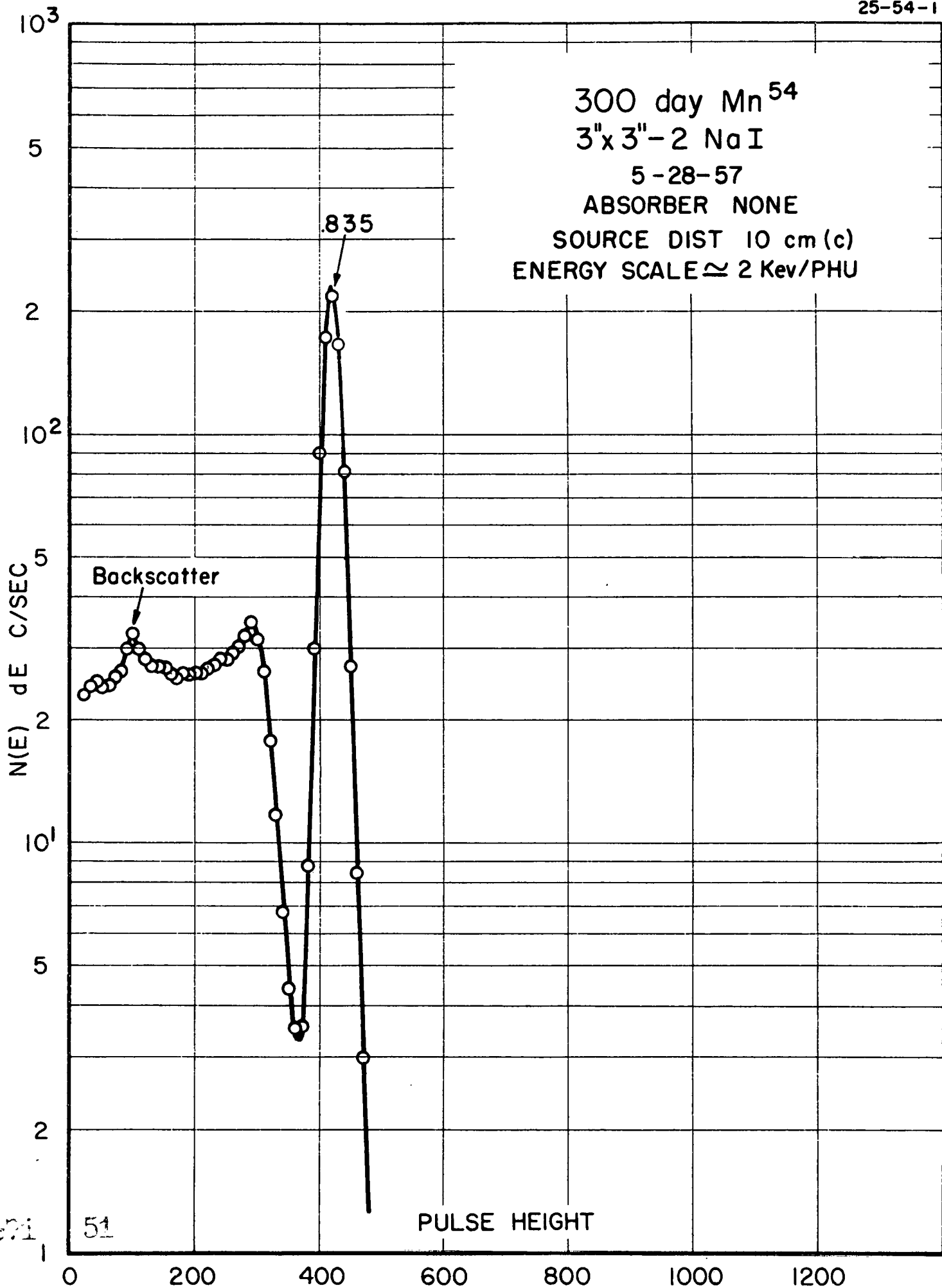
ENERGY SCALE  $\approx$  0.5Kev/PHU



971 50

PULSE HEIGHT

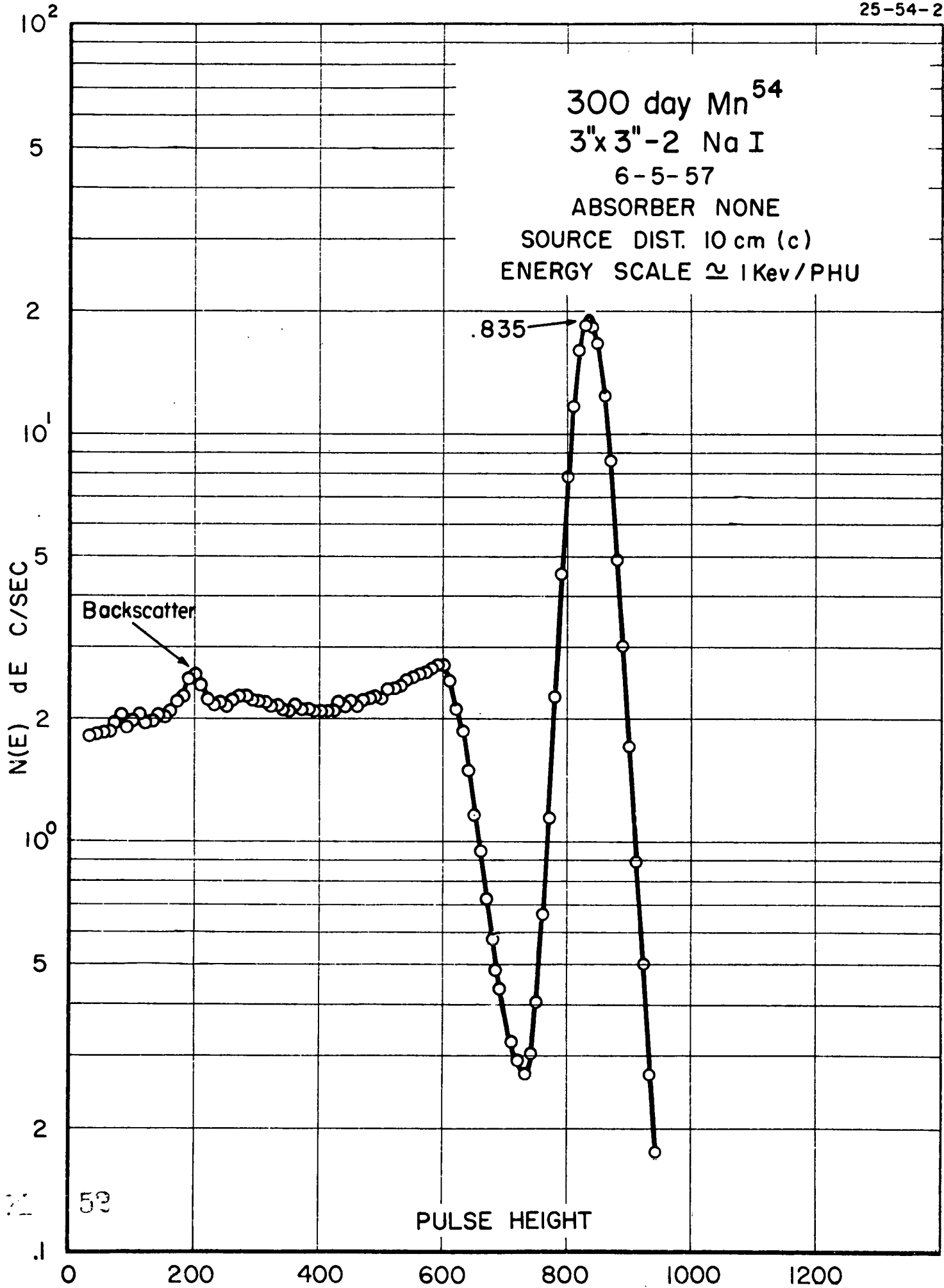
300 day Mn<sup>54</sup>  
3"x 3"-2 NaI  
5-28-57  
ABSORBER NONE  
SOURCE DIST 10 cm(c)  
ENERGY SCALE  $\approx$  2 Kev/PHU



51

PULSE HEIGHT

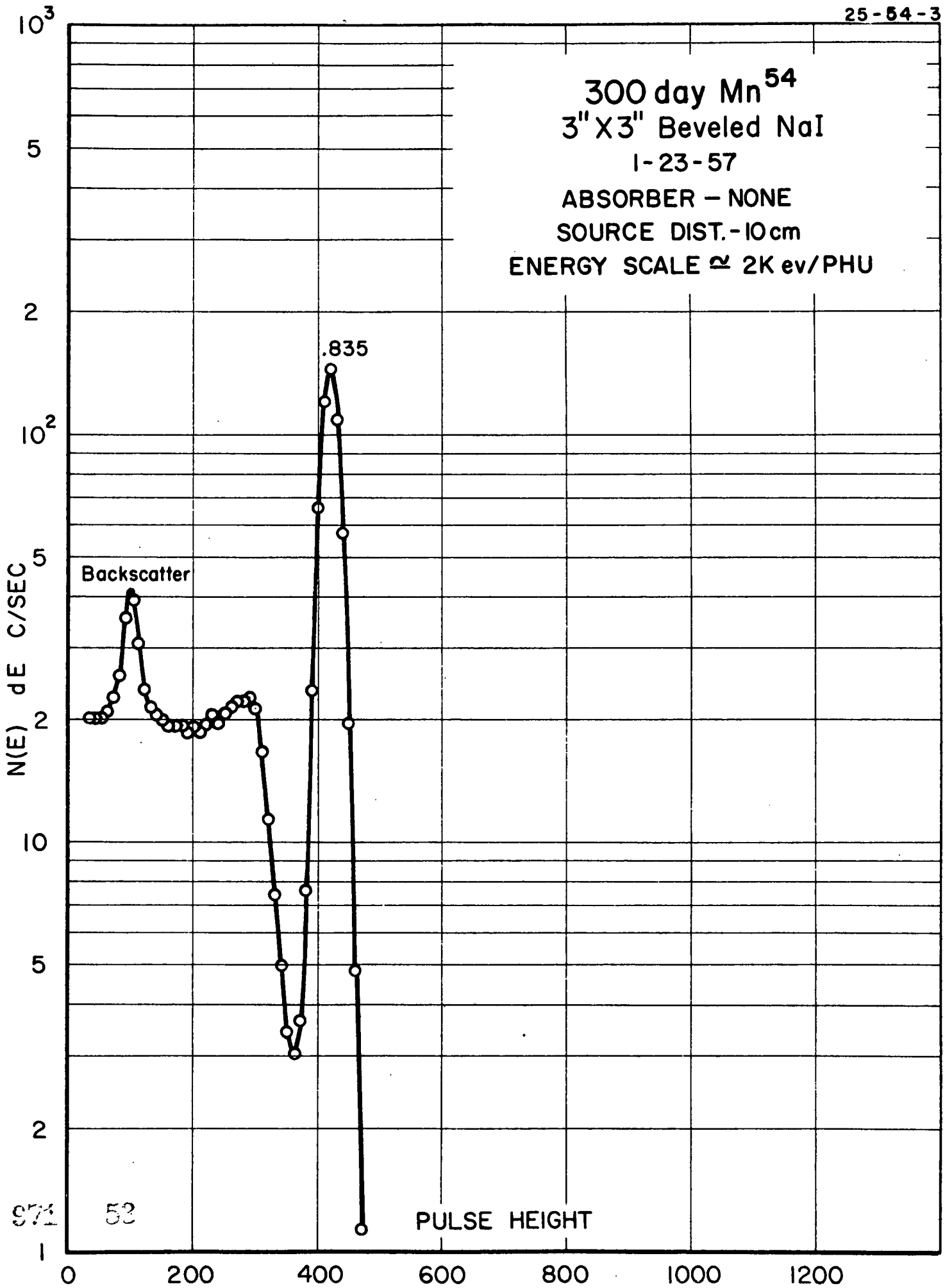
300 day Mn<sup>54</sup>  
3"x3"-2 Na I  
6-5-57  
ABSORBER NONE  
SOURCE DIST. 10 cm (c)  
ENERGY SCALE  $\approx$  1 Kev/PHU

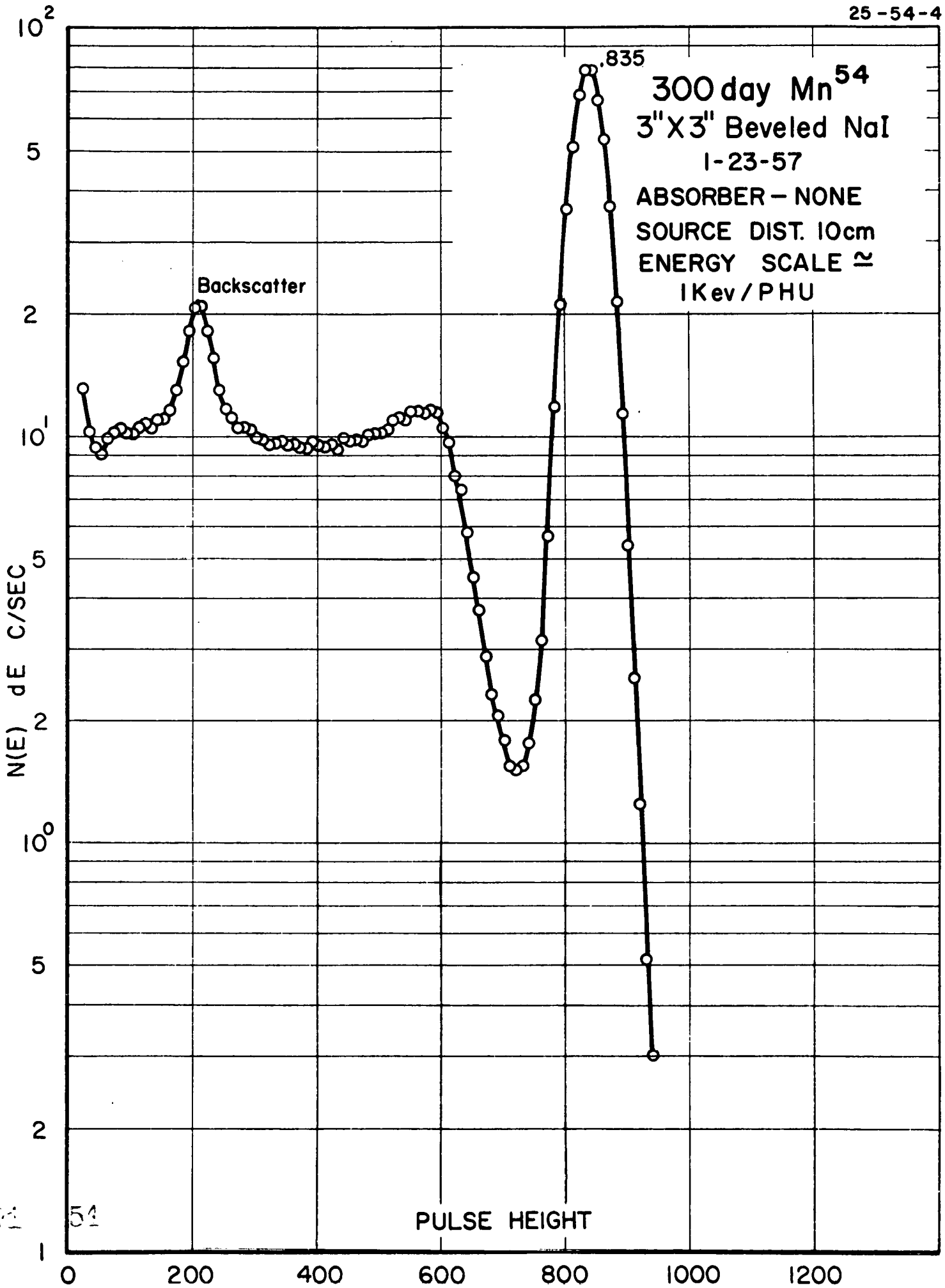


59

PULSE HEIGHT

300 day Mn<sup>54</sup>  
3" X 3" Beveled NaI  
1-23-57  
ABSORBER - NONE  
SOURCE DIST. - 10 cm  
ENERGY SCALE  $\approx$  2K ev/PHU



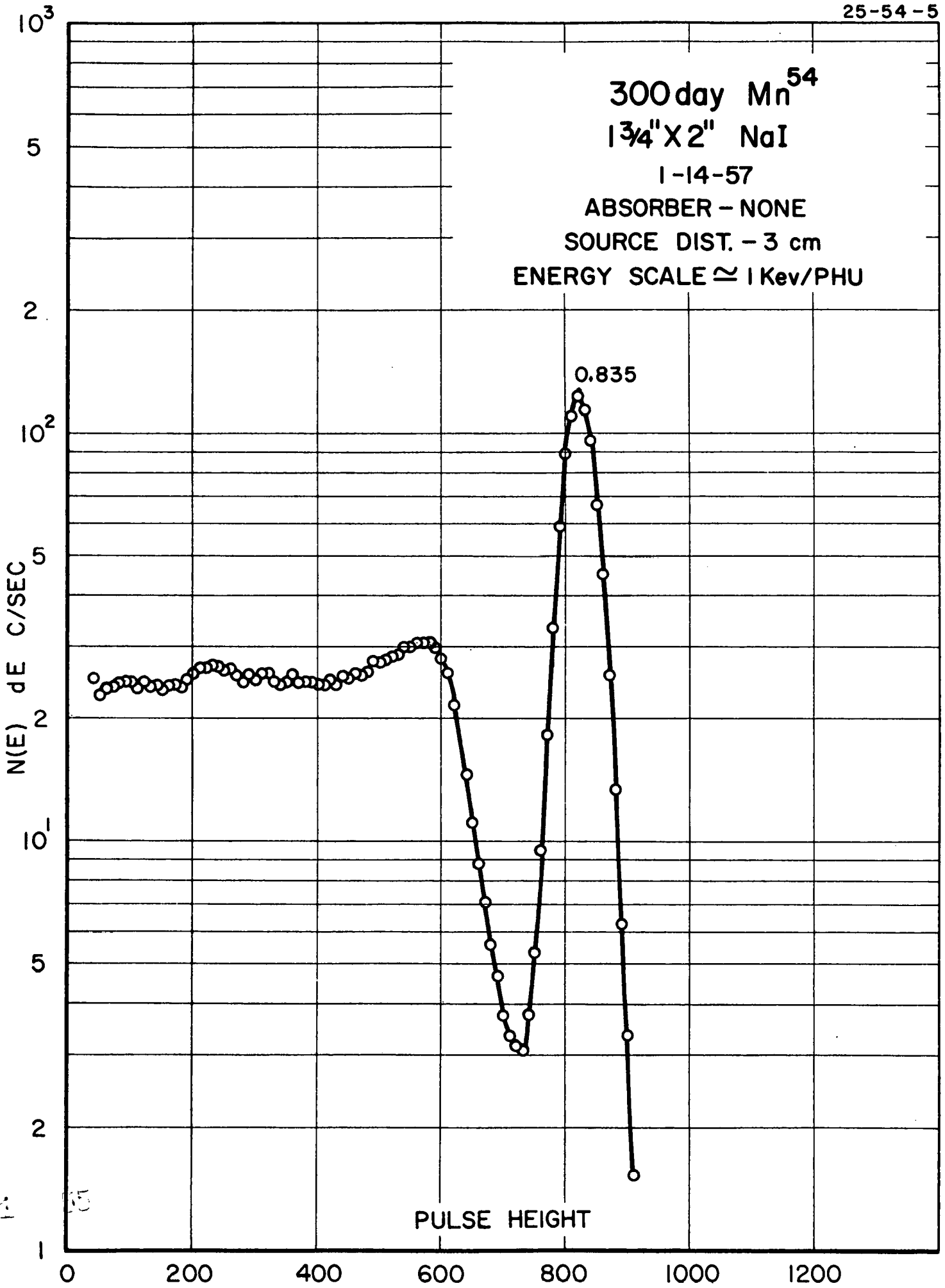


971

54

1

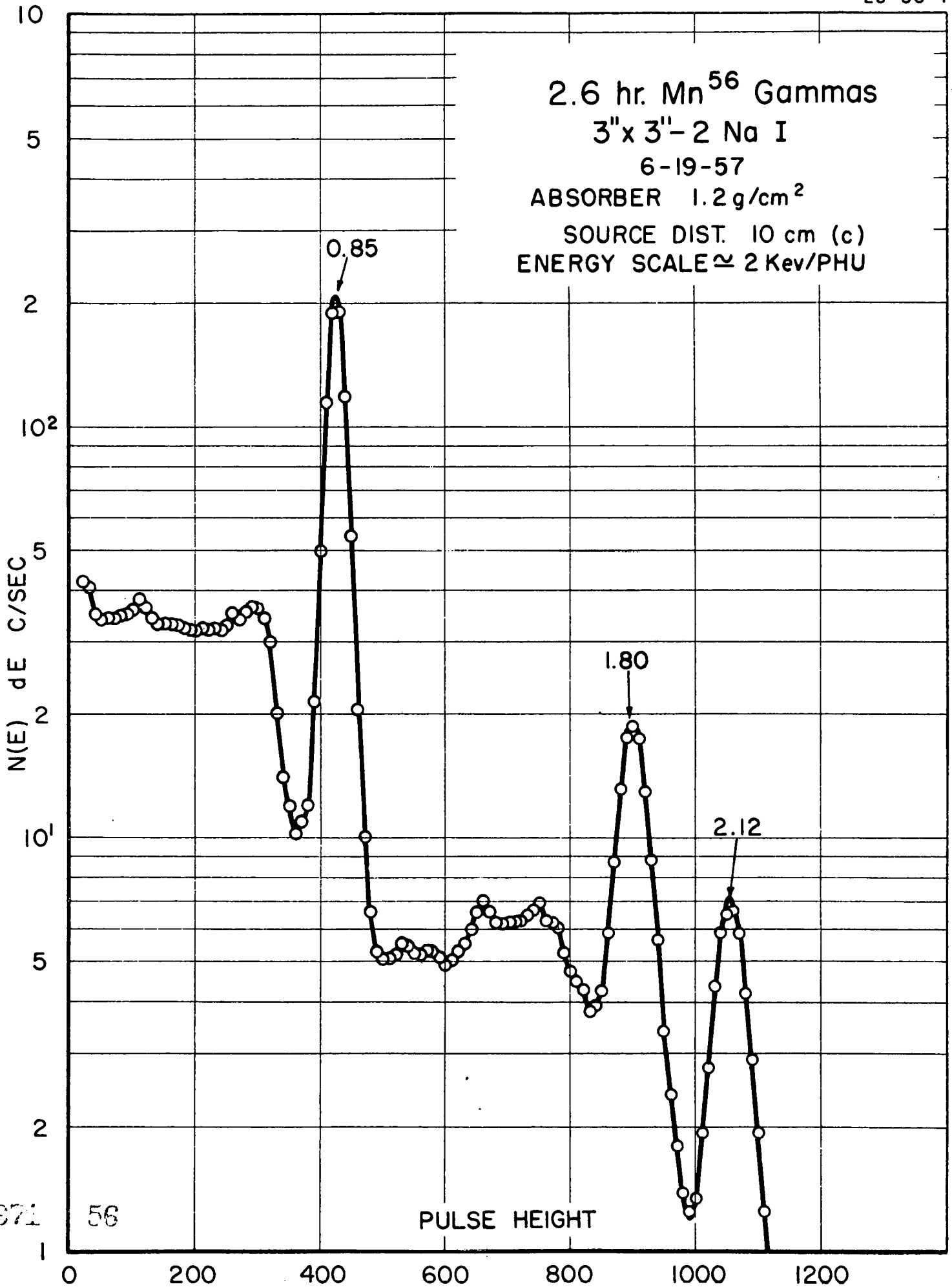
300 day Mn<sup>54</sup>  
1 3/4" X 2" NaI  
1-14-57  
ABSORBER - NONE  
SOURCE DIST. - 3 cm  
ENERGY SCALE ≈ 1 Kev/PHU



971 15

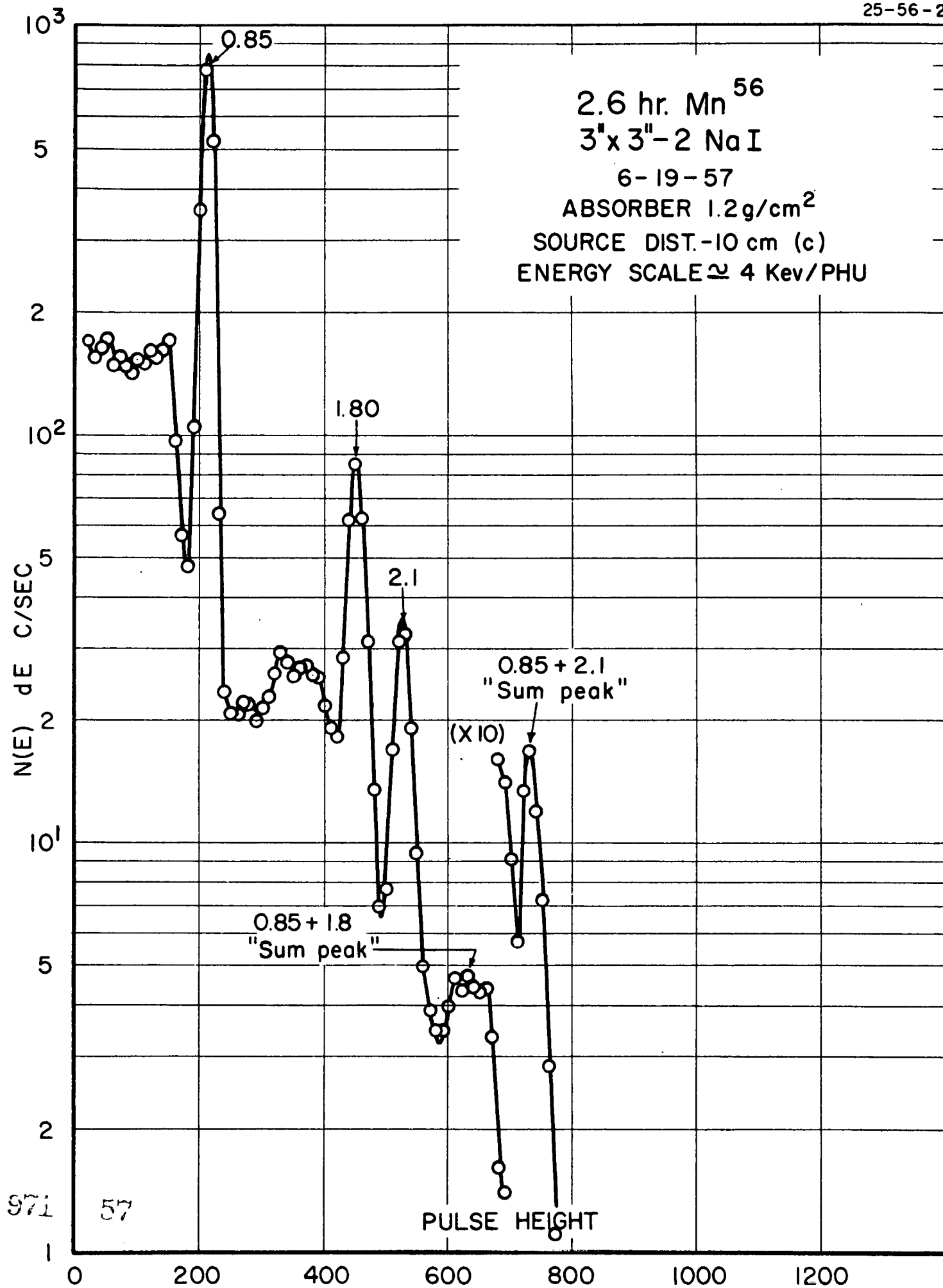
PULSE HEIGHT

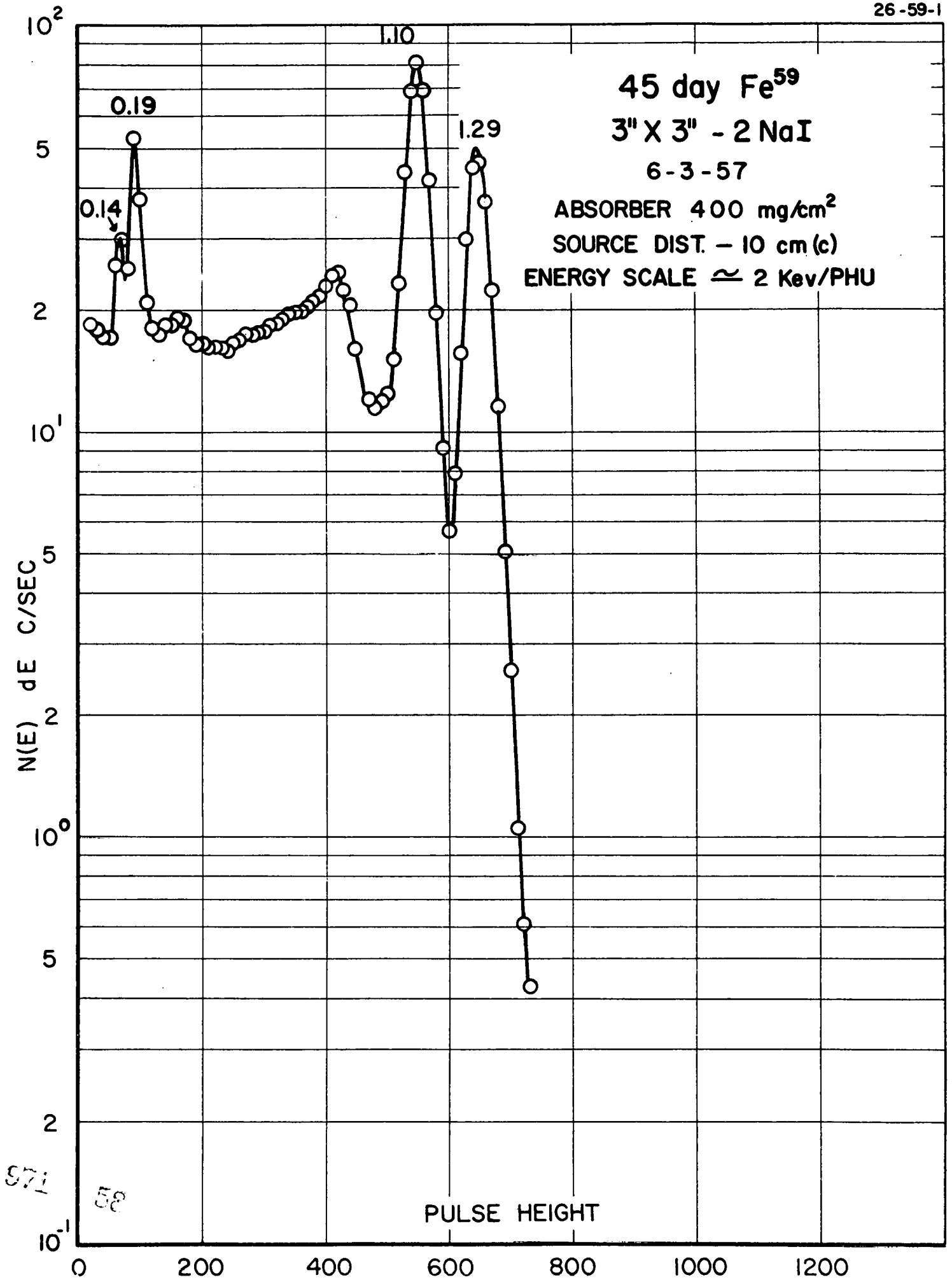
2.6 hr. Mn<sup>56</sup> Gammas  
 3" x 3" - 2 Na I  
 6-19-57  
 ABSORBER 1.2 g/cm<sup>2</sup>  
 SOURCE DIST. 10 cm (c)  
 ENERGY SCALE  $\approx$  2 Kev/PHU



56

PULSE HEIGHT

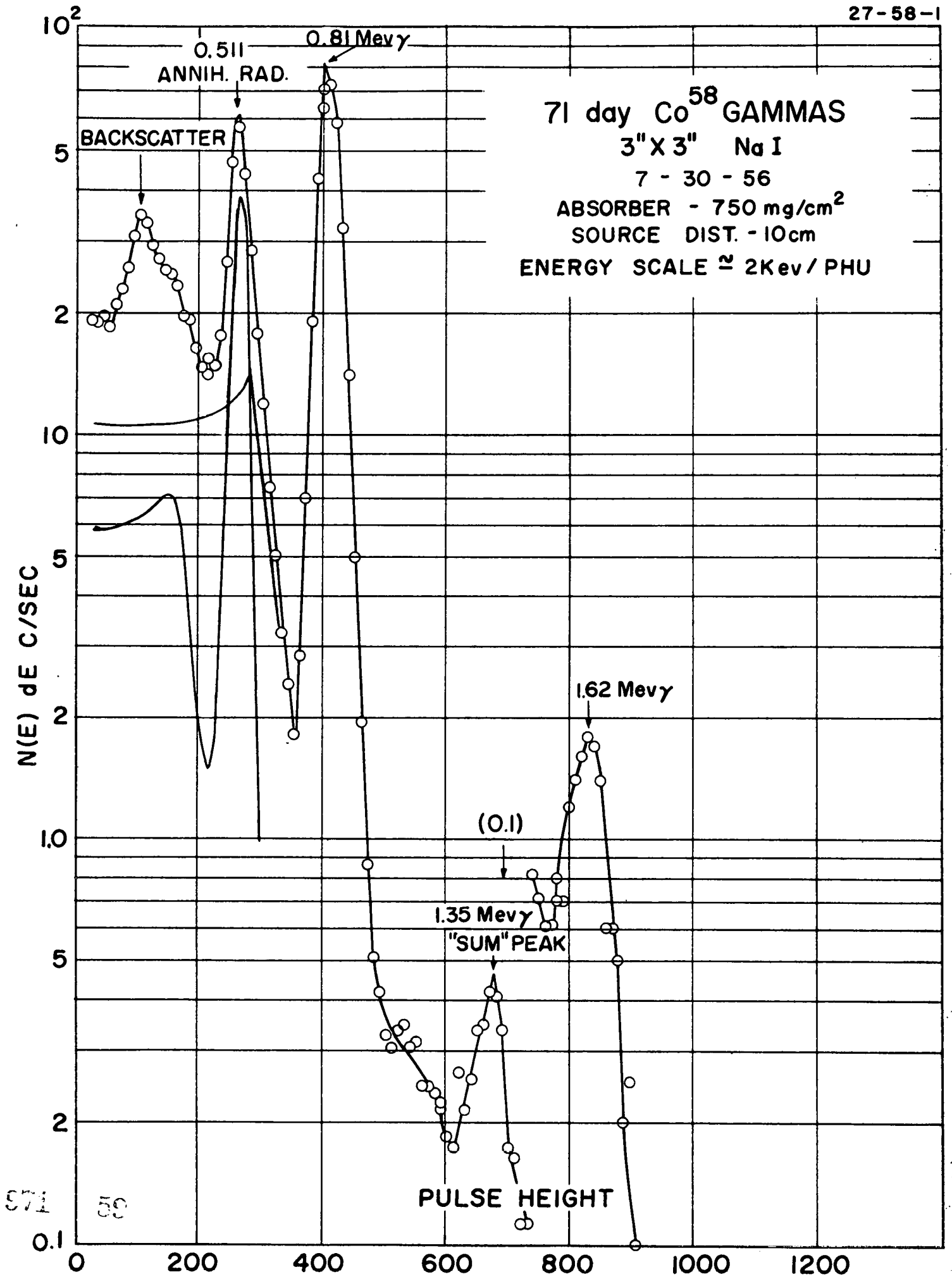




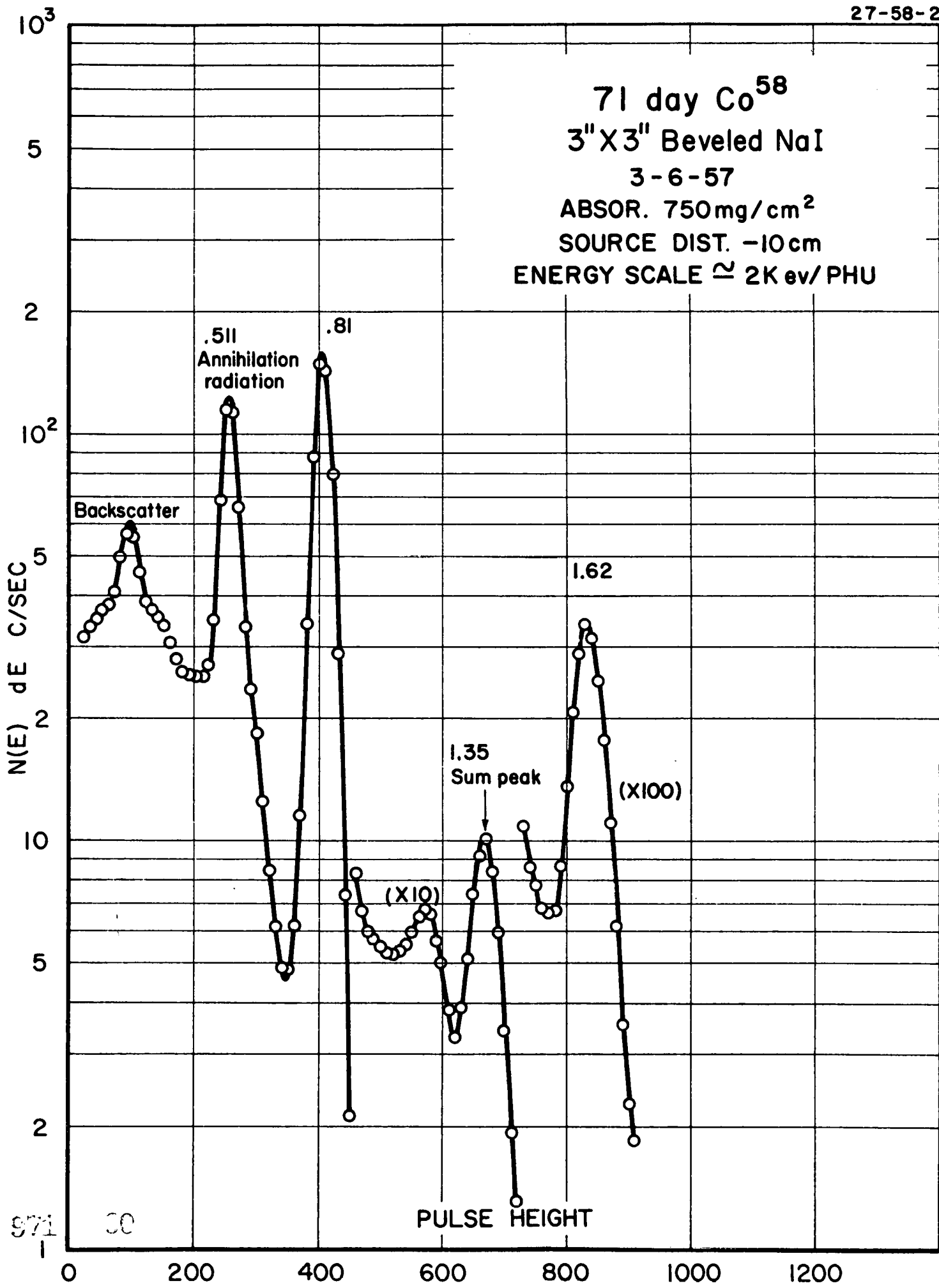
571

58

PULSE HEIGHT



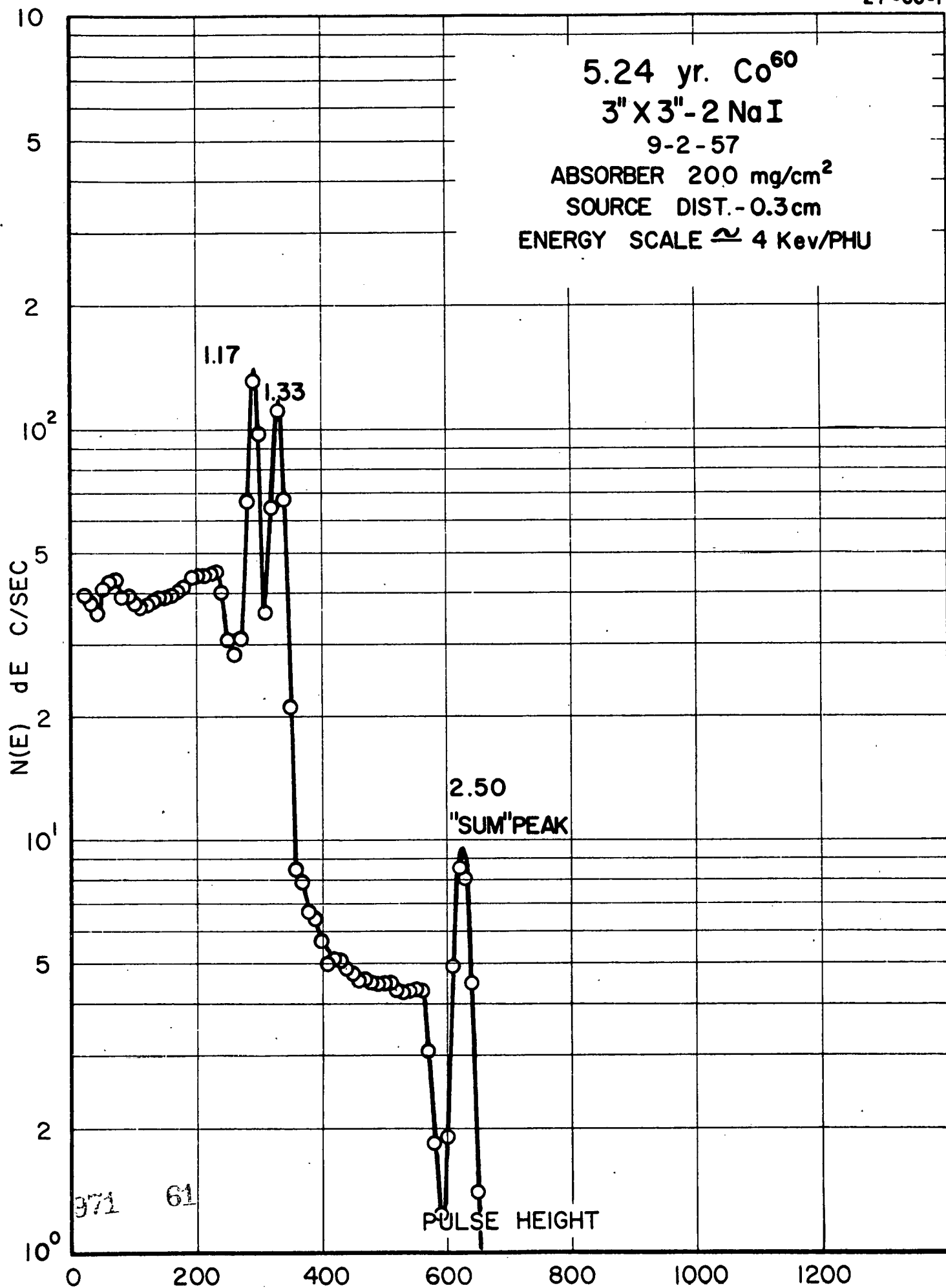
71 day  $\text{Co}^{58}$   
3" X 3" Beveled NaI  
3-6-57  
ABSOR. 750mg/cm<sup>2</sup>  
SOURCE DIST. -10cm  
ENERGY SCALE  $\approx$  2K ev/PHU



971  
1  
CO

PULSE HEIGHT

5.24 yr.  $Co^{60}$   
3" X 3"-2 NaI  
9-2-57  
ABSORBER 200 mg/cm<sup>2</sup>  
SOURCE DIST. - 0.3cm  
ENERGY SCALE  $\approx$  4 Kev/PHU



5.24 yr.  $Co^{60}$

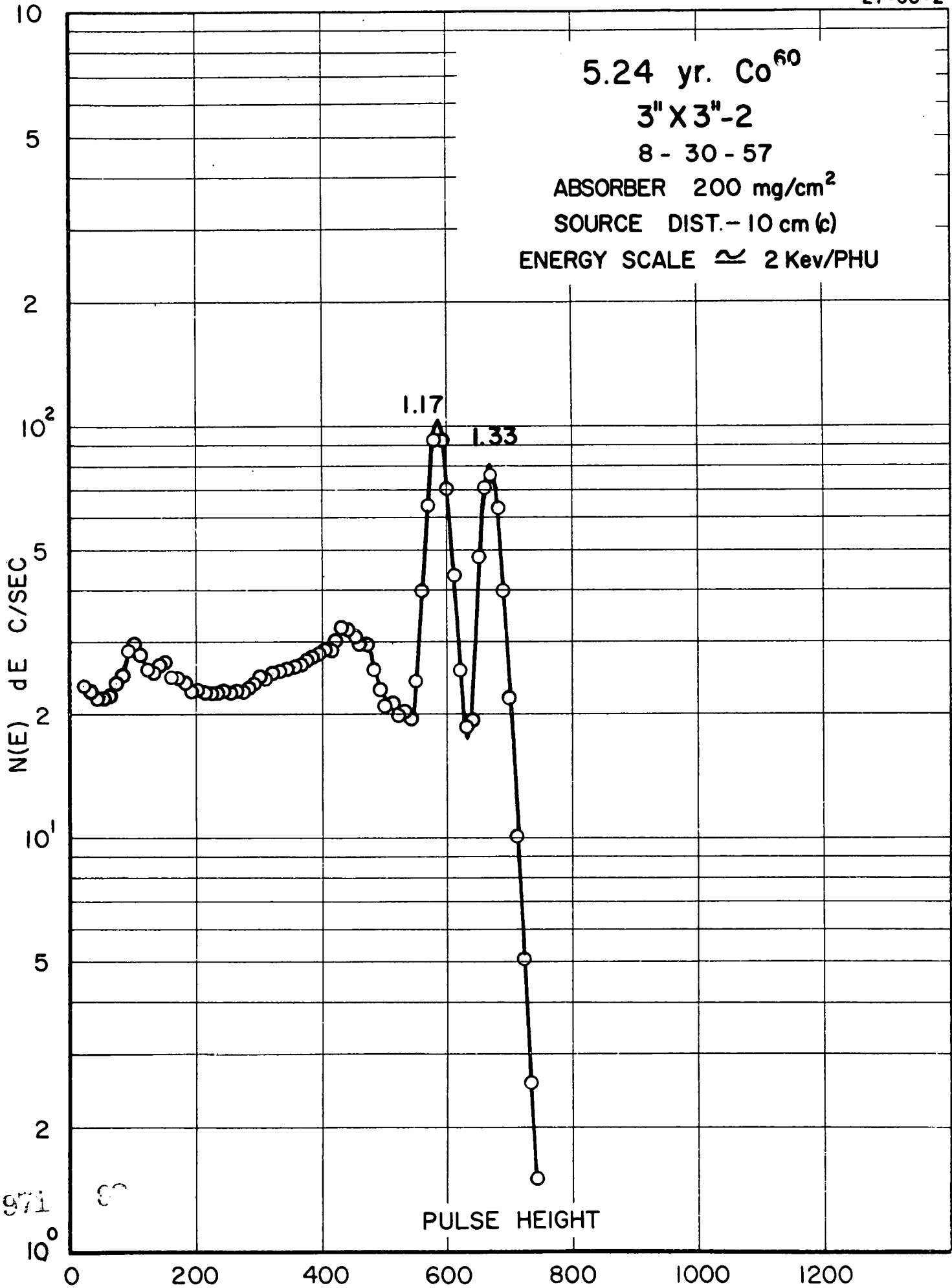
3" X 3"-2

8 - 30 - 57

ABSORBER 200 mg/cm<sup>2</sup>

SOURCE DIST. - 10 cm (c)

ENERGY SCALE  $\approx$  2 Kev/PHU



97i 57

PULSE HEIGHT

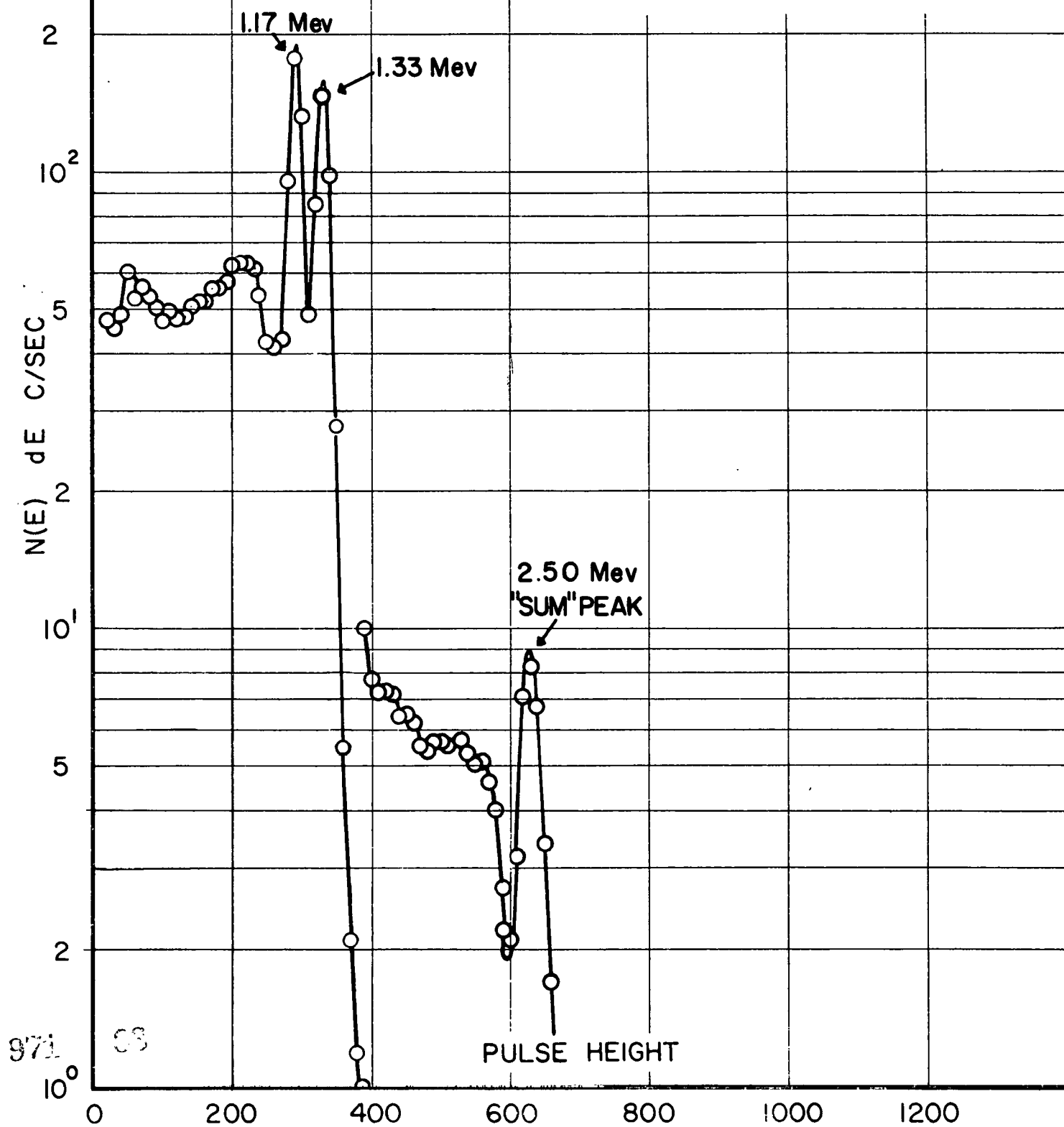
5.24 yr.  $\text{Co}^{60}$ 

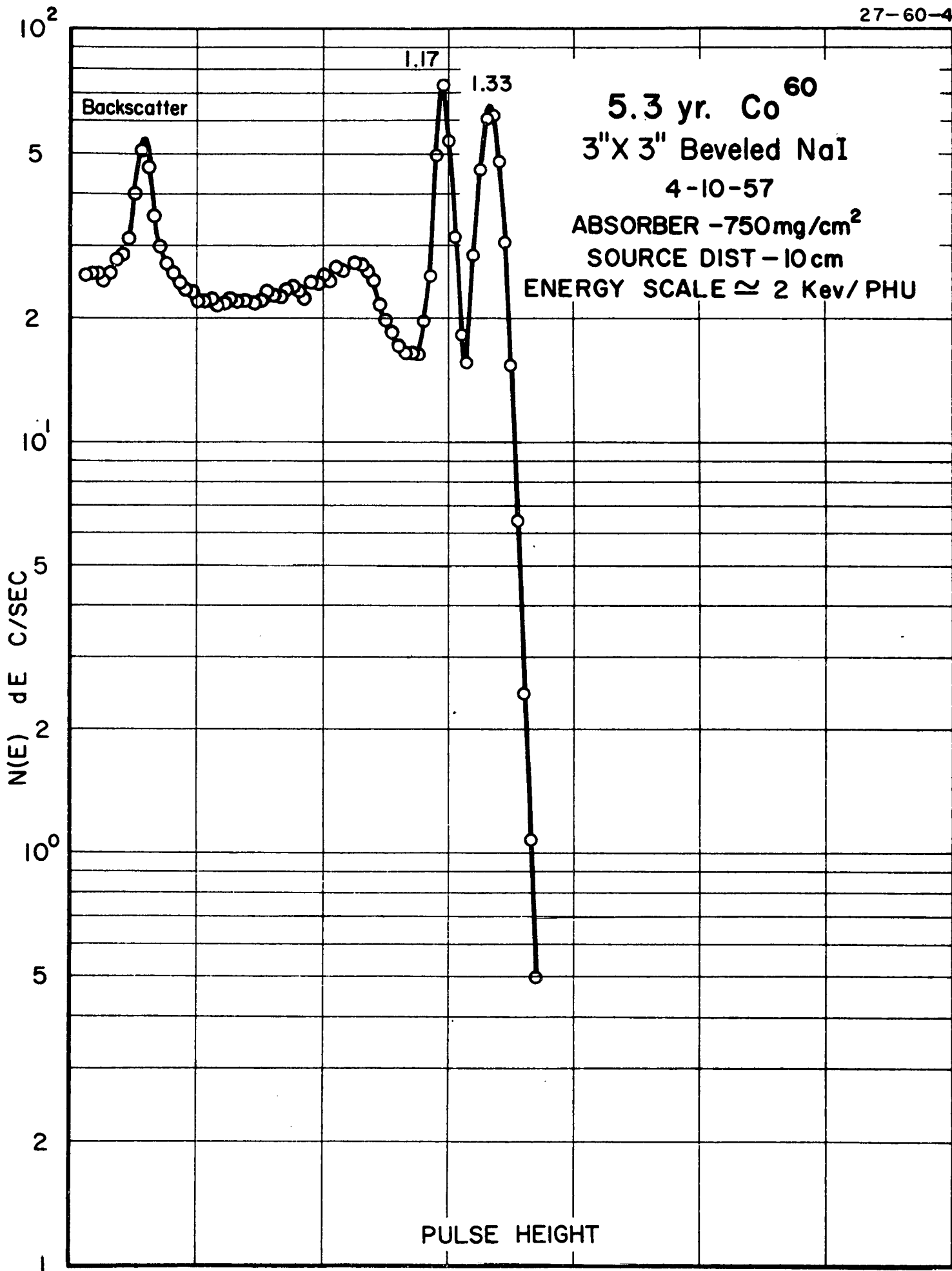
3" X 3"-2NaI

8-30-57

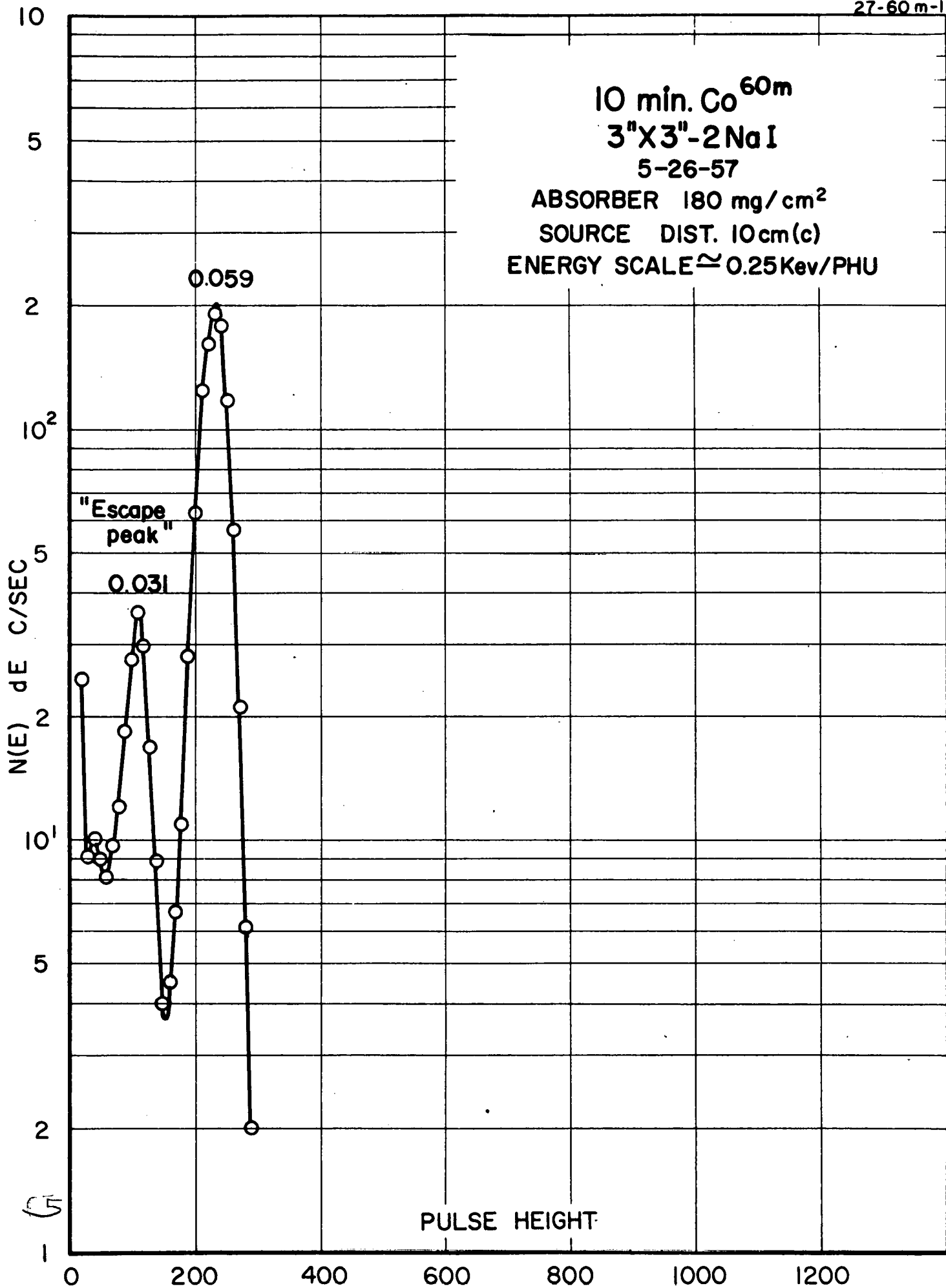
ABSORBER 200 mg/cm<sup>2</sup>

SOURCE DIST. 10cm (c)

ENERGY SCALE  $\approx$  4 Kev/PHU



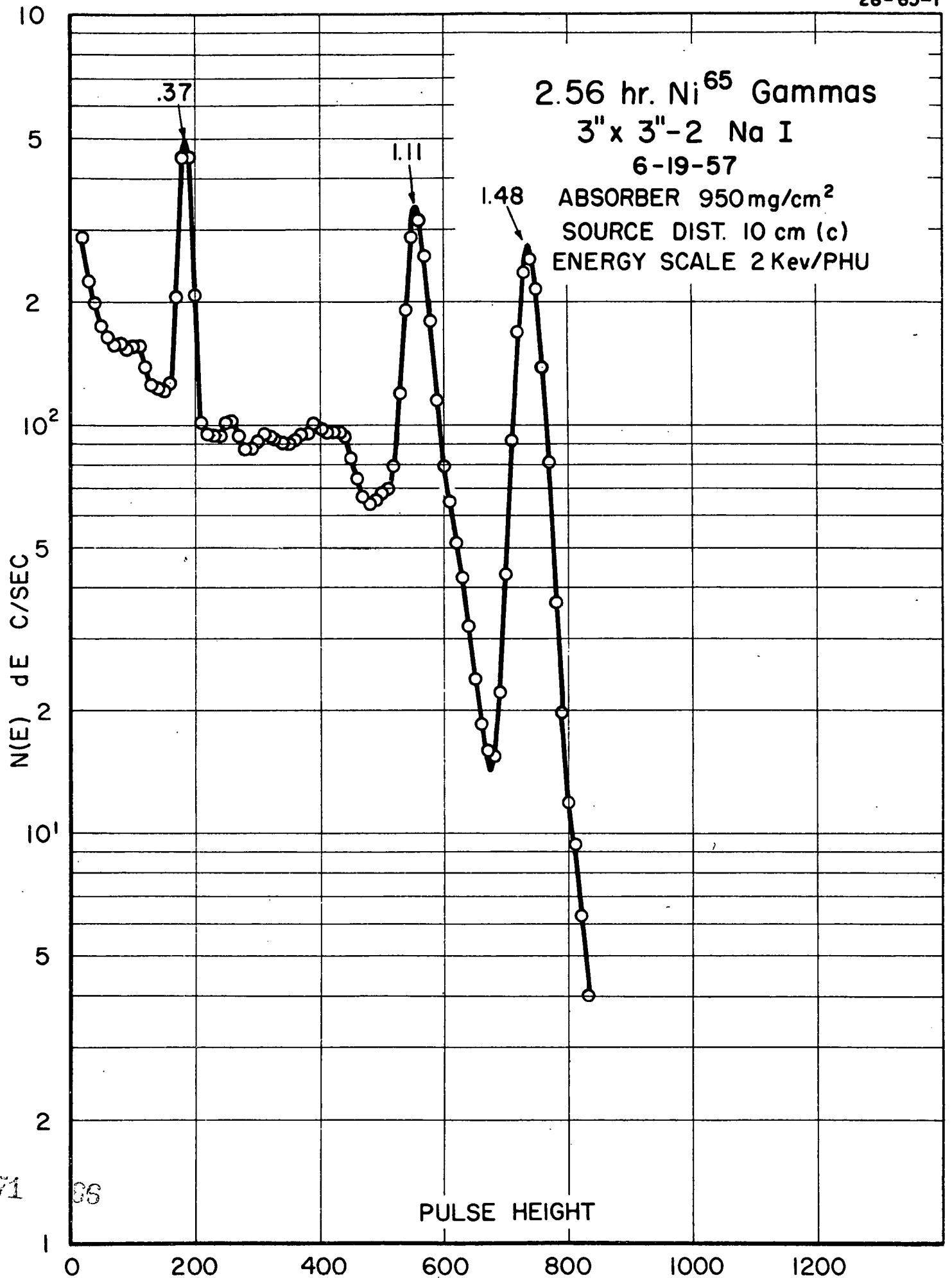
10 min. Co<sup>60m</sup>  
3"X3"-2NaI  
5-26-57  
ABSORBER 180 mg/cm<sup>2</sup>  
SOURCE DIST. 10cm(c)  
ENERGY SCALE  $\approx$  0.25Kev/PHU



971

5

PULSE HEIGHT



971 86

12.8 hr.  $\text{Cu}^{64}$  GAMMAS  
3" X 3" NaI

9-21-56

ABSORBER - 250 mg Cu SANDWICH

SOURCE DIST. - 10cm

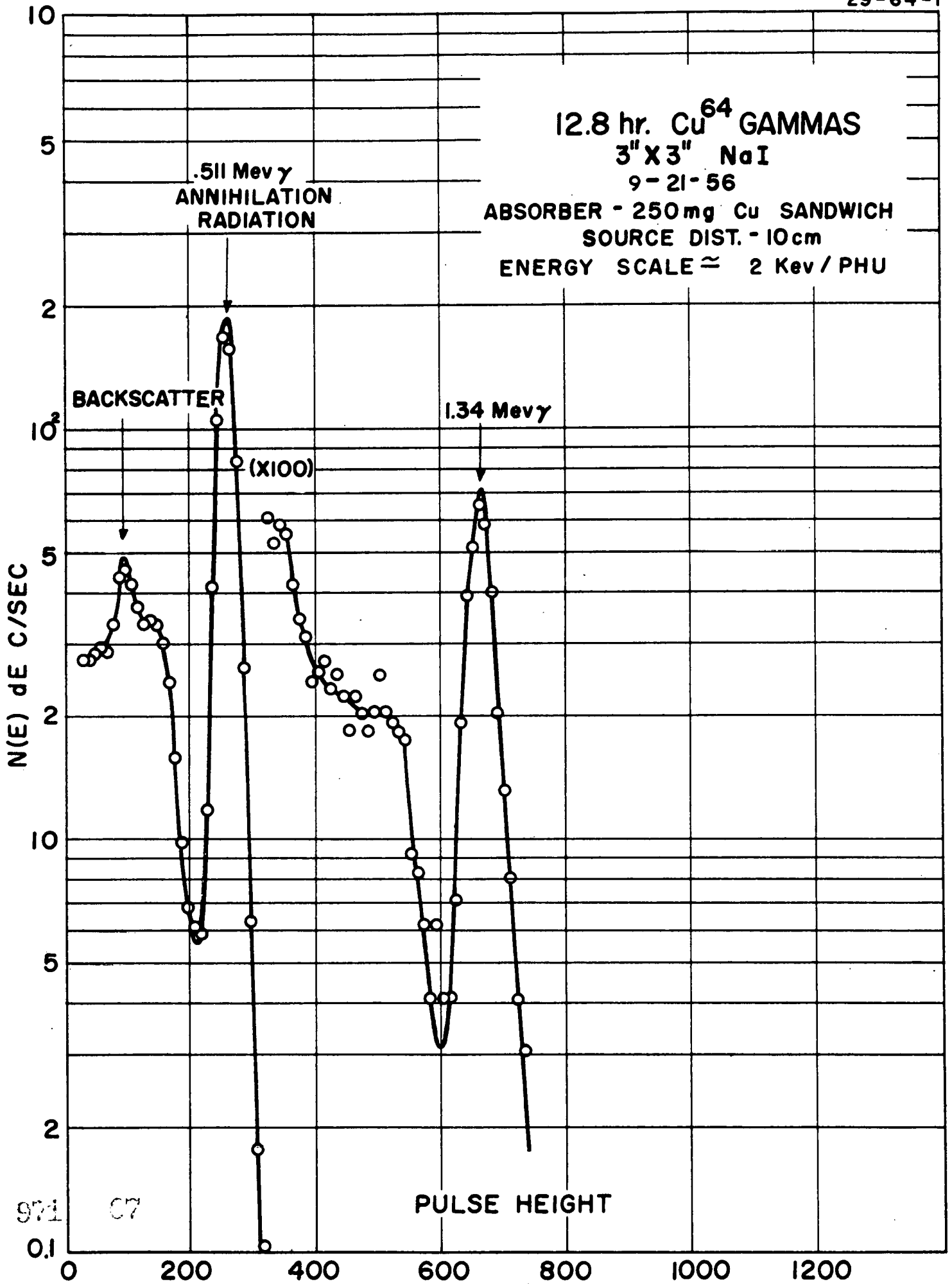
ENERGY SCALE  $\approx$  2 Kev / PHU

.511 Mev  $\gamma$   
ANNIHILATION  
RADIATION

BACKSCATTER

1.34 Mev

(X100)

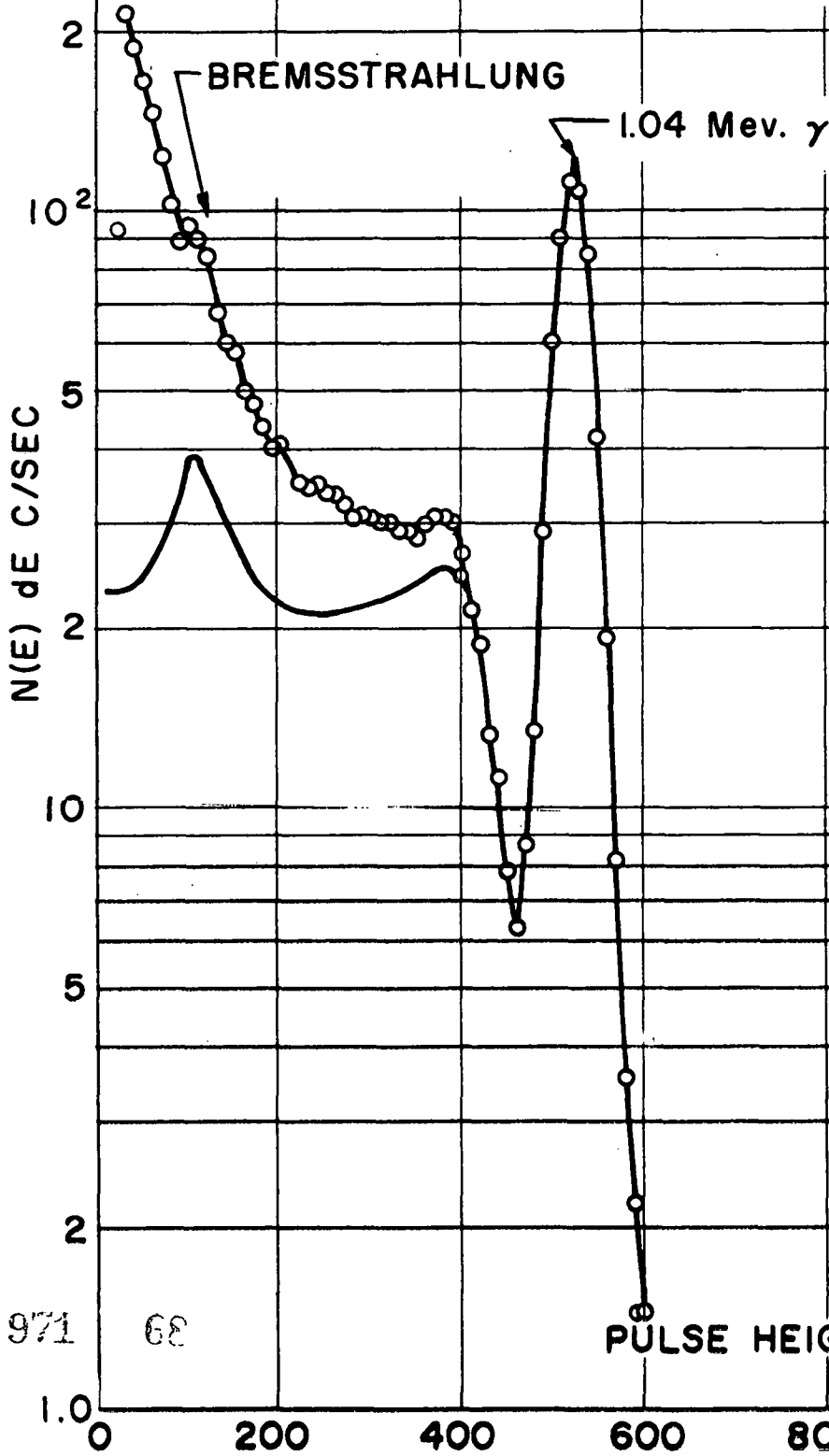


971 C7

PULSE HEIGHT

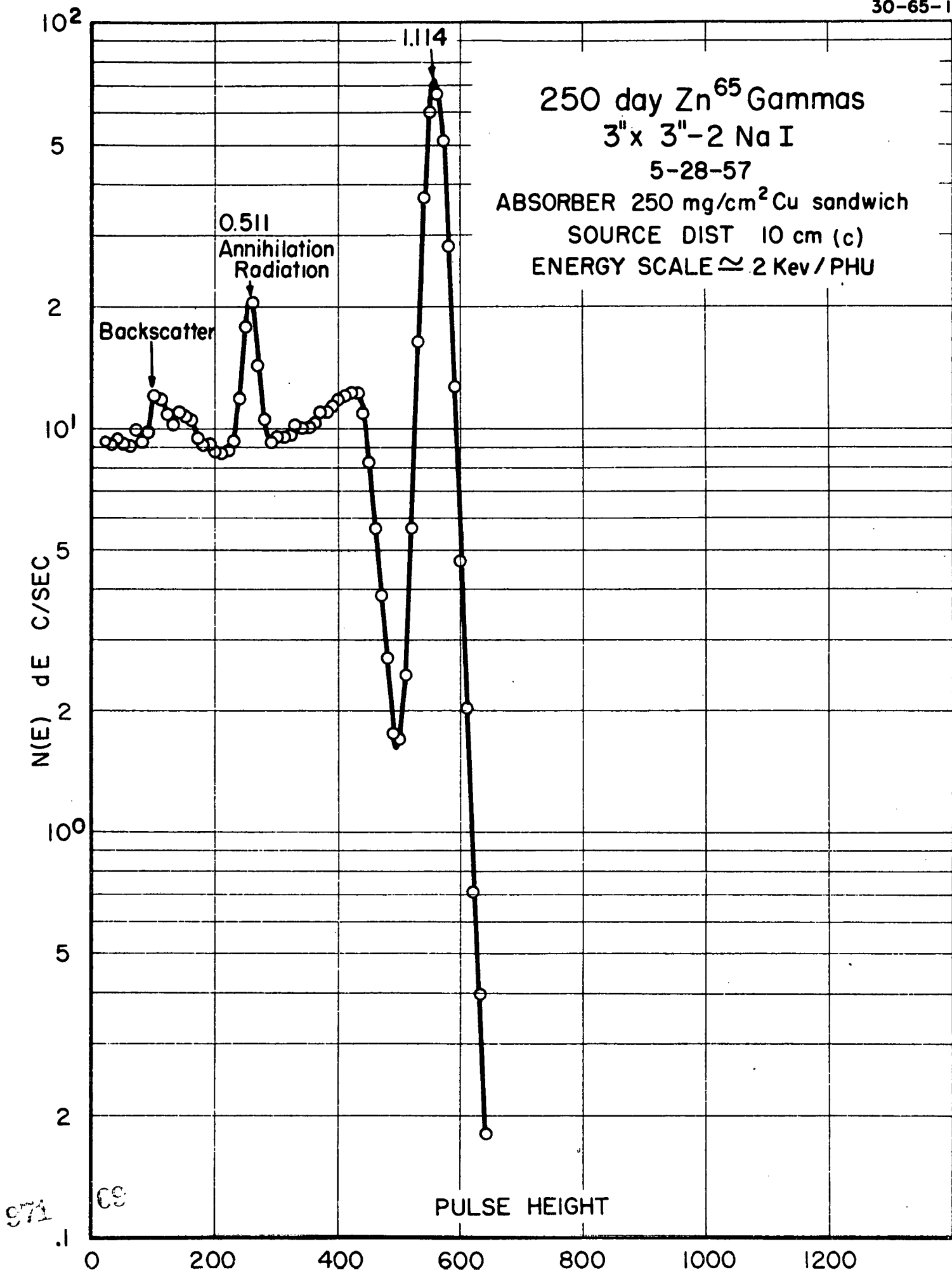
5 Min. Cu<sup>66</sup> GAMMAS  
3" x 3" Na I  
7-31-56

ABSORBER - 1.34 + .95g/cm<sup>2</sup>  
SOURCE DIST. - 12cm.  
ENERGY SCALE  $\approx$  2 Kev/ PHU



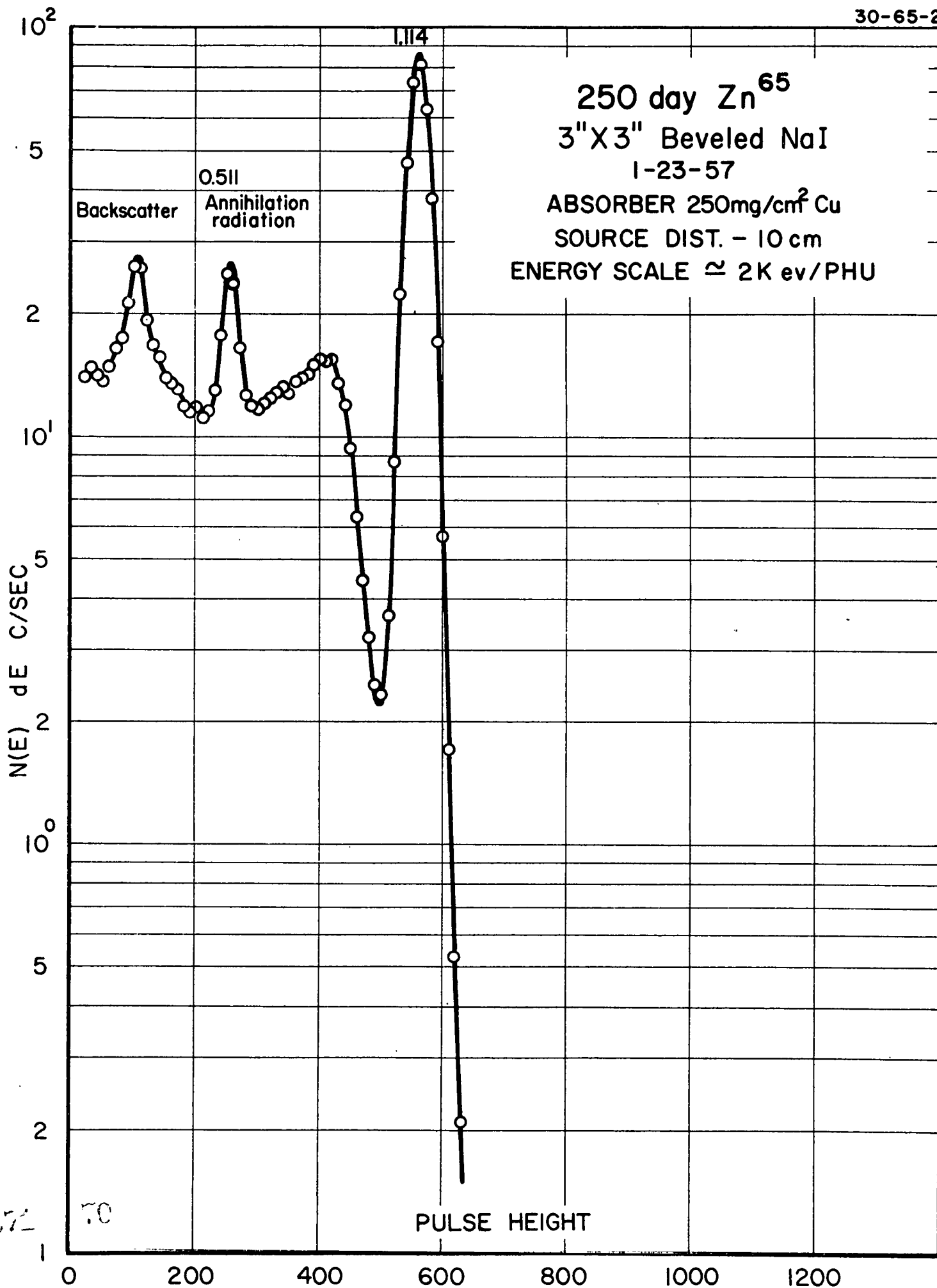
971 68

PULSE HEIGHT



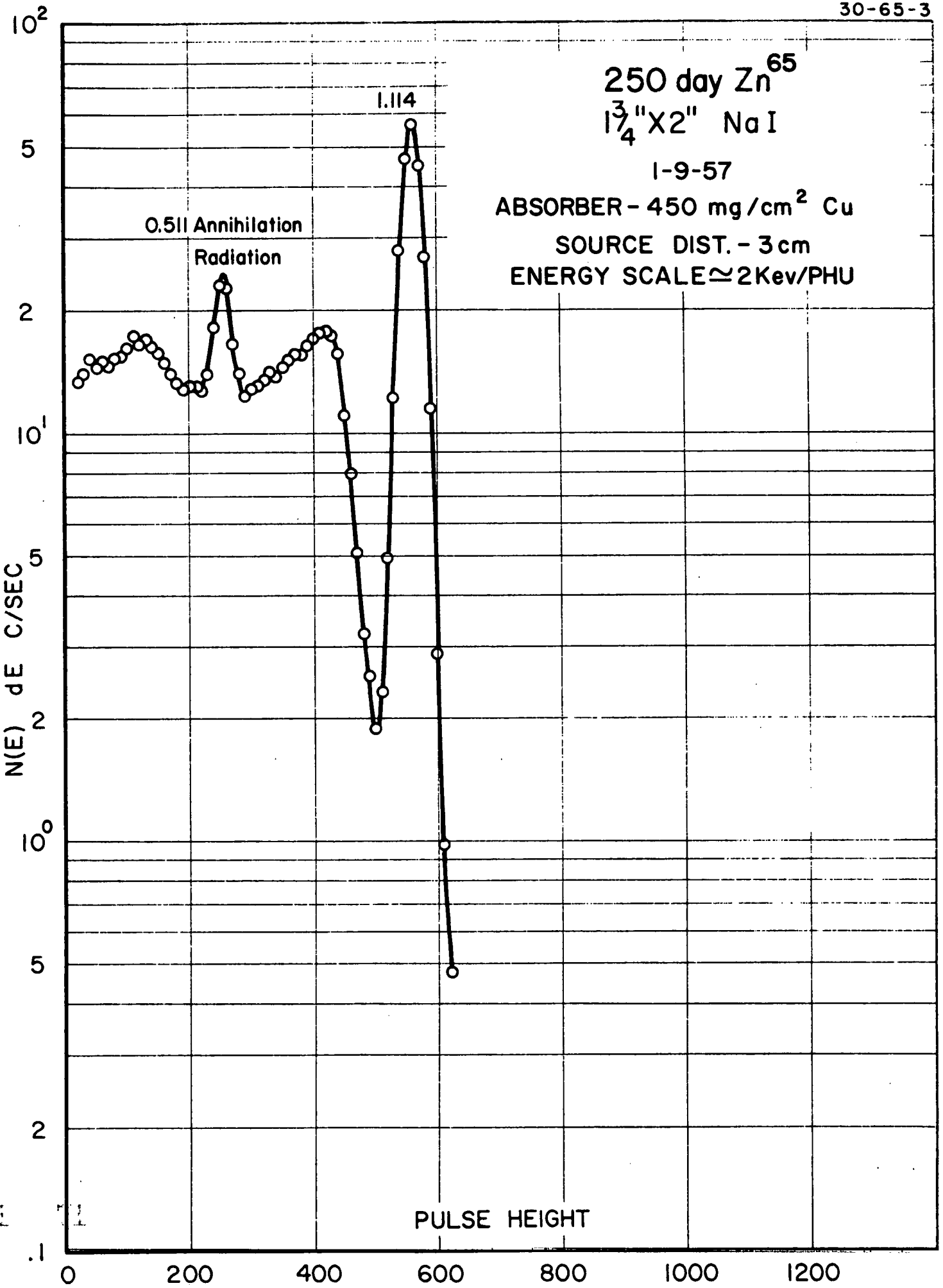
971

CS

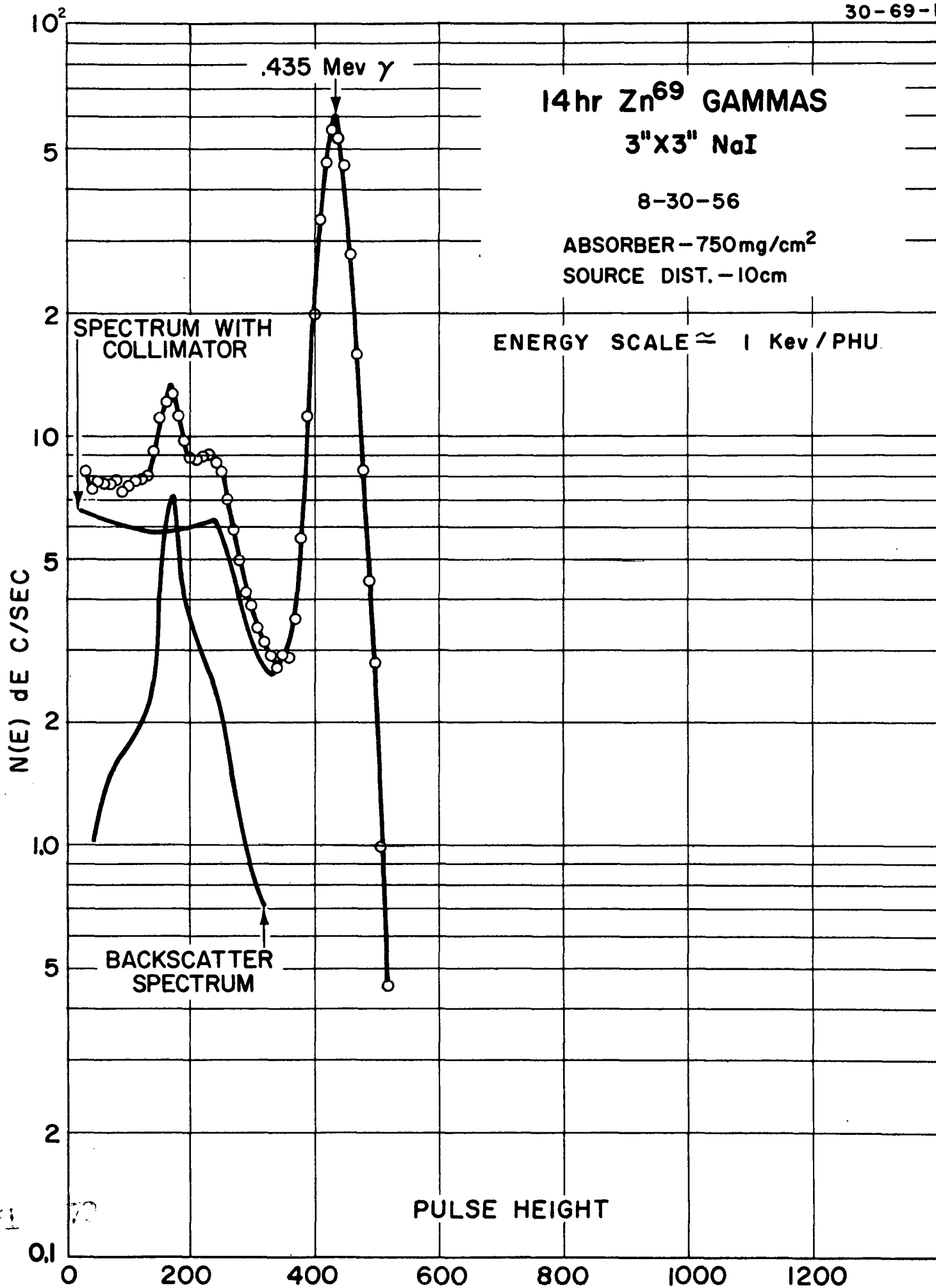


572 70

PULSE HEIGHT

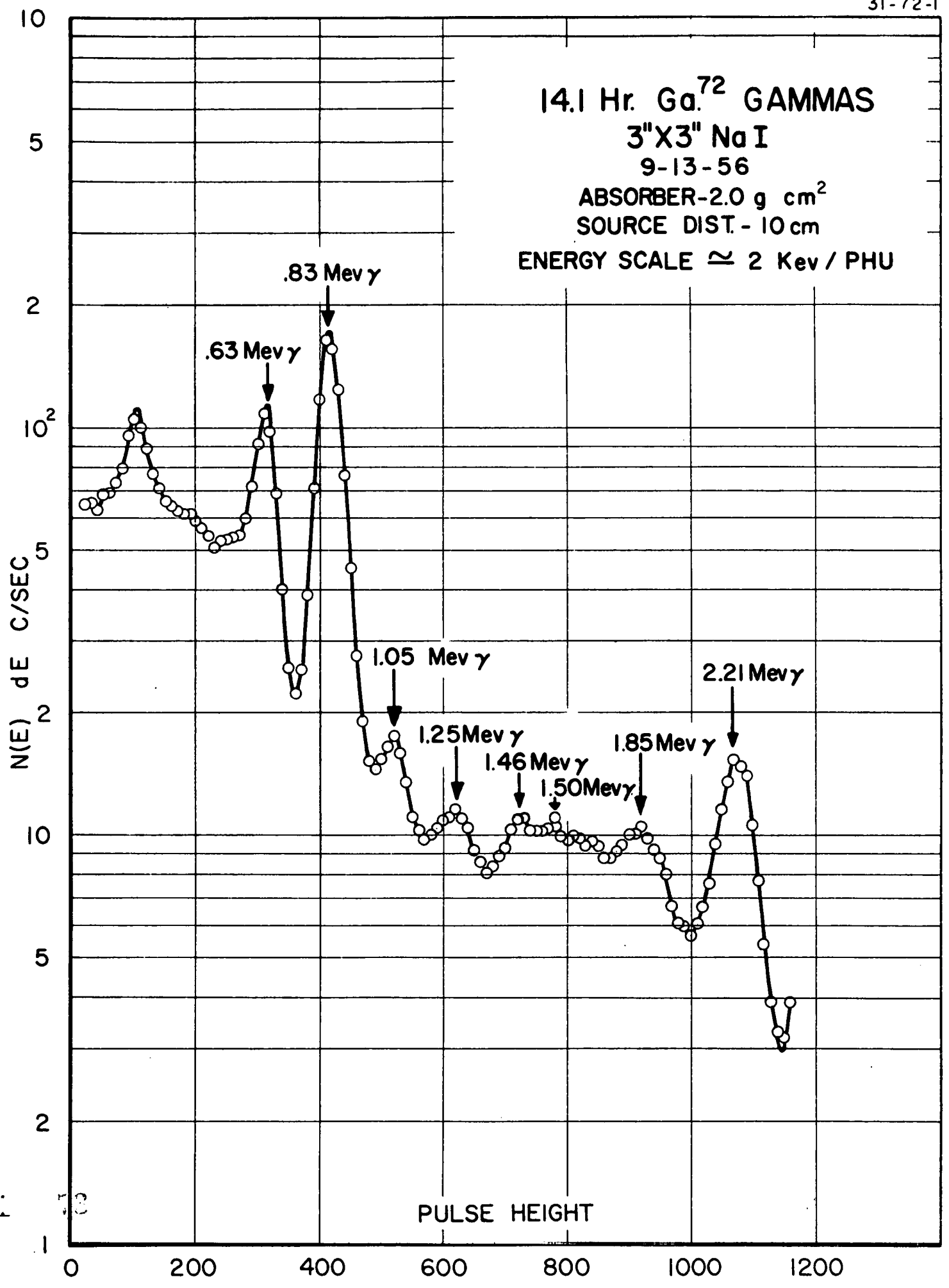


971



971 72

14.1 Hr. Ga.<sup>72</sup> GAMMAS  
3"X3" NaI  
9-13-56  
ABSORBER-2.0 g cm<sup>2</sup>  
SOURCE DIST.- 10 cm  
ENERGY SCALE  $\approx$  2 Kev / PHU



971 13

PULSE HEIGHT

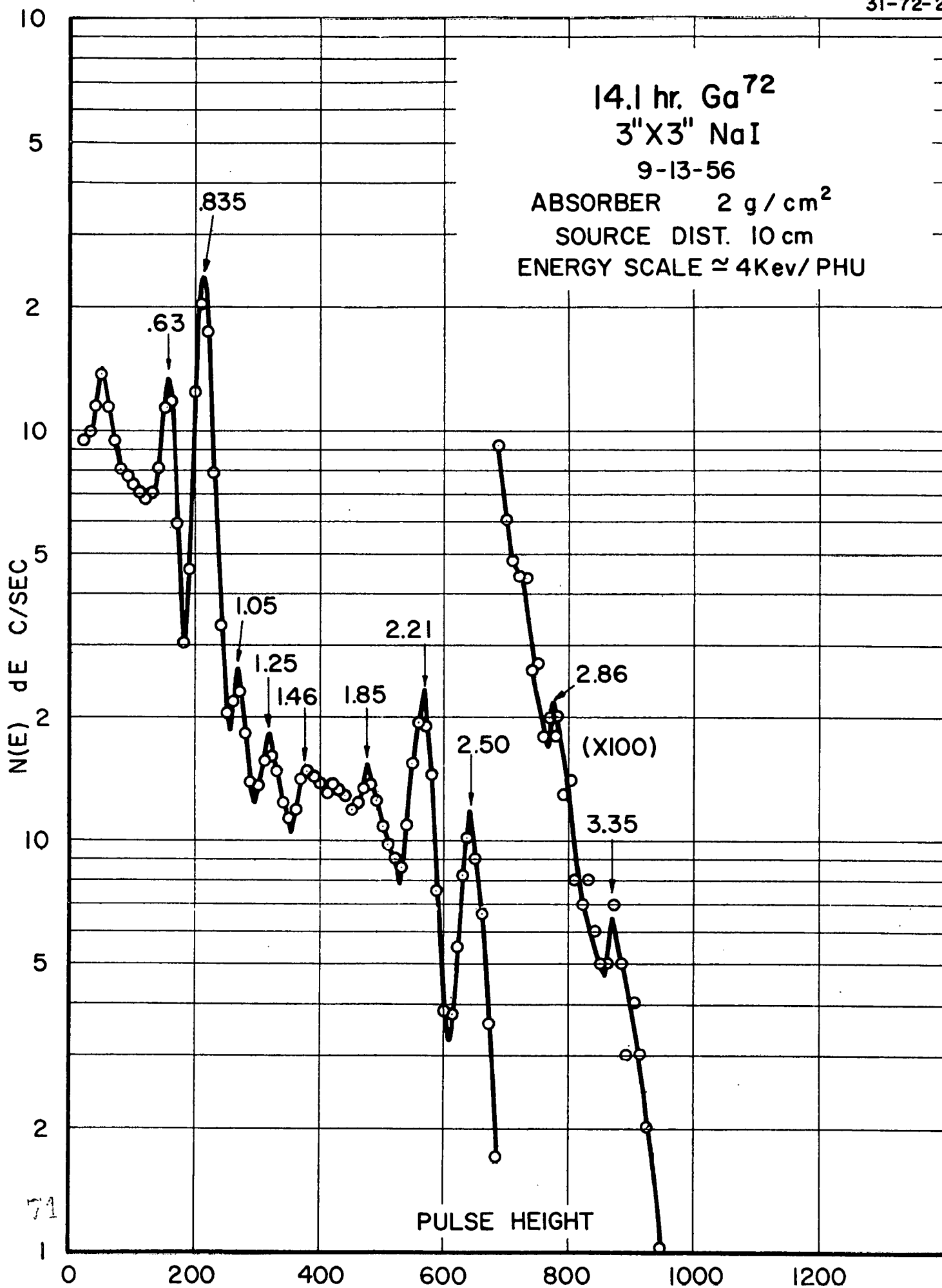
14.1 hr. Ga<sup>72</sup>

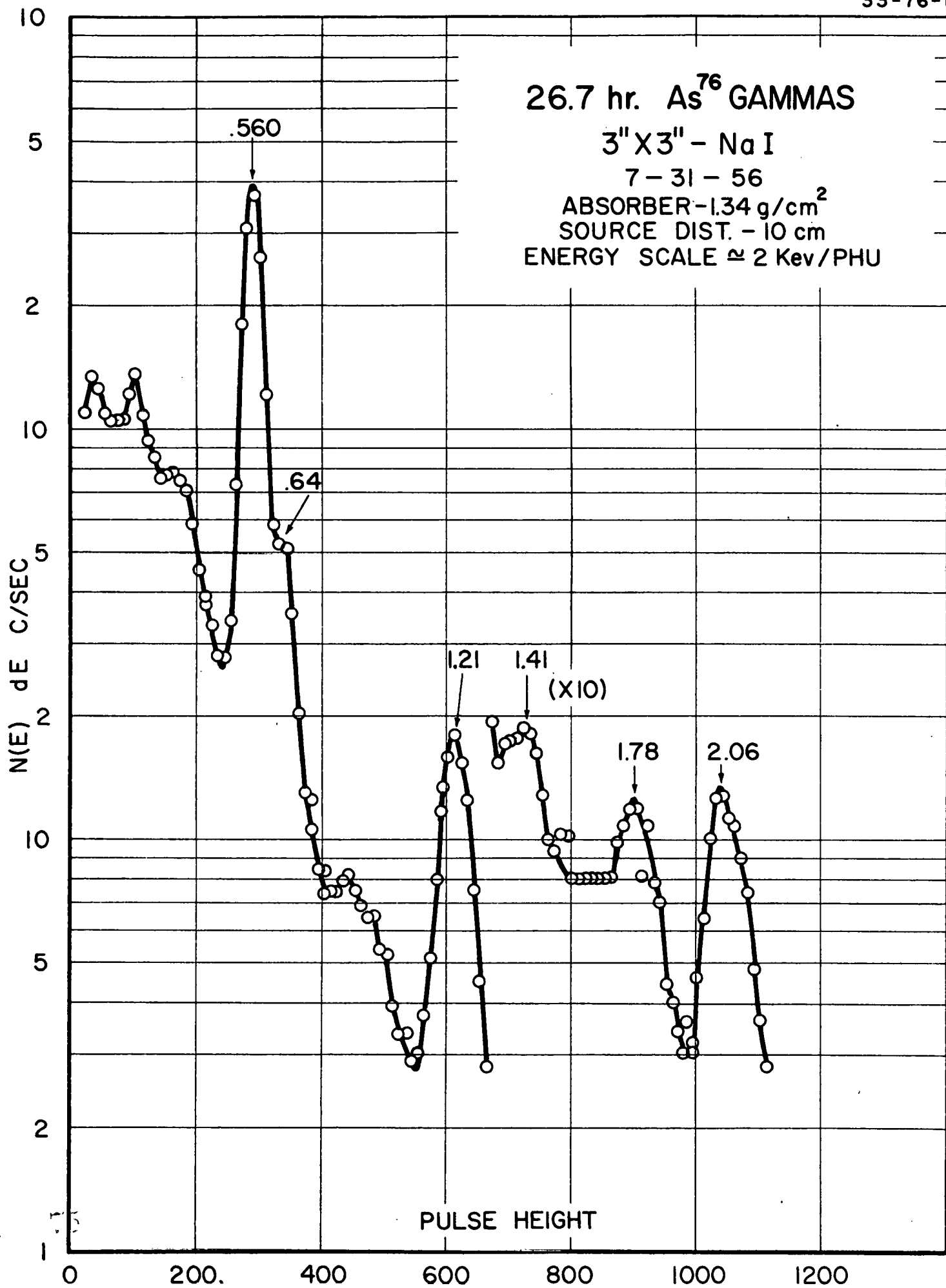
3"X3" NaI

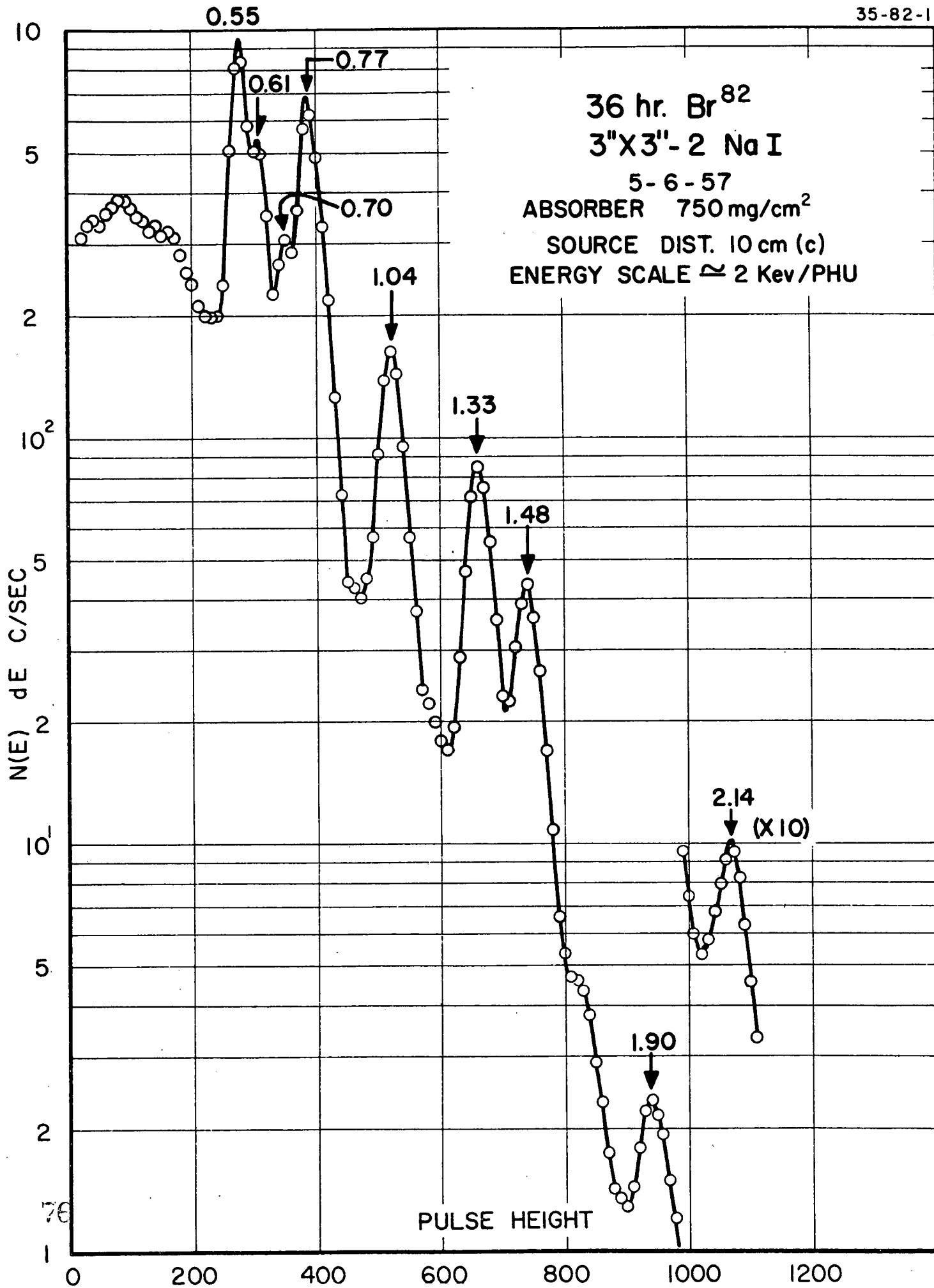
9-13-56

ABSORBER 2 g/cm<sup>2</sup>

SOURCE DIST. 10 cm

ENERGY SCALE  $\approx$  4Kev/PHU





971

76

PULSE HEIGHT

10.4 yr.  $Kr^{85}$

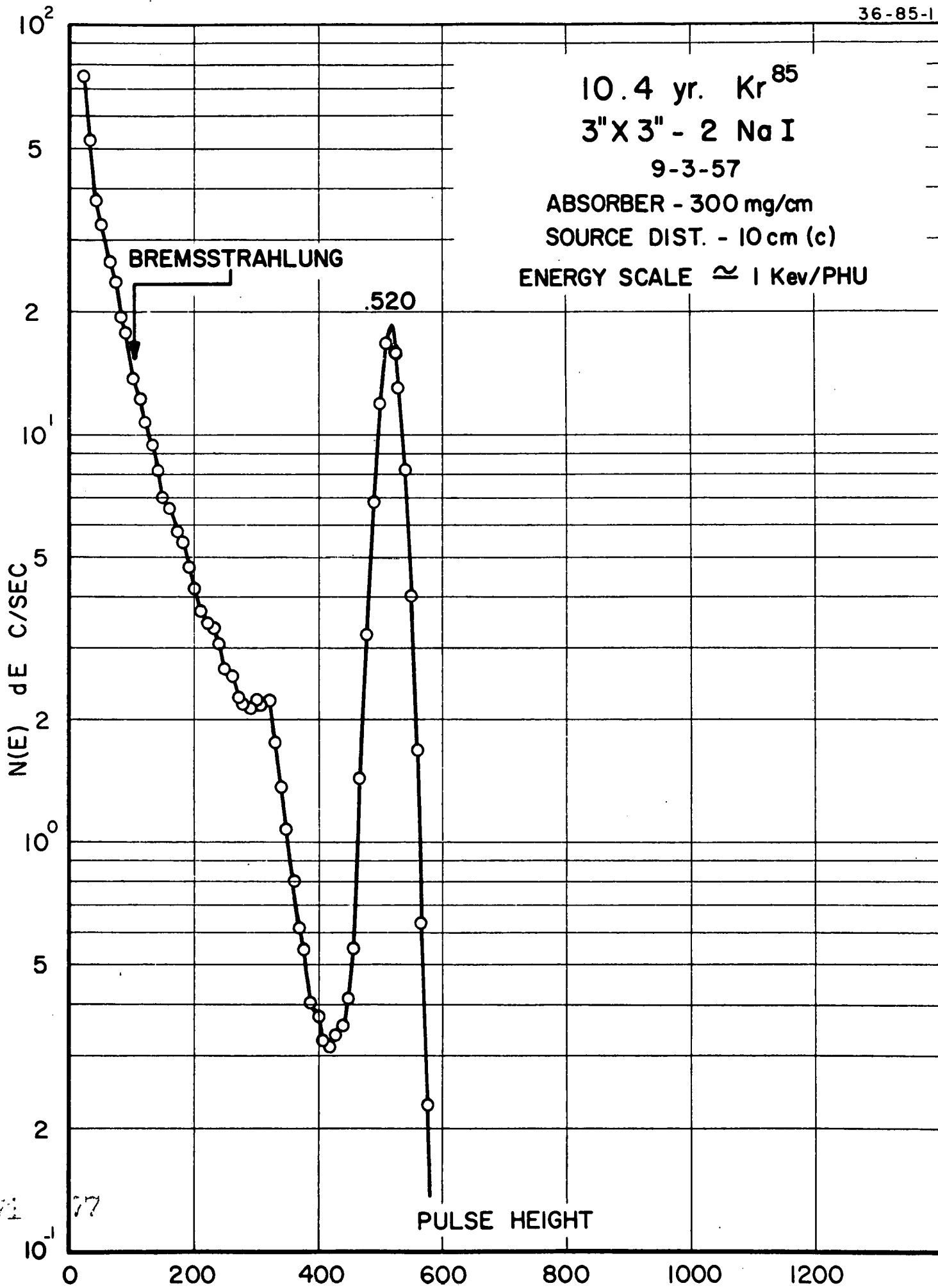
3" X 3" - 2 Na I

9-3-57

ABSORBER - 300 mg/cm

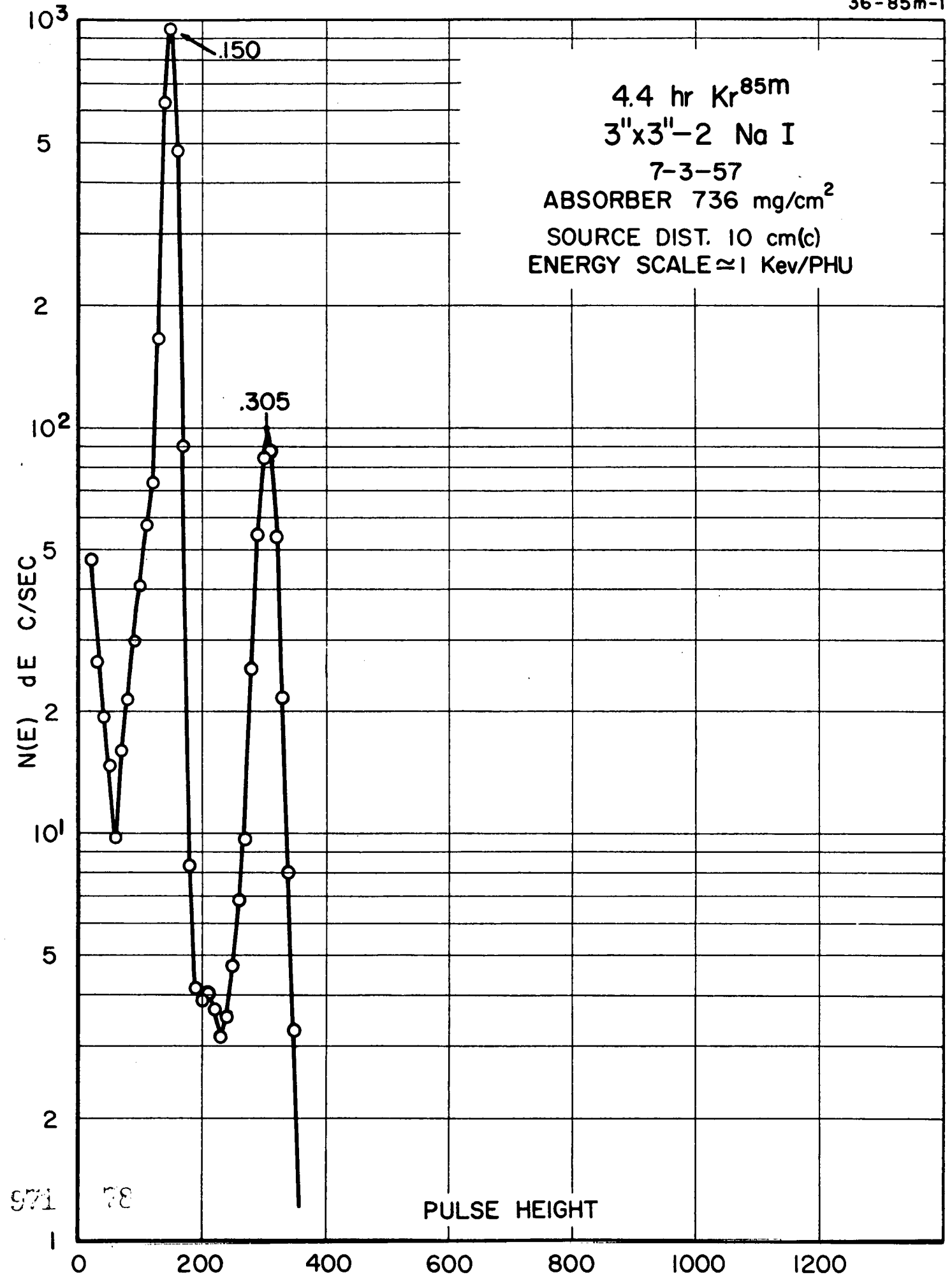
SOURCE DIST. - 10 cm (c)

ENERGY SCALE  $\approx$  1 Kev/PHU

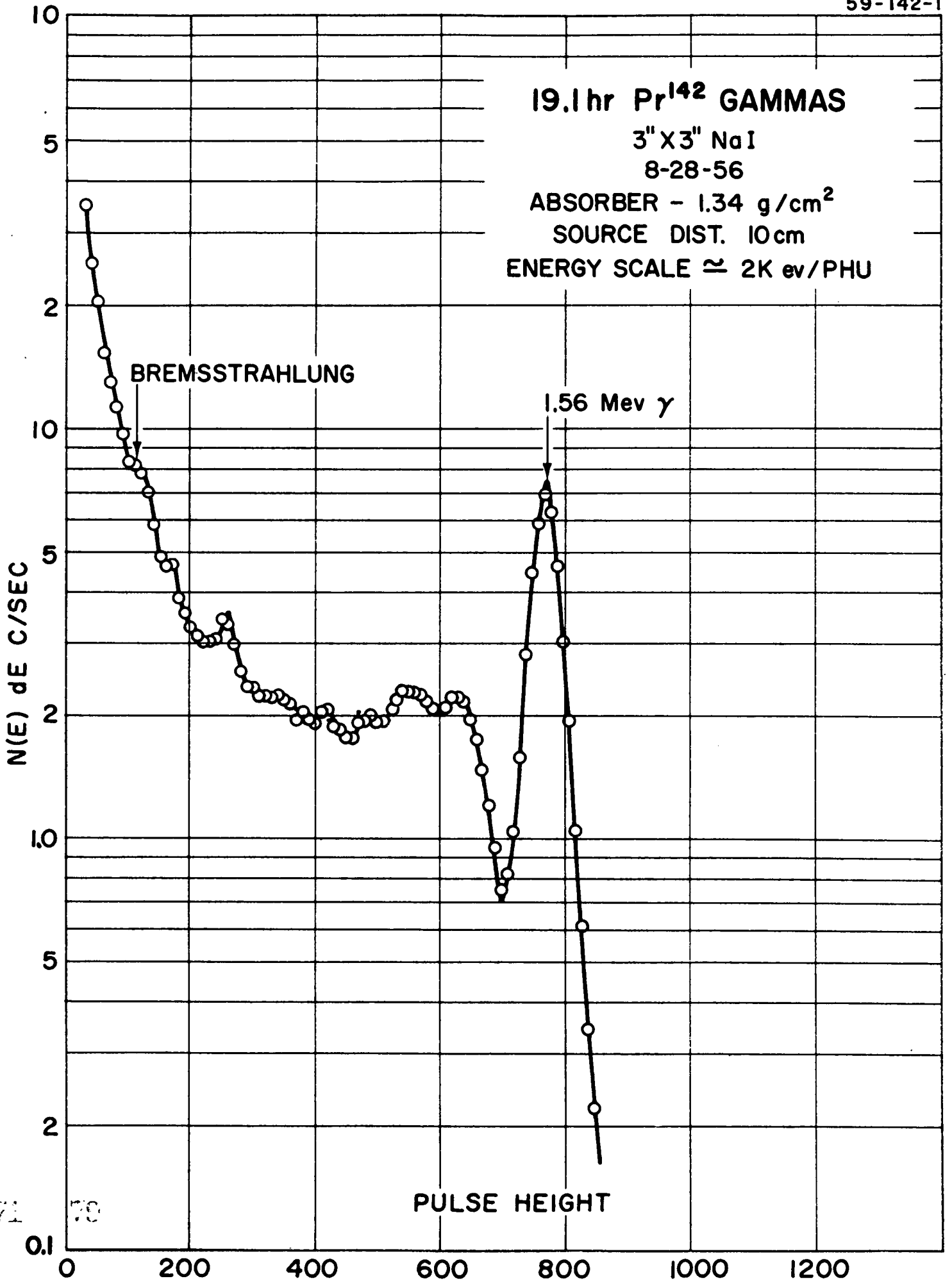


971 77

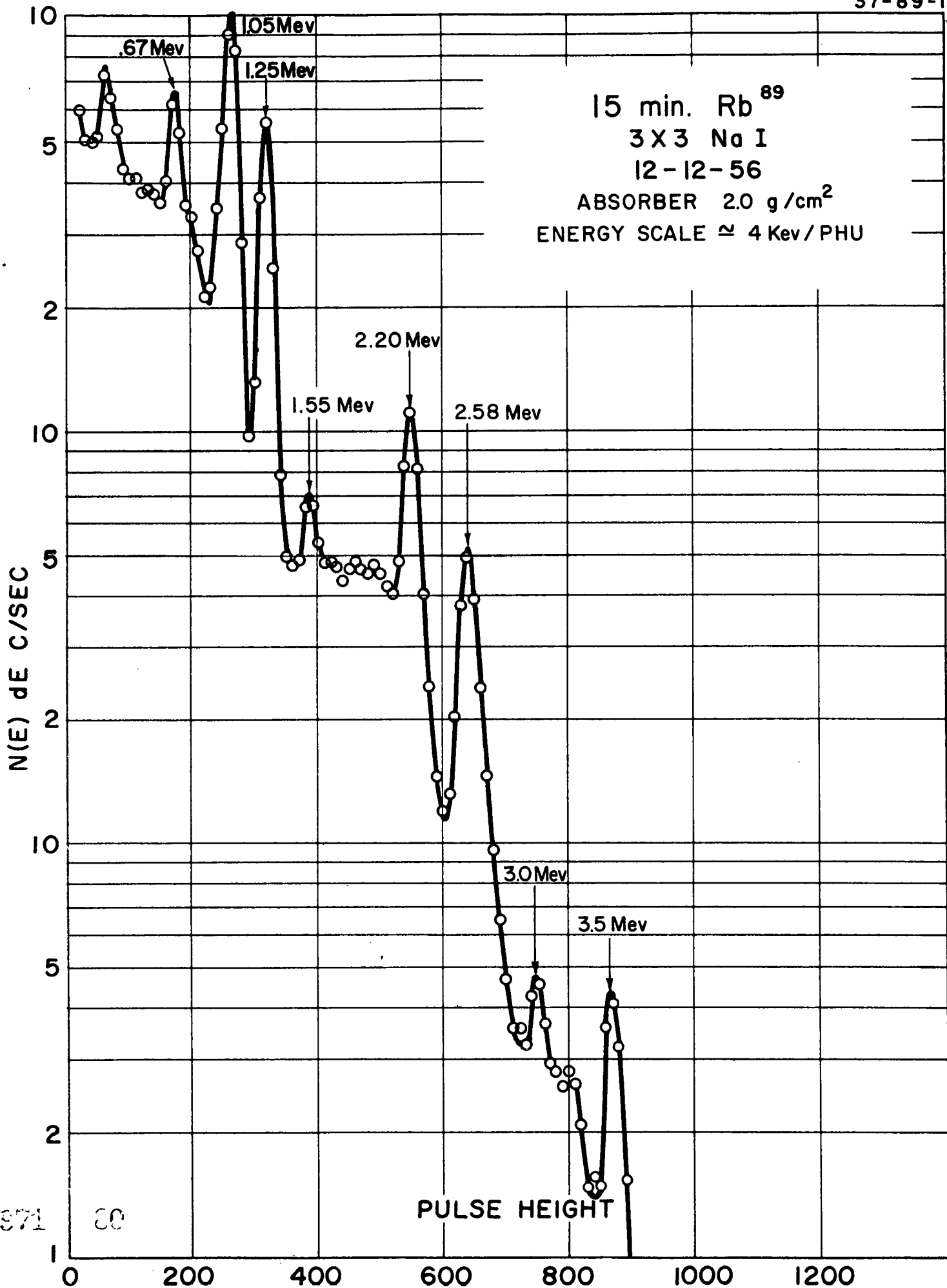
PULSE HEIGHT



19.1 hr Pr<sup>142</sup> GAMMAS  
3" X 3" NaI  
8-28-56  
ABSORBER - 1.34 g/cm<sup>2</sup>  
SOURCE DIST. 10 cm  
ENERGY SCALE  $\approx$  2K ev/PHU



971 79



371 00

PULSE HEIGHT

9.7 hr. Sr<sup>91</sup>

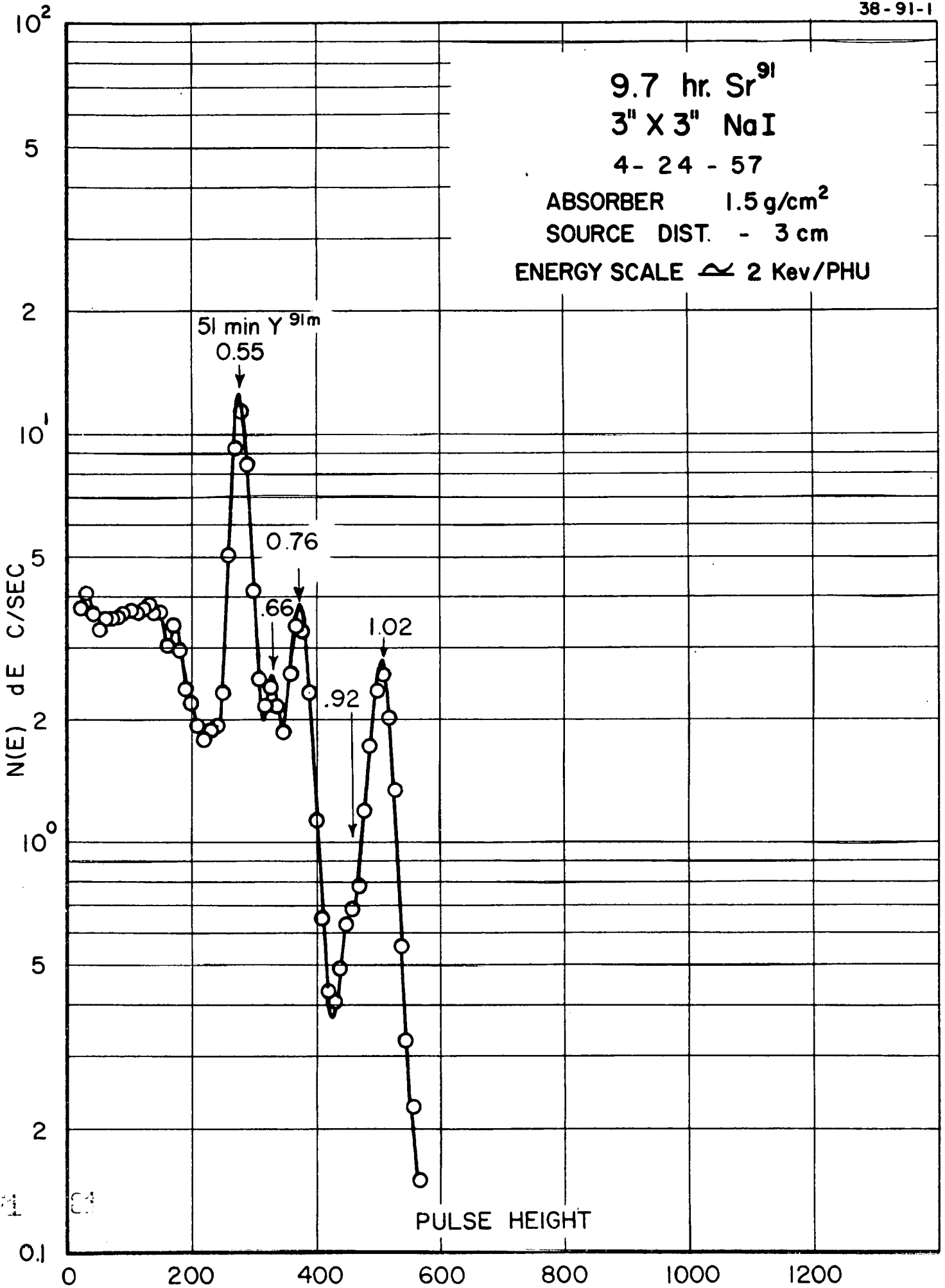
3" X 3" NaI

4-24-57

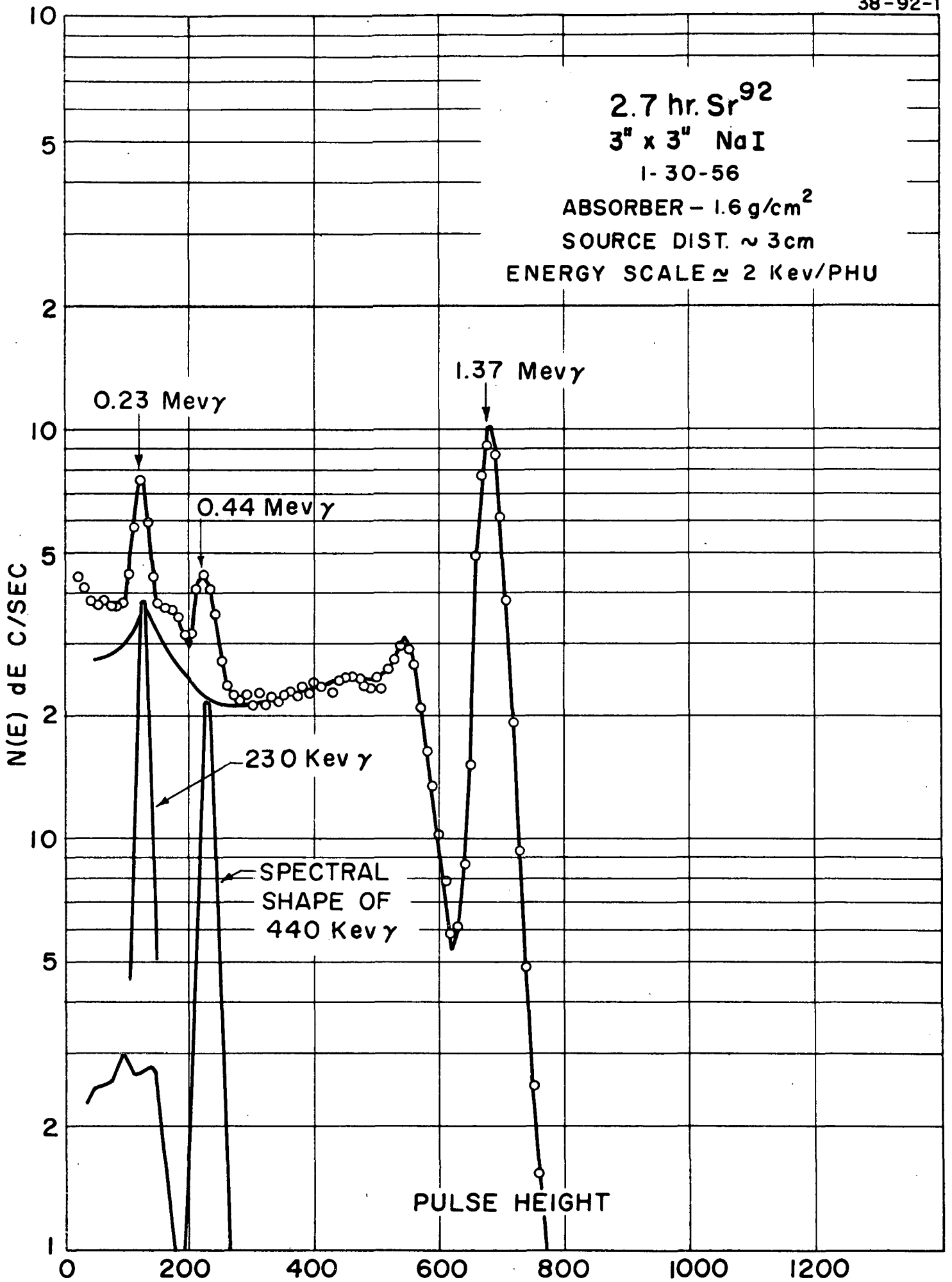
ABSORBER 1.5 g/cm<sup>2</sup>

SOURCE DIST. - 3 cm

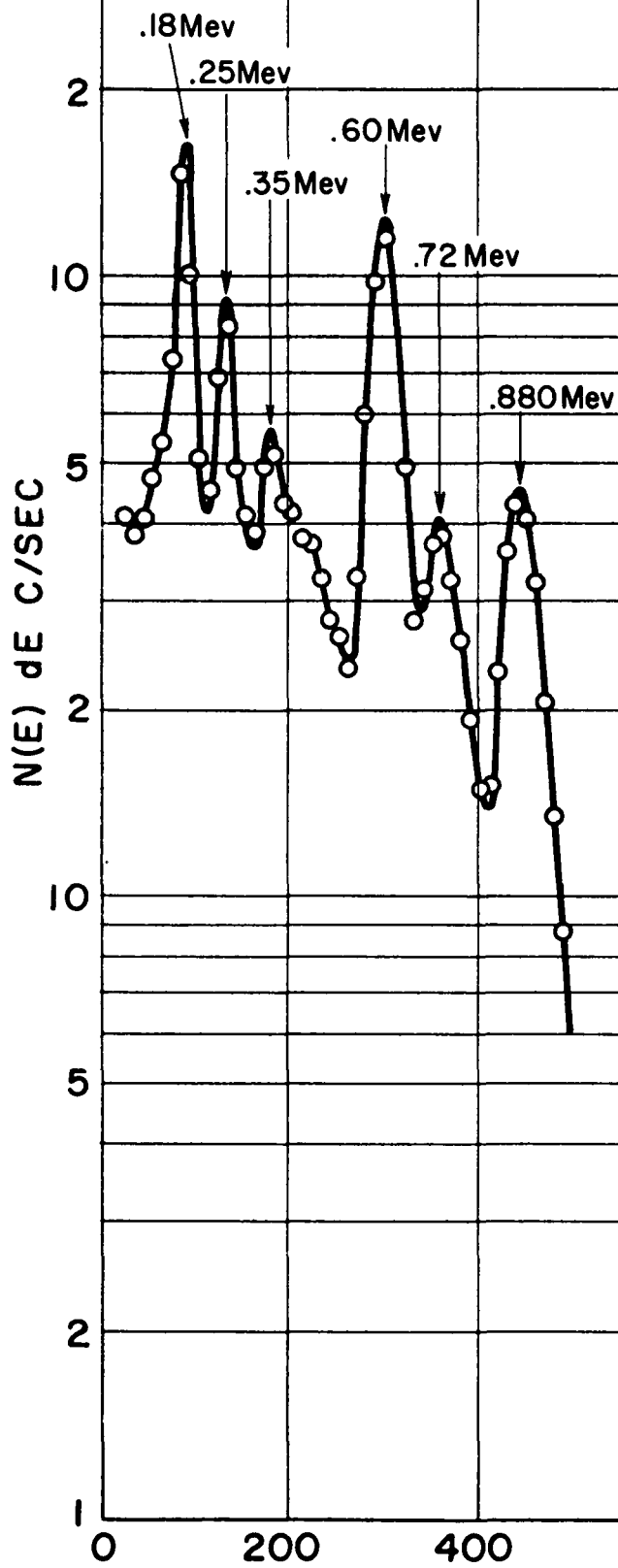
ENERGY SCALE  $\approx$  2 Kev/PHU



971



7.0 min  $\text{Sr}^{93}$  GAMMAS  
 3 X 3 Na I  
 4-20-56  
 ABSORBER 2.0 gm/cm<sup>2</sup>  
 SOURCE DIST. — 10 cm  
 ENERGY SCALE  $\approx$  2 Kev / PHU



PULSE HEIGHT

105 day  $Y^{88}$

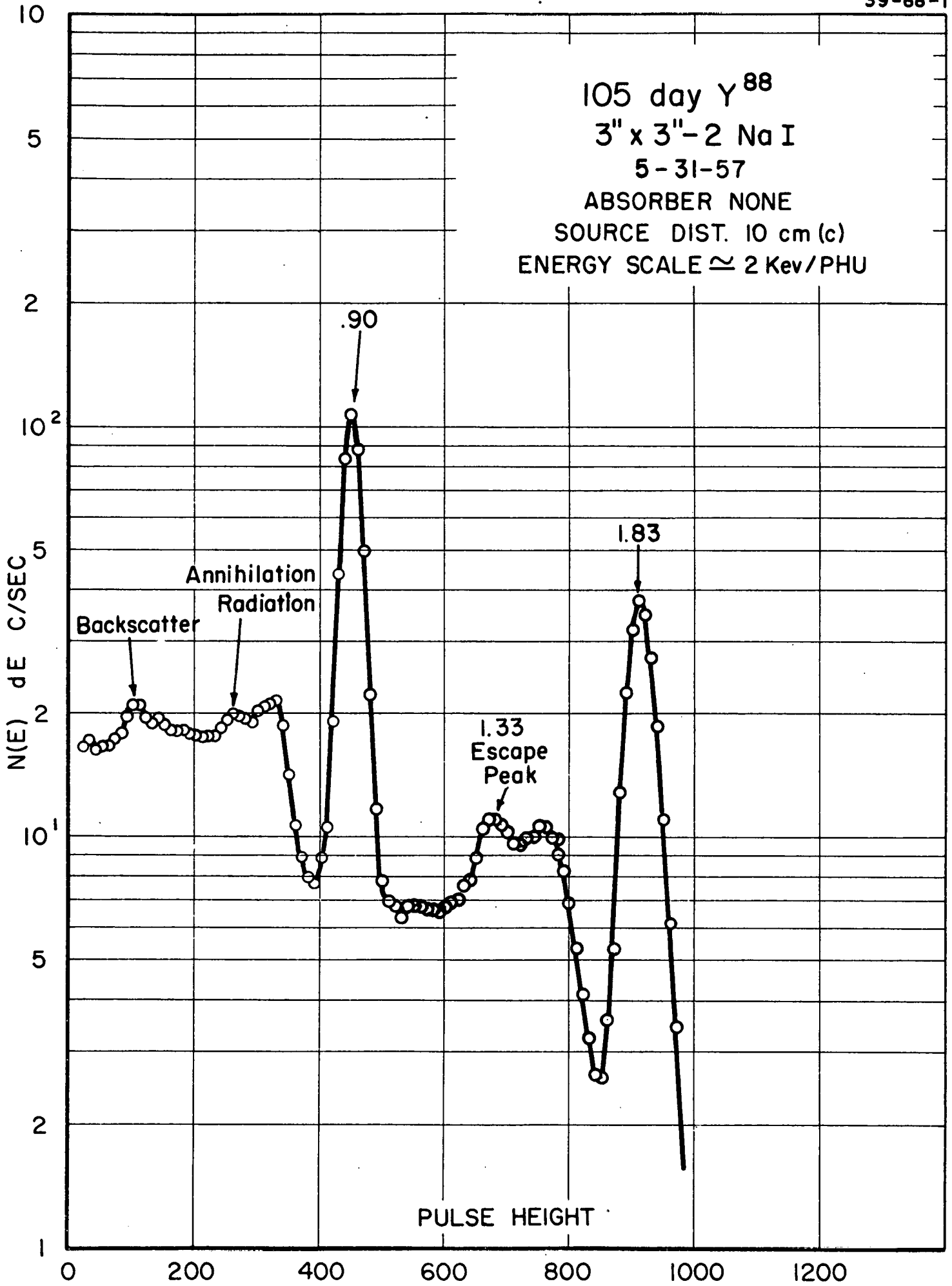
3" x 3"-2 Na I

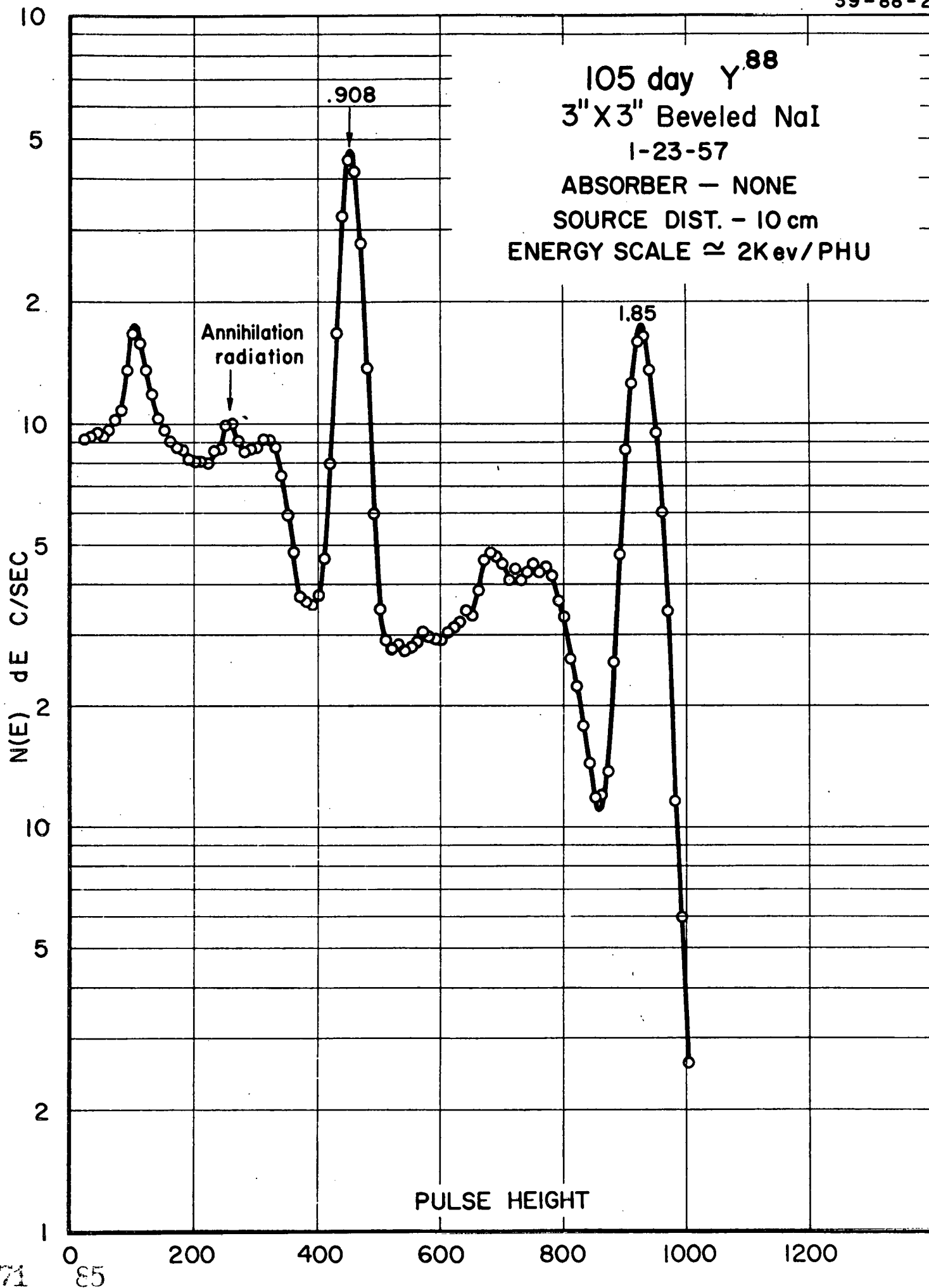
5-31-57

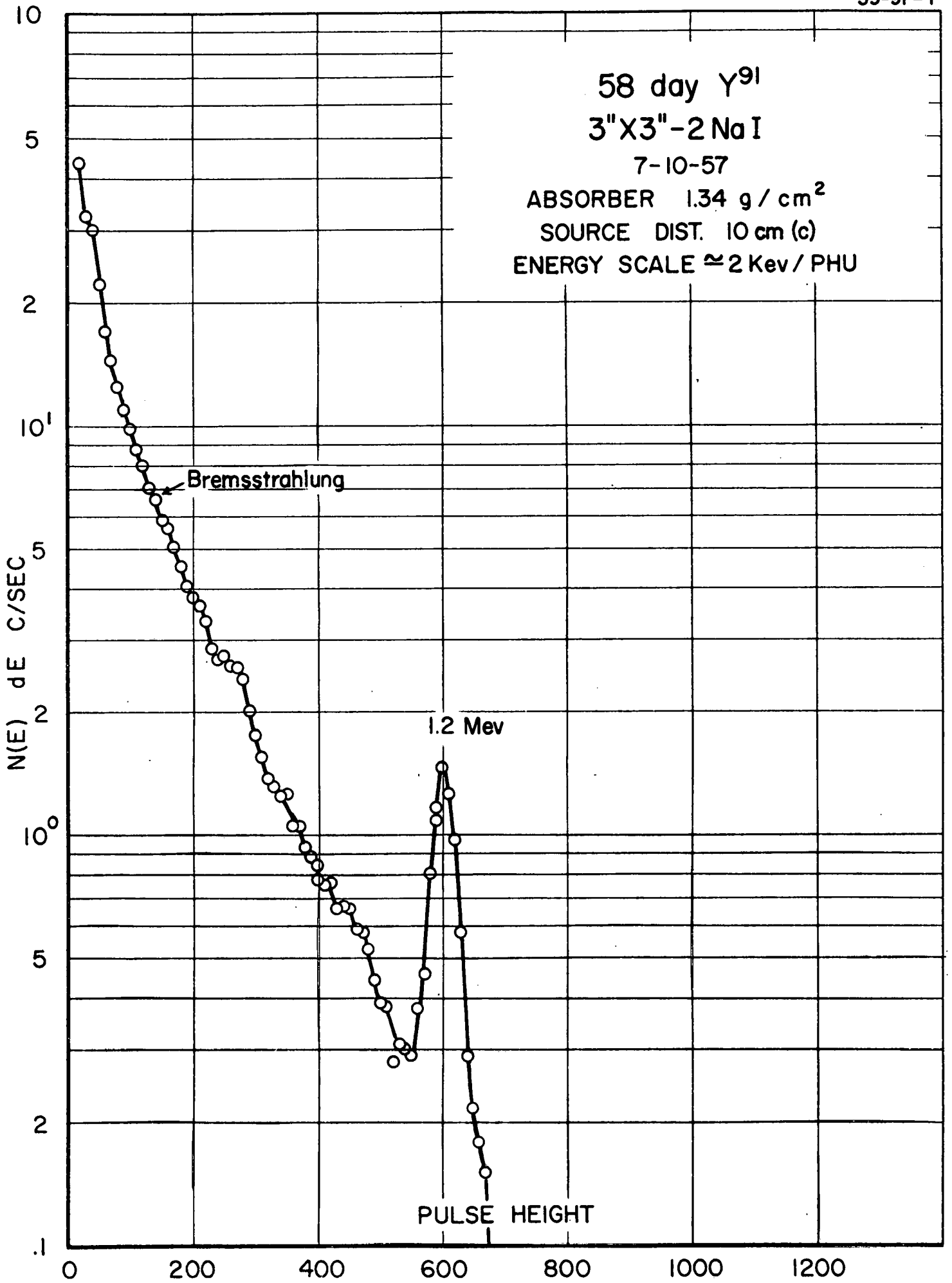
ABSORBER NONE

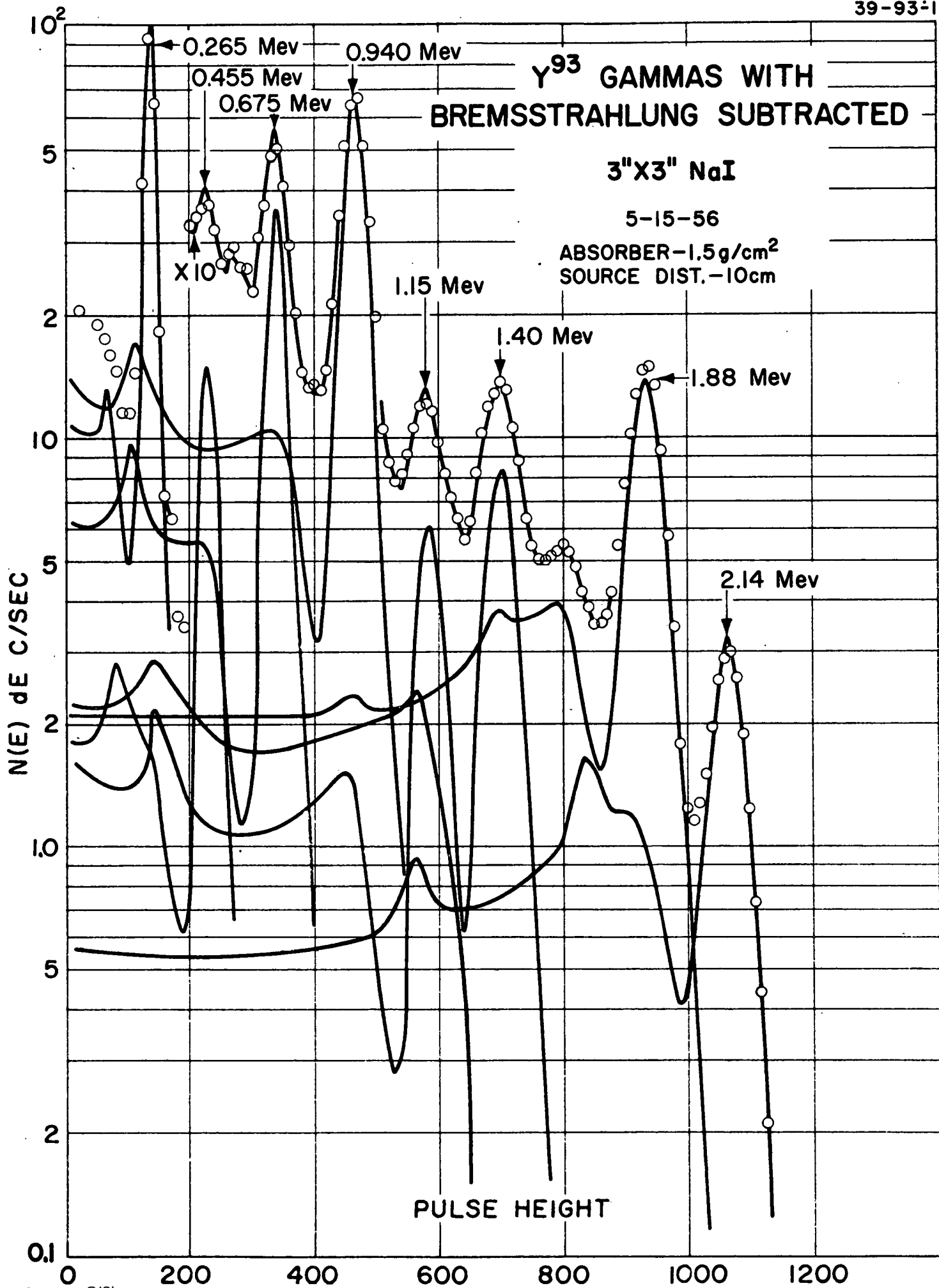
SOURCE DIST. 10 cm (c)

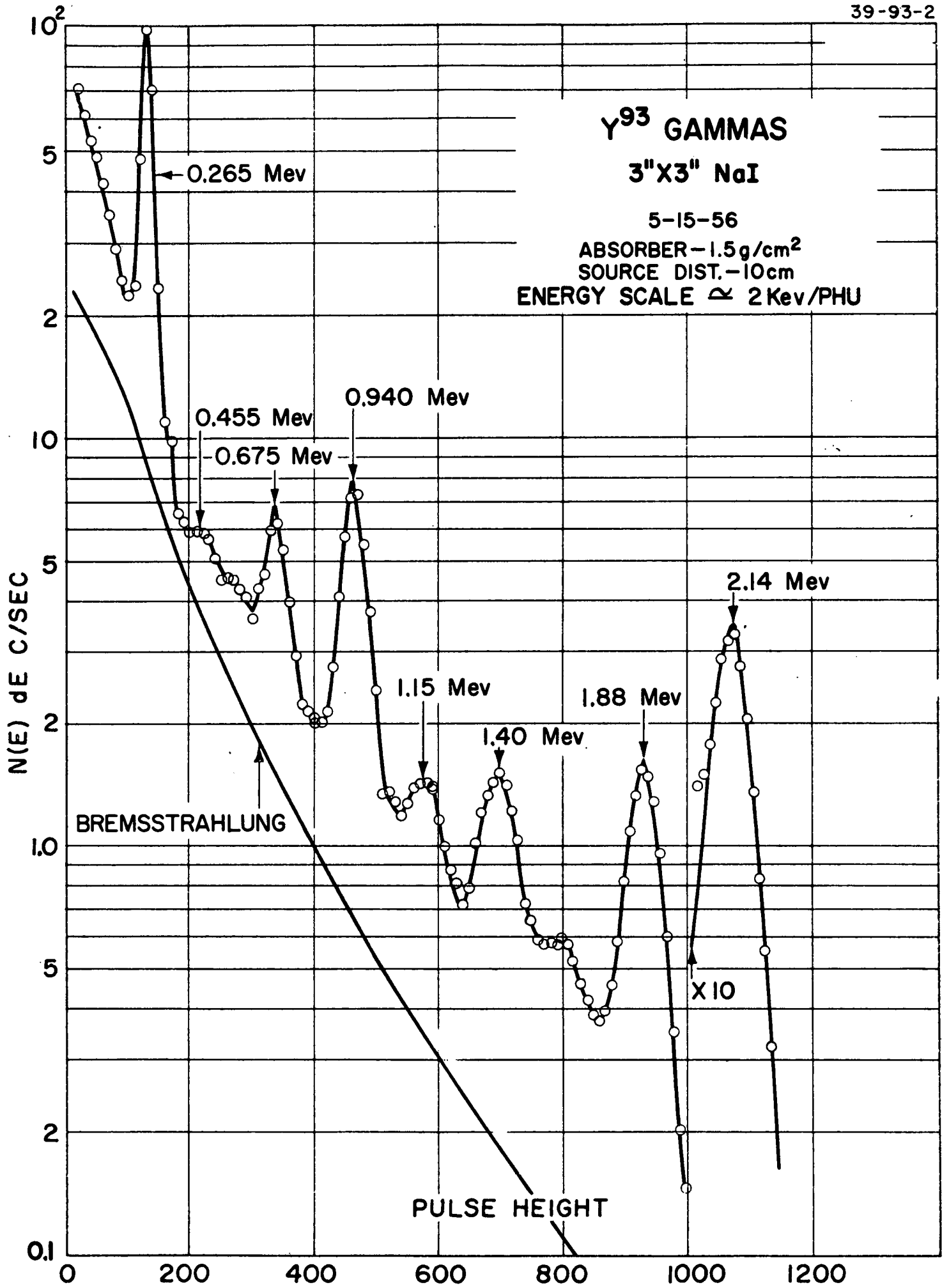
ENERGY SCALE  $\approx 2$  Kev/PHU

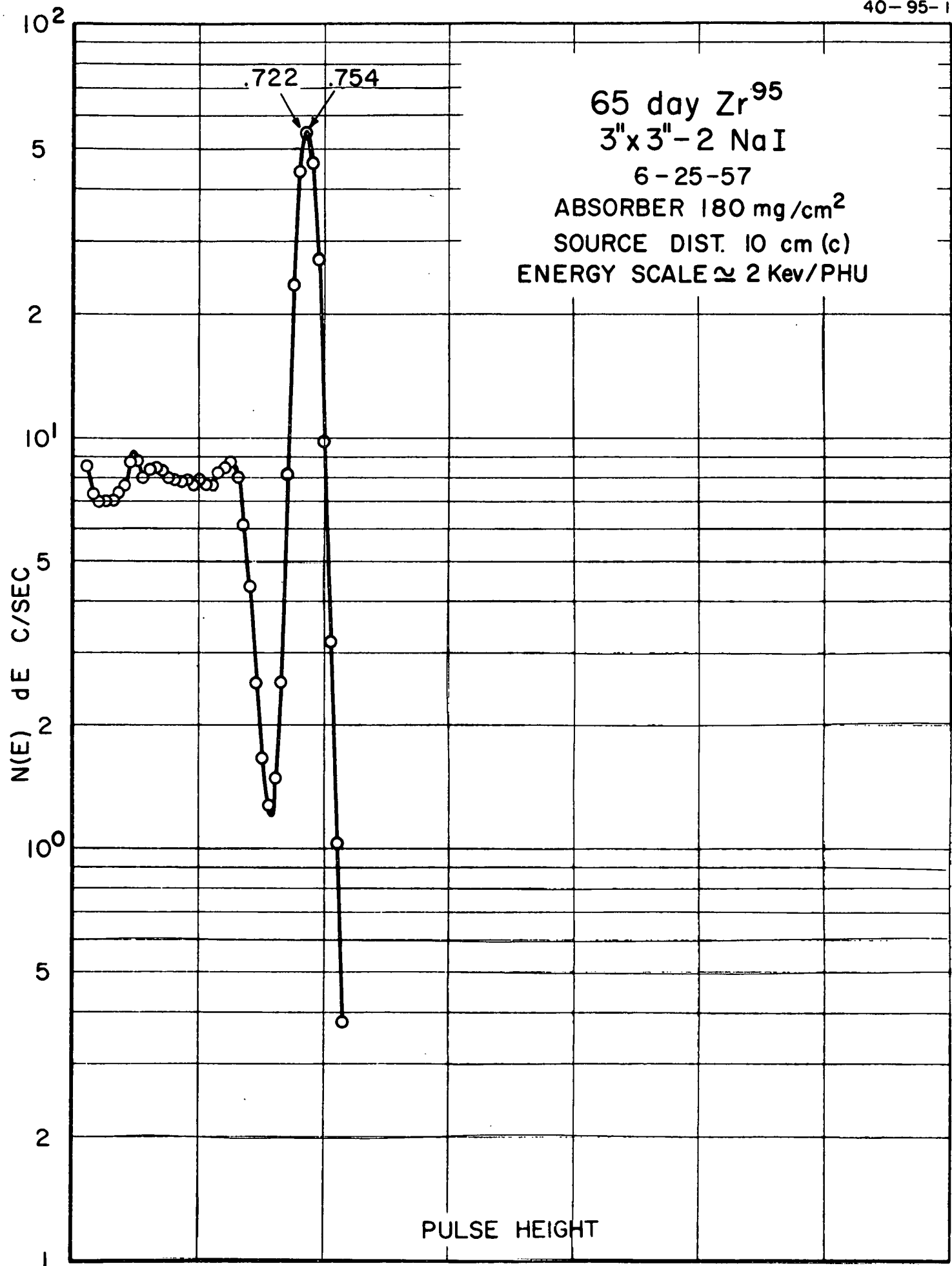


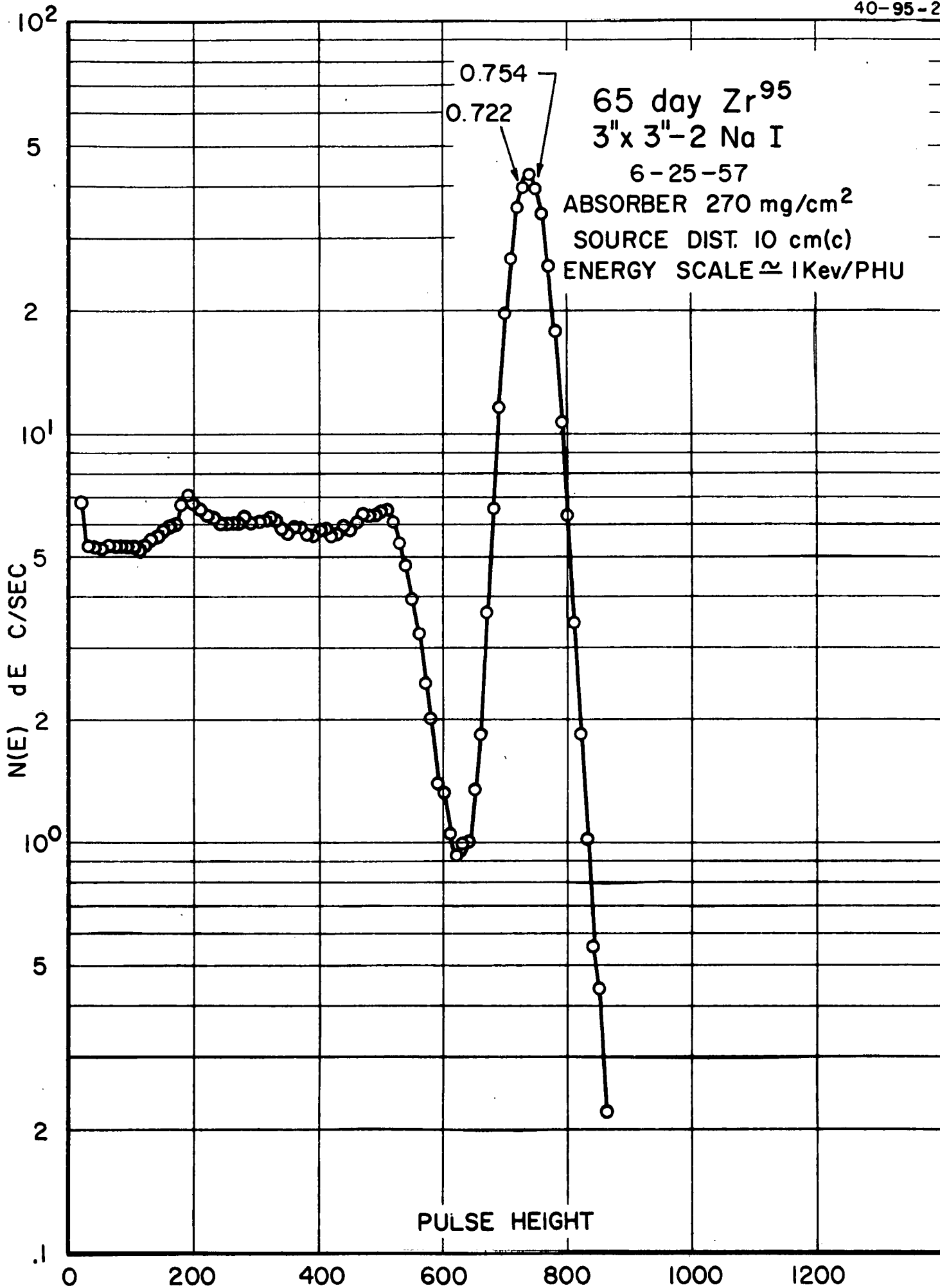


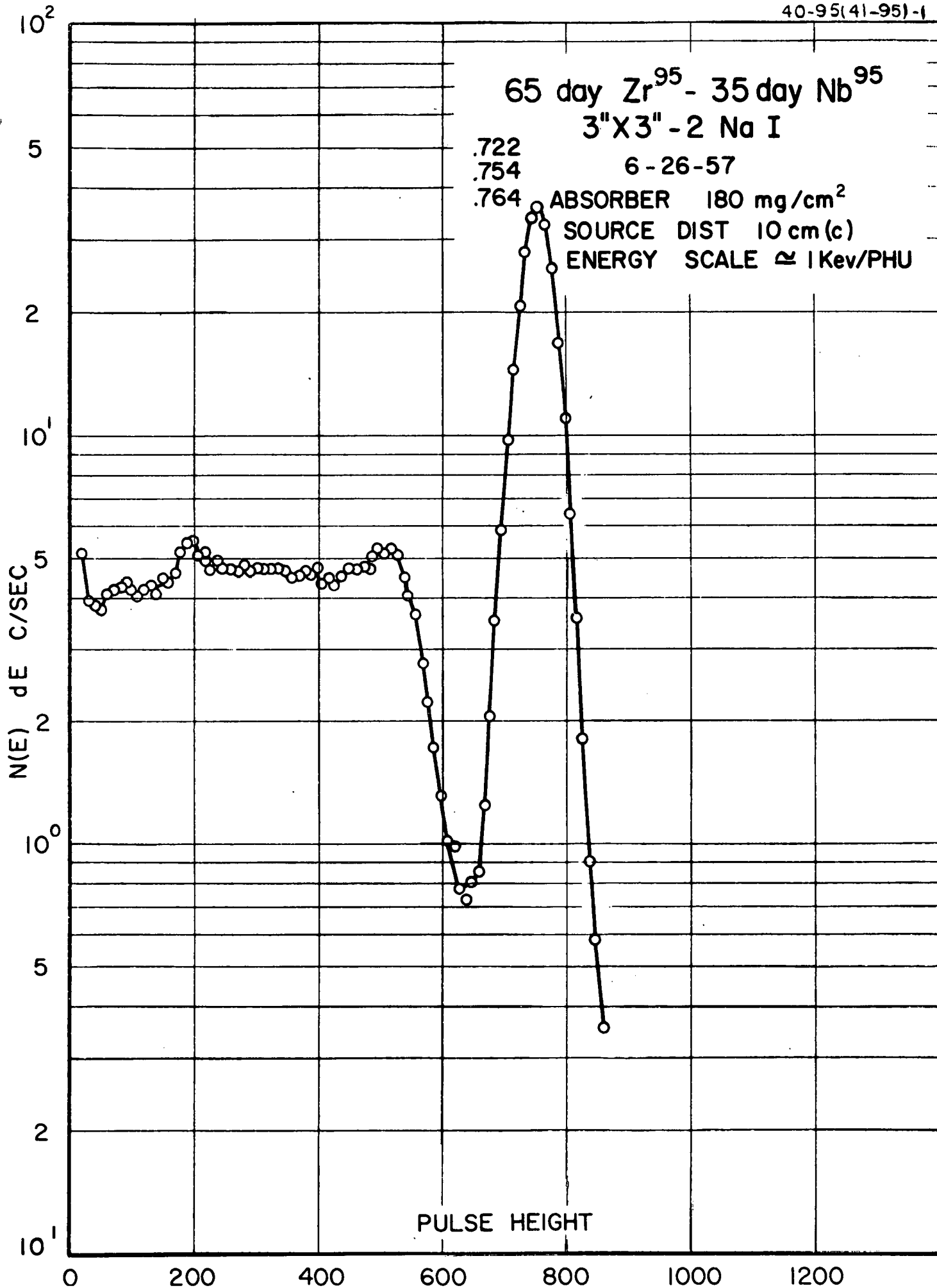




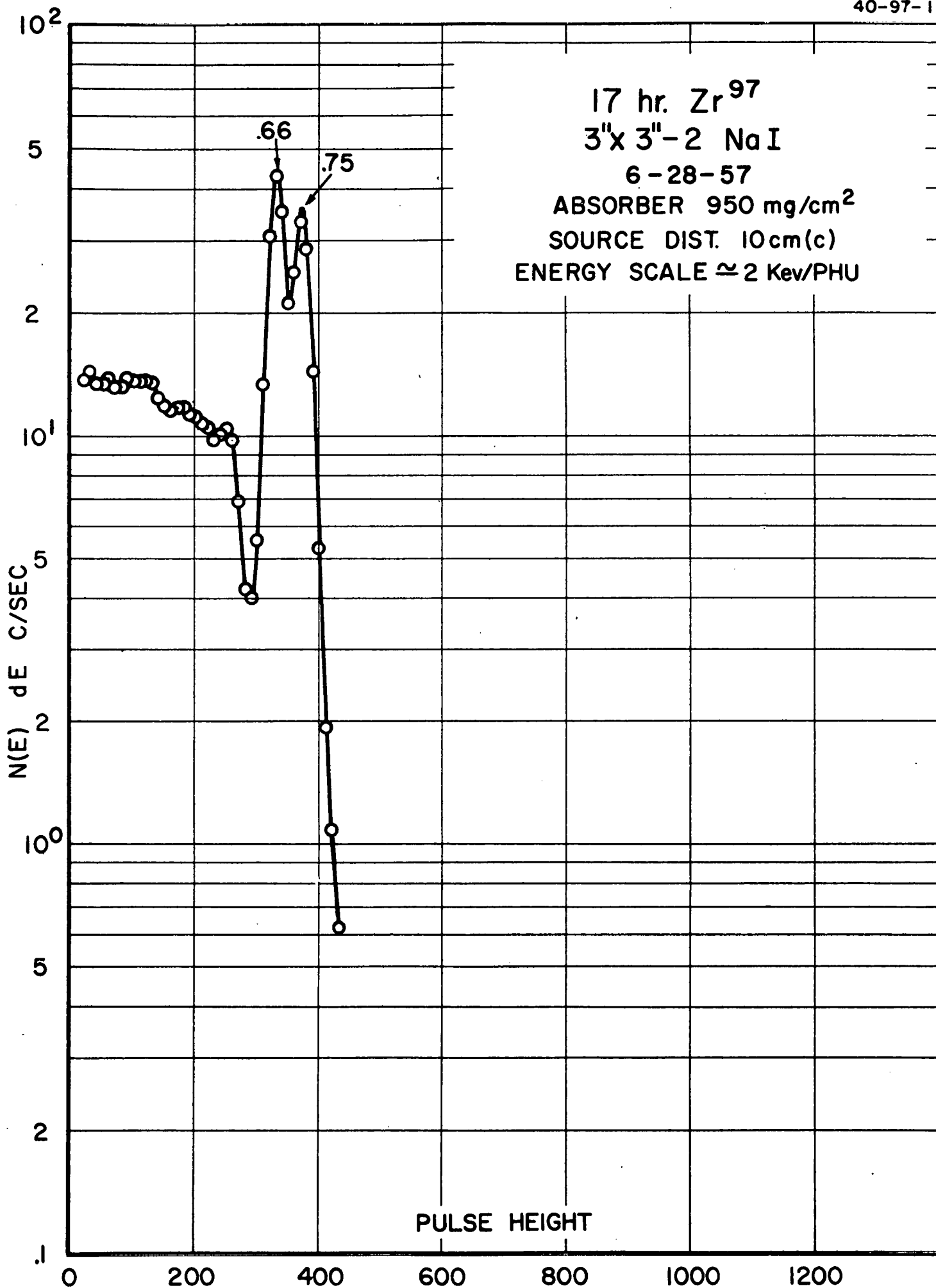




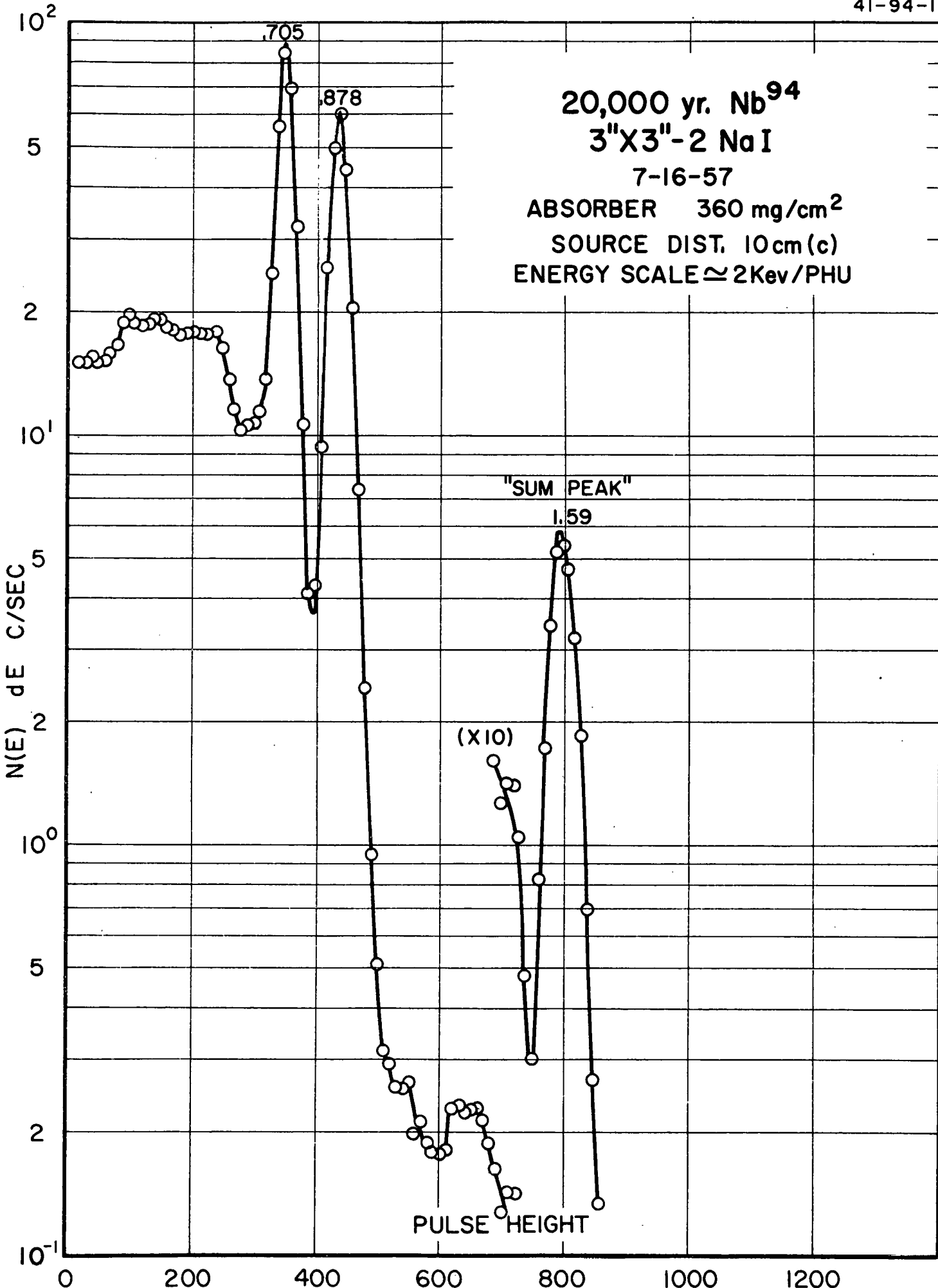


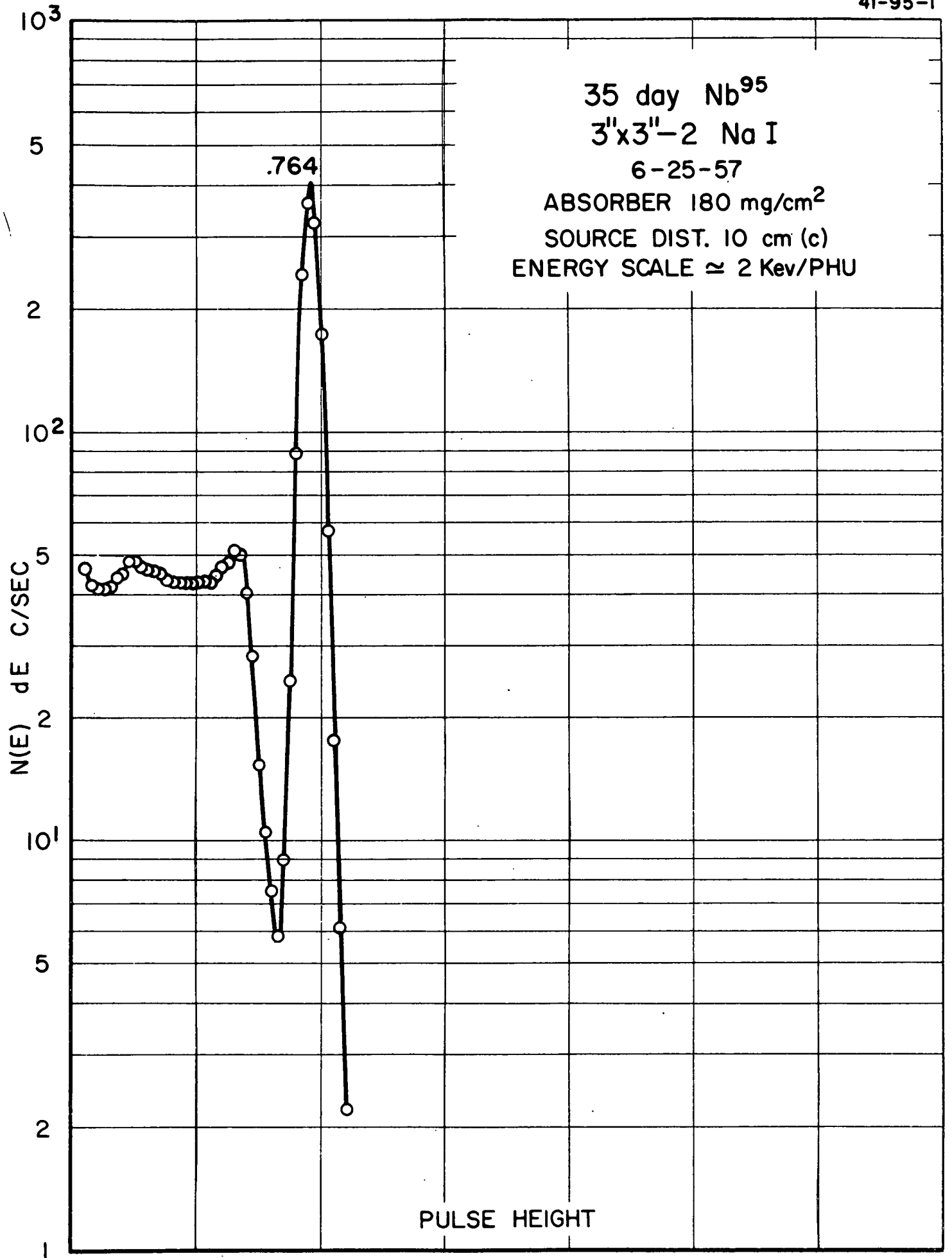


17 hr. Zr<sup>97</sup>  
3" x 3" - 2 NaI  
6-28-57  
ABSORBER 950 mg/cm<sup>2</sup>  
SOURCE DIST. 10cm(c)  
ENERGY SCALE ≈ 2 Kev/PHU

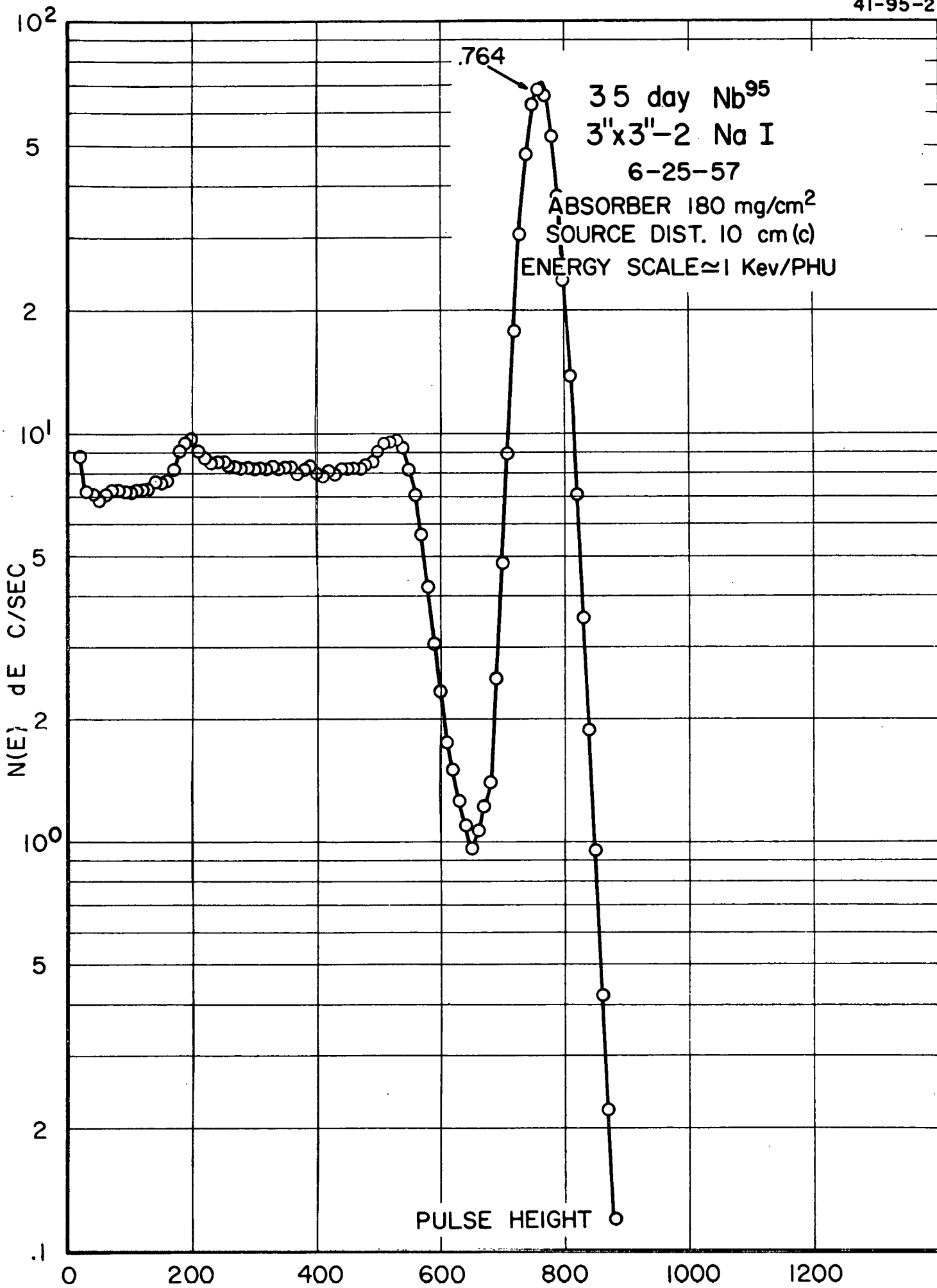


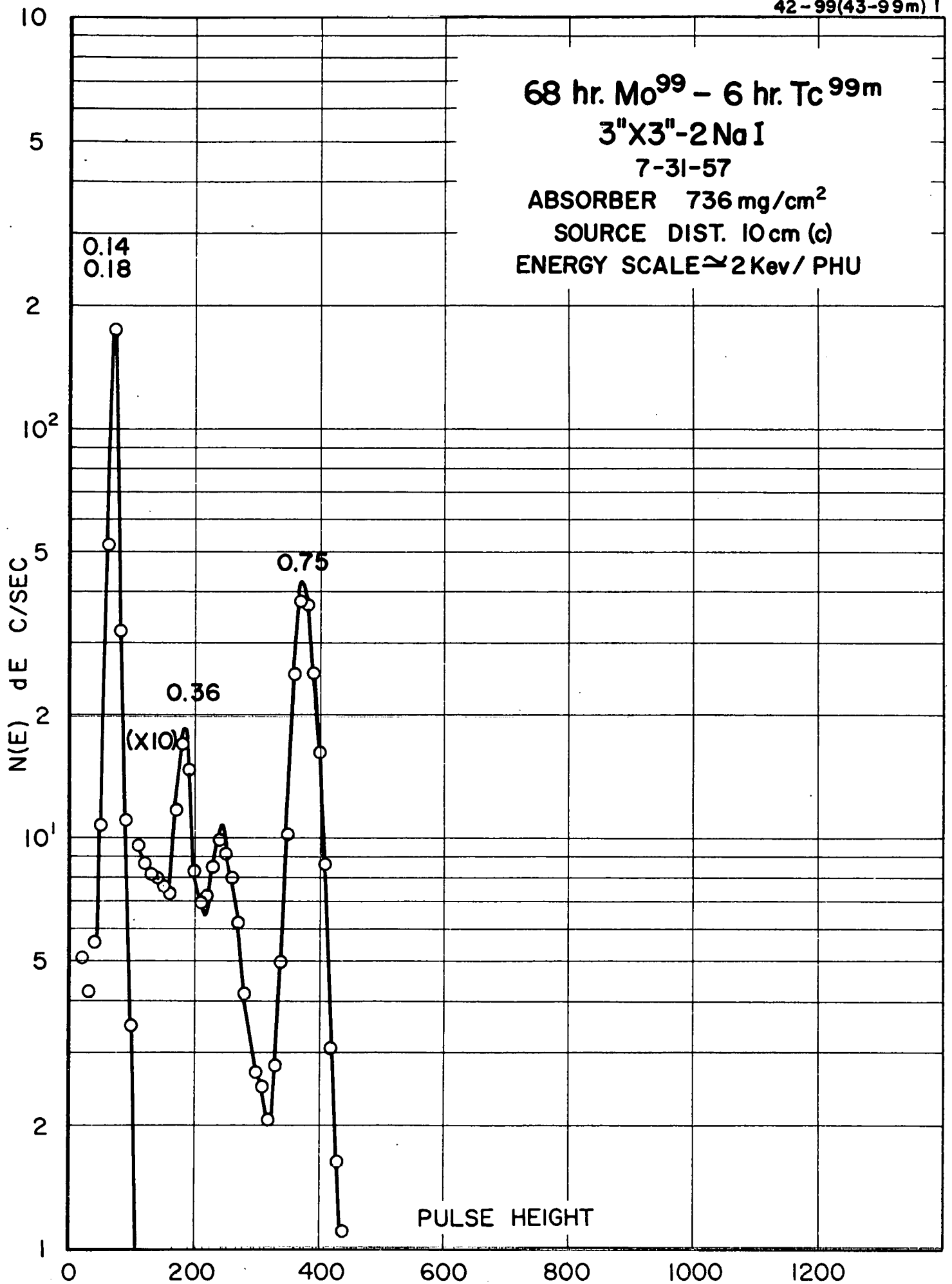
20,000 yr. Nb<sup>94</sup>  
3"X3"-2 NaI  
7-16-57  
ABSORBER 360 mg/cm<sup>2</sup>  
SOURCE DIST. 10cm(c)  
ENERGY SCALE  $\approx$  2Kev/PHU





971 0 54





68 hr. Mo<sup>99</sup> - 6 hr. Tc<sup>99m</sup>

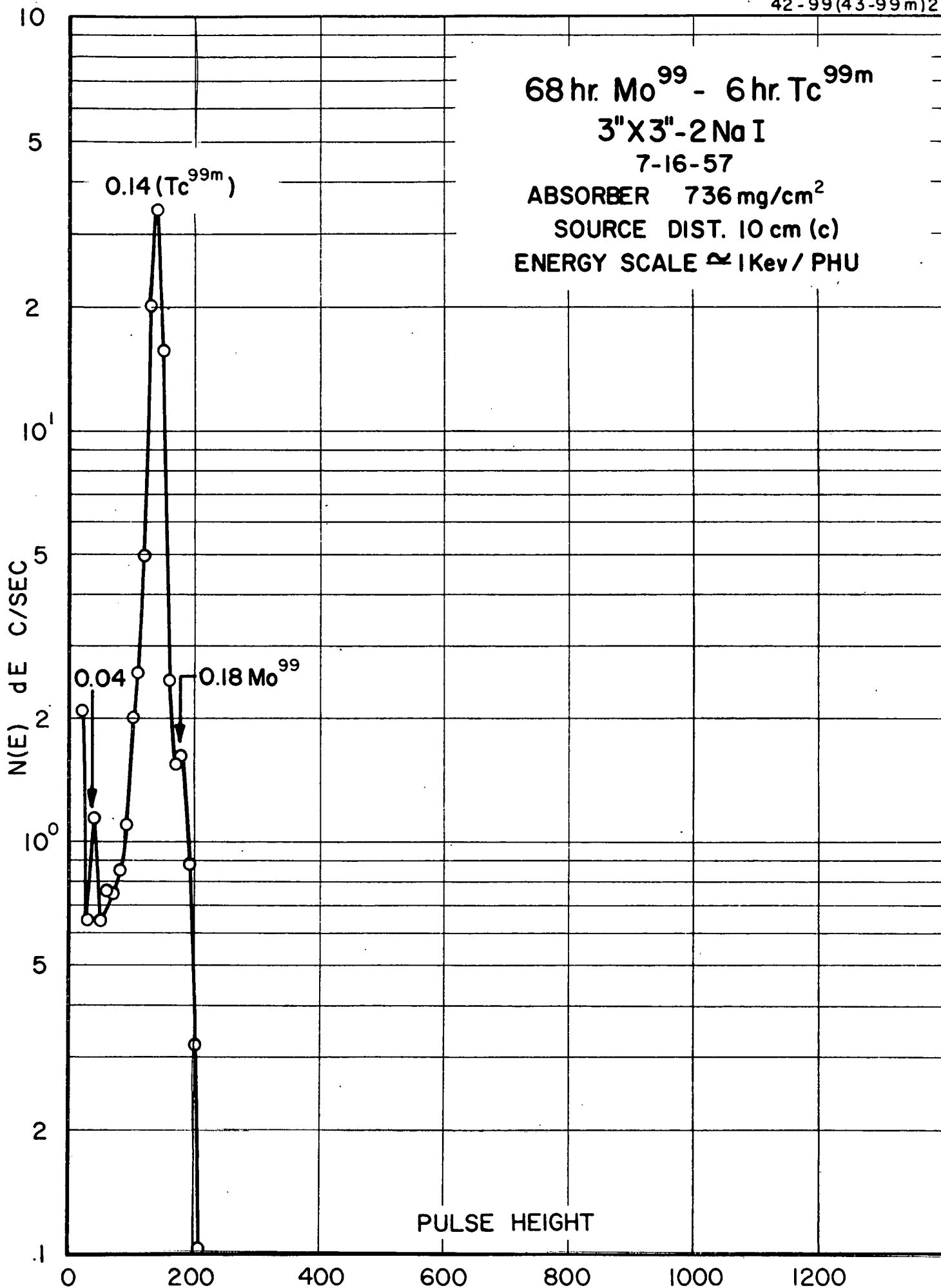
3"X3"-2 Na I

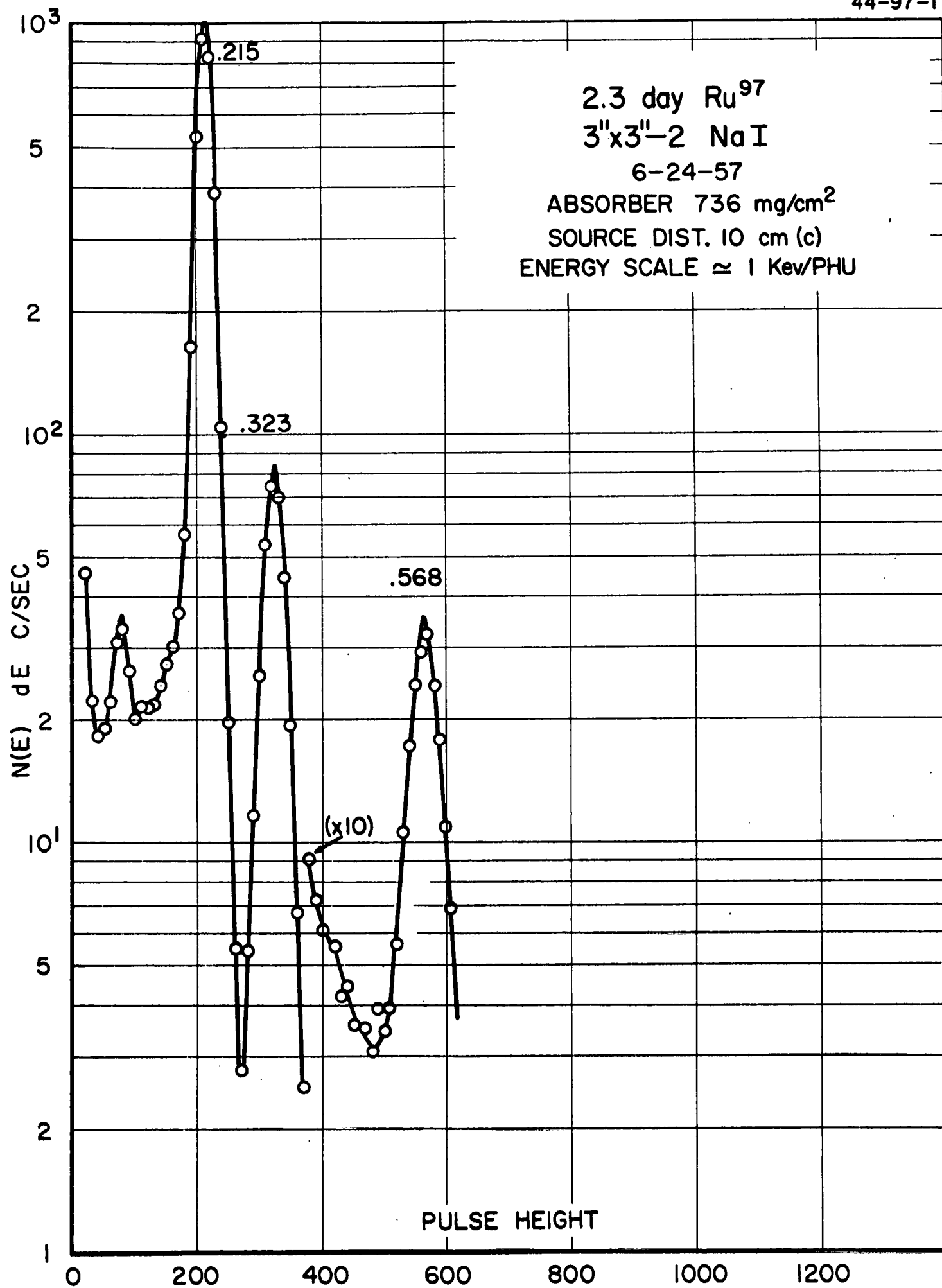
7-16-57

ABSORBER 736 mg/cm<sup>2</sup>

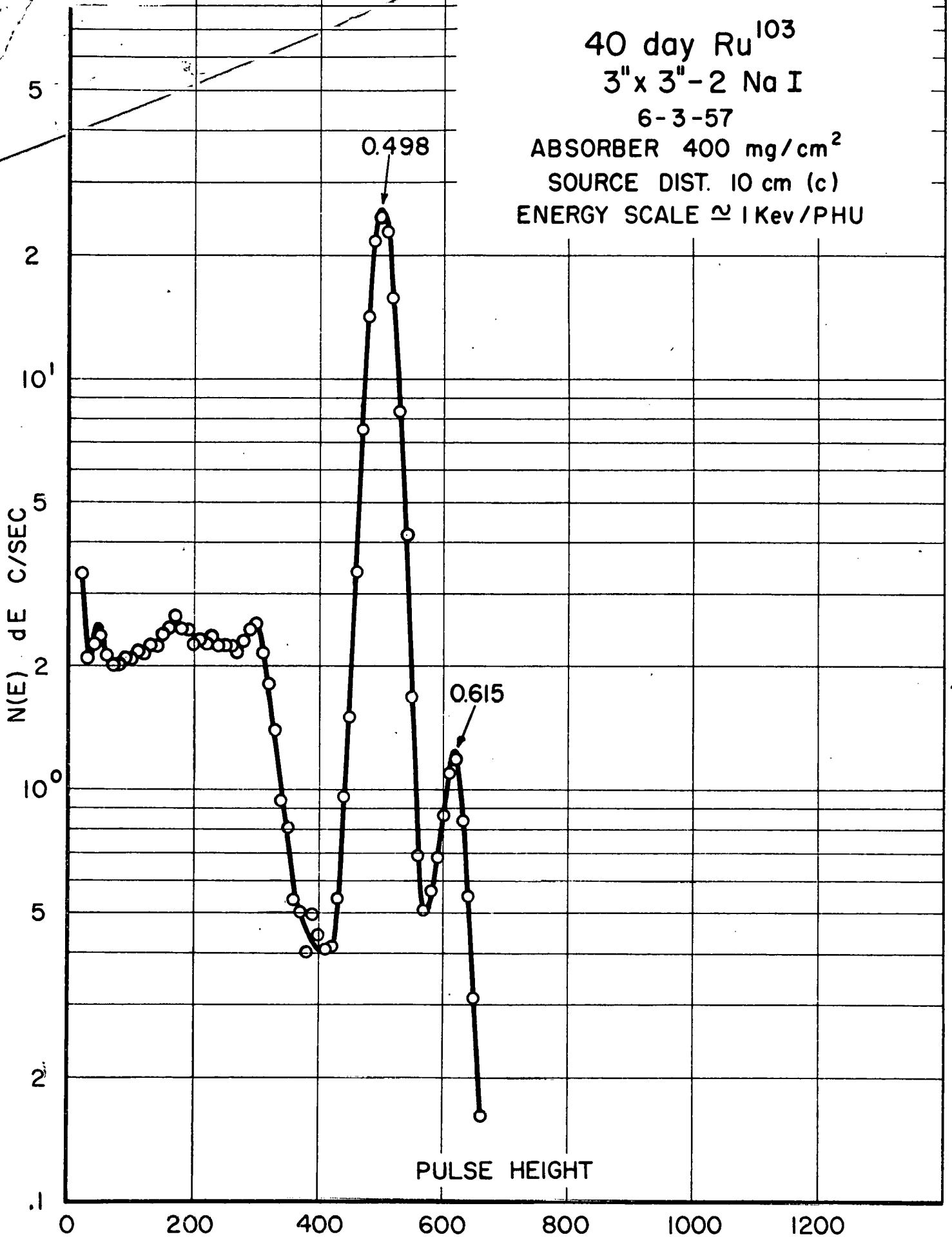
SOURCE DIST. 10 cm (c)

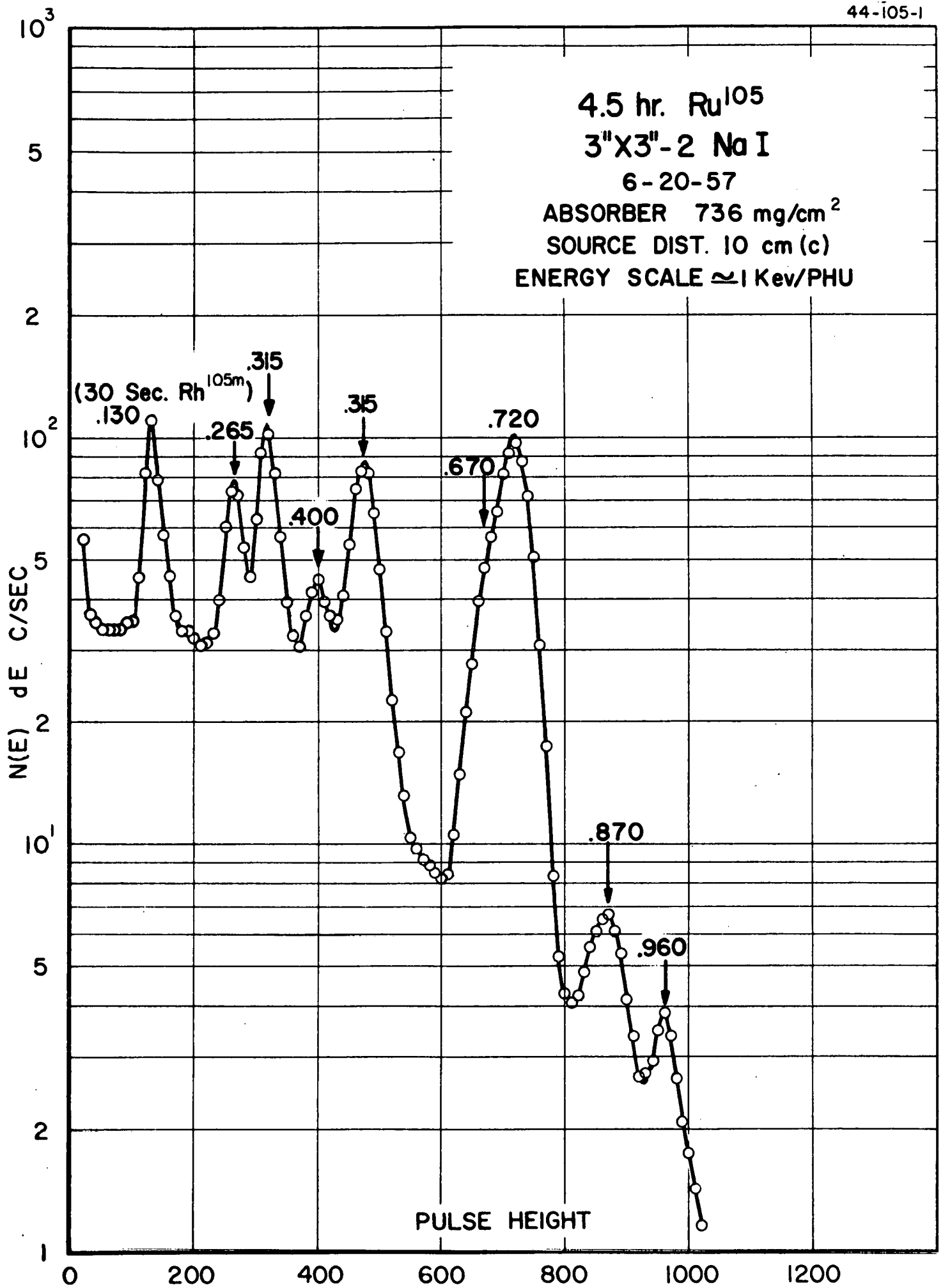
ENERGY SCALE  $\approx$  1 Key / PHU





40 day Ru<sup>103</sup>  
 3" x 3" - 2 Na I  
 6-3-57  
 ABSORBER 400 mg/cm<sup>2</sup>  
 SOURCE DIST. 10 cm (c)  
 ENERGY SCALE  $\approx$  1 Kev/PHU





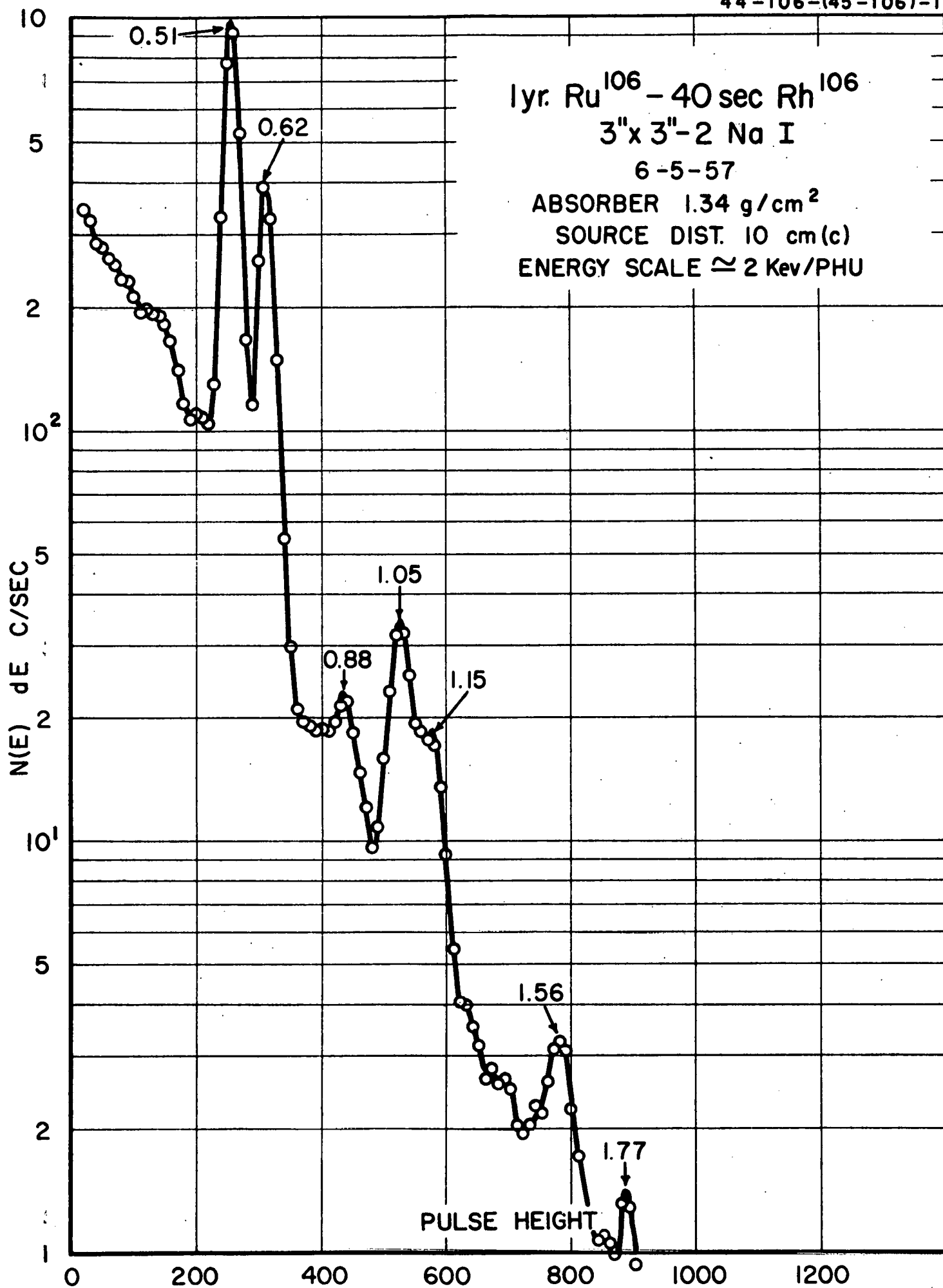
1yr. Ru<sup>106</sup> - 40 sec Rh<sup>106</sup>

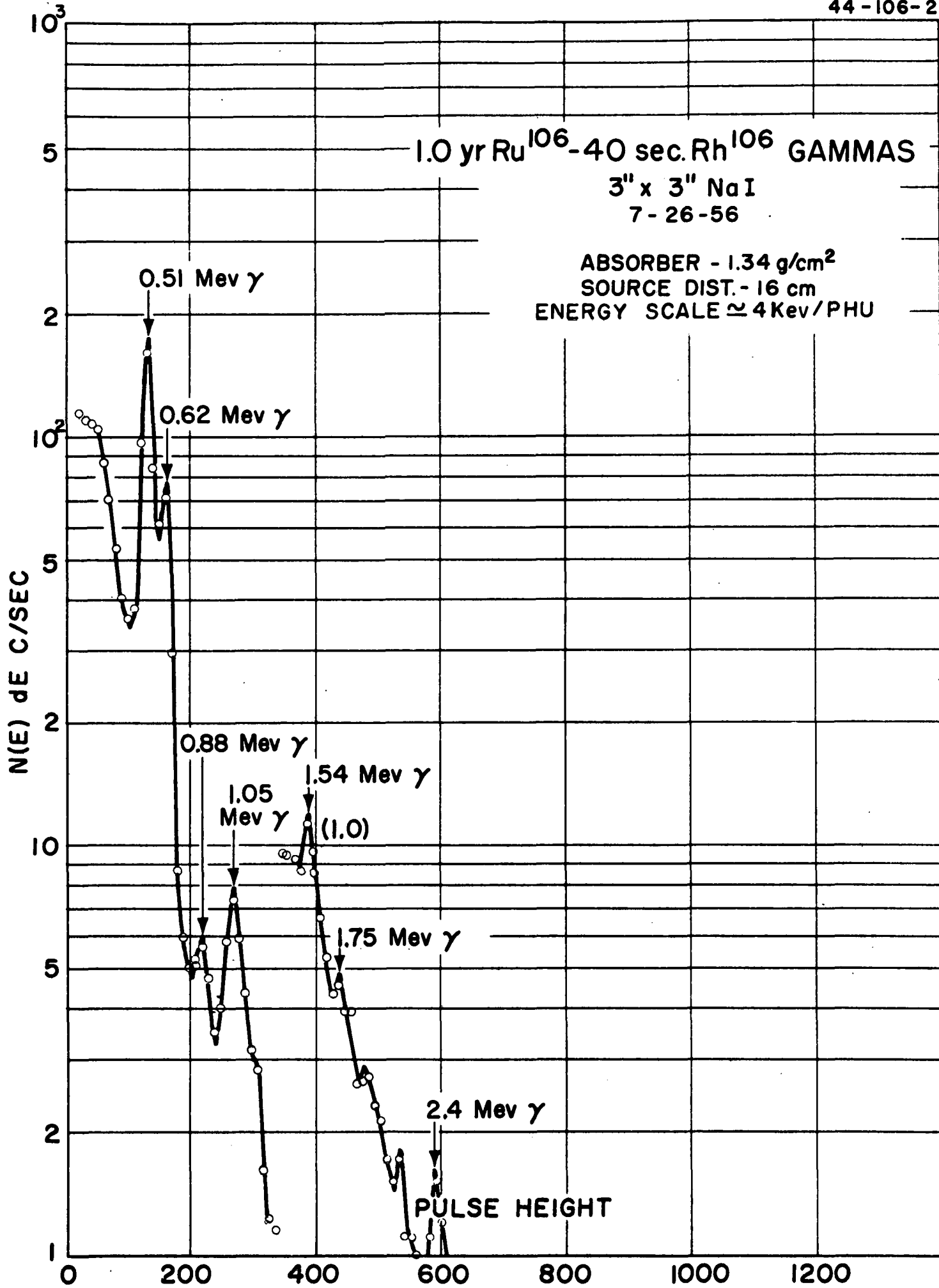
3" x 3" - 2 Na I

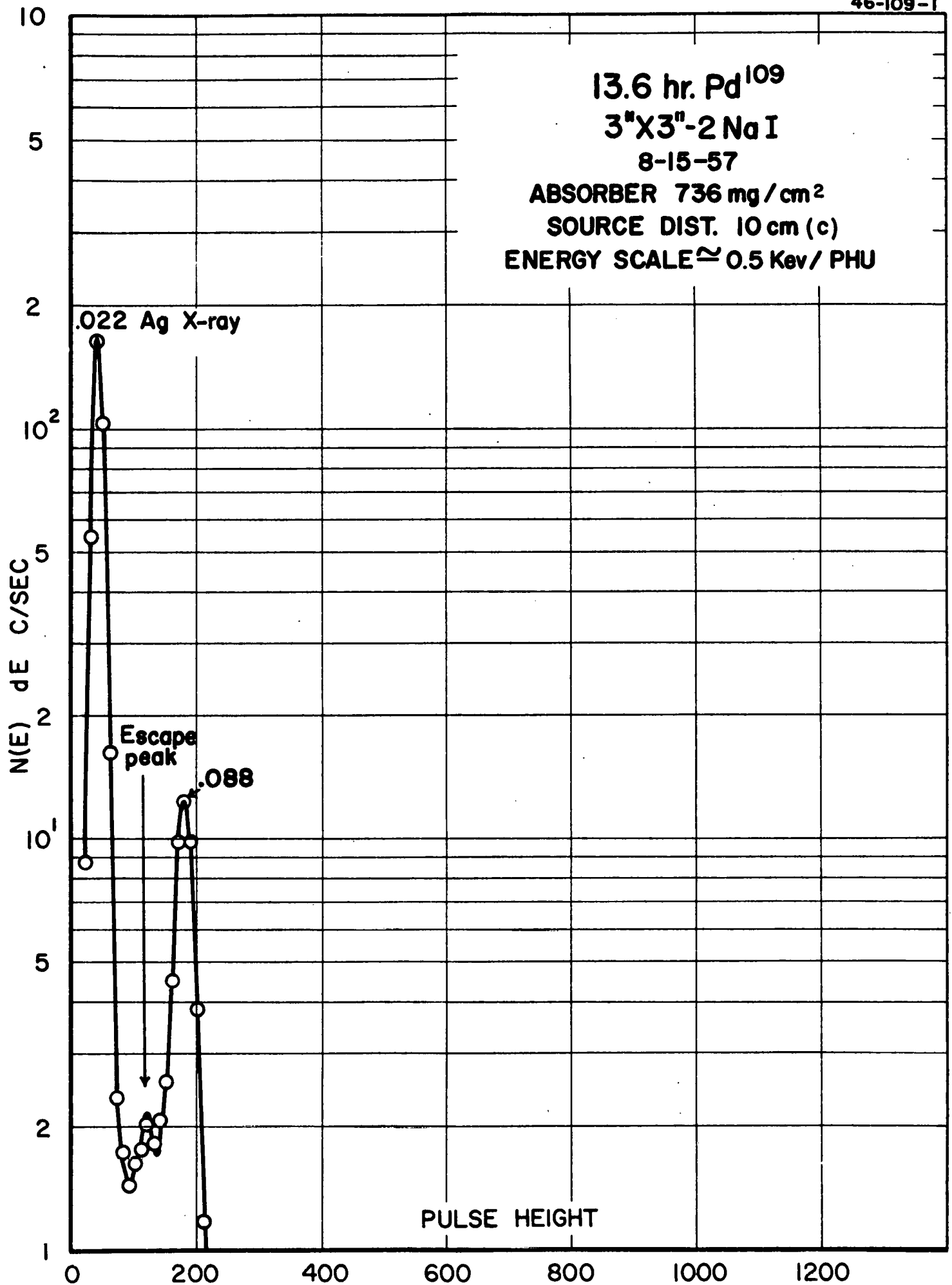
6-5-57

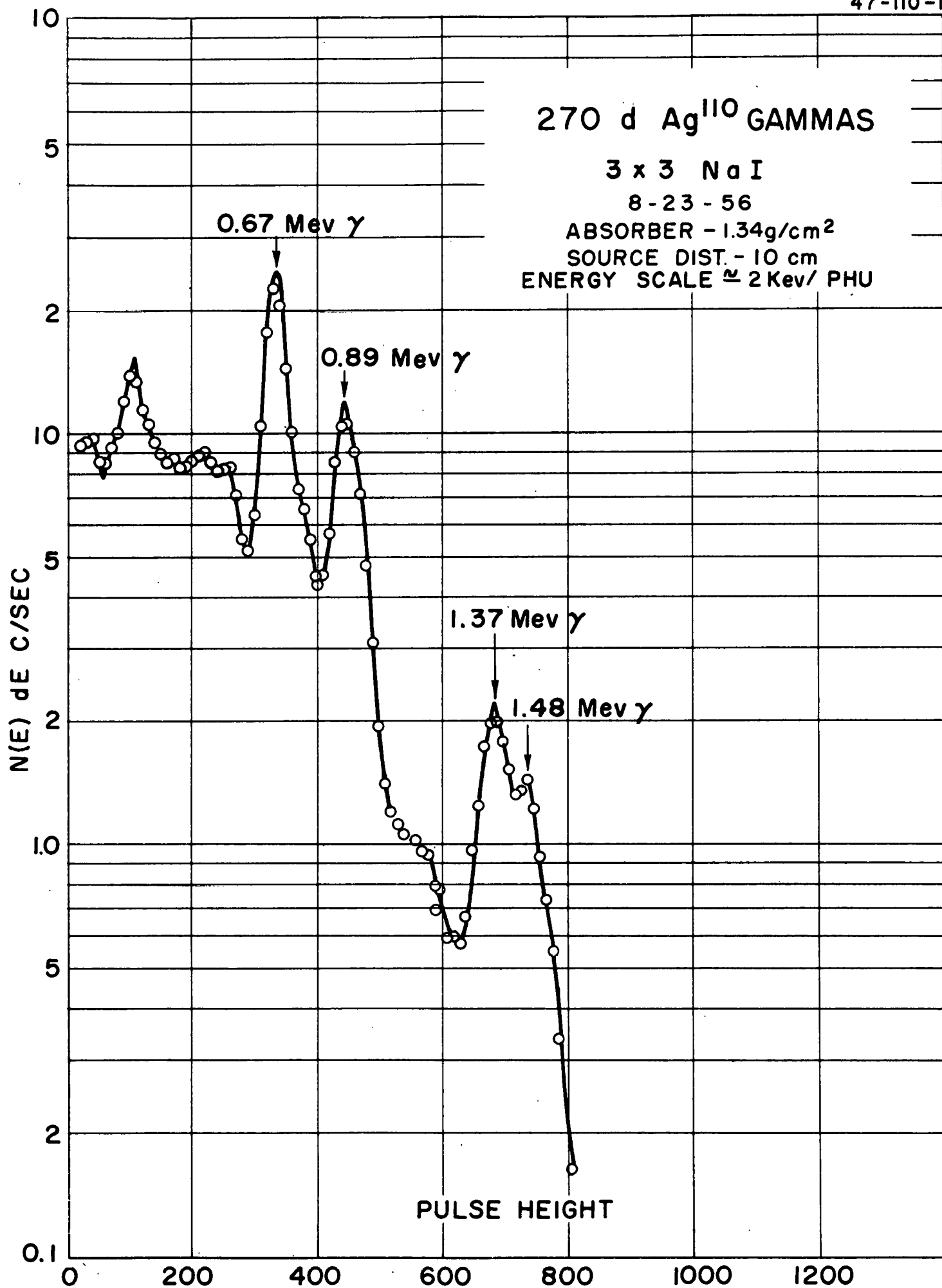
ABSORBER 1.34 g/cm<sup>2</sup>

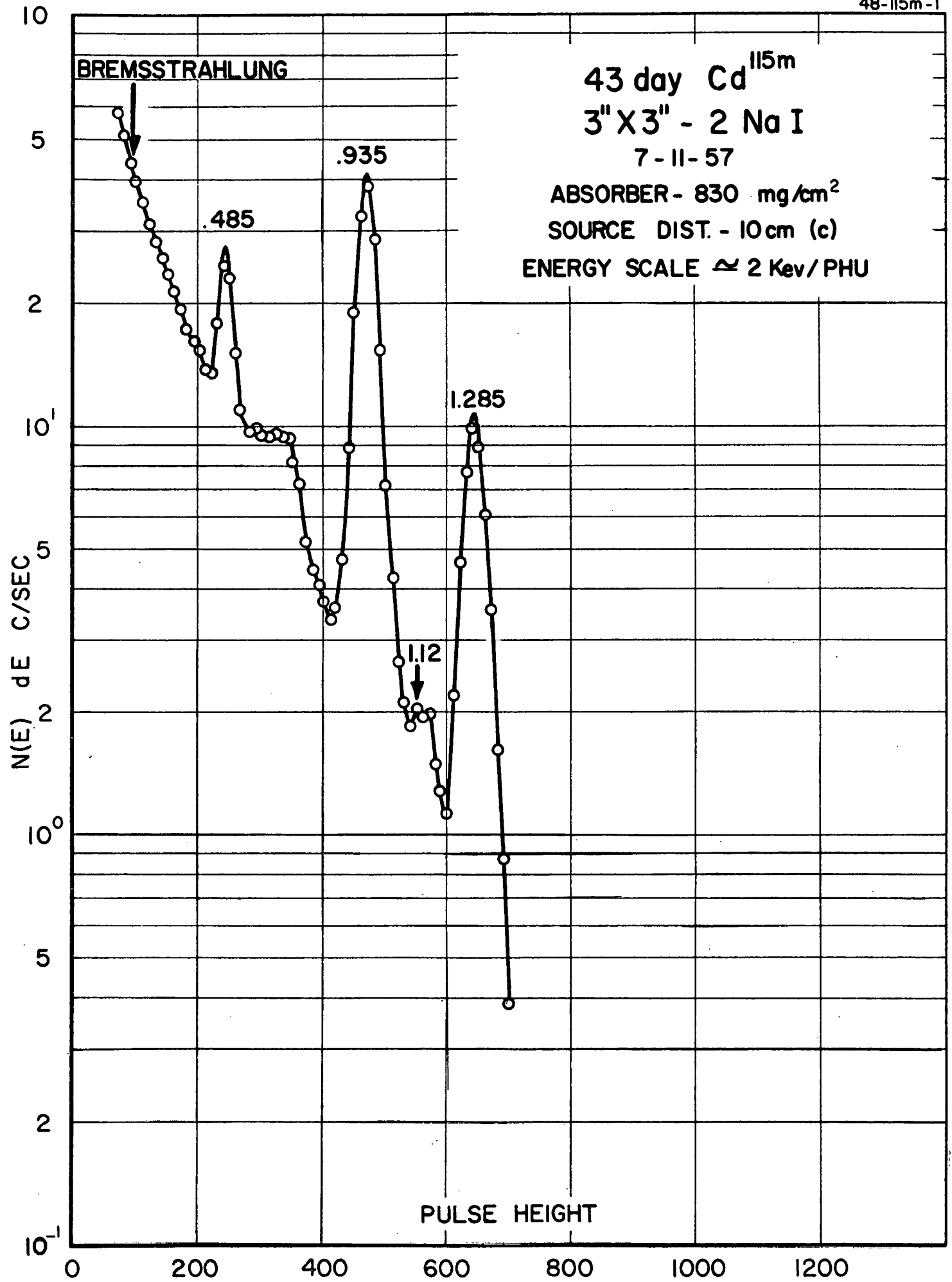
SOURCE DIST. 10 cm(c)

ENERGY SCALE  $\approx$  2 Kev/PHU









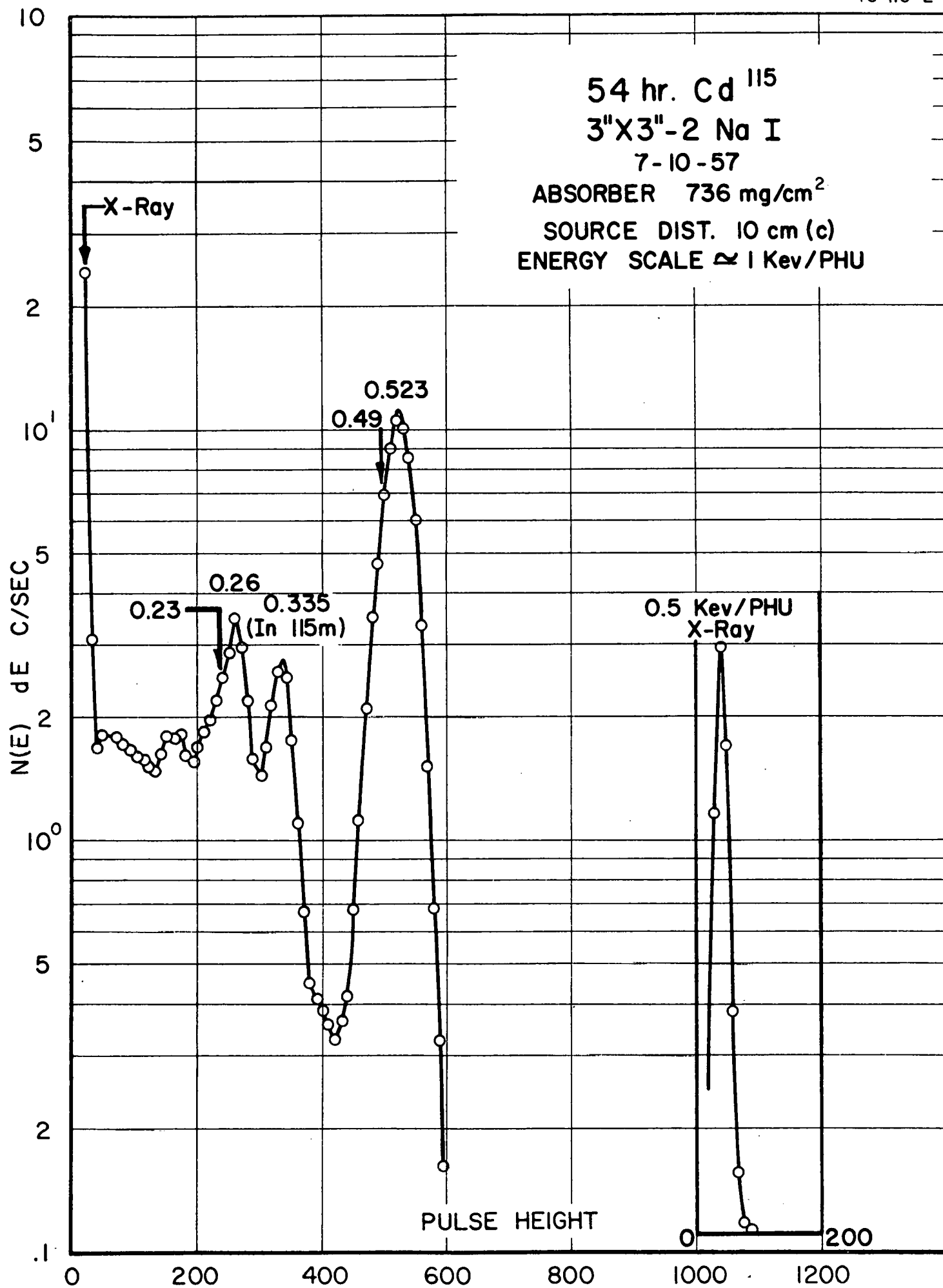
54 hr. Cd <sup>115</sup>

3"X3"-2 Na I

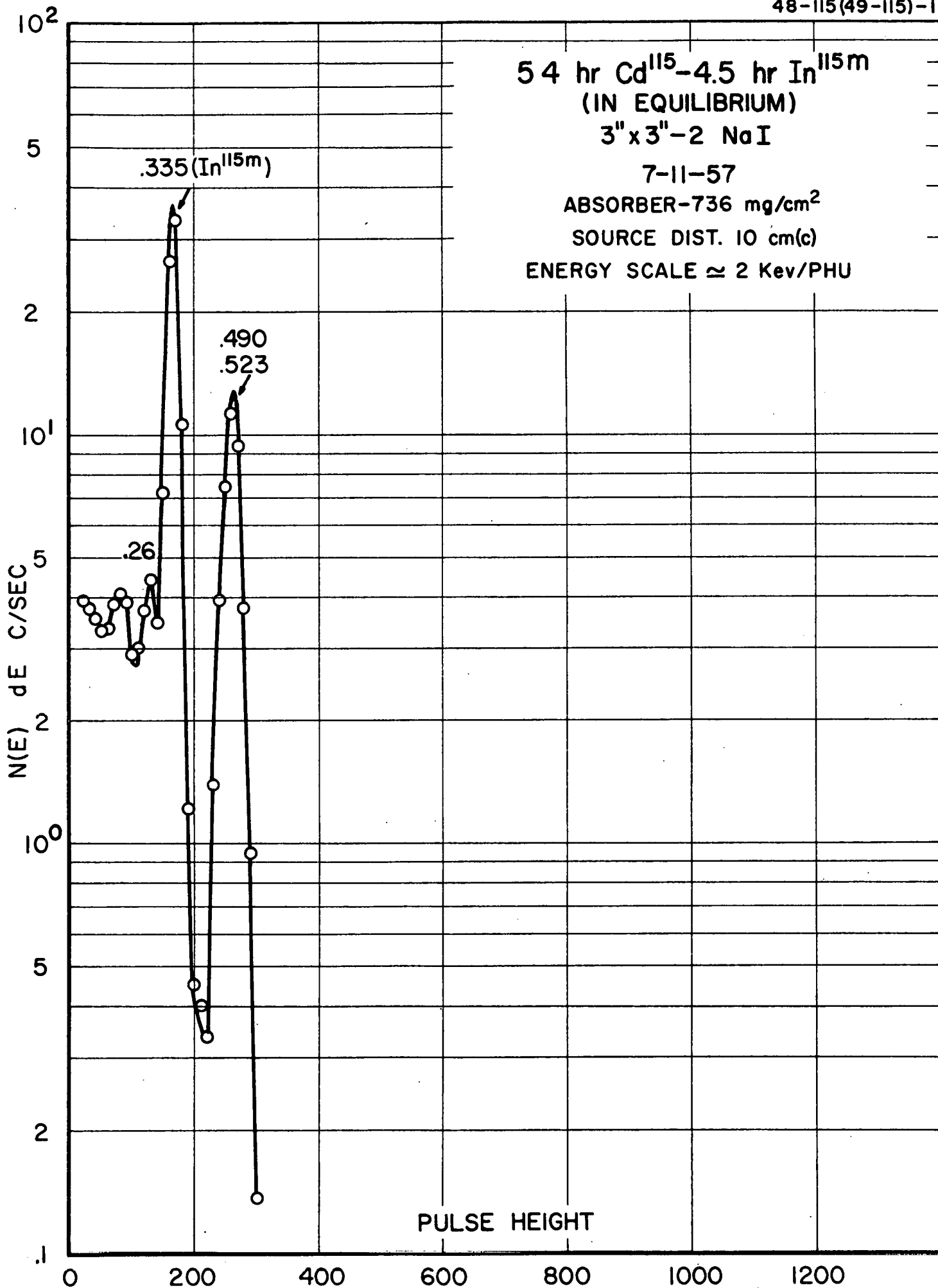
7-10-57

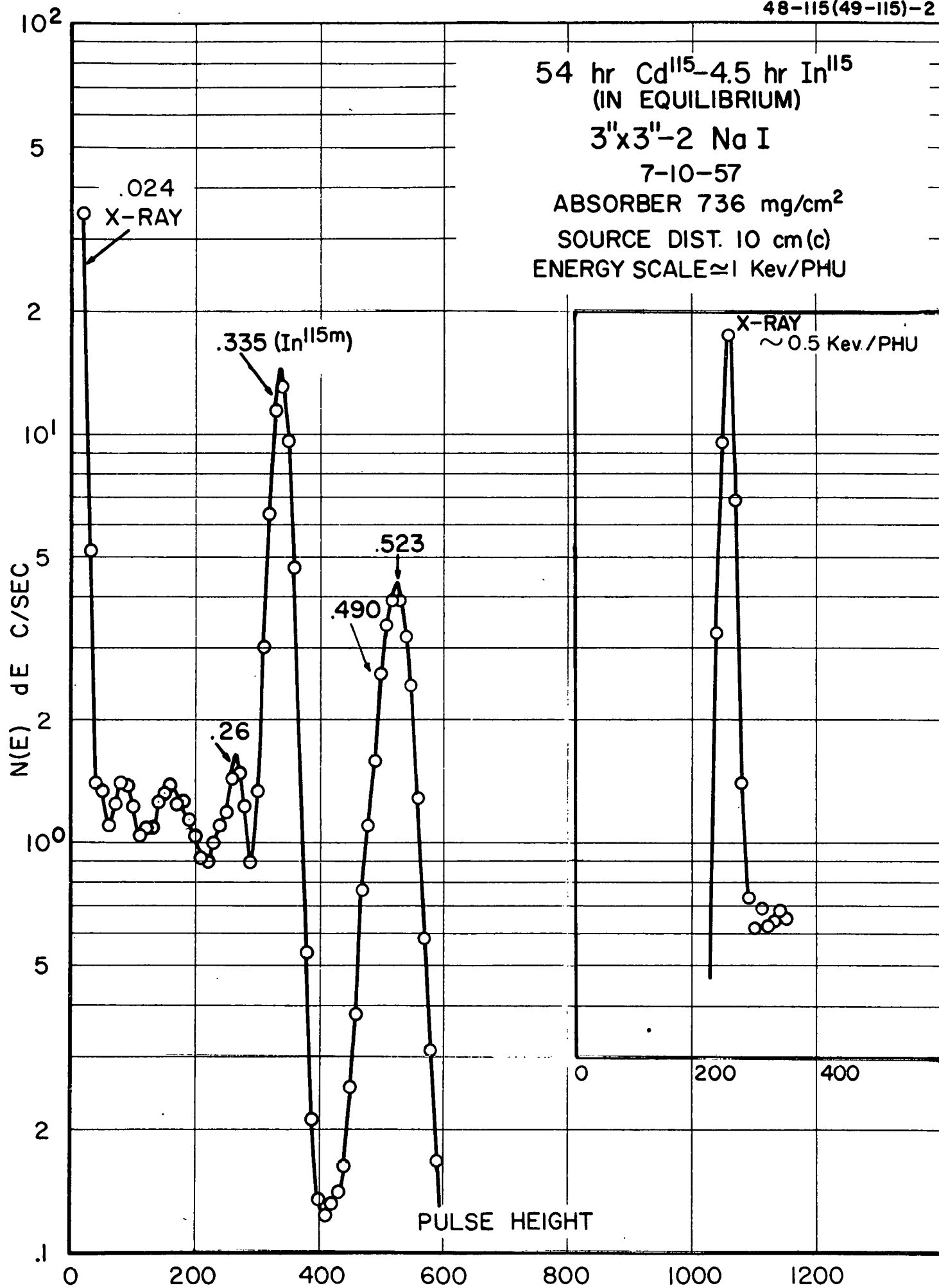
ABSORBER 736 mg/cm<sup>2</sup>

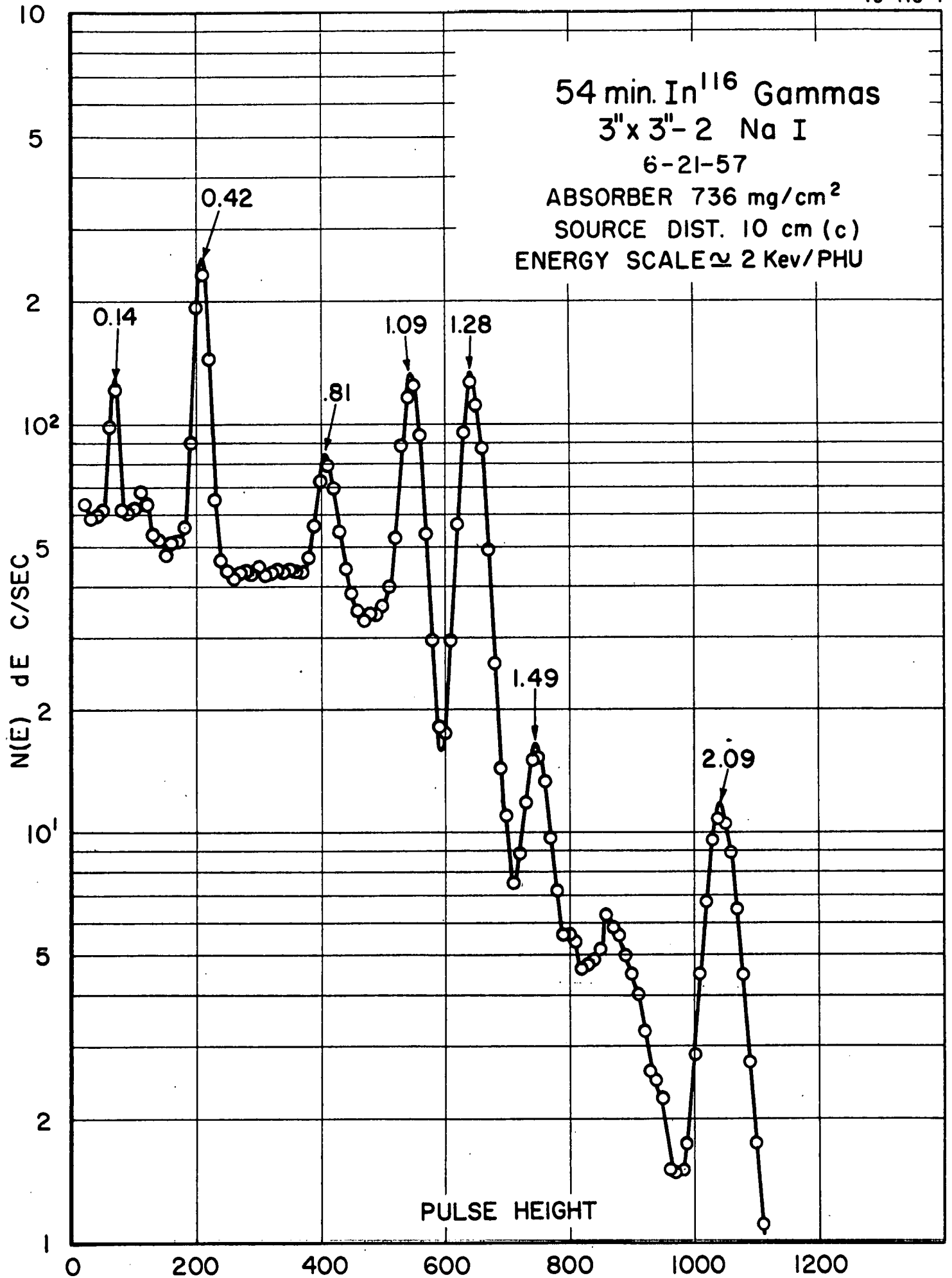
SOURCE DIST. 10 cm (c)

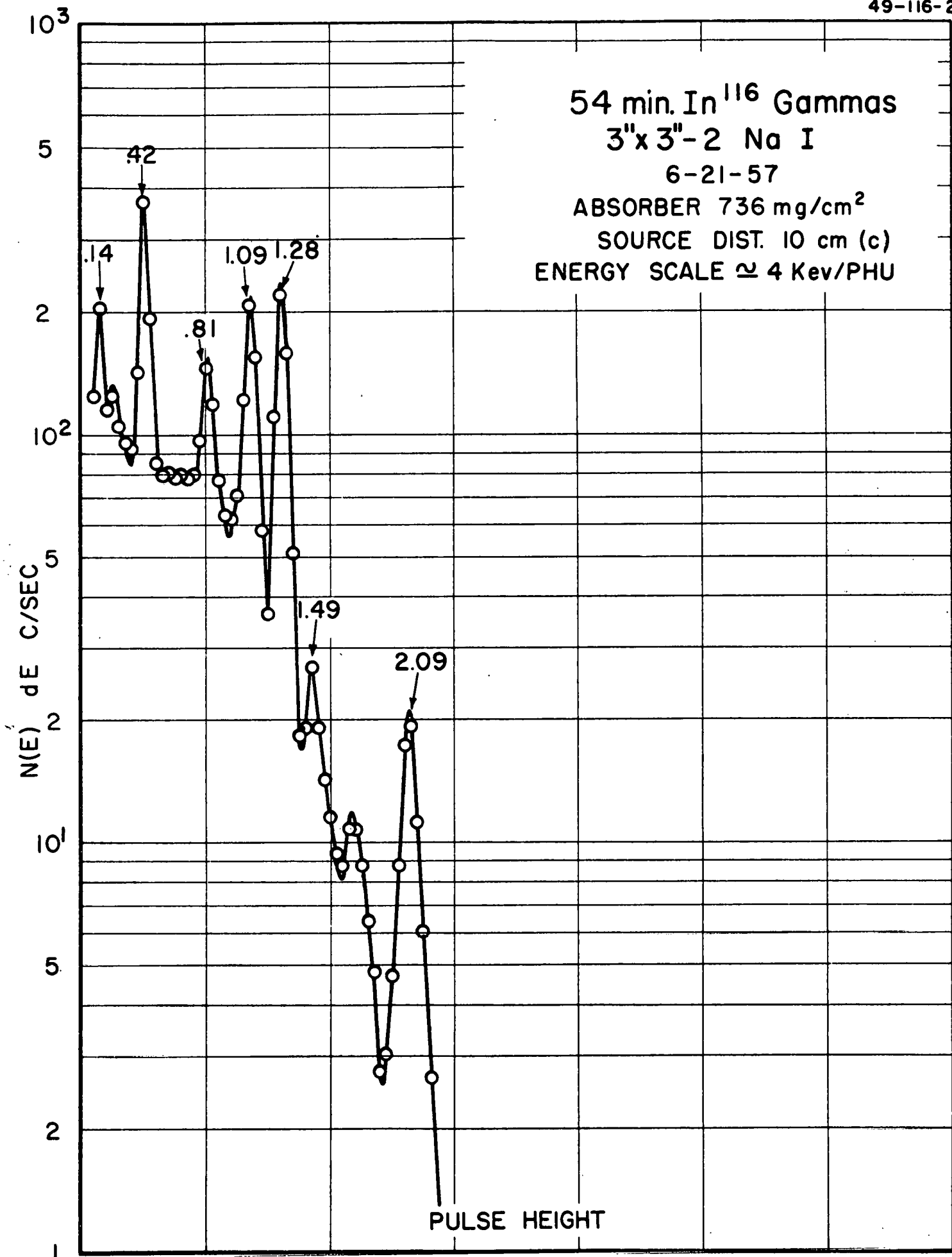
ENERGY SCALE  $\approx$  1 Kev/PHU

54 hr Cd<sup>115</sup>-4.5 hr In<sup>115m</sup>  
(IN EQUILIBRIUM)  
3" x 3"-2 NaI  
7-11-57  
ABSORBER-736 mg/cm<sup>2</sup>  
SOURCE DIST. 10 cm(c)  
ENERGY SCALE ≈ 2 Kev/PHU



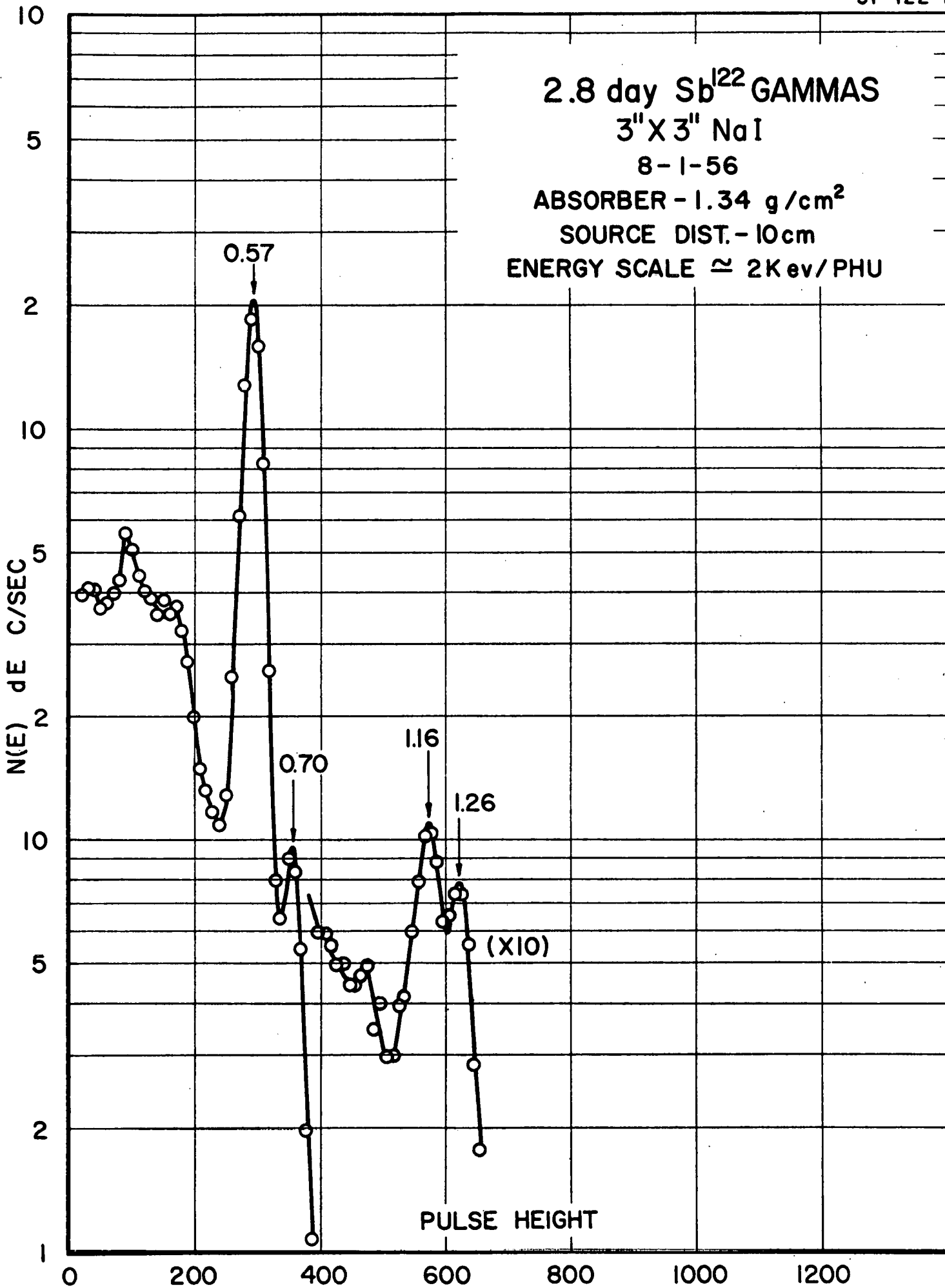




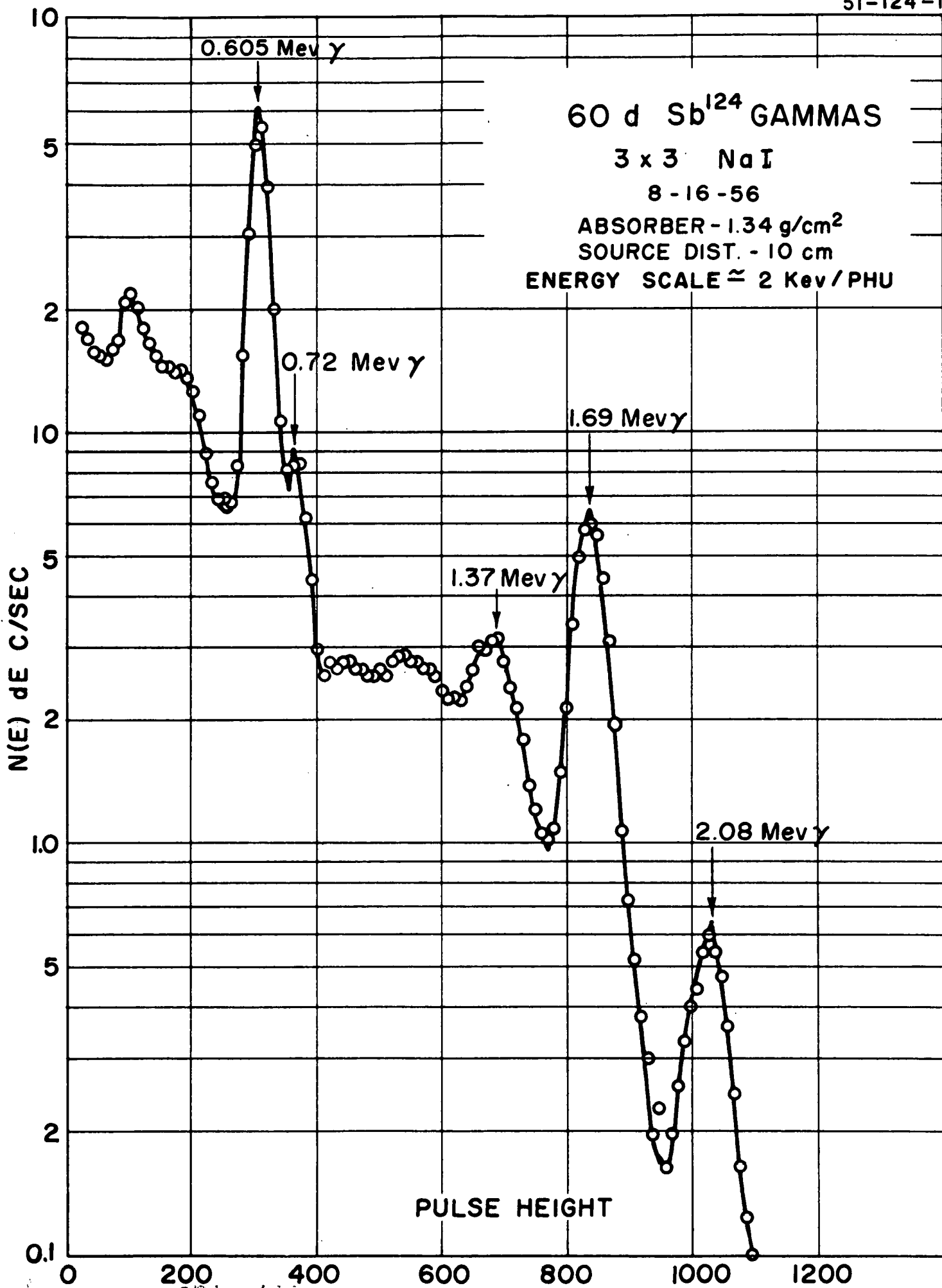


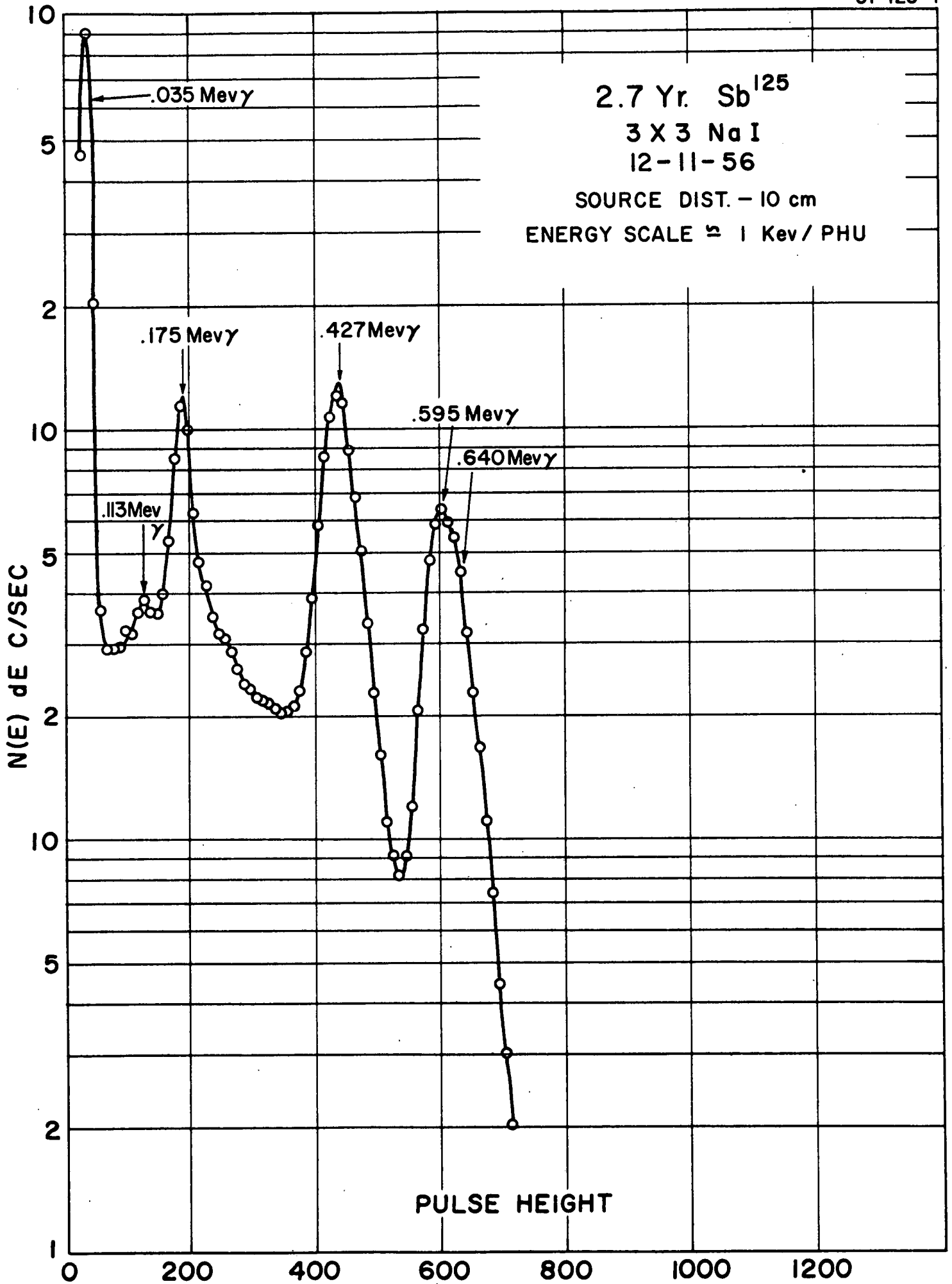
971 110

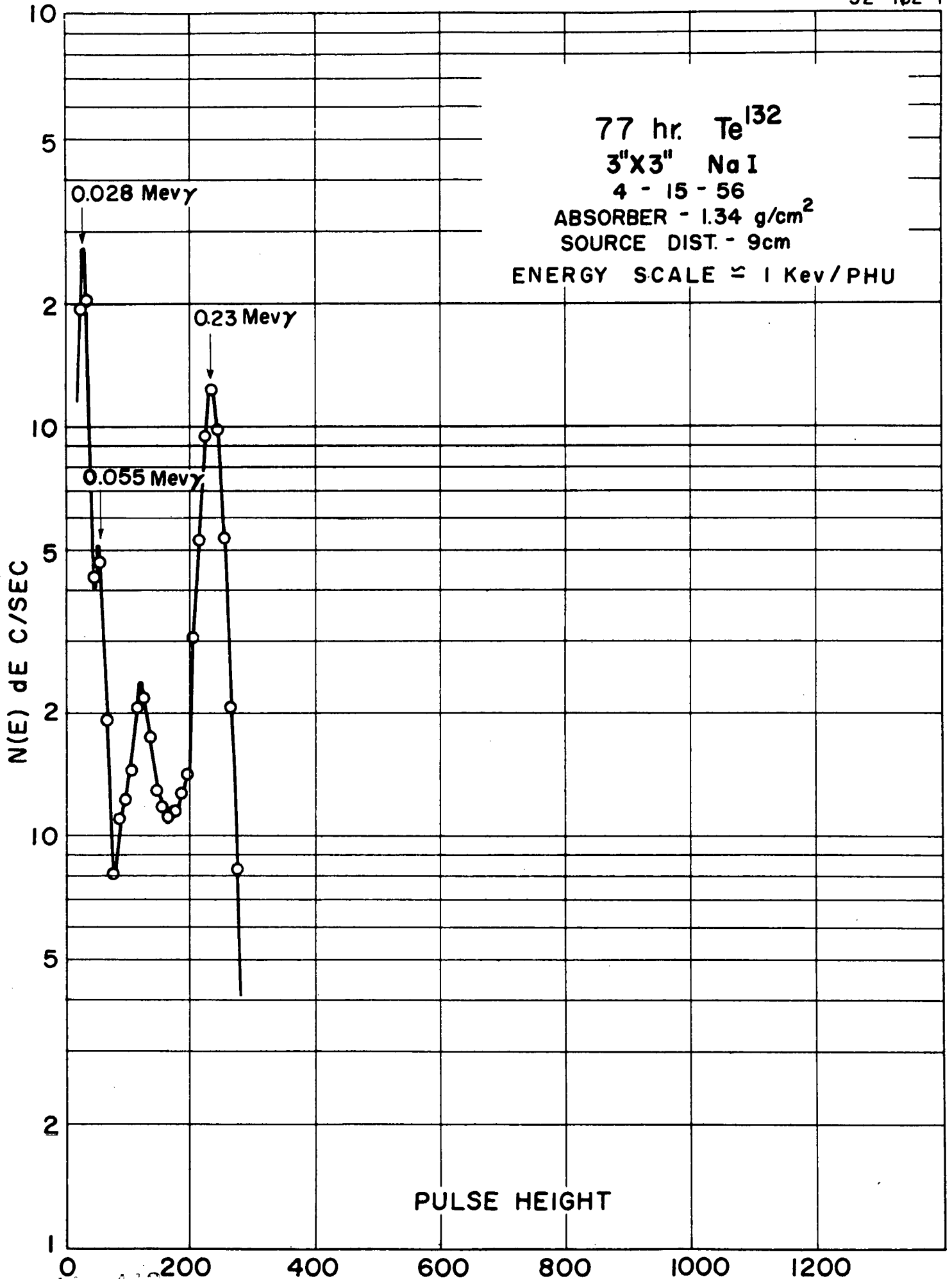
2.8 day  $Sb^{122}$  GAMMAS  
3" X 3" NaI  
8-1-56  
ABSORBER - 1.34 g/cm<sup>2</sup>  
SOURCE DIST. - 10cm  
ENERGY SCALE  $\approx$  2Kev/PHU

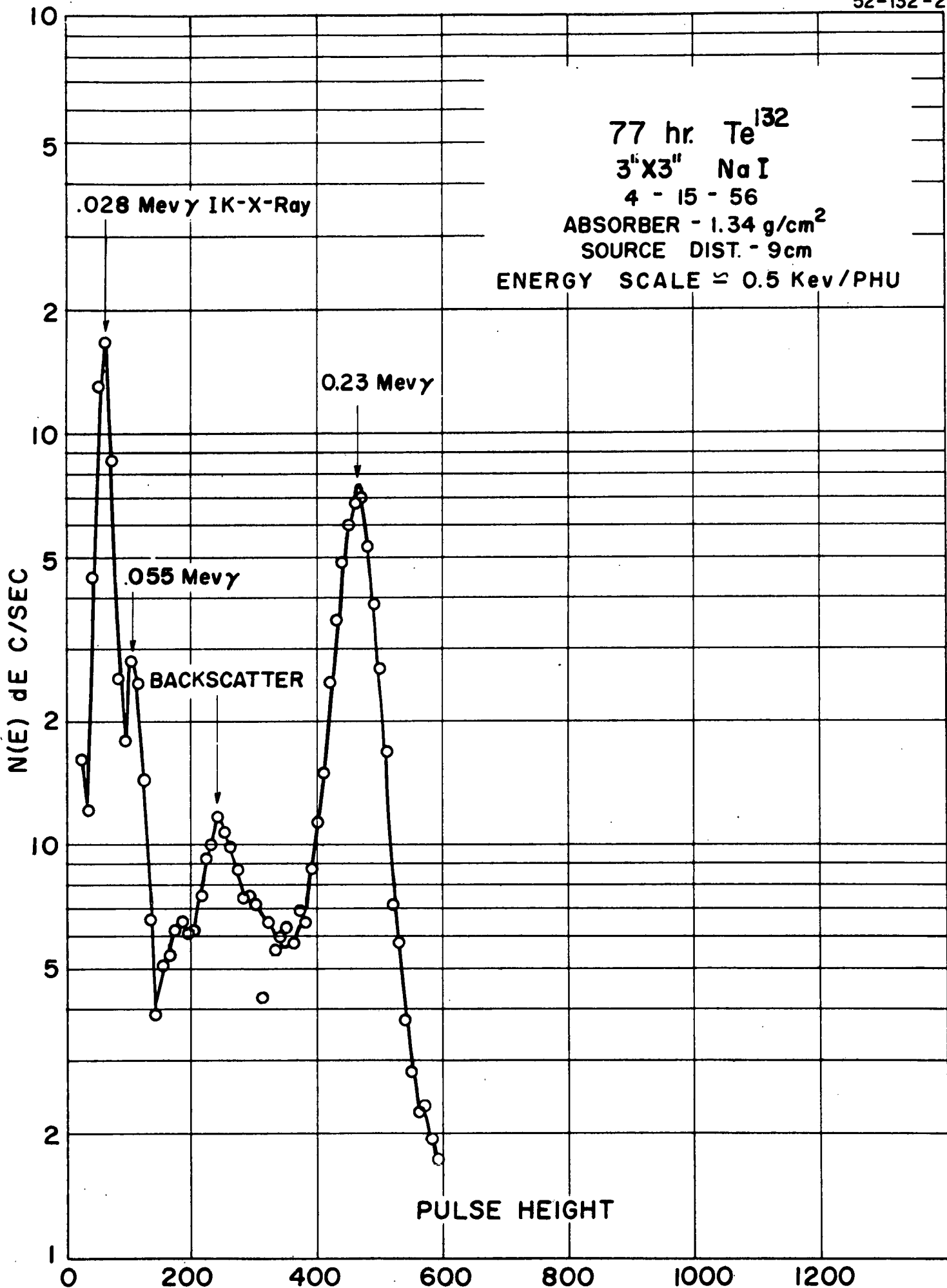


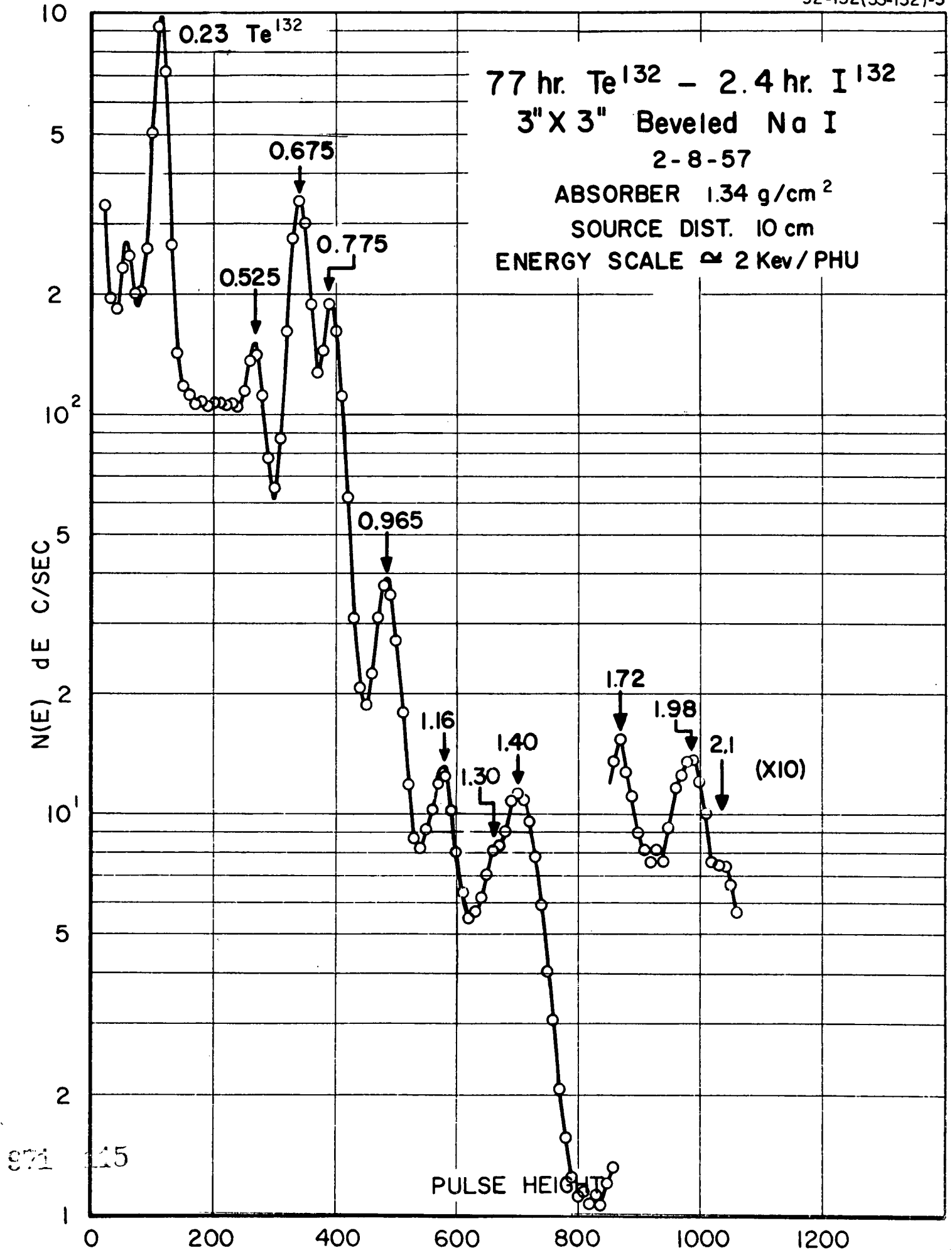
110A

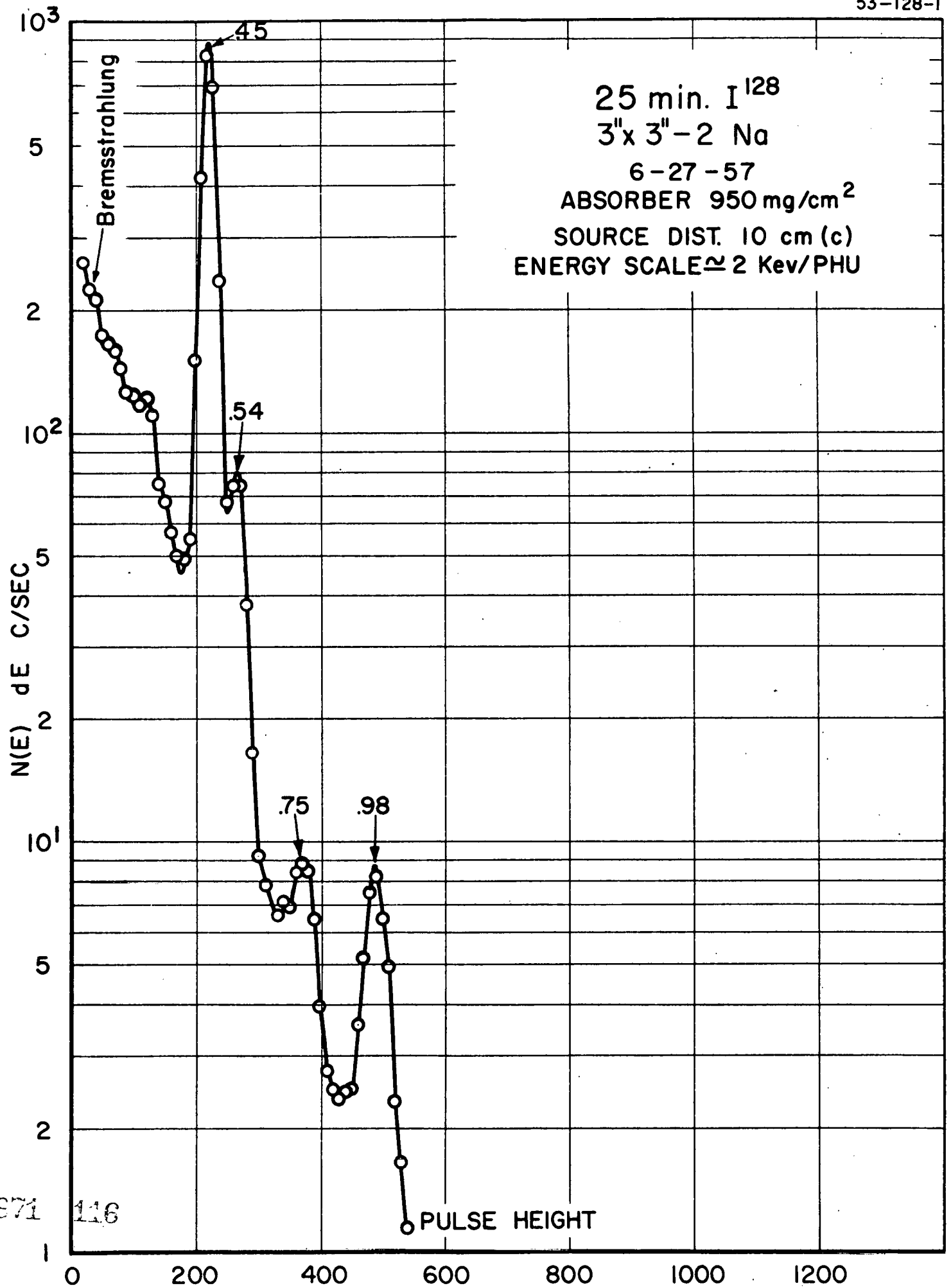






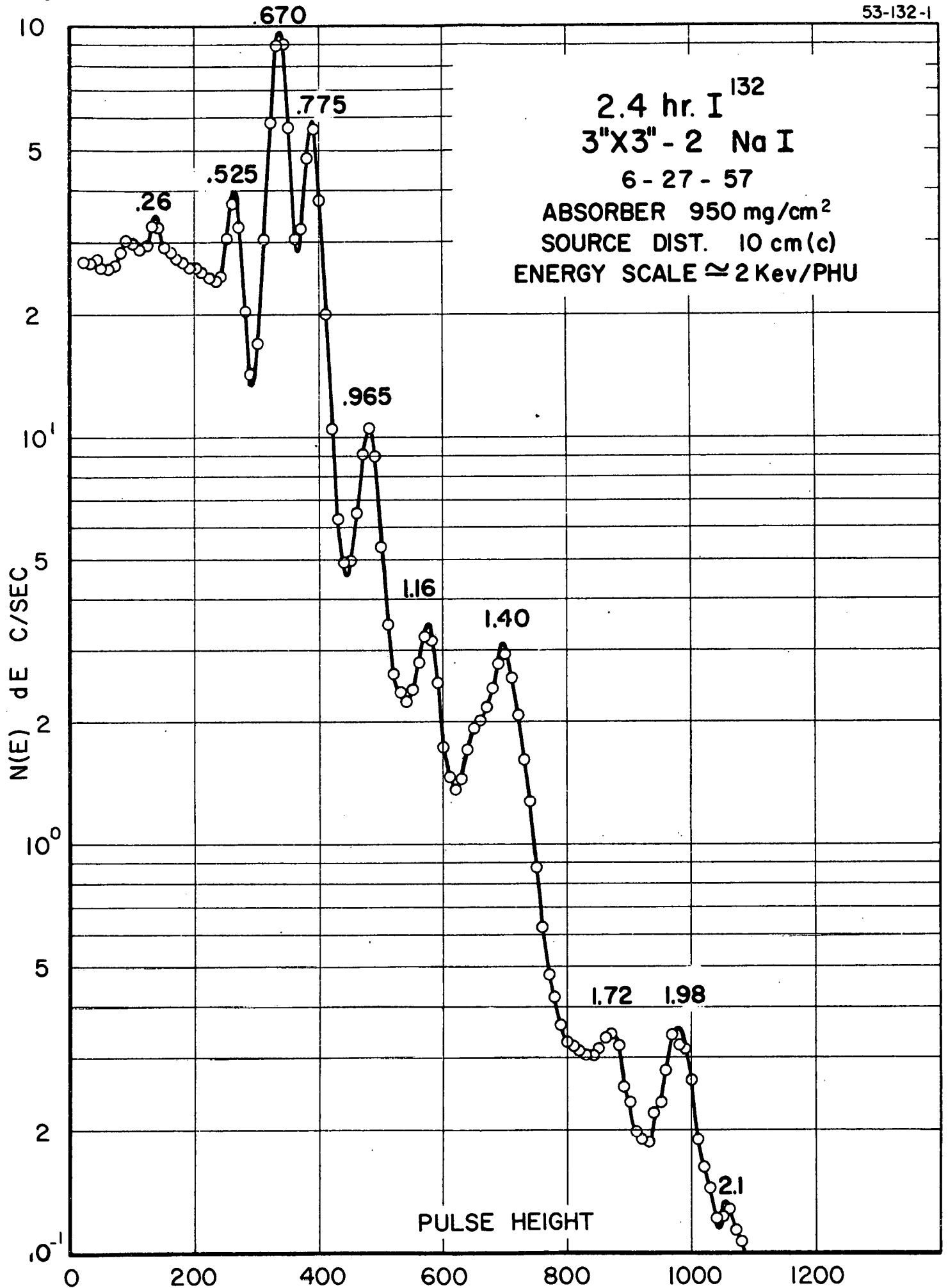


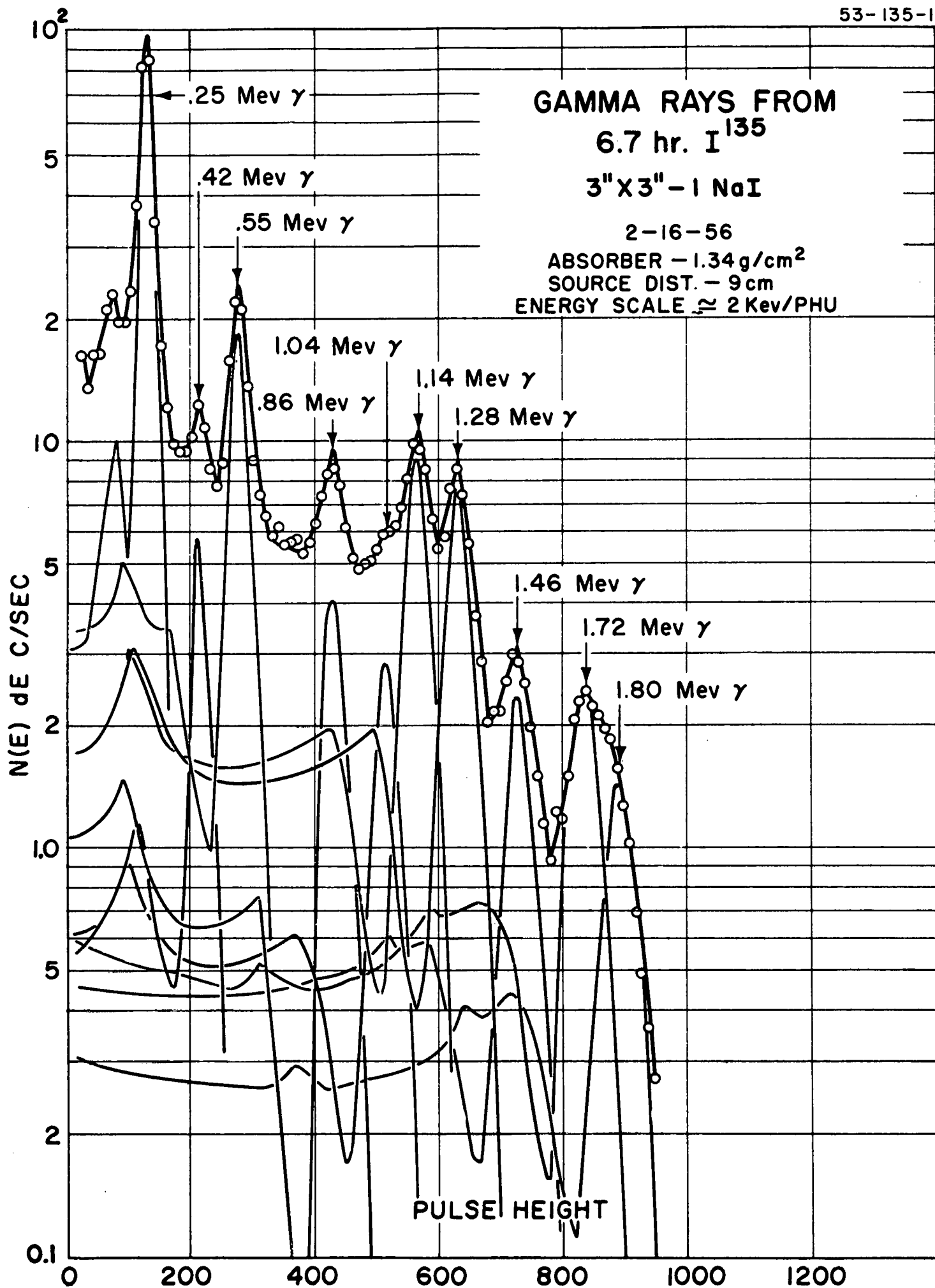


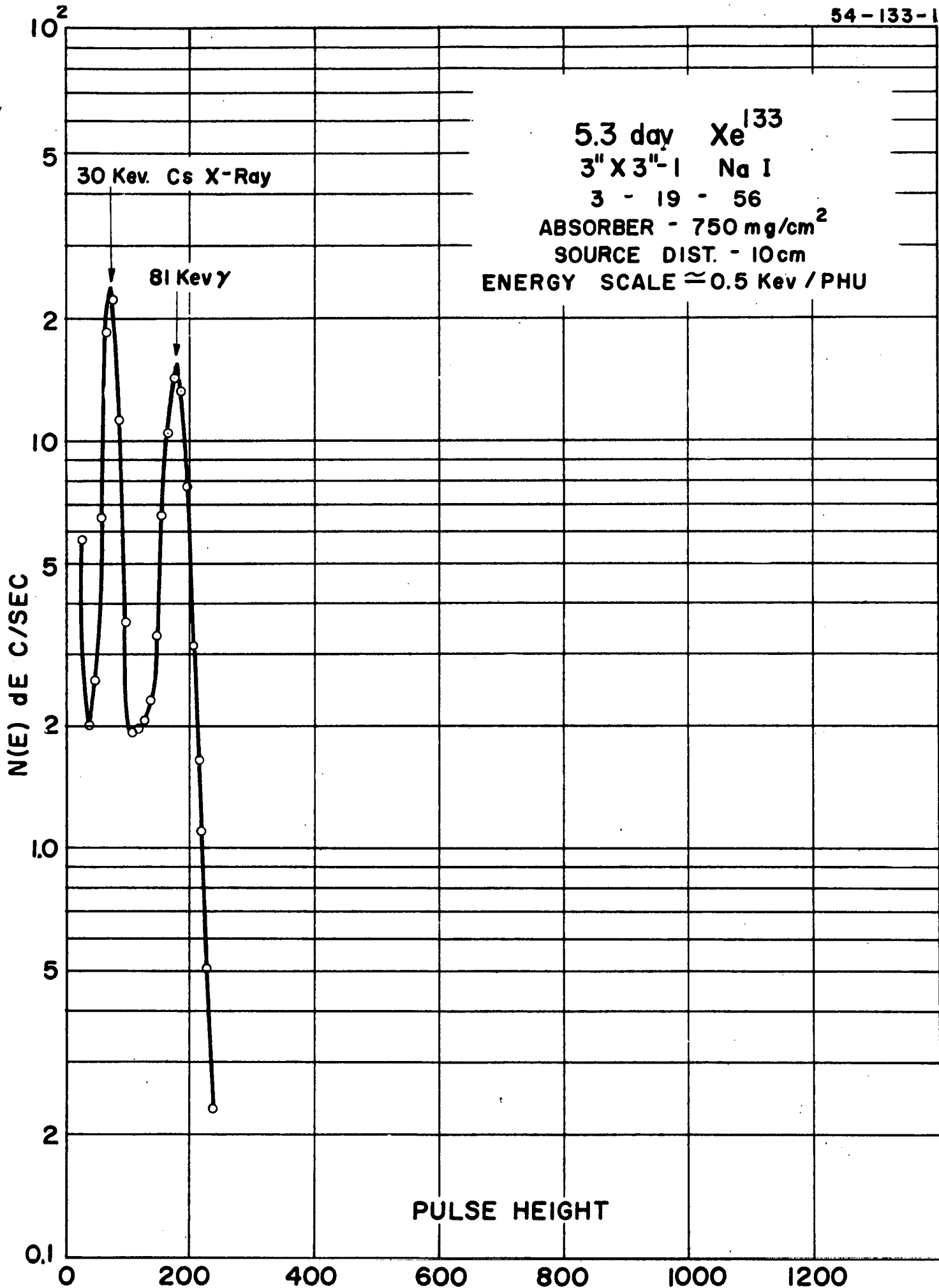


971 116









5.3 day -  $Xe^{133}$  9.2 hrs.  
 $Xe^{135}$  GAMMAS

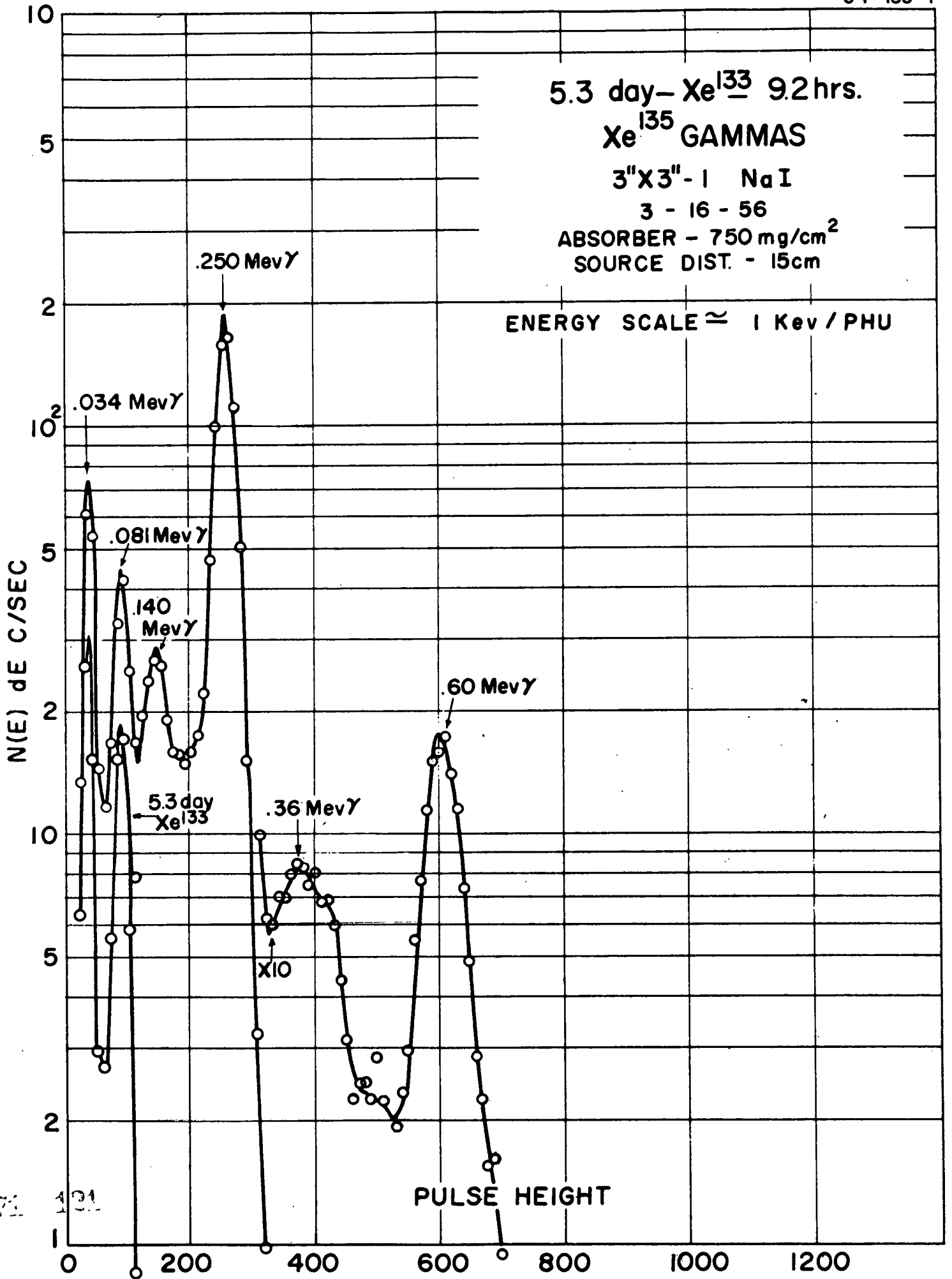
3"X3" - 1 NaI

3 - 16 - 56

ABSORBER -  $750 \text{ mg/cm}^2$

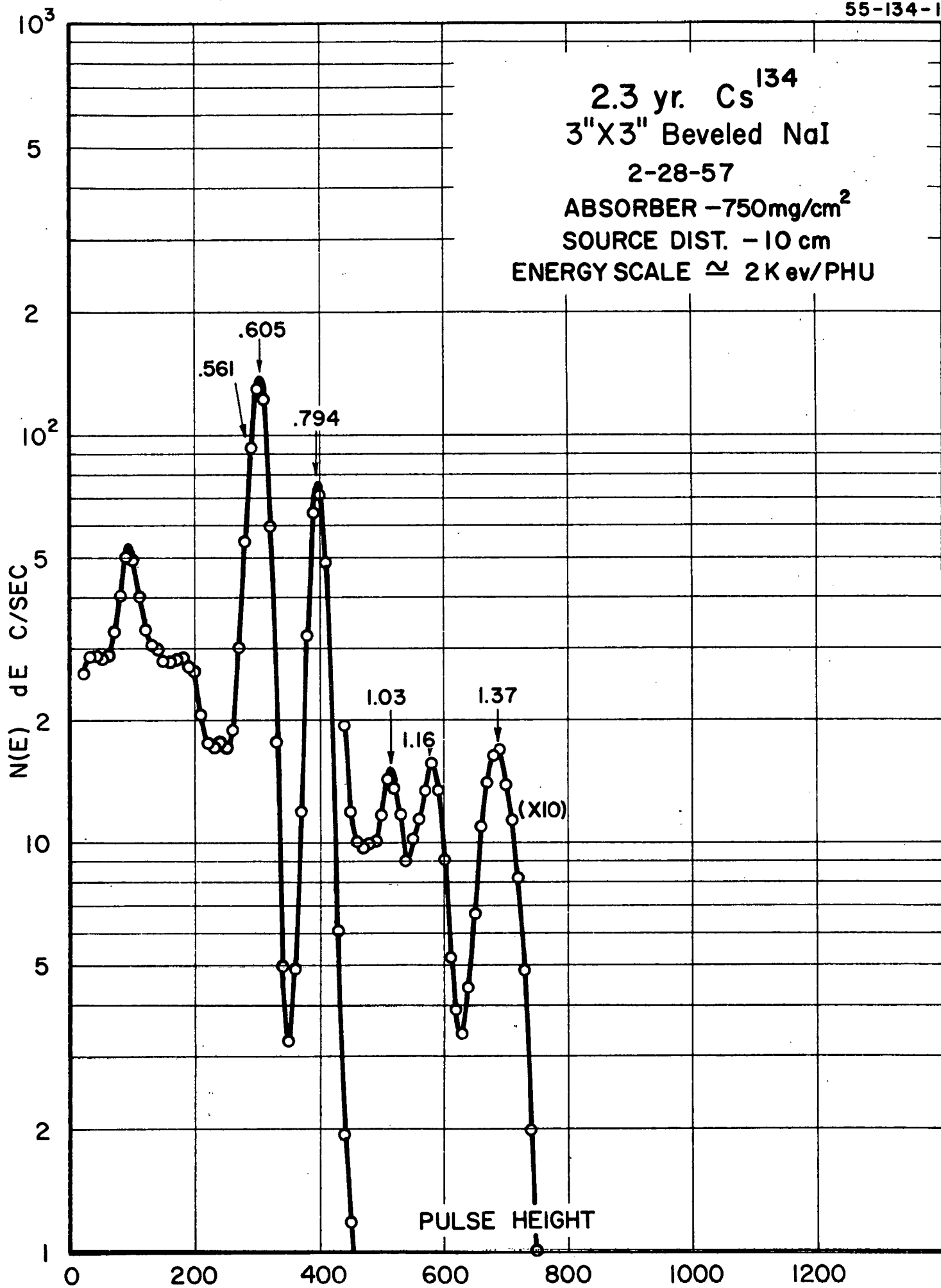
SOURCE DIST. - 15cm

ENERGY SCALE  $\approx 1 \text{ Kev / PHU}$



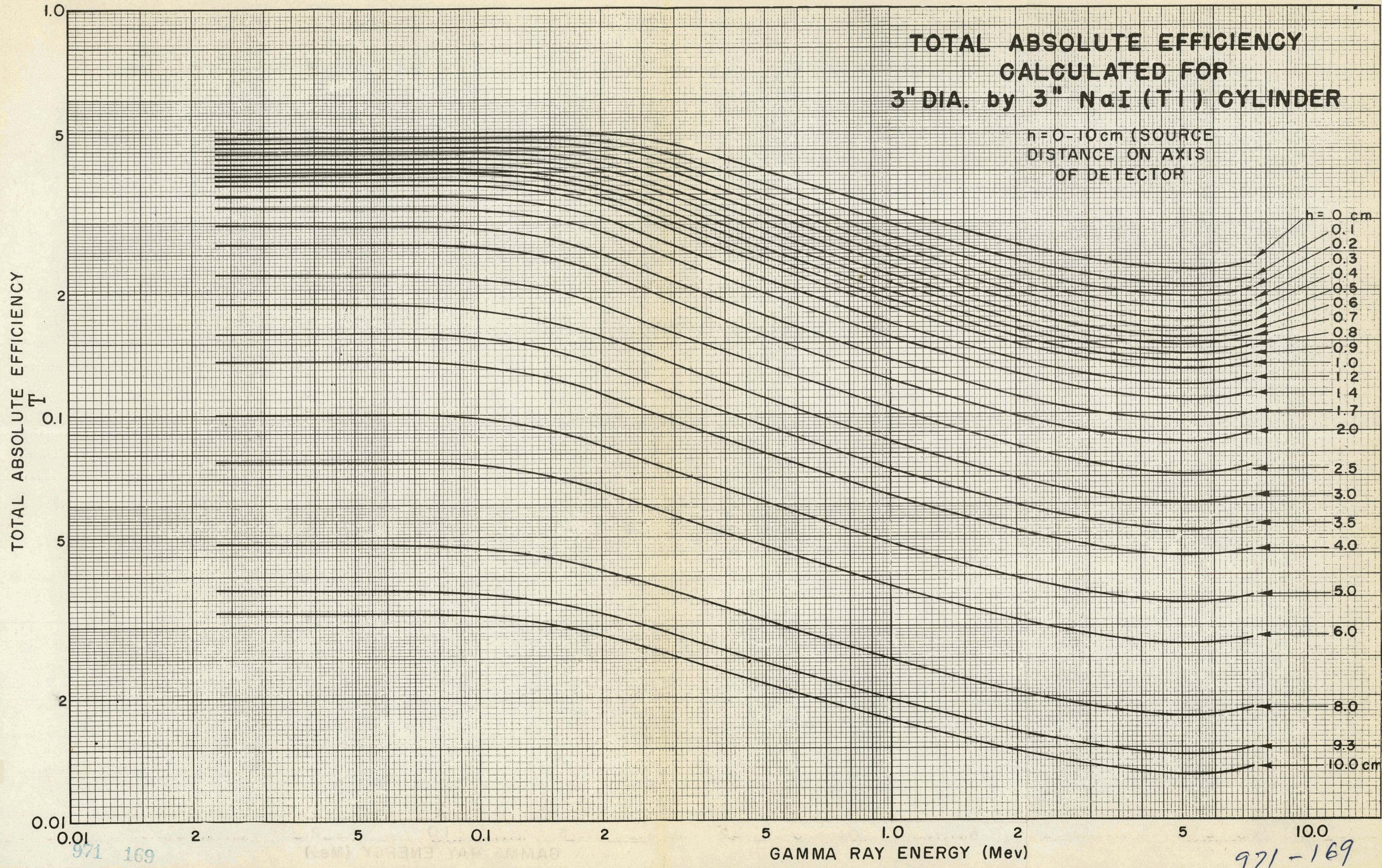
971 121

2.3 yr. Cs<sup>134</sup>  
3"X3" Beveled NaI  
2-28-57  
ABSORBER - 750mg/cm<sup>2</sup>  
SOURCE DIST. - 10 cm  
ENERGY SCALE  $\approx$  2 Kev/PHU



**TOTAL ABSOLUTE EFFICIENCY  
CALCULATED FOR  
3" DIA. by 3" NaI (TI) CYLINDER**

h = 0-10 cm (SOURCE  
DISTANCE ON AXIS  
OF DETECTOR)

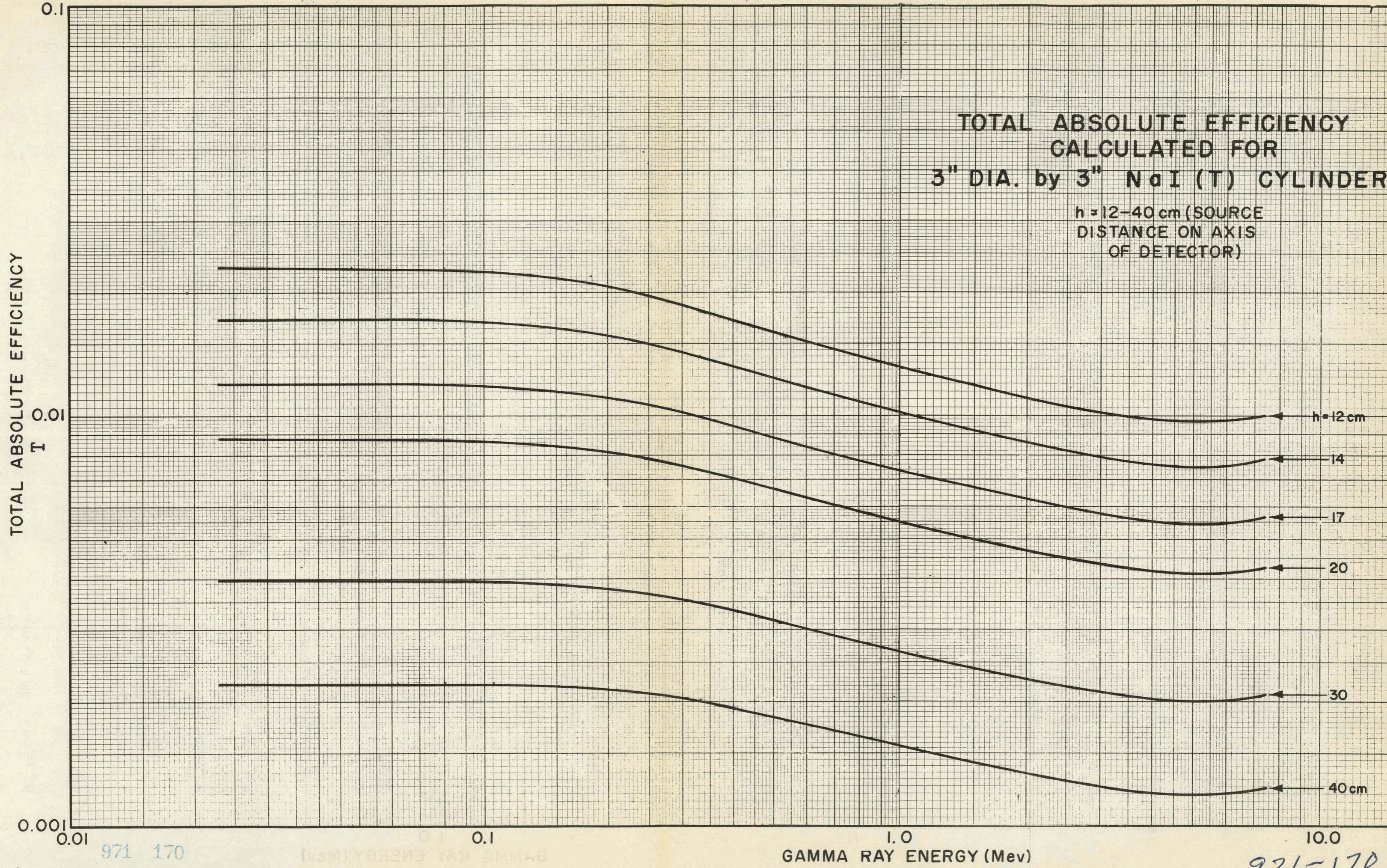


971 169

971-169

TOTAL ABSOLUTE EFFICIENCY  
CALCULATED FOR  
3" DIA. by 3" NaI (T) CYLINDER

h = 12-40 cm (SOURCE  
DISTANCE ON AXIS  
OF DETECTOR)



0.001  
0.01  
971 170

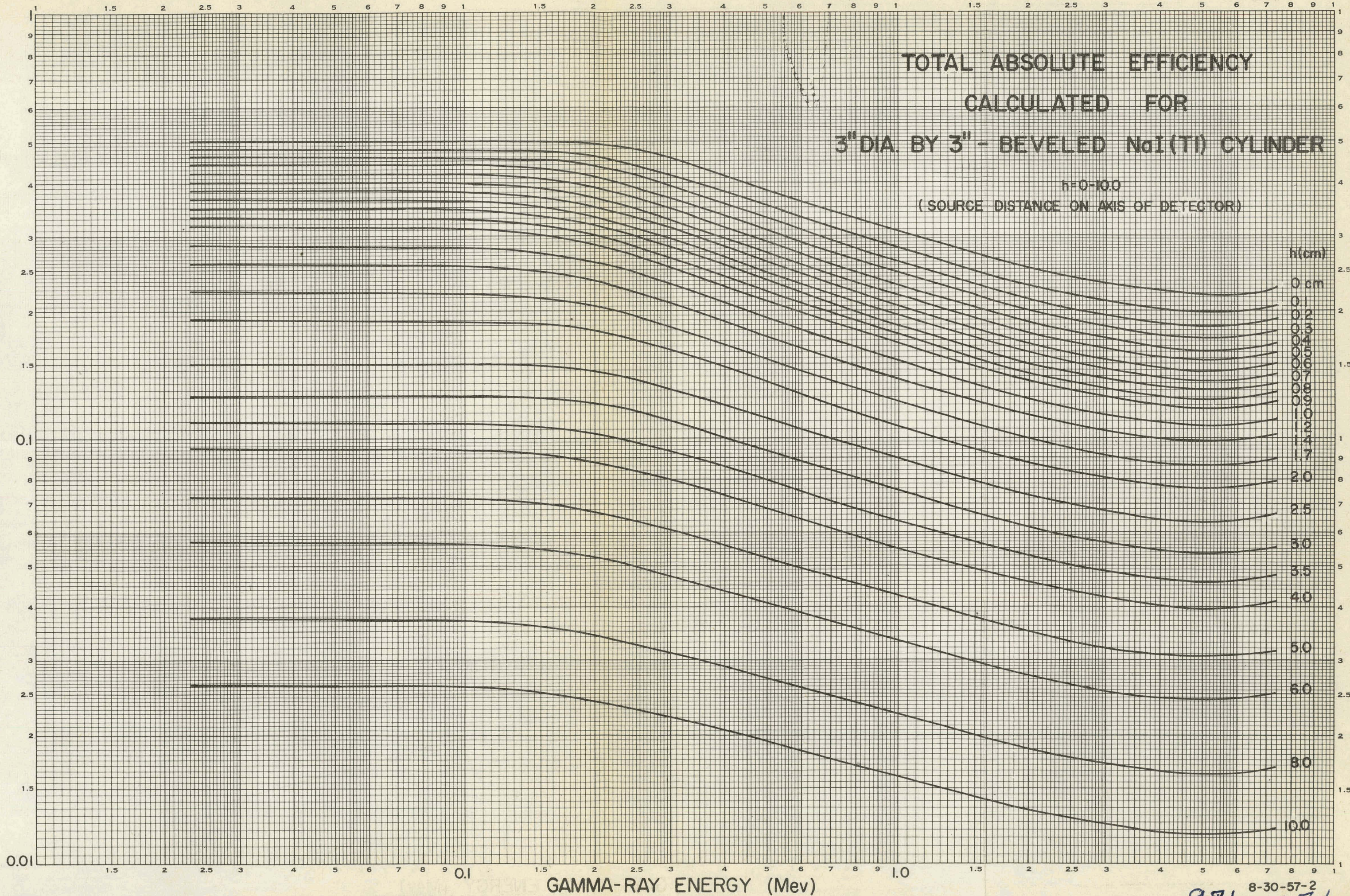
1.0  
10.0  
GAMMA RAY ENERGY (MeV)

971-170

TOTAL ABSOLUTE EFFICIENCY  
CALCULATED FOR  
3" DIA. BY 3" - BEVELED NaI(Tl) CYLINDER

$h=0-100$   
(SOURCE DISTANCE ON AXIS OF DETECTOR)

T  
TOTAL ABSOLUTE EFFICIENCY

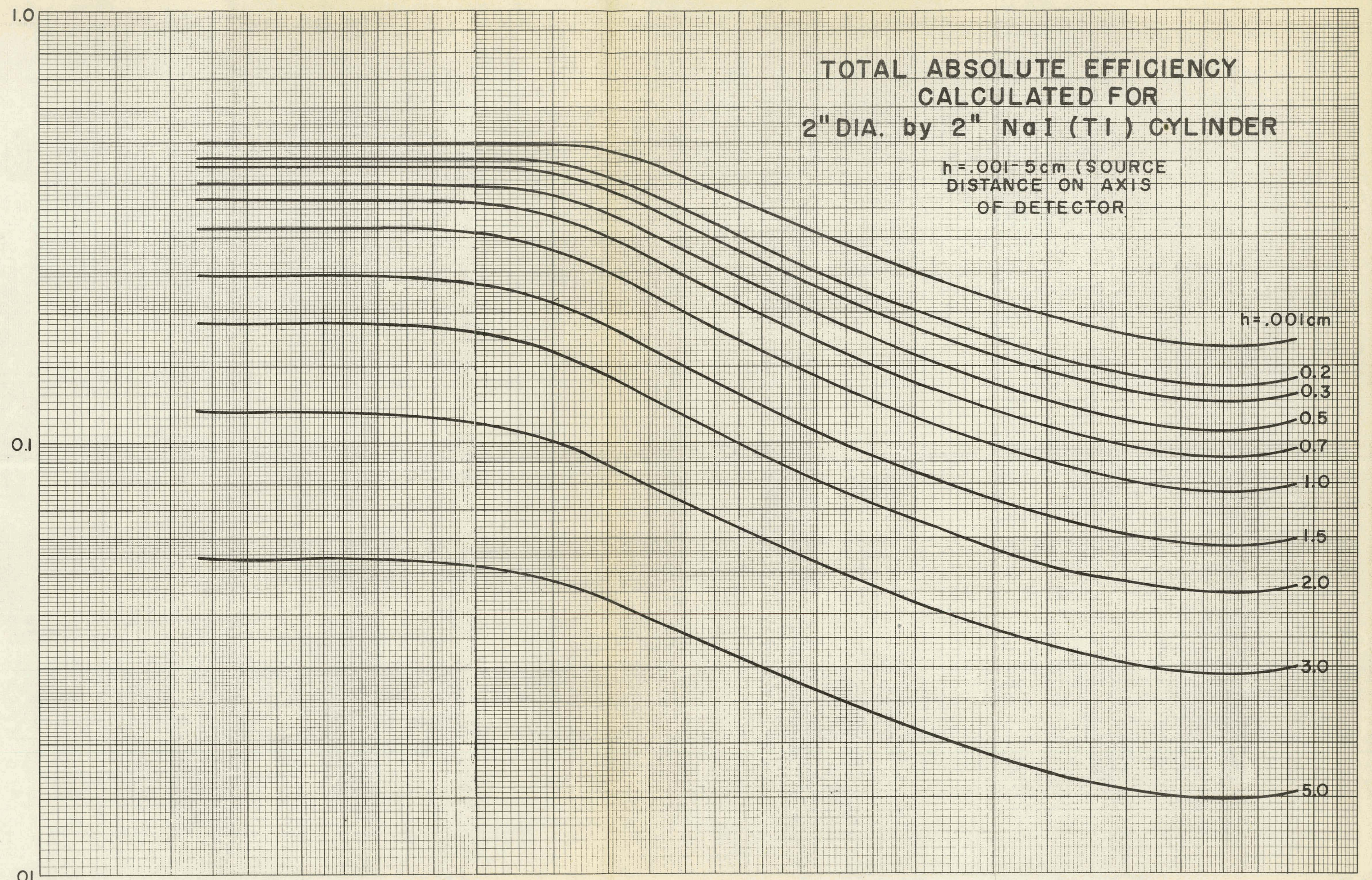


GAMMA-RAY ENERGY (MeV)

TOTAL ABSOLUTE EFFICIENCY  
CALCULATED FOR  
2" DIA. by 2" NaI (TI) CYLINDER

$h = .001 - 5\text{cm}$  (SOURCE  
DISTANCE ON AXIS  
OF DETECTOR)

TOTAL ABSOLUTE EFFICIENCY



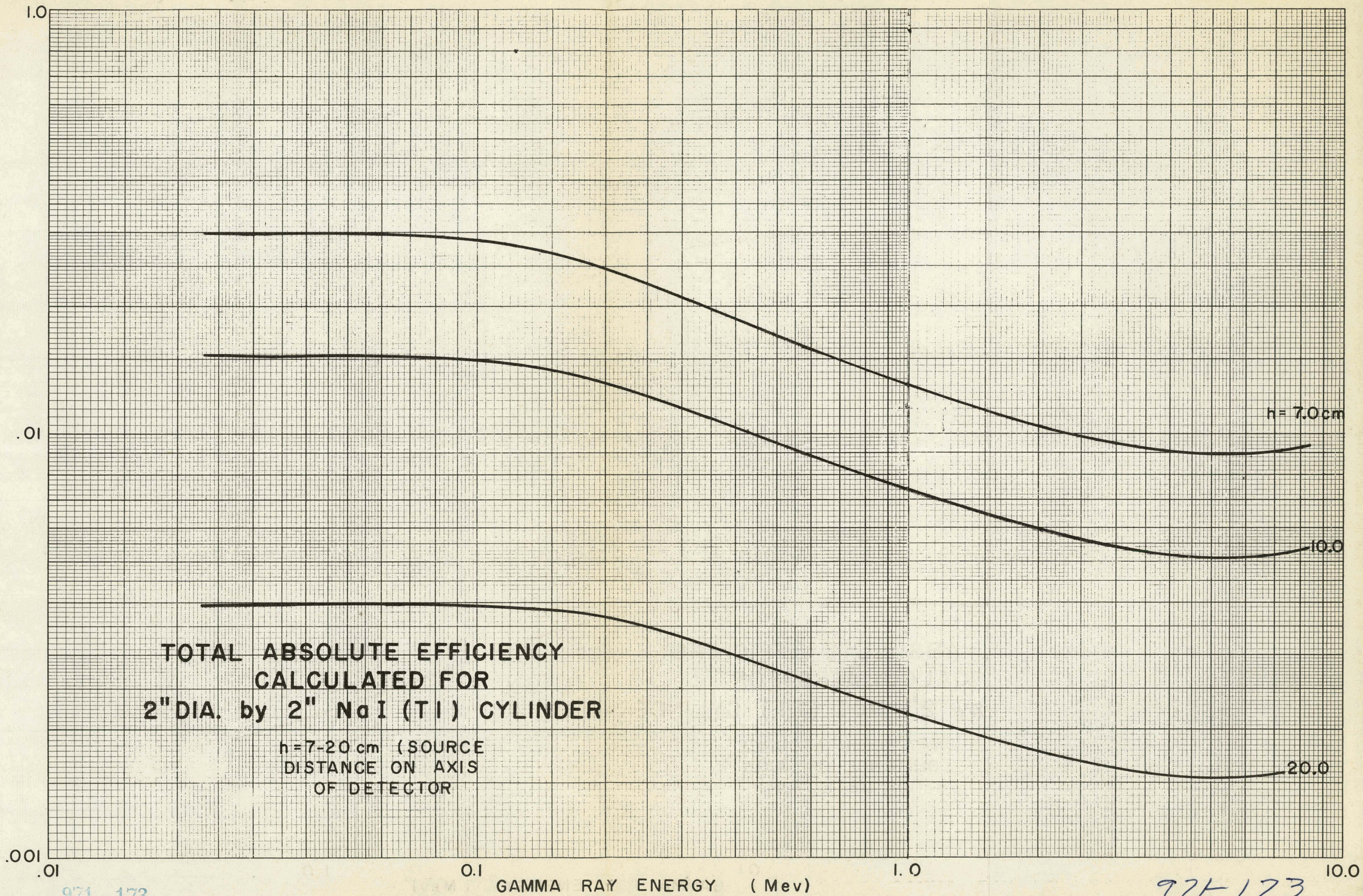
971-172

GAMMA RAY ENERGY (MeV)

971-172

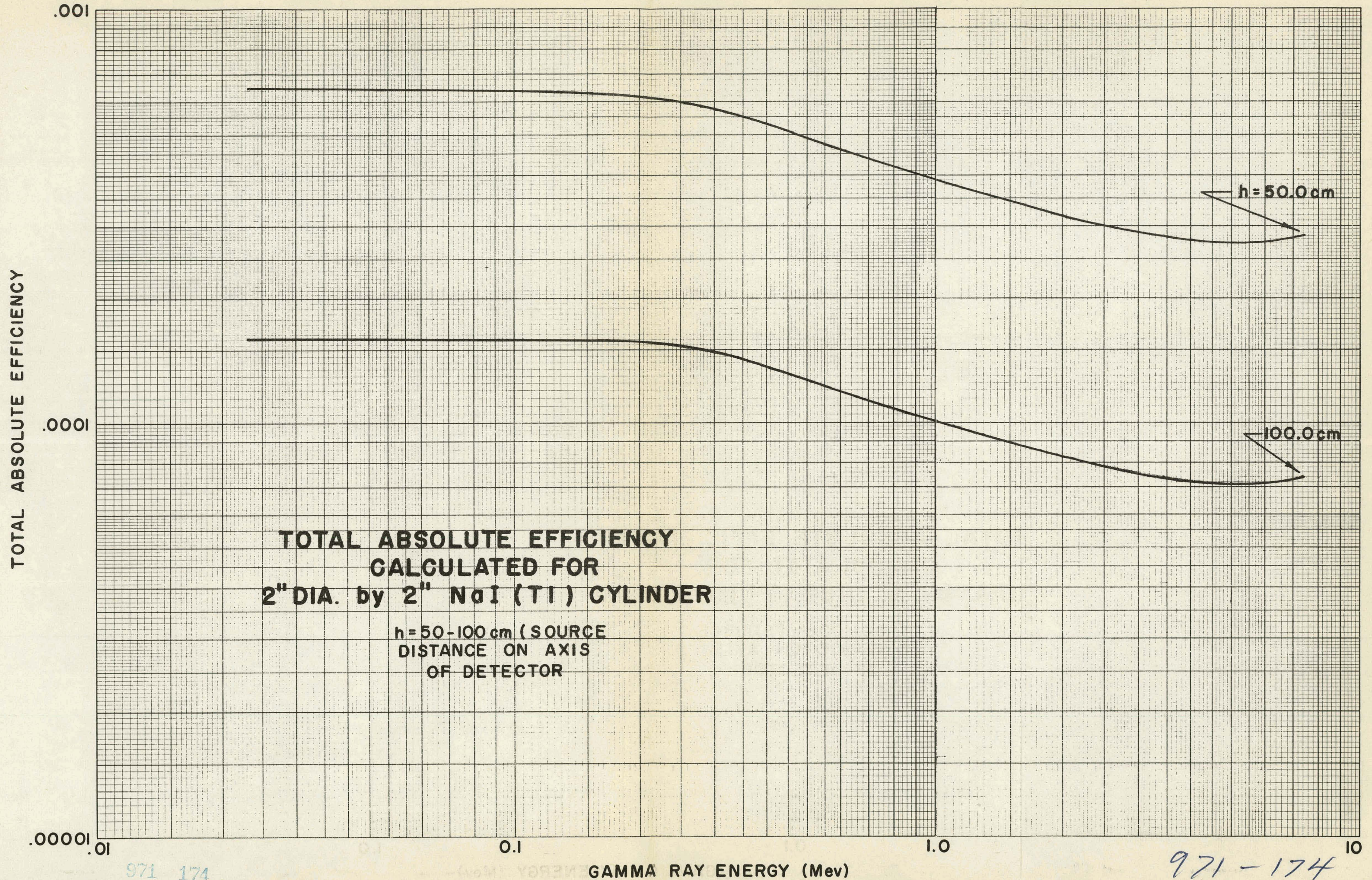
10.0

TOTAL ABSOLUTE EFFICIENCY



971 173

971-173



971 174

971-174

GAMMA RAY ENERGY (MeV)

APPENDIX II

PEAK-TO-TOTAL RATIOS

---

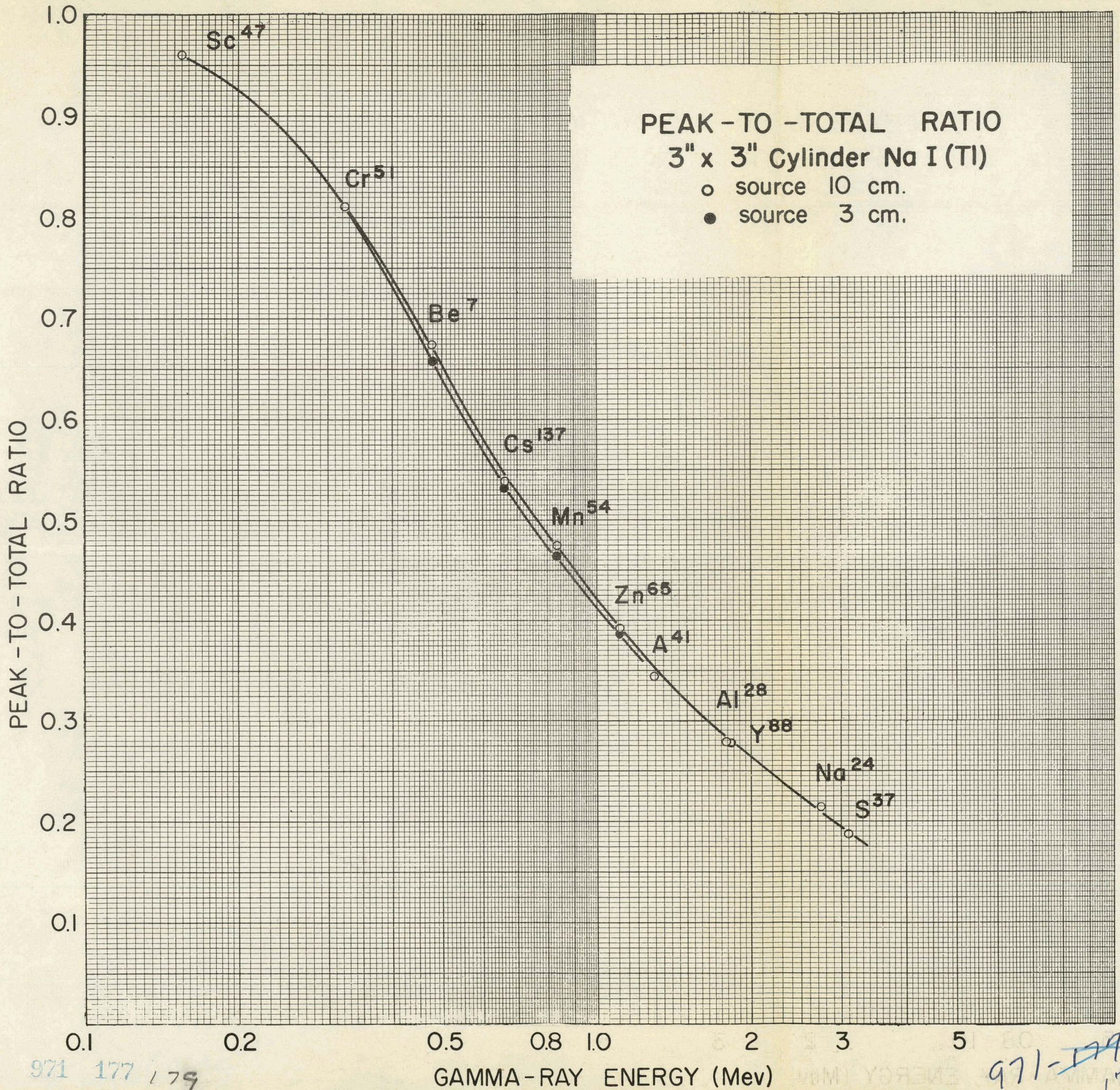
971 175

971-175

EXPERIMENTAL PEAK-TO-TOTAL RATIOS FOR NaI DETECTORS

Nuclide	$E_{\gamma}$ (Mev)	3" x 3" Cylinder				3" x 3" Cylinder (Bevelled for 1/2" at 45°)			
		0.2 cm.	3 cm.	5 cm.	10 cm.	0.2 cm.	3 cm.	5 cm.	10 cm.
Sc <sup>47</sup>	0.155	0.962	0.962	0.958	0.960	0.962	0.959	0.956	0.960
Cr <sup>51</sup>	0.323	0.814	0.813	0.812	0.811	0.815	0.823	0.818	0.814
Be <sup>7</sup>	0.478	0.652	0.657	0.672	0.674	0.650	0.668	0.662	0.667
Cs <sup>137</sup>	0.662	0.535	0.532	0.539	0.538	0.527	0.534	0.528	0.536
Mn <sup>54</sup>	0.835	0.461	0.464	0.470	0.474	0.457	0.465	0.468	0.473
Zn <sup>65</sup>	1.114	0.386	0.386	0.389	0.392	0.387	0.384	0.385	0.390
A <sup>41</sup>	1.29				0.344				
Al <sup>28</sup>	1.78				0.278				
Y <sup>88</sup>	1.83				0.276				
Na <sup>24</sup>	2.76				0.214				
S <sup>37</sup>	3.13				0.187				

Note: Experimental values above are for point source on central axis of detector. Error estimated to be  $\pm 2\%$  or better for all measurements.



971 177 179

971-179  
179